DIESEL AEROSOL SAMPLING METHODOLOGY - CRC E-43

FINAL REPORT

University of Minnesota
Department of Mechanical Engineering
Minneapolis, MN 55455

Principal Investigator:
David Kittelson

Co-Principal Investigator:
Winthrop Watts

Project Manager:
Jason Johnson

E-43 Sponsors:

Coordinating Research Council
Department of Energy National Renewable Energy Laboratory (DOE / NREL)
Engine Manufacturers Association (EMA)
South Coast Air Quality Management District
California Air Resources Board
Cummins Engine Company, Inc.
Caterpillar, Inc.
Volvo Truck Corporation
National Institute for Occupational Safety and Health (NIOSH)

8/19/2002

Table of Contents

Table of Figures

Table of Tables

COORDINATING RESEARCH COUNCIL E-43 SPONSORS

Coordinating Research Council
Department of Energy National Renewable Energy Laboratory (DOE / NREL)
Engine Manufacturers Association (EMA)
South Coast Air Quality Management District
California Air Resources Board
Cummins Engine Company, Inc.
Caterpillar, Inc.
Volvo Truck Corporation
National Institute for Occupational Safety and Health (NIOSH)

ACKNOWLEDGEMENTS

The University of Minnesota (UMN) research team would like to thank our subcontractors for their participation in the E-43 study. West Virginia University (WVU) contributed to the wind tunnel study, Carnegie Mellon University (CMU) modeled roadway aerosol and its lifetime, Tampere University provided the Electrical Low Pressure Impactor and technical assistance, and the Paul Scherrer Institute in Switzerland provided the surface area instruments used throughout the study. In particular, we wish to thank Drs. Nigel Clark and Spyros Spandis, from WVU and CMU, respectively, for coordinating the activities of their universities. We owe a great deal of thanks to Nick Bukowiecki from Paul Scherrer Institute (PSI) and Jyrki Ristamäki from Tampere University for their contributions to all phases of the E-43 project.

We are grateful for the cooperation and technical support provided by both Cummins and Caterpillar. We would like to acknowledge the monetary support and technical assistance provided by the Cummins Emissions Development Group. In particular, we want to thank John Wall, Chief Technical Officer, Pat Flynn, Vice President of Research (now retired), Dr. Shirish Shimpi, Senior Technical Advisor, Rory McCoy, Project Engineer, and Don McCloskey, Lab Manager. At Caterpillar, we would like to acknowledge the technical assistance provided by Rob Graze and other technical staff.

We would like to acknowledge the guidance and technical assistance provided by the Quality Assurance Team appointed by CRC. Drs. Bruce Cantrell, Alberto Ayala and Bernard Olson provided oversight, guidance and technical assistance throughout the project.

We would like to acknowledge the assistance of the CRC E-43 technical panel for their oversight and review of the many reports produced as a result of this project. Mr. Brent Bailey of CRC coordinated the activities of this panel and guided us through the contractual process. The E-43 project leader was Dr. Nicolas Barsic of Deere & Co. Dr. Doug Lawson with DOE/NREL and Dr. Steve Cadle with General Motors assisted Dr. Barsic. Dr. Barsic also spent time with the research team as a valued participant in the on-road and particle loss studies.

Finally, we would like to thank all of the undergraduate and graduate students at the University of Minnesota, and the Center for Diesel Research staff who participated in this project. In particular we wish to thank, Dwane Paulsen, Marcus Drayton, Qiang Wei, Megan Arnold, Erin Ische, Mindy Remerowski, Dick Beaudette, Hee Jung Jung, Alfred Ng, Feng Cao, Jungwoo Ryu, John Gage and Darrick Zarling. Without their assistance this project would not have been possible.

ACRONYMS AND ABBREVIATIONS USED IN THIS REPORT

	Acronyms
Avg DR	Mean dilution ratio
CARB	California Air Resources Board
CD	Chassis dynamometer
CDPF	Catalyzed Diesel Particulate Filter
CMU	Carnegie Mellon University
CO	Carbon monoxide
CO_2	Carbon dioxide
CPC	Condensation particle counter
CRC	Coordinating Research Council
CVS	Constant volume sample
CVS-1	First configuration of CVS dilution system
CVS-2	Second configuration of CVS dilution system
Dair	Dilution air
DC	Diffusion charger
DECSE	Diesel Emissions Control Sulfur Effects Program
Dg	Geometric mean diameter
DGN	Geometric mean number diameter
Dp	Particle diameter
DGS	Geometric mean surface diameter
DMA	Differential mobility analyzer
DOE/NREL	Department of Energy/ National Renewable Energy Laboratory
DR	Dilution ratio
DRI	Desert Research Institute
E-43	CRC Project Number
ECM	Electronic control module
ECOM AC	Raw exhaust gas analyzer
ELPI	Electrical low pressure impactor
EMA	Engine Manufacturers Association
EPA	Environmental Protection Agency
EPI	Epiphaniometer
FTP	Federal Test Procedure
HEI	Health Effects Institute
ISM	A Cummins test engine also referred to as M-11
ISO	International Standards Organization
L-10	A Cummins test engine
M-11	A Cummins test engine also referred to as ISM
Max DR	Maximum dilution ratio
MEL	Mobile emissions laboratory
Min DR	Minimum dilution ratio
MOUDI	Micro-orifice uniform deposit impactor

MTU	Michigan Technological University
nano-MOUDI	nano-Micro-orifice uniform deposit impactor
NDIR	Non-dispersive infrared
NIOSH	National Institute for Occupational Safety and Health
NO	Nitric oxide
NO_2	Nitrogen dioxide
NOx	Oxides of nitrogen
N_{30}	Number of particles <= 30 nm
N total	Total number of particles particles/cm^3
NIST	National Institute of Standards and Technology
N/V	Number/Volume = (Particles/cm^3)/($\mu m^3/cm^3$)
Part	Particles
PAS	Photoemission/photoelectric aerosol sensor
PAH	Polycyclic aromatic hydrocarbons
PDT	Primary dilution temperature
PRT	Primary residence time
PSI	Paul Scherrer Institute
PSL	Polystyrene latex
Pt	Particles
QA	Quality assurance
SBOCLE	Scuffing load ball-on-cylinder lubricity evaluator
S	Saturation ratio
SD	Standard deviation
SDOM	Standard deviation of the mean
SI	Spark ignition
SMPS	Scanning mobility particle sizer
SOF	Soluble organic fraction
TD	Thermal denuder
TDPBMS	Thermal desorber particle beam mass spectrometer
TL	Transfer line
UMN	University of Minnesota
UMN-1	First configuration UMN dilution system
UMN-2	Second configuration UMN dilution system
UV	Ultraviolet
V_{30}	Volume of particles <= 30 nm
V total	Total volume of particles $\mu m^3/cm^3$
WVU	West Virginia University

EXECUTIVE SUMMARY

The University of Minnesota and research partners West Virginia University, Carnegie Mellon University, Tampere University, Paul Scherrer Institute, University of California at Riverside, Caterpillar, Inc., and Cummins, Inc. undertook the study titled "Diesel Aerosol Sampling Methodology" to sample, characterize and quantify particles in Diesel exhaust. The goal of this project (E-43) was to develop Diesel aerosol sampling methods for the laboratory that would produce particle size distributions similar to those obtained under real-world roadway conditions.

The study was carried out at four locations with measurements on four test trucks powered by Caterpillar and Cummins engines and several engines installed on engine dynamometers. Standard certification (EPA) and market basket blends of California fuels (CA fuel) were used for all tests. A mobile laboratory was built and used to conduct on-road, chase studies, and a wind tunnel study was carried out at the Langley Wind Tunnel in Langley, Virginia. Engine and chassis dynamometer laboratory studies were carried out at Caterpillar, Cummins, and at the University of Minnesota.

To ensure quality processes and products for the E-43 project, CRC appointed a separate quality assurance (QA) team. The primary goal of the QA team was to provide independent opinions and guidance for the research team in the development of QA protocols for the research and final evaluation of project data. The QA team concluded that the project was consistent with QA level 3, "… projects producing results used to evaluate and select basic options, or to perform feasibility studies or preliminary assessments of unexplored areas which might lead to further work."

Laboratory measurement of combustion particle sizes and concentrations that represent typical on-road vehicle emission exposures requires approximately 1000:1 dilution. Several dilution techniques using state-of-the-art instrumentation were employed to cover the typical spectrum of lab equipment available today. Available dilution equipment allows considerable variation in operating parameters, such as dilution ratio, dilution rate, sample line size, residence time, heat loss, and dilution air temperature, but not all possible combinations of these produce results that simulate on-road exposures. Thus, the research team provided guidance for others to best simulate on-road exposures and to allow duplication of their results.

Diesel particle size distributions typically fit a lognormal, trimodal form consisting of nuclei, accumulation, and coarse modes. Nuclei mode particles measured on-road ranged in diameter from the 3 nm lower detection limit of available instrumentation to 30 nm. These nuclei mode particles are primarily volatile and consist of hydrocarbon or sulfur compounds that condense to the particle phase as their temperature decreases following release from the combustion process, cooling, and dilution with ambient air. A small amount of these nuclei mode particles contain solid ash from lube oil or wear metals; however, more research is needed to clearly determine their nature and quantities. Typically, 0.1-10 % of the particle mass and up to 90 % or more of the particle number

are found in the nuclei mode. Nuclei mode particles are a subset of the recently popular nanoparticle designation, which consists of particles smaller than 50 nm in diameter. Accumulation mode particles are 30 to 500 nm in diameter and are composed primarily of carbon agglomerates and nuclei mode particles that have collided with accumulation mode particles and contributed to their size. In addition, hydrocarbon vapors and sulfur compounds condense onto accumulation mode particles and thus contribute to the size and mass of accumulation mode particles. Approximately 10 % of the particle number count and 80 % to 90 % of the mass is contained in the accumulation mode. Coarse mode particles are larger than about 1 µm and contain 5-20 % of the mass, but this program focused on particles in the nuclei and accumulation modes.

The specific objectives and most significant findings are discussed below.

1. *Conduct on-road chase and wind tunnel experiments to determine the actual particle size distribution and particle number concentration in the exhaust plume from heavy-duty Diesel vehicles operated on the road or in the wind tunnel.*

For highway cruise and acceleration conditions all test vehicles produced bimodal size distributions in the submicron range with distinct nuclei and accumulation modes with both EPA and CA fuels. Old and new technology engines produced nuclei modes of similar magnitude.

Nuclei and accumulation mode geometric mean number diameters (DGN) ranged from 6-11 and 52-62 nm, respectively.

The fraction of particles found in the nuclei mode ranged from 37 to 87 % by number and from 0.3 to 2.1 % by volume. These fractions are considerably smaller than previously reported.

The accumulation mode was a repeatable function of engine and operating conditions, while the nuclei mode exhibited noticeable variation. The nuclei mode variability depended on engine operation, engine thermal history, roadway grade, interaction with other traffic, background aerosol, and ambient temperature.

The nuclei mode variability depended upon engine operation, engine thermal history, roadway grade, interaction with other traffic, background aerosol, and ambient temperature.

Cold temperatures favored nuclei mode formation.

Wind tunnel sampling conditions were quite different from those encountered on-road, with low dilution ratios and high background concentration. Size distributions were unlike on-road with no significant nuclei mode and a large accumulation mode.

2. *Conduct laboratory tests to compare on-road aerosol data with that generated in emissions test facilities to determine if current emission test facility sampling and analysis methods are adequate for characterizing particle size observed on the road.*

Current emission test facility sampling and analysis methods are not adequate for measuring particle size distributions and concentrations observed on a roadway, thus recommended modifications to those methods were made by the research team due to the following observations.

Composite average on-road size distributions under moderate summer conditions were similar to those obtained in the laboratory using typical systems modified to best simulate most on-road data, but it was not possible to duplicate all individual on-road size distributions.

Unsteady conditions encountered during normal on-road operation and a strong sensitivity to ambient conditions, especially temperature, make the duplication of on-road size distributions in the laboratory challenging.

The nuclei mode is much more sensitive to engine operation, dilution and sampling conditions than is the accumulation mode.

Storage and release of volatile material in the exhaust system, and prior engine operating history influence the formation of nuclei mode particles.

On-road size distribution measurements consistently showed a nuclei mode while laboratory measurements showed a nuclei mode in many but not all conditions.

The size distributions formed during on-road operation depend not only upon engine, fuel, lube oil, and exhaust system design, but also upon many other factors including instantaneous operating conditions, operating history, and environmental conditions.

Particle loss in sampling lines and instruments is an inherent characteristic of aerosol measurement, and a primary goal of aerosol research is to minimize loss, but these data are often not reported. This research team departed from tradition by reporting particle number count loss results as approximately 50 % at 10 nm, 20 % at 20 nm and 3 % at 60 nm.

To address the above observations and concerns, the best sampling strategy for measuring engine exhaust size distributions is to apply good particle technology principles in the laboratory using a standard set of sampling and dilution conditions that are reproducible, are sensitive to sampling the broad range of particle sizes known to exist in engine exhaust aerosols and minimize sampling artifacts. Well-designed two-stage dilution systems operating at constant first stage dilution ratio offer the most current promise; specific details are provided in the main text.

3. *Examine particle transformations as the plume disperses downwind of the roadway in a typical urban situation.*

A computer model was used to determine that for typical urban conditions, characteristic times and transit distances for 90 % reduction of total number (nearly all in the ultrafine range) concentrations are on the order of a few minutes and 100-1000 m, respectively. Thus, Diesel trucks and other mobile particle sources will influence the aerosol particle number concentrations within a limited area mainly near roadways.

For a given wind speed, these particles are expected to survive and travel a factor of ten greater distances in a rural flat area as compared to an urban downtown location. This is because of faster coagulation due to higher background particle concentrations and faster mixing and deposition due to rougher terrain in urban areas.

The influence of roadway sources on particle mass distribution was not modeled and is more complex than number concentration due to the combination of fresh combustion, existing aerosol, meteorological conditions and photochemical aerosol generation.

4. *Characterize the bulk Diesel particulate matter chemical composition to determine surface properties and composition.*

The organic component of total Diesel particulate matter and nuclei mode particles appears to be mainly comprised of unburned lubricating oil for the engines and operating conditions sampled. The major organic compound classes (alkanes, cycloalkanes, and aromatics) appear to be distributed fairly uniformly across the volatility spectrum.

Heating can be used to differentiate volatile and solid particles, while the smallest particles are nearly all volatile. The fraction of solid particles decreased as particle size decreased, and only a volatile mode was detectable for the smallest particles tested (7 nm). It was found that more than 97 % of the volume of the volatile constituents of 12 and 30 nm particles disappeared on heating to 400°C. The volatility of these particles resembles that of C24-C32 n-alkanes, which implies a significant contribution of lubricating oil.

Sulfuric acid is a minor component (a few percent) of the nuclei mode for Diesel engines operating at light and medium loads using a 400 ppm sulfur diesel fuel with a trend of moderately increasing concentration with decreasing particle size.

Much was learned from this research, but further work remains. This program showed that the formation of on-road size distributions is strongly dependent upon operating and environmental conditions, especially temperature. The on-road vehicle operating conditions to be simulated must be defined before standard laboratory procedures can be finalized. More information on roadside and on-road nanoparticle concentrations is needed so that critical conditions can be identified. Standardized particle calibration and loss determination methods for particle sizing instruments and related measurements are needed. Laboratory sampling methods and recommended practices described here should

be validated, especially on very low emission engines. New instruments are becoming available for fast response particle sizing that may be useful for transient testing. They should be tested with engine and laboratory aerosols. Finally, the advanced combined physical chemical characterization methods developed in this program and related EPA, CARB, and DOE programs should be applied to ultra low emission engines.

E-43 PROJECT GOALS AND OBJECTIVES

The University of Minnesota formed an international research team to conduct the Coordinating Research Council (CRC) E-43 project, titled "Diesel Aerosol Sampling Methodology". The objectives of the E-43 project were:

- Determine the actual particle size distribution and particle number concentration in the exhaust plume from heavy-duty Diesel vehicles operated on the road.
- Compare on-road aerosol data with data generated in emissions test facilities to determine if current emission test facility sampling and analysis methods are adequate for characterizing particle size observed on the road.
- Examine particle transformations as the plume disperses downwind of the roadway in a typical urban situation.
- Characterize the bulk Diesel particulate matter chemical composition and to determine surface properties and composition.

The goal of the E-43 project was to develop laboratory methods to measure Diesel aerosol size that would mimic results obtained under real-world roadway conditions. To accomplish this goal, a fundamental understanding of aerosol formation, transformation, measurement, and the physical processes that affect the size distribution, such as dilution, nucleation, condensation, adsorption and coagulation was required. The research team measured and characterized Diesel aerosol on the roadway and in the laboratory to try to establish a link between aerosol size characteristics measured under real-world conditions on the roadway and those measured in the laboratory.

CRC E-43 OVERVIEW

The CRC E-43 project was carried out in distinct phases using trucks and engines supplied by the Cummins and Caterpillar engine companies. The engines supplied by each of the companies were quite different, and the study was not designed to compare results between Cummins and Caterpillar engines. The project began in September 1998 and was completed in June 2002. The specific study events and dates are listed below.

- Design and build Mobile Emissions Laboratory (MEL) - 10/98 to 5/99
- Develop and validate on-road test procedures - 6/99 to 9/99
- Cummins engine tests
  - On-road chase tests - 9/16 to 11/18/99
  - Wind Tunnel Study - 10/22 to 10/28/99
  - Chassis dynamometer study - 4/27 to 5/3/00
  - Testing in CVS tunnel - 5/16 to 5/24/00
    - Cummins sponsored fuel sulfur and lube oil study – 5/25 to 6/2/99

- Caterpillar Engine Tests
  - On-road chase tests - 7/11 to 8/8/00

- CVS tests - 8/16 to 8/25/00
- Performance cell tests - 8/29 to 9/6/00
- Chassis dynamometer tests - 9/30 to 10/6/00

➢ Data Analysis and reporting – project initiation to 6/15/02

Cummins provided two test trucks powered by Cummins engines (L-10 and ISM or M-11) that were used throughout the Cummins portion of the research. Chase studies were carried out in MN using both trucks and the MEL. Following these tests, the UMN, WVU and others conducted a wind tunnel study using the ISM truck at the Langley wind tunnel in Langley, VA. This study was followed by chassis dynamometer and CVS studies carried out at Cummins test facility in Columbus, IN. The wind tunnel research resulted in reports prepared by UMN and WVU. The UMN produced a data volume summarizing the on-road and laboratory tests conducted at Cummins. CMU prepared a report using size distribution data from the on-road Cummins chase tests.

Caterpillar provided two trucks powered by 3406C and 3406E engines, respectively. The same engines and trucks were evaluated on-road and at the Caterpillar chassis dynamometer facility in Peoria, IL. Similar, but not identical, 3406E engines were tested in the Caterpillar CVS (one engine) and performance test cells (two engines). The Caterpillar portion of the research resulted in a data volume prepared by the University of Minnesota.

Test fuels for the research program included Environmental Protection Agency (EPA) certification fuel supplied by either Cummins or Caterpillar and two batches of market basket blend California (CA) fuel supplied by CRC. In addition, Cummins sponsored additional tests to determine the impact of specially-formulated fuel and lube oil on the particle size distribution.

A major goal of the E-43 project was to reproduce on-road size distributions using laboratory-type dilution systems in the engine laboratories by simulating the on-road operating conditions. Three dilution systems were tried in the laboratory in an effort to simulate the atmospheric dilution processes. One of these dilution systems was partially based on a commercial unit.

Finally, a number of related projects were conducted at the same time as the E-43 project. Results from these projects impact the interpretation of the E-43 results. These projects include:

- Studies conducted in the Power and Propulsion Laboratory at the University of Minnesota by Qiang Wei and others using a Caterpillar C-12 engine and the Cummins ISM engine used in the E-43 project.
- Studies conducted by Drs. Ziemann, McMurry and Kittelson using the Thermal Desorption Particle Beam Mass Spectrometer (TDPBMS) (Ziemann, *et al.*, 2002).
- Studies conducted in the Power and Propulsion Laboratory by Drs. Kittelson and Watts to assess particle bounce and particle losses in the micro-orifice uniform deposit impactor (MOUDI).

- Studies conducted by Hee Jung Jung, Dr. Zachariah, Dr. Kittelson and others on the response of the photoemission aerosol sensor (PAS) and diffusion charger (DC) using flame aerosols (Jung, *et al*., 2001).
- Studies conducted by Drs. Sakurai, McMurry and Kittelson using the nano-differential mobility analyzer (nano-DMA) to measure the water uptake and volatility of Diesel aerosols (Sakuria, *et al*., 2001).
- Chemical analysis of Diesel particulate matter samples collected by the MOUDI and nano-MOUDI by Dr. Zielenska and colleagues at Desert Research Institute and by Dr. Cahill and associates at University of California Davis.
- Kinetics of soot oxidation by Higgins and colleagues at the University of Minnesota (Higgins, *et al*., 2001).

CHAPTER 1 - BACKGROUND

Diesel and other aerosols are often characterized by measuring particle diameters of individual particles making up the aerosol. The aerodynamic diameter, defined as the diameter of a unit density (1 g/cm^3) spherical particle that has the same settling velocity as the measured particle, is frequently used to classify particles to determine the mass size distribution by gravimetric measurement. Typically, the electrical mobility diameter is used to classify aerosols to determine the number size distribution. The electrical mobility diameter is a close approximation of the Stokes diameter, which is defined as the diameter of a spherical particle having the same density and settling velocity as the measured particle. The Stokes diameter determines the particle diffusion coefficient and its diffusional deposition characteristics. The densities of Diesel particles are typically less than 1 g/cm^3 so that aerodynamic diameters are less than the Stokes diameters. Other parameters, such as surface area and volume, are useful in characterizing aerosols. In the E-43 project, multiple measures were used to characterize Diesel aerosols. These measures include particle number, volume, surface area and mass.

Diesel particle size distributions typically fit a lognormal, trimodal form with the concentration in any size range being proportional to the area under the corresponding curve in that range. The nuclei, accumulation and coarse modes make up the trimodal size distribution. Nuclei mode particles range in diameter from ~ 0.003 to 0.03 micrometers (μm) or ~ 3 to 30 nanometers (nm). In the past, the nuclei mode was defined as particles between 5 and 50 nm. However, in light of the E-43 work, it is appropriate to redefine the nuclei mode to encompass the range between 3 and 30 nm. These particles consist mainly of volatile organic and sulfur compounds in varying proportions, as well as a small amount of solid material likely to consist of carbon and metallic compounds. Most of the volatile particles form during exhaust dilution and cooling. The nuclei mode typically contains 0.1 to 10 % of the particle mass and up to 90 % or more of the particle number. The accumulation mode ranges in size from roughly 0.03 to 0.5 μm (30 to 500 nm). Most of the mass, composed primarily of carbonaceous agglomerates and adsorbed materials, is found in the accumulation mode. The coarse mode consists of particles larger than 1 μm (> 1,000 nm) and contains 5 to 20 % of the Diesel aerosol mass. These relatively large particles are formed by reentrainment of particulate matter, which was deposited on cylinder and exhaust system surfaces (Kittelson, 1998).

Ultrafine and nanoparticles have diameters less than 100 and less than 50 nm, respectively. There is some disagreement about the most appropriate boundary for the nanoparticle range, but 50 nm is widely used. The nuclei mode falls nearly entirely within the nanoparticle range while the accumulation mode straddles the fine, ultrafine and nanoparticle ranges. The nuclei and accumulation modes formed by Diesel engines are formed at different times and have different compositions. It is more convenient and meaningful to describe Diesel exhaust size distributions in terms of the characteristics and sizes of the nuclei and accumulation modes rather than focusing on ultrafine and nanoparticle fractions. However, if there is a significant nuclei mode, nearly all of the

nanoparticles are found in this mode and the terms are nearly synonymous. This approach is followed throughout this report.

Particulate matter emissions from internal combustion engines have traditionally been regulated solely on the basis of total particulate matter mass. The regulations do not refer to either the size or the number concentration of the emitted particles. Modern Diesel and spark ignition engines emit lower exhaust particulate matter mass concentrations than their predecessors. MTU did exploratory work on the mass and number of particles emitted from older and newer Diesel engines. They reported higher than expected number concentrations for the newer engine (Bagley, *et al*., 1996 and Johnson, *et al.*, 1996). This research was recognized as exploratory by HEI and it was recommended that it be confirmed by other laboratory studies. In the MTU study, a prototype 1991 Cummins LTA10-310 engine, designed to meet 1991 Federal on-highway emissions limits, was evaluated. The engine had a high pressure, mechanically controlled fuel-injection system, as well as other design features commonly used in heavy-duty, high-speed, on-highway Diesel engines. MTU showed that this technology significantly reduced mass emissions, but caused a prominent shift in the size distribution of Diesel aerosol towards smaller nuclei-mode particles when compared to emissions from a 1988 Cummins L10 engine. Under steady-state conditions, the LTA engine produced up to 40 % of the particle volume in the nuclei-mode range. These findings were considered preliminary and subject to verification with representative engines from different manufacturers.

The MTU finding that the large concentration of nuclei mode particles accounted for a large percentage of the total volume of particles in the exhaust is unusual in that it differs from results reported by others. Previous research measuring the size distribution of Diesel aerosol found bimodal, lognormal distributions (Abdul-Khalek, *et al.*, 1995, Baumgard, *et al.*, 1985, Kittelson, *et al.*, 1988, Kittelson and Johnson, 1991). Typically, the majority of the mass or volume concentration of the Diesel aerosol was found within the accumulation mode of the particle size distribution as opposed to the nuclei mode. However, the engines and sampling conditions used in these studies were not of the same type as used by MTU. On the other hand, roadway studies done in the late 1970s and early 1980s reported nearly as large fractions of aerosol in the nuclei mode as MTU (Whitby, *et al.*, 1975 and Kittelson, *et al.*, 1988). A strong correlation appears to exist between local traffic patterns and ambient particle number concentration, while there is less correlation with ambient mass concentration. Measurements in urban areas show that ambient number concentrations reach 4×10^6 particles/cm^3, even though ambient mass concentrations are below regulated limits (McAughey, 1997 and Booker, 1997).

Results from the Northern Front Range Air Quality Study (Watson, *et al*., 1998 and Cadle, *et al.*, 1998) suggest that the direct $PM_{2.5}$ contribution from gasoline powered vehicles and engines was three times the direct $PM_{2.5}$ contribution from Diesel-powered vehicles and engines during the winter in Denver. Laboratory studies (Graskow, *et al.*, 1998, Greenwood, *et al.*, 1996 and Maricq, *et al.*, 1999a, b) have suggested that nanoparticle emissions from spark ignition (SI) engines are much more speed and load dependent than Diesel engines. High speed and load conditions, such as high-speed

cruise and hard acceleration, may produce number emissions approaching those of Diesel engines. However, under less severe conditions, SI emissions are considerably lower.

UMN Minnesota Department of Transportation (Mn/DOT) Study

A study of on-road aerosol measurements was recently completed in Minnesota (Kittelson, *et al*., 2001). On-road particulate matter emissions ranged between 10^4 to 10^6 particles/cm^3, with the majority of the particles by number being less than 50 nm in diameter. An association was observed between traffic speed and nanoparticle concentration: The higher the speed the greater the nanoparticle concentration and the smaller the particle size, as illustrated in Figure 1. This is a reasonable finding, because when the MEL was going 55 mph, the surrounding traffic was going 60 to 70 mph. At high vehicular speeds, particulate matter emissions increase because of higher engine load and fuel consumption. Researchers at the University of California Los Angeles have also observed the relationship between the on-road size distribution and vehicular speed (Zhu, *et al.*, 2002a,b). Some of the particles observed at higher speeds are likely due to transient release of particle-associated materials stored in exhaust systems during lower speed operation. Passing Diesel traffic was also observed to increase particle number concentrations.

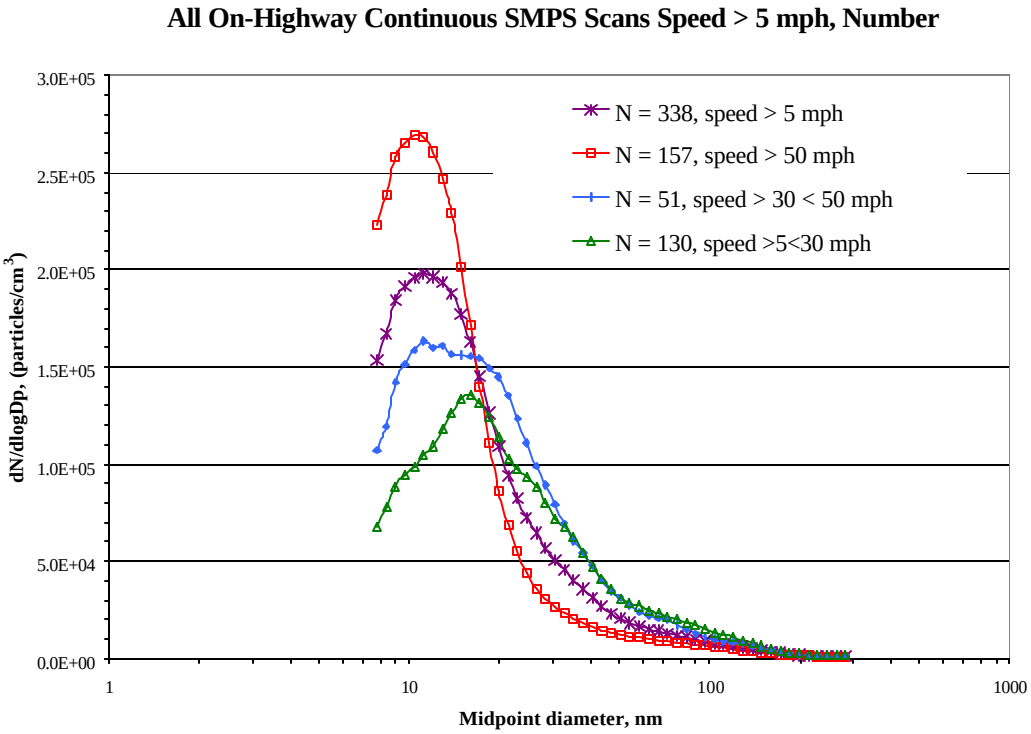

Figure 1. On-highway SMPS number distributions grouped by MEL highway speed (Kittelson, Watts, Johnson, 2001)

Slower speeds resulted in larger particles and larger aerosol volumes as illustrated by the volume distributions in Figure 2. Particle volume is a surrogate measure of particle mass, and is conserved while the particle number is constantly changing due to adsorption, coagulation and other physical and chemical mechanisms. The increase in particle volume or mass at lower vehicle speeds was consistent with expectations of higher concentrations under congested conditions. Less variation was observed in particle volume compared to particle number size distributions.

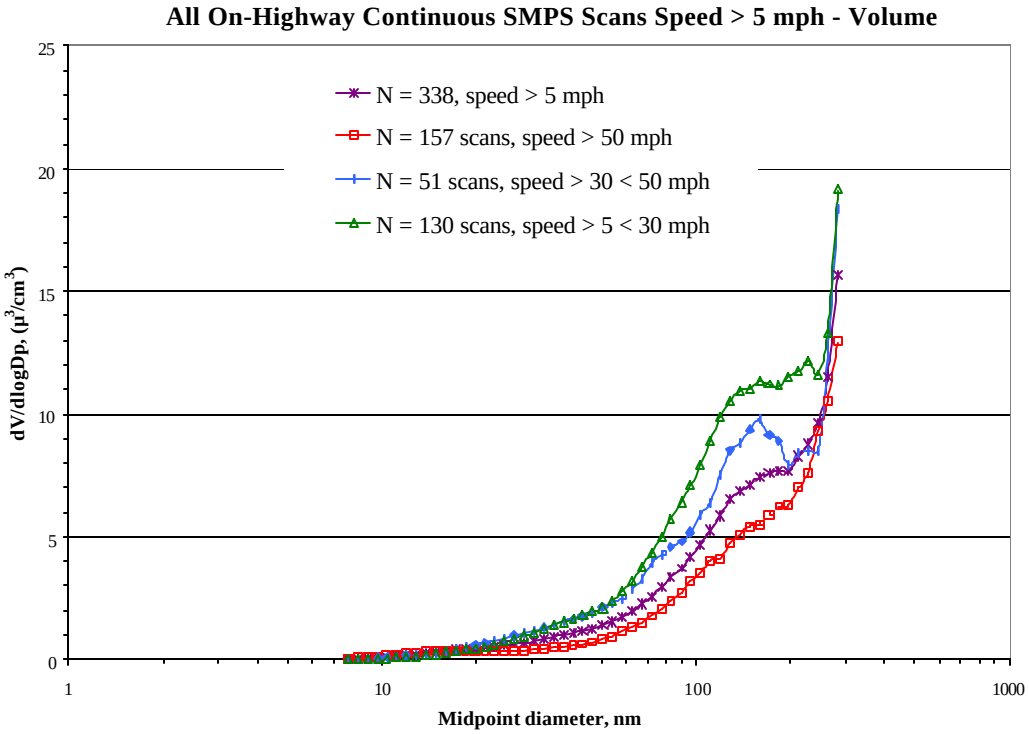

Figure 2. On-highway SMPS volume distributions grouped by MEL highway speed (Kittelson, Watts, Johnson, 2001)

Measurements made 10-30 m from the highway, in residential areas where highway airflow was not obstructed by barriers, demonstrated that aerosol concentrations approached on-road concentrations. The size distribution in these areas was similar in shape to on-road aerosol, with high concentrations of very small (< 20 nm) particles. Lower concentrations, lower by a factor of 10 or more, were observed in residential areas located 500 to 700 m from the highway. No distinct nuclei mode was apparent at these locations.

Better agreement between the TSI 3025A Condensation Particle Counter (CPC) and the scanning mobility particle sizer (SMPS) was found at slower speeds and less agreement at higher speeds where the particles were smaller. Under these conditions, CPC concentrations were generally at least 3 times higher. We believe the difference results from the CPC's ability to count particles between 3-8 nm, below the range of the TSI 3071 SMPS. We also found that the absolute number concentrations derived from the

SMPS, Dekati Electrical Low Pressure Impactor (ELPI) and CPC measurements differed. The lower counting limit of the ELPI as configured for this work was 30 nm so that ELPI number concentrations were nearly always lower than either the CPC or the SMPS. However, the concentrations measured by the instruments generally went up and down together. These points are illustrated in Figure 3, which shows a period of time when the MEL was making measurements on the highway at various cruise speeds. Note how the absolute difference between the SMPS, ELPI and CPC is greatest when the MEL speed is the highest. Also note that peak number concentrations were observed when the MEL was traveling at 55 mph.

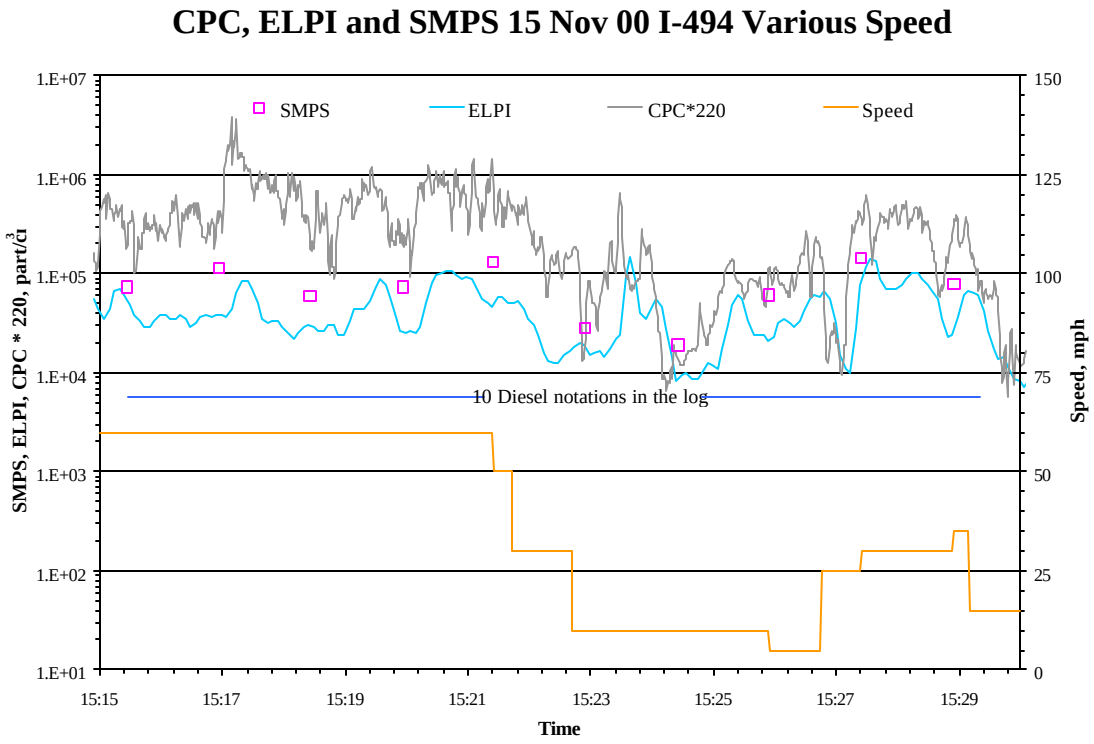

Figure 3. CPC, ELPI, SMPS 15 Nov 00 I-494 various speeds (Kittelson, Watts, Johnson, 2001)

The overall average size distribution obtained on Minneapolis freeways was nearly identical to the overall average on-road chase distribution measured during the E-43 study. These data are shown in Figure 23 and discussed in the results section.

UMN Health Effects Institute (HEI) Study

The UMN conducted a study of Diesel aerosol measurement for the HEI (Paulsen, 2001 and Kittelson *et al.*, 2002). This project evaluated alternative metrics of exposure in an occupational setting where low exposures of mixed combustion aerosol were present, and attempted to partition exposure by source. Traditional exposure assessment of Diesel and other combustion aerosols has been based on the measurement of mass concentration. However, this may not accurately reflect the full complexity of the exposure. Particle

number and surface area concentrations may be more health-relevant indices of exposure. Further, it may or may not be possible to partition exposure by source because of similarities in the composition of combustion aerosols.

The exposures of three occupational groups were evaluated using a variety of metrics including the mass concentration of elemental carbon, the mass concentration of black carbon, surface area, the number concentration, and the aerosol size distribution. Sampling focused on the Minneapolis/St. Paul and University of Minnesota transportation systems. Personal samples were collected on bus drivers, parking garage attendants, and mechanics to obtain distributions of exposures for these similarly exposed groups. Area samples were collected in buses, parking garages, and garage maintenance and repair facilities. These sampling locations represent environments where both Diesel and gasoline-powered vehicles operate on a regular basis in various ratios. The relationships between different exposure metrics (based on mass, surface area, number) were studied, and it was possible to identify differences in the exposures of the three occupational groups, as measured by these exposure metrics. However, we were not successful in separating Diesel and spark ignition exposure in mixed aerosol environments.

The size distributions measured in this study were lognormal and bimodal. Parking ramp aerosol (primarily from spark ignition sources) was calculated to have modal diameters of 14 to 29 nm and 37 to 134 nm, for mode 1 and mode 2, respectively. As shown in Figure 4, the number concentration measured by the CPC was 3 to 4 times greater than the SMPS integrated number concentrations. We believe that the CPC counted a high number of small particles (3-8 nm) below the range of the SMPS. In addition, the TSI SMPS 3071A does not account for diffusional losses within the classifier column or plumbing.

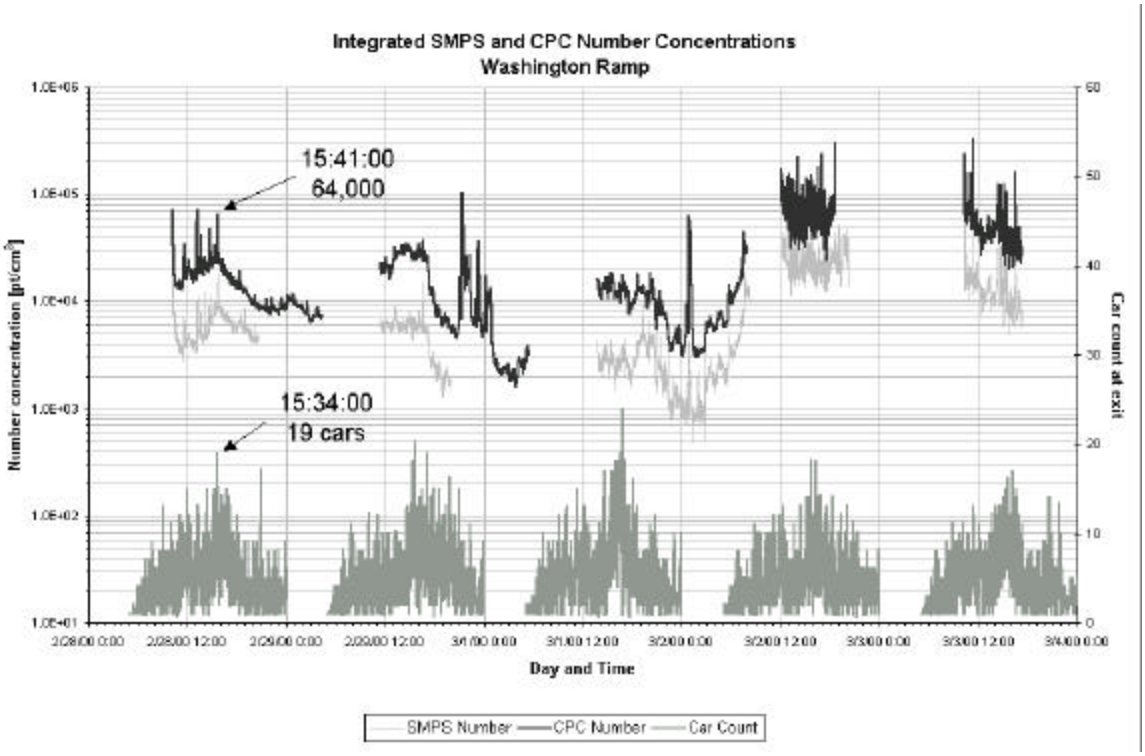

Figure 4. SMPS and CPC number concentration at the parking ramp (Paulsen, 2001)

The diurnal pattern observed from the concentration measurements demonstrated the dependence on traffic (primarily spark ignition traffic) at the exit of the ramp. The first three periods shown on Figure 4 (28 - 29 February, 1 March) were made inside the attendant's booth, while the last two (2 - 3 March) were made directly outside the booth. Particle concentrations were reduced considerably in the attendant's booth with average inside and outside concentrations of 12,900 and 60,500 part/cm^3, respectively.

The particle concentrations measured outside contained a high fraction of very small combustion nuclei that were less than 10 nm in diameter. Physical changes, such as coagulation and condensation, are likely occurring on a timescale of minutes for the nano-sized particles (D_p<50 nm). Size distributions taken inside and outside the parking ramp attendant's booth are shown in Figures 5 and 6. The particle sizes inside and outside the booth were essentially the same. The aerosol in the booth was a mixture of clean air and air coming through the attendants window. The concentrations inside the booth were low enough, about 10,000 particles/cm^3, that coagulation was not an issue.

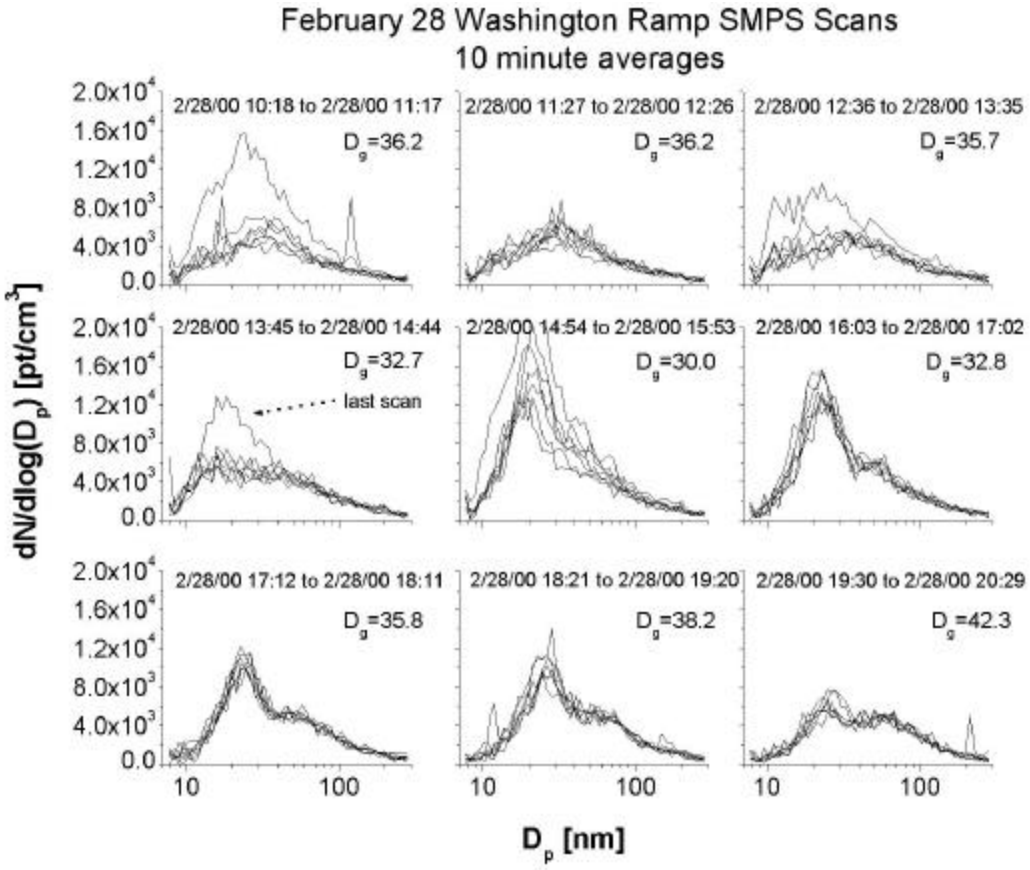

Figure 5. SMPS size distributions taken inside the parking ramp attendant's booth (Paulsen, 2001) D_g = Geometric mean diameter; D_p = Particle diameter

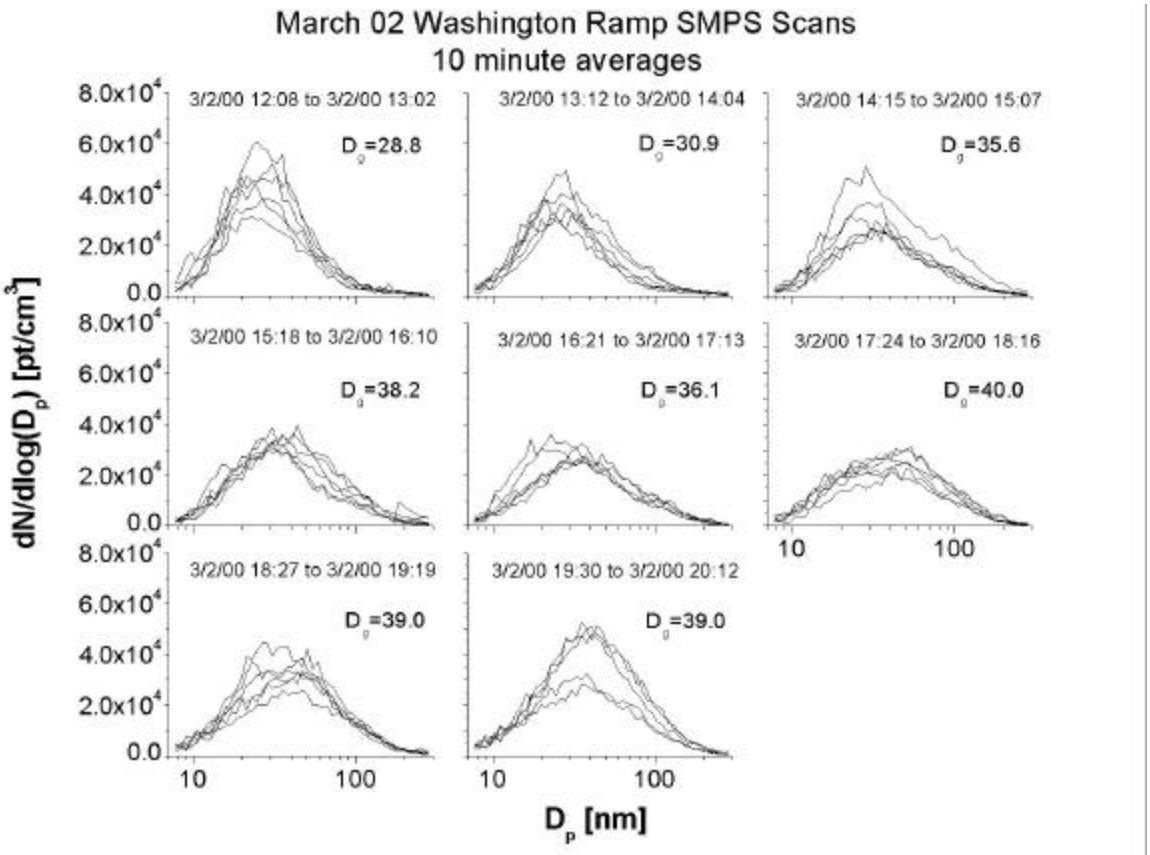

Figure 6. SMPS size distributions taken outside the parking ramp attendant's booth (Paulsen, 2001) D_g = Geometric mean diameter; D_p = Particle diameter

Our findings from the HEI study include:

- The parking ramp size distributions consisted of a nuclei mode at about 20 nm and a smaller accumulation mode at about 50 nm. These modes were sometimes merged.
- The CPC number concentrations were consistently 3 to 4 times higher than SMPS number concentration. We believe that particle losses within the SMPS and a large number of particles smaller than the SMPS lower limit of 8 nm were present.
- The CPC tracked best with the traffic pattern due to fast response time and lower size detection limit. By particle number, much of the fresh aerosol had a diameter smaller than ~10 nm.
- The diameter of average surface calculated from the SMPS measurements tracked well with traffic but was larger than that measured with the DC and CPC. This difference is mainly due to the lower size cutoff of the CPC and SMPS, 3 nm vs. 8 nm, respectively.

The Minnesota Hypothesis

We believe that the literature can be used to formulate a hypothesis to explain the magnitude of nanoparticle concentration in Diesel exhaust. The University of Minnesota has published some of this research, and Kittelson (1998) published a review of engines and nanoparticles. Other laboratories, including many European laboratories, have also contributed heavily in this area. In this hypothesis, we consider the ratio of solid accumulation mode carbon mass to the mass of volatile precursor material to be critical, as well as the many parameters that affect dilution and sampling such as dilution ratio, residence time and dilution rate. We present this information to provide a background for understanding the research findings from the E-43 project. The theory behind the Minnesota hypothesis is presented in detail in Appendix D.

In contrast to the MTU study (Johnson and Baumgard, 1996, and Bagley, *et al.,* 1996), work in our laboratory (Abdul-Khalek, *et al.*, 1998a) suggests that increased injection pressure is not the principle reason for the increased emissions of nanoparticles. A Perkins T4.40, 4 cylinder direct injection, turbocharged and aftercooled Diesel was operated under International Standards Organization (ISO) type C1 8 mode and type B Universal 11 mode cycles. The highest injection pressure (1200 bar) was produced at engine mode 1, yet mode 1 produced a relatively small number concentration. Furthermore, a systematic study of the influence of injection pressure on particle mass and number emissions in the 400 to 1000 bar range showed a continuous decrease in both mass and number emissions with increasing pressure (Jing, *et al.*, 1996).

We believe that higher nanoparticle emissions are a consequence of reducing the mass of carbon particles in the accumulation mode with respect to the mass of volatile material likely to become solid or liquid by homogeneous nucleation or condensation/adsorption, as the products of combustion expand and cool, then dilute and cool. The driving force for nucleation is the saturation ratio S, the ratio of the partial pressure of a nucleating species to its vapor pressure. As shown in Appendix D, after particles are formed, growth rates depend both upon the saturation ratio and the concentration of the material undergoing gas-to-particle conversion. For materials like the constituents of the soluble organic fraction (SOF) or sulfuric acid, the maximum saturation ratio is achieved during dilution and cooling of the exhaust (Abdul-Khalek, *et al*., 1999) and typically occurs at dilution ratios between 5 and 30:1.

The relative rates of nucleation and condensation/adsorption are an extremely nonlinear function of S. Low values of S favor adsorption/condensation, high values of S favor nucleation. The rate of adsorption/condensation is proportional to the surface area of particulate matter already present (Friedlander, 2000). Thus, the large mass and consequently surface area of carbonaceous agglomerates present in the exhaust of old technology engines will take up supersaturated vapors quickly and prevent S from rising high enough to produce nucleation. On the other hand, in a modern low emission engine there is little carbonaceous surface area available to adsorb or condense supersaturated vapors making nucleation more likely. This is especially true if the solid carbon emissions have been reduced relatively more than sulfuric acid and material that makes

up the SOF. The solid carbon should play less of a role under atmospheric dilution conditions than under typical laboratory conditions because the short time scale of atmospheric dilution allows little time for adsorption to the carbon particles.

The engine used at MTU emitted low concentrations of particles in the accumulation mode diameter range, where carbonaceous agglomerates reside, and had very high SOF ranging from 60 to 75 %. These factors would favor nucleation of the SOF as nanoparticles. The high fuel injection pressure and the fuel-air mixing strategy used in their engine probably led to more effective reduction of carbonaceous material than SOF. Thus, the high injection pressure may have indirectly led to an increase in number emissions. However, other engine modifications or aftertreatment devices that reduce carbonaceous emissions more effectively than SOF or sulfuric acid are also likely to increase particle number emissions. In fact, this was exactly what has been observed downstream of some trap oxidizer systems (Suresh, *et al.*, 2001, Kruger, *et al.*, 1997 and Mayer, *et al.*, 1995).

The same arguments just made about the role of carbonaceous agglomerates in suppressing nucleation during dilution and cooling of the exhaust also apply to nucleation of ash constituents that are volatilized at combustion temperatures, except that in the case of ash constituents, the nucleation takes place inside the engine during the expansion stroke immediately after combustion. We use the term ash to describe inorganic solid materials present in exhaust particulate matter (including for example metal sulfates and oxides). Prior to our recent work and similar work in Switzerland (Mayer, *et al*., 1998 and 1999), we had not seen evidence of significant solid ash particle nucleation except when high concentrations of metals were added with fuel additives. Tests using the Perkins engine suggest that carbonaceous agglomerate emissions may have been reduced to such a low level that the agglomerates no longer provide enough surface area to relieve ash supersaturation and prevent nucleation of ash derived from lube oil. Once ash nuclei are formed, they may serve as heterogeneous nucleation sites for SOF and other species during dilution and cooling of the exhaust. In fact, some of the particles in the high SOF nuclei mode observed in the past may have had ash cores. Tests made as part of the E-43 program and related tests supported by Caterpillar shed further light on this question. Tests made during E-43 at Cummins showed that the thermal denuder removed nearly all of the nuclei mode particles, except at idle which showed a distinct non-volatile residue mode. This was true for both the L10 and ISM engines. Recent tests done in our laboratory for Caterpillar (Jones and Kittelson, 2002) with the Caterpillar C12 engine (similar combustion system to the 3406E engines used in E-43) show similar behavior. A non-volatile nuclei mode residue is only present at very light loads and idle. In all cases these residue modes are small and constitute no more than a few percent of the nuclei mode volume.

Thus, the nanoparticles observed in the diluted exhaust of low emission Diesel engines may consist of volatile nuclei formed by homogeneous nucleation or volatile nuclei with a solid core formed by heterogeneous nucleation on existing particles. Small concentrations of non-volatile carbon or ash particles may be present under some conditions. It is clear that a number of factors affect the fine particle aerosol size

distributions, and if not properly understood and accounted for, can create an aerosol artifact that is not representative of human exposure. Representative measurements of such particles can be made only if the sampling and dilution system simulates atmospheric dilution to the extent necessary to reproduce size distributions observed under atmospheric dilution conditions. Volatile nuclei are the most sensitive to sampling biases, but even with solid particles, care must be taken to avoid coagulation and wall losses. Regardless of how particles are formed, the relationships between lab and atmospheric dilution ratio, dilution rate, saturation ratio and the other processes affecting particle formation must be understood. Recently, other groups (Ping, *et al*., 2000, and Ristimaki 2001) have reported that the particle size distributions and number concentrations were significantly affected by dilution conditions.

Another problem with laboratory data is that, typically, the exhaust is diluted with particle free air. This precludes interaction between the exhaust and the particles in the ambient environment. This interaction is strongly influenced by particle size and concentration, which determine atmospheric residence time, rates of coagulation, and available surface area for adsorption of volatile materials present in the atmosphere and surface chemical reactions.

The residence time of engine-generated particles in the atmosphere is particularly important because it impacts what size area roadways influence and what particles are available for inhalation and deposition. The typical residence time for 10 nm particles is quite short (on the order of minutes) (Harrison, 1996), because these particles have high diffusion rates and coagulate with larger accumulation mode particles. Although their individual particle identity is lost, these particles remain in the atmosphere as part of larger particles, which have lower alveolar deposition rates. Particles in the 0.1 to 10 µm diameter range have a much longer residence time, on the order of days, while larger particles are removed from the atmosphere quite quickly by gravitational settling. The Carnegie Mellon E-43 report provides much more information on atmospheric behavior of roadway aerosols (Capaldo and Pandis, 2001).

Further information on the theory behind nanoparticle formation and growth is found in Appendix D.

Chapter 1 Summary

- The presence of nanoparticles near roadways is not a new finding, as studies conducted in the late 1960s and 1970s measured high concentrations of these particles.
- Laboratory studies have shown that both SI and Diesel engines emit nanoparticles.
- Roadway studies suggest that there is a stronger correlation between local traffic patterns and ambient particle number concentration than there is with ambient mass concentration.
- More nanoparticles are found on-road when traffic is moving at high speeds.

- CPC number concentrations are frequently higher than the integrated SMPS number concentration. We believe that this is because particles in the 3 to 8 nm range are counted by the CPC, but not by SMPS. Further, particle losses within the SMPS contribute to this difference.
- Many factors influence the formation and measurement of nanoparticles, such as engine type, fuel, and sampling conditions.
- The MN hypothesis suggests that nucleation and growth of volatile nuclei mode particles is driven by particle precursors like sulfuric acid and heavy hydrocarbon fractions in the SOF.
- Further, the MN hypothesis suggests that solid carbonaceous particles present in the exhaust adsorb particle precursors and suppress nucleation and growth of volatile particles.

CHAPTER TWO – METHODS AND MATERIALS

MEL

The UMN MEL was used to collect plume samples during on-road chase tests. A 1998 Volvo tractor powered by a 350 hp Diesel engine was configured with a roll-on roll-off platform capable of carrying a 20 ft box container housing the MEL operator(s) and instrumentation. Power is supplied to the MEL by two Onan 12.5 kW Diesel generators that get their fuel from the tanks of the Volvo. Since on-road plume aerosols are inherently unsteady, and because the SMPS is not a real-time instrument, a bag sampler was designed and built for the MEL. The bag sampler allowed a discrete sample of air to be captured in 5.5 s so that a steady aerosol source was available for determination of the size distribution using the SMPS. Upon completion of the SMPS scan, the bag was purged with filtered air and reset for another sample. Filling, scanning, and purging a bag sample generally took between 3 and 4 min. Bag particle losses, to be discussed later, were determined early in the program during the wind tunnel study and found to be small (< 10%) and essentially independent of particle size. More information on particle losses is provided later in this report.

Test Engines

Cummins provided two test trucks. Test truck 47 was a 1980 Kenworth HCOE K100C repowered with a 1989 Cummins L10, 270 hp mechanically controlled engine. Truck 61 was a 1993 Kenworth 76 powered by a 1999 Cummins ISM (M-11) engine. The ISM is a 6 cylinder, 4-cycle 10.8-L engine with a peak torque of 1831 N-m at 1200 rpm. The rated maximum power is 386 hp at 1800 rpm. Cummins also provided a loaded trailer (gross vehicle weight 73,000 lbs). Cummins provided technical assistance so that a limited amount of engine data (fuel rack, turbo boost, RPM, air temperature exiting the turbocharger, and exhaust temperature) could be obtained from the 1989 engine when it was operated on road. A proprietary Cummins data acquisition system was provided with the ISM truck to record engine data from the engine's electronic control module (ECM). The engines in these trucks were used throughout all phases of the Cummins portion of the CRC E-43 project. The ISM engine was also evaluated in the Power and Propulsion Laboratory upon completion of the E-43 testing. Neither the L-10 nor the ISM engines were identical to the engines evaluated by MTU (1988 LTA10-300 and LTA10-310) as reported by Bagley, *et al*, 1996.

Truck 61 was equipped with a horizontal muffler and a vertical stack. The pipe had a 4 in diameter and the height to top of the stack was about 13 ft. Truck 47 was equipped with a vertical muffler mounted behind the cab. The exhaust pipe had a 4 in diameter and the height was about 13 ft.

Caterpillar also supplied two tractors and two 53 ft trailers. One trailer was loaded and the other was empty. The gross vehicle weight with the loaded trailer was approximately 80,000 lbs and the gross vehicle weight with the empty trailer was about 30,000 lbs. A

model year 2000, 3406E, 550 hp engine powered one of the tractors, while a model year 1993, 3406C, 425 hp engine powered the other. Both of these engines had more than sufficient power to pull the loaded trailer and outpace the MEL, hauled by a Volvo truck with 350 hp engine. Both Caterpillar trucks were equipped with electronic control modules that were used to obtain on-road engine data. The 2000 model year truck had an exhaust duct (253 x 5 in) followed by a muffler (45 x 10 in). The older truck had a similar configuration (187 x 5 in exhaust duct with a similar muffler). The 3406E and 3406C engines were evaluated on-road and in the chassis dynamometer facility at Caterpillar. A different 3406E engine was evaluated in the Caterpillar CVS laboratory. Caterpillar supplied two additional 3406E engines for evaluation in the performance cell. The objective of these tests was to determine if engines of the same series showed significant variation.

The Caterpillar test protocol differed from the Cummins test protocol in that the same two Cummins engines were evaluated throughout the E-43 project while Caterpillar provided multiple 3406E engines for testing.

The Cummins and Caterpillar tractors were evaluated with oil in an "as is" condition. The oil was broken in during normal vehicle use prior to arriving in Minneapolis.

E-43 Test Fuels

CRC arranged for two types of fuel to be used in the E-43 project, an EPA certification fuel that was provided by either Cummins or Caterpillar and a market basket blend CA fuel provided in two batches by the California Air Resources Board (CARB). Table 1 shows the results of the fuel analysis provided by CRC for all fuels used in the E-43 project. The average results from three laboratories are shown.

The original plan called for the Cummins EPA fuel and the first batch of CA fuel to be used in the Cummins tests and for the Caterpillar EPA fuel and second batch of CA fuel to be used in the Caterpillar tests. However, this did not happen. The Cummins EPA and first year CA fuels were used as planned, but the first year CA fuel was also used for all on-road Caterpillar chase tests. The second year CA fuel was used for all tests conducted

Table 1. Specifications for the fuels used in the E-43 project

Test	CA market basket blend		EPA certification	
	Year 1*	Year 2	Year 1**	Year 2
Spec Grav (60 deg F)	0.8332	0.8354	0.8455	0.8538
API Grav	38.4	37.9	35.9	34.2
Sulfur (wt %)	0.0050	0.0096	0.0326	0.0406
Flash Pt (deg C)	72	71	70	75
Cloud Pt (deg C)	-11	-10	-18	-21
Pour Pt (deg C)	-19	-16	-20	-25
Visc @ 40 C (cSt)	2.555	2.82	2.405	2.67
Cetane Index	51.7	53.0	46.9	44.1
Cetane Number	53.5	54.0	45.7	45.6
Hydrocarbons (wt %)				
aromatics	21.3	21.9	29.7	31.5
olefins	1.1	1.2	1.5	1.8
saturates	77.7	76.8	68.8	66.7
PNA (wt %)				
anthracene	*	0.092	**	0.065
pyrene	*	0.156	**	0.081
napthalene	*	5.759	**	8.767
CHN (wt%)				
carbon	86.9	86.2	86.5	86.2
hydrogen	13.3	13.8	13.2	13.3
nitrogen	0.0056	0.013	0.008	0.002
Gross Heat of Combustion (BTU/lb)	19846	19767	19561	19540
SBOCLE (pass/fail gms)	*	>4700	**	>4700
D-86 Distillation (deg F)				
Vol, %				
IBP	363	365	353	373
5	401	405	400	406
10	415	425	420	420
20	439	450	446	443
30	460	476	466	463
40	481	498	483	480
50	503	519	498	497
60	526	540	513	515
70	551	563	532	536
80	579	588	556	560
90	615	622	591	596
95	646	648	619	627
FBP	665	658	640	645
Recovery	97.5	97.5	98.1	98.2
Residue	1.8	1.3	1.2	1.0
Loss	0.7	1.2	0.7	0.8

* Blend of three major fuels marketed in CA supplied by CARB; inspections are an average of results from two laboratories; a third laboratory measured SBOCLE lubricity at >4700grams and PNA wt% at 0.56376, 0.18444, and 3.5403 for anthracene, pyrene, and napthalene respectively, but sample contamination was suspected.

** Average of results from three laboratories; SBOCLE lubricity was measured at 3600/3700 grams and PNA wt% at 0.13081, 0.15916, and 18.8148 for anthracene, pyrene and naphthalene respectively by a single laboratory.

at the Caterpillar laboratories in Peoria. As shown in Table 1, there are differences between the EPA and CA fuels, and there is also year-to-year variation between fuels. For instance, the sulfur content of the CA fuel was 50 or 96 ppm, and either 326 or 406 ppm for the EPA fuel.

Only the Cummins ISM and Caterpillar 3406E engines were evaluated with both EPA and CA fuel.

Cummins Specially Formulated Fuel and Lube Oil Tests

Cummins sponsored additional research immediately following the Cummins phase of the E-43 project. This research benefited from the fact that the test engine, apparatus and aerosol instrumentation were already in place at the Cummins CVS facility. The purpose of these tests was to evaluate the impact of specially formulated fuel and lube oil content on nanoparticle emissions.

The Cummins ISM engine was used for all tests. Cummins provided the fuels, oil, and a catalyzed Diesel particulate filter (CDPF). Break-in periods for the new fuels were typically about an hour at a heavy load condition selected by Cummins. The break-in period for the specially formulated lube oil was between 4-6 hr. A longer break-in period would have been better, but the test schedule did not permit it. Table 2 shows the matrix of fuels and oils that was evaluated in these tests. The test fuels were all the same base stock doped to the different sulfur contents. The low S lube oil was specially formulated to compensate for the removal of sulfur containing additives. Lubrizol provided this oil and no other information other than its sulfur content is available. Only the Cummins ISM engine was used during these tests.

Table 2. Fuel and oil sulfur (S) matrix used in the Cummins fuel/oil S tests

Fuel S, ppm	Oil S, ppm
1	4000
49	4000
1	385
26	385
49	385
325	385

Instrumentation

A suite of aerosol instrumentation was used in the E-43 project to size aerosol from < 10 nm - 10 µm in near real-time. The particle size instruments include the ELPI, the TSI 3934 SMPS, and a stand-alone TSI 3025A CPC. A MOUDI and a nano-MOUDI were

also used to collect size-fractionated samples for chemical analysis. In addition to these particle-sizing instruments, a PAS, a DC, and an epiphaniometer were used.

Three ambient gas analyzers were used in the E-43 project to measure diluted gas concentrations. Two were Rosemount Analytical 880A non-dispersive infrared (NDIR) analyzers used to measure carbon monoxide (CO) and carbon dioxide (CO_2) concentrations. The third gas analyzer was an EcoPhysics CLD 700 AL chemiluminescence oxides of nitrogen (NOx) analyzer. Measurement ranges for these instruments were; CO analyzer 0-1100 ppm, CO_2 analyzer 0 - 2500 ppm and NOx analyzer 0 - 10 ppm. The instruments all have a response time of about 1 s. Caterpillar and Cummins provided additional gas analyzers to measure raw exhaust gas concentrations.

A portable ECOM AC raw exhaust gas analyzer was used to measure raw exhaust gas concentrations [CO, CO_2, nitric oxide (NO) and nitrogen dioxide (NO_2)] during the on-road chase experiments. The ECOM AC uses an electrochemical cell to measure gas concentrations, and when compared to the laboratory grade gas analyzers, it has a slow response time. A stainless steel probe located in the exhaust stack of the truck collected a raw exhaust gas sample. Gas was transported to the instrument that was located in the truck cab through a Teflon line that was typically 10 - 12 ft long.

CPC

A standalone TSI 3025A CPC was used to measure total particle number concentrations. The CPC counts particles in the range of 3 - 1000 nm (0.003 µm – 1 µm), and works by condensing butyl alcohol on the particles to grow them to an optically detectable size, approximately 10-12 µm (Agarwal and Sem, 1980). TSI reports a counting efficiency of 50 % at a particle size of 3 nm, which has been confirmed by at least two studies (Kesten, *et al*., 1991 and Wiedensohler, *et al.*, 1990). Pui and Chen (2001) discuss the operation of the CPC. They state that detailed calibration studies of the CPC have shown that below a particle size of 5 nm the response of the instrument begins to drop off as a function of particle size. The counting efficiency decrease can be attributed to particle loss in the flow passages in the instruments due to diffusion and the lack of 100 % activation due to inhomogeneous vapor concentration distribution in the condenser. Counting efficiency for larger particles is much higher (approaching 100 %). Further details can be found in the TSI manual and literature cited previously.

The CPC has a sensitive flow system. The sheath air (270 cm^3/min) is supersaturated with alcohol vapor in the heated saturator. This vapor sheath is then used to confine a small amount of sample aerosol (30 cm^3/min) to the centerline of the condenser, where supersaturation is the greatest. The result is a reduction of diffusion losses to the walls, finer nuclei activation, and a sharply defined lower size detection limit. This special flow design allows detection of ultrafine particles in concentrations up to 10^5 part/cm^3. If concentrations are higher than 10^5 part/cm^3, a dilutor must be used to dilute the aerosol concentration before it reaches the CPC. The two types of dilutors used with the CPC are described below. The CPC response time is approximately 1 s and measures rapidly

changing aerosol concentrations, which make it ideal for measuring transient aerosols such as aerosols created from hydrocarbon combustion. Further information on the CPC is available elsewhere (Pui and Chen, 2001).

Parallel Flow Dilutor

During the Cummins on-road chase tests and the wind tunnel study, a parallel flow dilution system was used to dilute the aerosol concentration to a measurable range for the CPC, < 100,000 particles/cm^3. Figure 7 is a schematic diagram of the parallel flow dilutor. Three toggle valves were used to set the sampling mode for the dilutor; diluted aerosol, undiluted aerosol, or absolute filter zero. The loading of the cartridge filter was monitored by a differential pressure gauge. Another pressure gauge was used to monitor the pressure drop across the orifice. In addition, a needle valve was used to set the pressure drop across the orifice and filter.

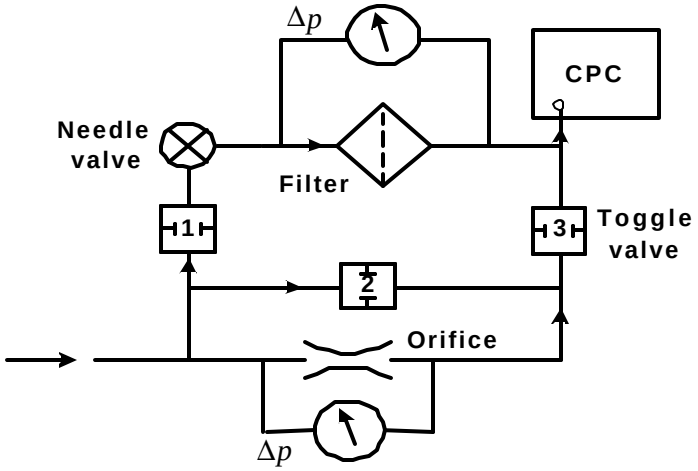

Figure 7. Schematic diagram of the parallel flow dilutor

The pressure across the orifice was maintained at 1 cm of H_2O (98 Pa). The instrument system flow for the CPC was 2.5 L/min. The actual instrument flow for the CPC is 1.5 L/min; however, a pressure equalization loop was added to minimize the pressure differential between inlet and outlet of the CPC. A flow of 1 L/min is maintained through the loop.

The dilution ratio was determined experimentally in the laboratory with ammonium sulfate (with the size distribution centered at 28-30 nm) using two flow calibrated CPCs. One CPC continually measured the aerosol concentration while the other was toggled between the diluted and undiluted conditions. The measured dilution ratio was 14.4 with a standard deviation of 0.3 for 5 data points, which is within 12 % of the calculated value.

Wind tunnel data, as seen in Figure 8, shows that the dilution ratio was not stable and was dependent upon the aerosol size distribution. As the aerosol decreased in size, the dilution ratio increased, probably due to particle losses within the dilutor. The range of dilution varied from 25-90:1. This increase in dilution ratio cannot be explained by

diffusion losses of particles in the normal sizing range of the SMPS. For particle losses to explain this difference, the particles must be much smaller, near the lower detection limit of the CPC (3 nm). As a result of this apparent size dependence, a second dilution system was designed and built for use in all subsequent E-43 tests.

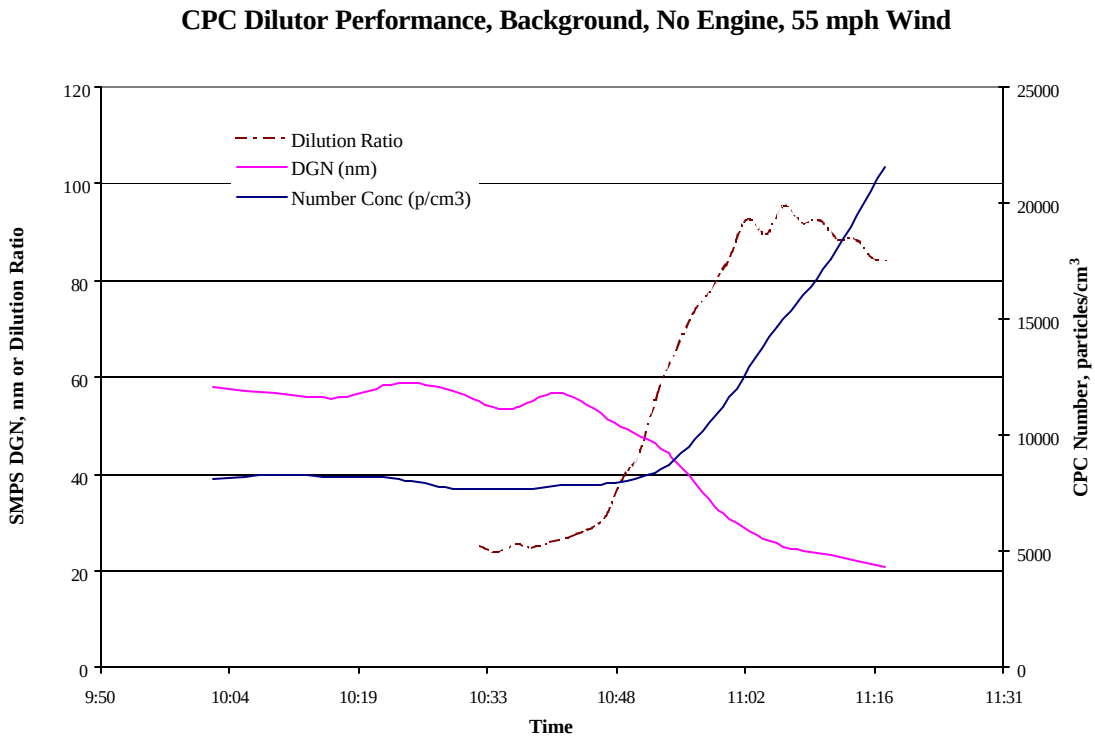

Figure 8. CPC parallel flow dilutor performance

Leaky Filter Dilutor

A glass capillary tube was placed inside a capsule absolute filter (No. 12144, Pall-Gelman Laboratory) to create a leak through the filter. The diameter of the capillary tube determines the dilution ratio. The 0.2 cm diameter capillaries were made at the UMN glass blowing shop to attain a dilution ratio, between 14 and 16:1. Figure 9 is a schematic diagram of a leaky filter dilutor.

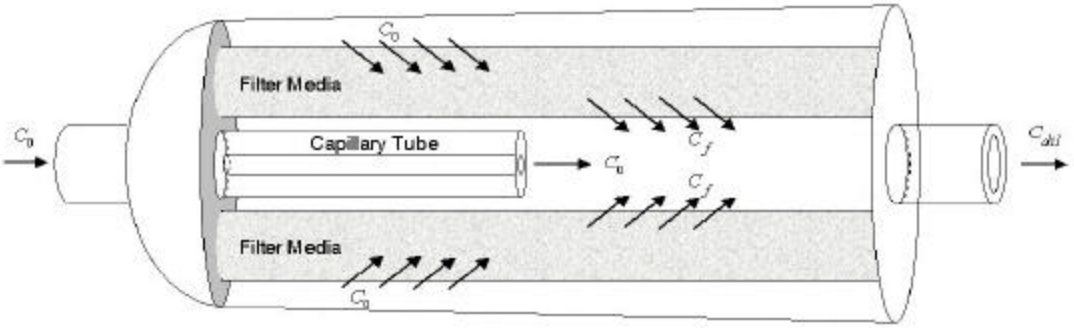

Figure 9. Schematic of the leaky filter dilutor

The dilution ratio provided by a single leaky filter was often insufficient to bring the number concentration below the 100,000 particles/cm^3 required by the CPC. This difficulty was resolved by placing two leaky filters in series; however, this introduced additional variability in the system because the dilution ratio was not constant from day to day. A variety of approaches were used to attempt to solve the leaky filter variability problem. Near the end of the program it was determined that increased flow rate combined with an orifice and mixing tube solved the problem. Unfortunately, this came too late to influence the main experimental phase of the E-43 program.

SMPS

The SMPS, consisting of a TSI 3071A Electrostatic Classifier and TSI 3025A CPC, was used to classify particles by an electrical mobility equivalent diameter. A greased 0.0508 mm impactor was used to prevent the introduction of measurement errors from particles larger than 1.0 µm. For the E-43 project, the SMPS was configured to cover the range of 7.5 to 305 nm in the low flow mode (10 L/min sheath air flow and 1 L/min aerosol flow) or the range of 7.5 to 283 nm in the high flow mode (10 L/min sheath air flow and 1.5 L/min aerosol flow). The low flow mode was used for the Cummins chase and wind tunnel work and the high flow mode was used for the rest of the project. The high flow mode reduces internal particle losses. Scan times ranging from 60 to 300 s for the up scan and 30-60 s for the down scan were used. The majority of the E-43 data were collected using 60 s up scan and 30 s down scan with the CPC in the high flow mode. Data were analyzed using version 3.2 of the TSI SMPS software.

For transient tests in which the engine exhaust did not reach a steady-state condition, the SMPS was sometimes configured to run in the single-size mode (Greenwood, *et al.*, 1996). In this mode, the SMPS continuously measures a single particle size range (channel) with a time resolution of a few seconds. The disadvantage of this approach is that the transient test must be repeated many times so that the SMPS can be reset to measure additional particle sizes to build the size distribution. As a result, this approach is time consuming and expensive.

ELPI

The ELPI (Keskinen, *et al.*, 1992) was developed to measure number distributions in real-time and to obtain mass size distributions by gravimetric analysis. The instrument sizes particles by their aerodynamic diameter in the range from 30-nm to 10-µm. The ELPI charges the particles prior to entering the impaction section, and each impaction stage is connected to an electrometer that detects the current produced by the impacting particles. This current is converted into a particle concentration for that size range. This approach allows the instrument to make essentially real-time size distribution measurements with a time resolution of about 1 s. The ELPI is very sensitive and can measure particle concentrations at ambient levels. It can also be used to measure size distributions during transient tests. However, some uncertainties regarding particle bounce and calibration have been reported. During the E-43 project, we tried both the

sintered metal and traditional greased plates provided by Dekati to try to reduce the bounce problem.

Calibration experiments have compared the ELPI with the SMPS (Dickens, *et al.*, 1997, Maricq, 1998 and Maricq, *et al.*, 2000). The ELPI measured lower concentrations and larger particle diameters in the submicron diameter range, and calibration difficulties in the upper end of the ELPI size range were also reported. The ELPI has a lower size cutpoint of 30 nm that is too large to detect the bulk of nanometer particles produced by new technology engines.

We report no ELPI data in the final report. Our experience with the instrument suggests that the presence of a large concentration of Diesel particles smaller than about 30 nm (*i.e.*, a large nuclei mode) causes substantial distortion of the size distribution. This problem will have to be resolved by revisions to the analysis software and/or instrument modification. We also found that the ELPI corona was fouled by deposits resulting from the repeated use of ammonium sulfate as the calibration aerosol. In the future, calibration should be done using an oil-based aerosol. We are continuing to analyze the ELPI data collected for the E-43 project, but do not believe that is appropriate to report results at this time in view of the uncertainties. Results will be reported when the analysis is completed.

Nano-MOUDI

During the E-43 project, both a MOUDI (Marple, *et al*., 1991) and a nano-MOUDI (Marple, *et al*., 1994) were used to determine the aerosol size distribution and to collect size fractionated samples for chemical analysis. A MOUDI has the following impactor plate cut-sizes 18, 10, 5.62, 3.20, 1.80, 1.00, 0.56, 0.32, 0.18, 0.10, and 0.056 µm followed by an after filter. The prototype nano-MOUDI used in the E-43 project was composed of a MOUDI plus additional low-pressure impactor stages. The additional low-pressure impactor stages are 0.032, 0.018, and 0.010 µm followed by an after filter. The prototype nano-MOUDI low-pressure impactor stages, on loan from the EPA, were mated with a MOUDI, on loan from National Institute for Occupational Safety and Health (NIOSH). The NIOSH MOUDI was not equipped with the 0.056 µm, but Dr. Bernard Olson from the Quality Assurance (QA) team added that stage and modified the MOUDI to accommodate the low-pressure stages. The MOUDI stages were rotated using a MOUDI turner. The nano-MOUDI stages do not rotate. Two pumps are required to operate the nano-MOUDI, the upper 10 stages have a flow rate of 30 L/min and the lower 4 stages have a flow rate of 10 L/min.

Different types of substrates and after filters were used in the E-43 project. These included 37 mm greased or ungreased, Al foil, Mylar, and Teflon substrates and 37 mm or 47 mm ultra pure quartz fiber or Teflon filters. The exact array of substrates and filters were selected based upon the type of experiment being conducted.

PAS

The PAS responds to photo emitting substances on the surface of aerosol particles. Ultraviolet irradiation of the sampled aerosol leads to the emission of photoelectrons from surface material that readily undergoes photoemission (Burtscher, 1992). The remaining positively charged aerosol particles are separated from the electrons and collected on a filter connected to an electrometer. The measured current is a function of the UV irradiation wavelength and intensity, the total available surface area and the photoemission properties of the surface materials. Commercially available instruments usually have a wavelength of 222 nm. Diesel accumulation mode particles strongly respond to the PAS (Matter *et al*., 1999). Although the PAS was originally promoted as a monitor for surface-bound polycyclic aromatic hydrocarbons (PAHs), recent investigations more generally stated that PAHs show a high photoelectric (PE) yield, causing a high PAS signal, while EC, which has a significantly lower PE yield, leads to an only moderate PAS response (see Baltensperger *et al*., 2001; Siegmann and Siegmann, 2000). However, for Diesel accumulation mode particles, the contribution from PAHs to the PAS signal may be much lower than the EC contribution. In such cases, the PAS signal for Diesel aerosol measurements is predominantly correlated with the EC surface concentration of the Diesel accumulation mode particles, despite the lower PE yield of the EC surface. In mixed urban aerosols, on the other hand, where the PAH surface concentration (for example from spark ignition engines) may be much higher, the high PE yield of the PAHs dominates the PAS response. Therefore, PAS signals can only be quantitatively interpreted in a certain context. Nevertheless, PAS signal observations are useful for monitoring of relative changes using the measured electrometer response (usually fA units). These values are corrected for lamp fluctuations, which enables good instrument-to-instrument comparability in commercially available instruments.

DC

The diffusion charger measures the total active surface area of particulate matter. Positively charged ions are produced by a glow discharge forming in the neighborhood of a very thin wire. These ions attach themselves to the sampled aerosol stream with a certain probability. The charged aerosol particles are then collected on a filter. The electric current flowing from the filter to ground potential is measured and is proportional to the number of ions attached to the particles. For particles in the free molecular range, the attachment is proportional to the surface area of the particles, but is independent of the composition of the particles (Adachi *et al*., 1985). Siegmann *et al*., 1999 contend that the DC measures the so-called "active surface" in the size range from slightly above ten to a few hundred nm. The active surface is the effective surface area available for mass transfer in a kinetically limited situation and should be appropriate for describing the gas to particle mass transfer taking place in a diluting exhaust plume.

Epiphaniometer

Gäggeler *et al.*, (1989a,b) and Pandis *et al.*, (1991) have described the epiphaniometer in detail. Aerosols are pumped through a chamber containing the radioactive lead isotope ^{211}Pb. These lead atoms are produced at a constant rate by the decay of a short-lived radon isotope (^{219}Rn) emanating from a long-lived actinium source (^{227}Ac). ^{211}Pb atoms attached to aerosol particles are transported through a capillary acting as a diffusion barrier for non-attached lead atoms. At the end of the capillary, the aerosol particles, and with them the attached lead atoms, are deposited on a filter. A surface barrier detector measures the resulting activity on the filter continuously. Due to the relatively short half-life of ^{211}Pb (36 min), the device allows continuous monitoring of aerosols without changing or transporting the filter. At small aerodynamic diameters (d < 100 nm) the epiphaniometer signal is roughly proportional to the surface area of the aerosol particles, whereas at large aerodynamic diameters (d > 3 µm) the signal is proportional to d. In the intermediate regime, the obtained signal is proportional to d^x, with x varying between 1 and 2, depending on particle diameter. Therefore, for a polydisperse aerosol the obtained signal is proportional to the integral of the differential products $dN \cdot dS_F$, with N = particle concentration and S_F = "Fuchs surface" = $\pi \cdot d^x$. In the size range of Diesel aerosol, the exponent varies little with the diameter (Pandis *et al.*, 1991), so that calibration is possible. The instrument has an upper cut-off at d = 7 µm.

The epiphaniometer accumulates alpha counts for time intervals Δt, typically 5-30 min. The total number of counts in this interval Y_i depends on the amount of lead deposited during the count interval and also on previously deposited lead. The average rate of deposition of lead over the count interval $i + 1$ is therefore approximately (Rogak *et al.*, 1991):

$$f_{i+1} = \frac{Y_{i+1} - Y_i \exp(-\Delta t \lambda)}{1 - \exp(-\Delta t \lambda)} \qquad (1)$$

where $\lambda \cong \ln 2 / 36.1$ min^{-1} is the decay constant resulting in alpha particles. While the simplified inversion code according to equation (1) is sufficient if processes with time scales of about 30 min are investigated, a rigorous inversion giving a time resolution of a few minutes has been developed (Pandis *et al.*, 1991).

Procedures

A polydisperse, ammonium sulfate aerosol was used for daily, morning calibration and consistency checks. Aerosol was introduced into the sampling manifold so that the response of all of the aerosol instruments could be checked simultaneously. In retrospect, ammonium sulfate was probably not the best aerosol for ELPI calibration because of bounce related and corona fouling problems. Two configurations of a similar polydisperse aerosol generation system were used during the E-43 project. These systems were capable of generating large volumes of dry calibration aerosol. Aerosol was nebulized using a Collison nebulizer (model CN-24, BGI Inc., Waltham, MA). In addition to ammonium sulfate, monodisperse polystyrene latex (PSL) aerosol was used to check the size consistency of the SMPS and ELPI. Typically, PSL ranging in size from

30 to 100 nm was used. The QA team, using PSL and the TSI Electrospray, conducted particle loss experiments that are described in detail in the QA reports.

The Rosemount and EcoPhysics gas analyzers were calibrated each day prior to the beginning of tests using National Institute of Standards (NIST) traceable gases. Zero, low and high span calibrations were done for CO and CO_2. The EcoPhysics NOx analyzer has an electronic zero and only one span gas was used due to the high cost and difficulty of generating low NOx concentrations. The use of a gas divider or permeation tubes on a daily basis in the field was not practical.

Further details of the calibration procedures are found in the final QA report (Ayala, *et al.*, 2002).

Test Conditions

On-road Versus Laboratory

One of the underlying assumptions of the E-43 project was that real world engine conditions encountered on-road could be simulated in the laboratory. Planned test conditions included idle, 40 and 55 mph cruise with and without a loaded trailer, 40 to 55 accelerations with and without a loaded trailer, and decelerations. For the Cummins on-road tests, the no load condition referred to bobtail tests conducted with no trailer. For the Caterpillar tests we used an empty trailer provided by Caterpillar. The empty trailer assisted in directing the plume to the rear for sampling by the MEL. Bobtail accelerations were generally unsuccessful because the test trucks accelerated more quickly than the MEL, resulting in the rapid loss of the exhaust plume. Deceleration tests were also difficult because of the inability to differentiate the plume from background aerosol concentrations. The common on-road test conditions for both the Cummins and Caterpillar tests are listed below.

On-road engine test conditions:

- Idle
- 55 mph cruise control light load (60 mph for Caterpillar)
- 55 mph cruise control heavy load (60 mph for Caterpillar)
- 40-55,60 mph acceleration without load
- 40-55, 60 mph acceleration with load

The test truck driver in the Caterpillar test series also tried maintaining vehicle speed using a steady accelerator pedal position. Tests were conducted on both hills and flat areas, and some cruise tests were conducted at 40 mph. As expected, maintaining "steady engine conditions" on-road was very difficult. On the other hand, engine test laboratories are specifically designed to conduct either steady-state or transient conditions that are repeatable with minimal variation. Thus, one of the problems encountered in the E-43 project was difficulty in duplicating real world, on-road engine conditions in the laboratory.

Daily weather conditions also played a significant role in our on-road chase experiments. Tables 3 and 4 show weather data collected for the on-road chase tests conducted in 1999 and 2000, and it is clear that the ambient temperature and humidity fluctuated from day to day and season to season.

Table 3. Cummins chase test weather information from Anoka County

Date	Statistic	Temperature, °C	Dewpoint, °C	Pressure, kPA	
09/22/99	Mean	21.5	8.0	101.2	
	SD	2.9	1.0	0.2	
09/27/99	Mean	13.0	6.6	101.8	
	SD	2.1	0.9	0.1	
09/29/99	Mean	13.2	1.0	102.2	*
	SD	1.8	1.4	0.3	
10/01/99	Mean	5.5	0.2	101.7	
	SD	1.1	1.3	0.1	
10/04/99	Mean	10.7	1.0	102.0	
	SD	2.2	0.8	0.3	
10/06/99	Mean	8.0	1.2	101.9	*
	SD	5.7	1.8	0.3	
10/07/99	Mean	18.5	7.4	100.6	
	SD	5.9	2.0	0.2	
11/12/99	Mean	7.4	4.3	101.8	*
	SD	4.6	2.5	0.1	
11/17/99	Mean	3.6	-3.5		**
	SD				
11/18/99	Mean	6.2	-1.2		**
	SD				

* Data set not complete

** Very Minimal Data SD = standard deviation

Table 4. Caterpillar chase test weather information Minneapolis St. Paul airport

Date		Dry Bulb Temp (oC)	Dew Point Temp (oC)	Wet Bulb Temp (oC)	Relative Humidity (%)	Station Pressure (kPa)
7/17/2000	AVG	21.7	9.6	14.9	46.5	98.7
	StDev	1.0	1.8	0.9	7.0	0.0
7/19/2000	AVG	18.3	11.5	14.5	64.7	98.7
	StDev	0.9	0.7	0.7	2.4	0.1
7/20/2000	AVG	21.1	9.4	14.5	47.6	98.5
	StDev	1.2	0.9	0.7	5.4	0.0
7/26/2000	AVG	23.8	17.1	19.5	66.2	98.2
	StDev	0.9	0.7	0.5	5.9	0.0
7/27/2000	AVG	26.7	17.4	20.7	57.1	98.4
	StDev	1.3	0.4	0.6	4.7	0.0
7/28/2000	AVG	23.0	17.0	19.1	69.3	98.5
	StDev	1.2	0.5	0.6	4.2	0.0
7/31/2000	AVG	29.3	18.0	21.9	50.9	98.3
	StDev	1.1	1.2	0.8	5.9	0.1
8/1/2000	AVG	27.5	18.1	21.3	56.8	97.9
	StDev	1.3	1.8	1.1	6.0	0.0
8/2/2000	AVG	25.4	11.9	17.4	43.7	98.4
	StDev	1.3	2.1	0.8	9.1	0.0
8/3/2000	AVG	23.1	13.5	17.4	56.3	98.7
	StDev	1.4	2.2	0.7	12.4	0.0
8/7/2000	AVG	28.3	16.8	20.9	50.2	97.8
	StDev	1.6	1.8	1.1	7.4	1.2
8/8/2000	AVG	25.5	20.5	22.1	74.1	97.8
	StDev	1.0	1.0	0.8	4.8	0.5

Another source of unknown variability between on-road and laboratory tests is the history of the engine conditions prior to collection of an on-road sample. A brief description of how we collected on-road samples will clarify why this variability occurred.

For each on-road test, a bag sample was collected to determine the plume size distribution. The MEL operator, vehicle spotter and test truck observer would coordinate sample collection. For steady-state conditions, the sample would be triggered when the MEL operator observed a high CPC concentration or NOx concentration indicating that the MEL was capturing the plume. The time limit for these samples was established by on-road conditions and traffic. During loaded accelerations the MEL operator typically had a 20 - 30 s window to trigger a sample before the test truck was out of range. This window was between 10 and 20 s for unloaded accelerations. Collecting a sample did not guarantee that the plume was captured; a criterion was used to judge whether the sample had collected mainly background aerosol or plume aerosol. A good sample had more than 3 times the SMPS integrated number concentration of a non-plume background sample. During data analysis, we refined the criterion for a good sample, because our previous criterion gave too much weight to nanoparticles and insufficient weight to the accumulation mode. Therefore, for data analysis, a sample was included if the total

integrated SMPS number concentration of plume particles > 30 nm was > 2 times that of the > 30 nm background particle number concentration. The accumulation mode size range is associated with aged background aerosols so we wanted to be sure that our samples were enough above background to be meaningful. Particles in this size range are typically solid and not strongly influenced by dilution conditions. Each bag took about 3-4 min to process and during this time the trucks would slow to 40 mph or whatever speed highway traffic would allow. Thus, the engine history between samples was variable for the on-road tests, and it is impossible to quantitatively determine how this variability affected our results.

Finally, background aerosol samples were obtained either while the lab was in front of the chase truck, during periods of crosswind or at a rest stop. On average, 10 background bag samples were collected each day. It should be noted that on-road background air samples are not the same as background samples taken in the laboratory where filtered dilution air is used. Again the impact of this parameter on our results is unknown. We correct for background by subtraction. While care was taken to avoid sampling in the presence of significant traffic, we cannot be sure that the background during plume sampling was the same as the average background. Other influences of the background are impossible to determine, although concentrations were generally low enough that suppression of nanoparticle nucleation and growth by adsorption of particle precursors by background particles during dilution is unlikely.

Transient Versus Steady-state

Transient and steady-state tests were conducted during the E-43 project. Most of the laboratory testing was done under steady-state conditions that were a mixture of ISO conditions and conditions selected to mimic on-road test conditions. Some transient testing was conducted, primarily at Cummins, and consisted of ramp, simulated "real" cruise conditions with varying speed and load (wiggle) and FTP tests.

Dilution Systems

Multiple dilution systems were used in the E-43 project. These included multiple variations of the University of Minnesota two-stage dilution system, a Sierra BG-1 system with secondary dilution (BG-1/ejector) and a system similar to the one used by MTU during the HEI (CVS/ejector) investigation. An overview of each of these systems is provided. It is important to recognize that the UMN two-stage dilution systems were setup in five different laboratories for use with different engines. Every effort was made to minimize the differences in tunnel configuration. For instance, we tried to maintain a constant length of exhaust probe and exhaust transfer line from one laboratory to the next.

University of Minnesota 2-stage Dilution System

Three versions of the UMN 2-stage dilution system were used during the E-43 project. These systems were either similar to or the same as the tunnel described by Abdul-

Khalek, *et al*, 1999. Exhaust enters through a 3 in long, 0.25 in diameter stainless sampling probe immersed in the exhaust flow, and passes through a section of stainless steel tubing referred to as the transfer line (TL). To prevent particle losses the TL is insulated and maintained at approximately (300°C) exhaust temperature. Recent information (Wei, *et al.*, 2001a,b) has shown that the TL length and the sample flow rate are critical if nanoparticles are going to be measured successfully. A long TL and a low flow rate result in a substantial loss of nanoparticle precursors. We believe that volatile compounds are lost by mass transfer to the walls that might be enhanced by localized cold spots on the heated walls. A low sample flow rate enhances adsorption of this material to carbonaceous accumulation mode particles by increasing the residence time in the TL. Shortening the TL and increasing the flow rate reduces the opportunity for loss of precursor material and favor nanoparticle formation. Unfortunately, the laboratory facilities at Caterpillar and Cummins did not lend themselves to setting up the 2-stage tunnel with a very short TL, as the TL was approximately 36 in long at the Cummins CVS facility and 27 in long in the Caterpillar test facilities.

At Cummins, a TD 260-air ejector pump (a TD 110 was used at Caterpillar) with a critical flow orifice provided the first stage of dilution. The system was designed to give a primary dilution ratio ranging from 10 to 15:1. The sample aerosol then passed through a residence time chamber (labeled as UMN-3 in Figure 10) and a second TD 260 air ejector pump with a 0.48 mm critical orifice that provided second stage dilution. Secondary dilution increases the total dilution ratio and suppresses further nucleation and aerosol growth. The dilution ratio (DR) was determined as follows: DR = (raw NOx – background NOx)/(diluted NOx – background NOx).

The configuration of the 2-stage tunnel was similar for all tests. Different first stage ejector pressures and orifices were tried. The critical flow orifices ranged from 0.7 to 1.5 mm in diameter. The primary ejector pressure ranged from 15 to 40 psi, and the secondary ejector pressure varied from 30 to 36 psi. The typical sample flow rate was approximately 3 lpm. Increasing the ejector pressure and increasing the ejector size increases the dilution ratio, while increasing the critical orifice size, decreasing the size of the ejector and reducing the ejector pressure decreases the dilution ratio. Figure 10 illustrates the 2-stage tunnel as it was used at the Caterpillar CVS facility.

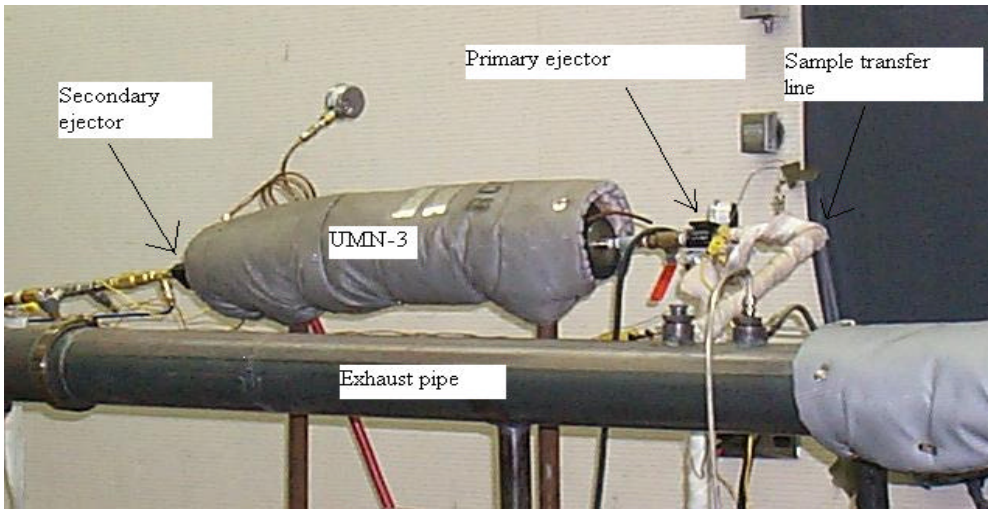

Figure 10. UMN two-stage tunnel in the Caterpillar CVS test facility

Table 5 shows the mean, standard deviation and range for the mixing temperature and dilution ratio for the various dilution tunnels used at Cummins. The residence time in the 2-stage tunnel used in the CVS laboratory varied from 0.85 to 1.48 s. The residence time of the 2-stage tunnel used at the chassis dynamometer facility varied from 0.21 to 0.36 s.

Table 5. Mixing temperatures and dilution ratios for dilution systems used at Cummins

Type	Primary Dilution Tunnel Mixing Temperature (C)			Total Dilution Ratio		
	Mean	SD	Range	Mean	SD	Range
UMN CD	22	6	6-36	1200	600	500-3100
UMN-2 CVS	29	5	17-44	1600	500	700-3700
CVS-1				1000	700	400-3900
CVS-2				1300	900	500-4500
CVS-1, Full Flow				300	40	300-400
CVS-2, Full Flow				900	400	300-1400

UMN CD = 2-stage tunnel used at the chassis dynamometer facility
UMN-2 CVS = 2-stage tunnel used at the CVS test cell
CVS-1 = first configuration of the CVS/ejector dilution system
CVS-2 = second configuration of the CVS/ejector dilution system
SD = standard deviation

At Caterpillar, the overall dilution ratios were lower than at Cummins. They were measured and found to be 460 $\pm$ 100 at the CVS tunnel and 760 $\pm$ 100 at the performance cell.

CVS/Ejector Dilution System

The dilution system used by MTU for the HEI study (Bagley, *et al*, 1996) consisted of a partial flow dilution system followed by a secondary dilution system consisting of an air ejector. At Cummins and Caterpillar, taking a sample from the CVS tunnel and using an

air ejector for secondary dilution, as illustrated in Figure 11, simulated this system. The sample probe had a total length of 18 in of which 4 in was in the CVS tunnel. The standard CVS tunnel used in heavy-duty engine test facilities is described elsewhere (Code of Federal Regulations, 2001). Dilution air used in the CVS tunnels was ambient filtered air with no humidity or temperature control. Figure 11 illustrates the system used at Caterpillar.

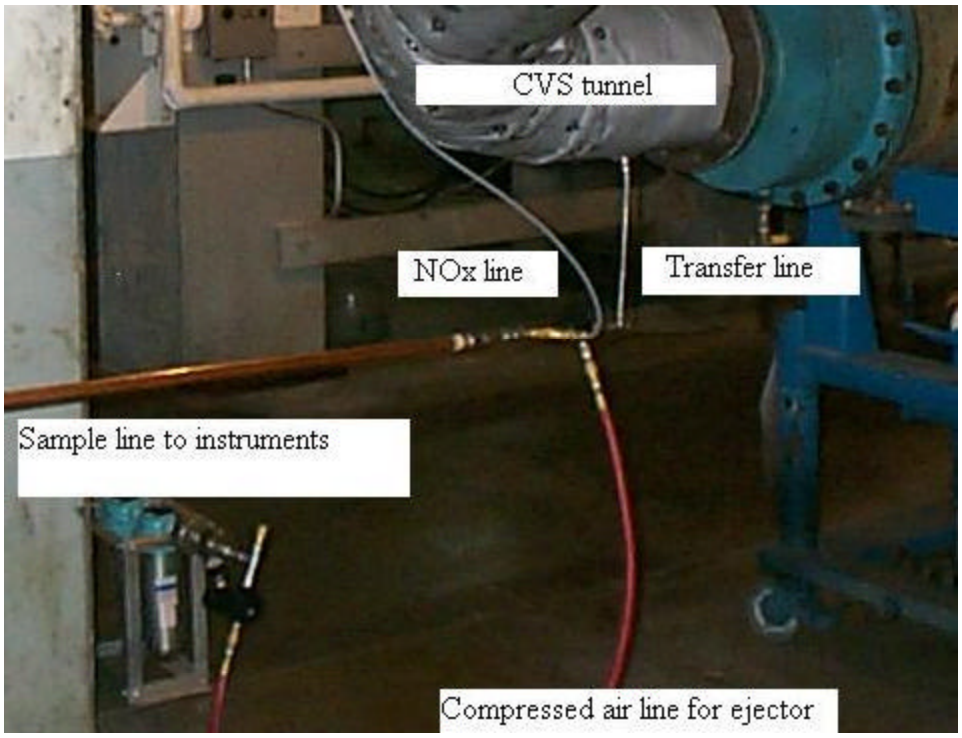

Figure 11. CVS tunnel and air ejector dilution system at Caterpillar

Sierra BG-1 Dilution System with Secondary Dilution (BG-1/ejector)

Caterpillar provided a BG-1 dilution system as an alternative to the 2-stage system. It was used during the chassis dynamometer and performance cell tests. The BG-1 is a fractional sampler that is insensitive to engine size and is fully described in the manufacturer's manual (Sierra, 1998). It is used to collect filter samples for gravimetric analysis. It acted as the first stage of a 2-stage dilution system. Caterpillar modified the BG-1 by adding a short aging section and a port, to accept our sampling probe prior, to the BG-1 filter. As engine exhaust was drawn from the exhaust system, it was diluted and cooled through mixing with a measured amount of dry, filtered, hydrocarbon-free air, and passed through an extension chamber prior to the filters. Dilution occurs in a chamber that consists of a porous stainless steel tube mounted concentrically within a stainless steel cylinder. During sampling, dilution air (25° ± 5°C maximum) is introduced under pressure into the chamber through the walls of the porous tube. The air permeates the porous tube creating a virtual "wall" of filtered, hydrocarbon-free air. As a result, particle and particle precursor losses are held to a minimum.

We modified the BG-1 to accommodate our sampling requirements. A 5.5 x 1 in pipe was inserted into the sampling system prior to the filter. An 18 in probe was inserted about 0.5 in into the residence time chamber to draw a sample from the BG-1 after primary dilution. This sample was passed through a TD 260 air ejector for secondary dilution. A major advantage of the BG-1/ejector system over the 2-stage system is that it uses a short double walled transfer line and the sample flow is more than double that used in the 2-stage system. These features lead to reduced heat and mass transfer and residence time, thus reducing particle losses.

All components of the BG-1, including pumps, desiccant, flow-monitoring system, calibration functions, dilution air conditioning and cooling are enclosed in a compact cabinet. The BG-1 computer allows control of all test procedures through simple data prompts and graphic displays. The computer controls sampling functions and the system's two mass flow controllers, allowing adjustment of flow rates and dilution ratios. Relevant test data were recorded during the test.

Database and Analysis Statistics

Data acquired during this research were collected and formed into a Microsoft® Access database to standardize and speed data reduction and analysis. The database consists of data tables that are related to one another by a number of codes.

Tables in the database contain data from the continuously recording instruments (gas analyzers, PAS, DC), reduced SMPS size distributions (in their uncorrected form), data related to engine operating conditions and performance (engine sensors, exhaust gases, etc.), data taken by the various laboratories used in the project (related to dynamometer conditions and dilution tunnel performance) and data related to mass particulate measurements (MOUDI, nano-MOUDI, and filter data). Code tables contain descriptions of these data.

Code tables are of four types. The most important of these is the condition index table that provides a schedule of testing for the entire project, covering all data in the database. An entry in the condition index table refers to a single repetition of a test condition. The test condition is described by the engine test condition, the aerosol source, the phase/location of the testing, the engine under test, the fuel and oil used for the test, and any aftertreatment device that may have been in place. Continuous data included in the analysis are data that have not been excluded based on mistakes or failures of some kind, are part of a verifiable test condition and occur one minute after and 30 s before any condition transition. In the case of on-road data, where no constant condition exists, and for calibration, where stabilization is required, all data for the researcher-defined condition period are used.

The second type of code describes the individual conditions of the engines. This code usually describes the load/speed combination of the condition or the type of on-road test, such as 55 mph cruise. The third type of code describes the source of the aerosol. This can be a nebulized calibration aerosol, such as ammonium sulfate or PSL, filtered air,

ambient aerosol, aerosol from a plume, or aerosol from the variety of dilution tunnel configurations used in the E-43 project. This code also delineates whether a sample was taken from a bag sample or directly from the boom.

The fourth and final code describes the state of individual continuous instruments. This code describes whether or not the instrument was functioning correctly, what type of dilution was used such as the leaky filters used with the CPC, and whether the instrument was connected to receive sample, background, or calibration aerosol.

Code tables provide the framework for analyzing the E-43 data. Condition indices are convenient for examining individual repetitions of a condition and dilution ratios are normally calculated for each condition index during laboratory tests.

In addition to standard codes, SMPS data are correlated with continuous data through the use of a sample ID. Within the continuous data, the window to which the SMPS sample corresponds is marked. Data in these windows are used for determining dilution ratios during chase testing and for correlating SMPS samples with specific sections of continuous data.

When analyzing data, a standard set of statistics is used. For gross values, averages, standard deviations (SD), and where appropriate, standard deviations of the mean (SDOM) are calculated. When a certain calculation requires multiple measured values, the error in the final calculation is estimated by error propagation assuming negligible covariance. If V is the value to be calculated and is a function of x_1, x_2, . . ., then

$$s_V^2 \approx s_{x_1}^2 \left(\frac{dV}{dx_1} \right) + s_{x_2}^2 \left(\frac{dV}{dx_2} \right) + \ldots$$

Where $V = f(x_1, x_2, \ldots)$, σ_v is the error in V, and σ_n is the error in x_n.

In cases where multiple repetitions of a condition generated averages and estimates of error for a given statistic, the average of these statistics was found by the method of weighted averaging. In particular, the averages were weighted by the inverse of the squared variance (the square of the standard deviation or standard deviation of the mean.) Thus, the contribution of a measurement to the grand average was inversely proportional to the square of its error. This allows more accurately known values to contribute more greatly to the calculation of the mean.

Calculation of Dilution Ratio

Atmospheric and laboratory dilution ratios were calculated in similar ways. In both cases, dilution ratio was calculated as follows:

$$DR = \left(\frac{C_{ExhNO} - C_{BgNO}}{C_{DilNO} - C_{BgNO}} \right)$$

Where DR is dilution ratio, C_{ExhNO} is exhaust NO concentration, C_{BgNO} is background NO concentration and C_{DilNO} is dilute NO concentration.

Dilution ratios for SMPS size distributions in the atmosphere were determined for the windows corresponding to a bag sample or a continuous direct sample. These windows were adjusted for instrument time delays. In the laboratory, dilution ratios were determined for a given condition repetition. These dilution ratios were applied to both continuous data and to SMPS size distributions.

Dilute NO was measured, in all cases, with the laboratory NO analyzer. In chase experiments, exhaust NO was measured with the portable ECOM AC exhaust analyzer. In laboratory tests, NO was measured with either the same portable exhaust analyzer or with exhaust NOx analyzers provided by the test laboratories. Where exhaust NO was not available, exhaust NOx was measured and NO_2 contribution was assumed to be minimal.

Background NO was also measured by the laboratory NO analyzer. In atmospheric testing, NO background was calculated as the daily average of NO measured during background test conditions. In the laboratory, background NO was measured by switching the NO analyzer sample source to measure NO in compressed air used for dilution. It was also measured as the dilute NO measured from a given tunnel with no engine exhaust present.

In laboratory tests where a particular condition repetition included some measures of background NO, an average of these values was used, otherwise a daily average background was used. During some test days, both at Cummins and at Caterpillar, background NO values were quite high and variable. The same NO analyzer was used for both diluted NO and background NO so the measurements could not be made simultaneously. This contributed to apparent variations in dilution ratio, especially at light loads where NO levels were low. In certain cases where continuous data did not exist (in the case of a data logger failure), the SMPS dilution ratio was determined as the dilution ratio average for that engine condition and dilution tunnel configuration.

Average SMPS Distributions

Average SMPS size distributions were calculated as averages of difference distributions. These difference distributions represent the difference between size distributions measured for a given test condition (and dilution method) and daily background/zero correction size distributions (for the given dilution method). These difference distributions were calculated for both atmospheric and laboratory conditions. Background distributions for atmospheric testing were determined from samples taken during measurement of ambient/roadway background aerosols. Background distributions for laboratory testing were determined from samples taken from the various dilution tunnels with no engine exhaust present. Aerosol calibration samples are not corrected for

tunnel or ambient backgrounds because the aerosol source was either an absolute filter or a nebulizer that uses filtered air.

Leaky Filter Dilution Ratios

The dilution ratio for the leaky filter was calculated based on a number of measurements for a given phase of testing. The concentration of an ammonium sulfate aerosol was measured by the CPC without a leaky filter dilutor and compared to the concentration of the same aerosol measured by the CPC with the leaky filter dilutor in place. Where multiple tests of this dilution ratio existed for a given test phase (as in most cases), an average of all measures was taken. In the case of the Caterpillar performance cell tests, due to the mixing problems and the change in bypass configuration, the leaky filter dilution ratio was determined on a daily basis. The dilution ratios determined for these days were checked for consistency with the ratio of CPC to (undiluted) SMPS integrated number. Absolute consistency between these values was not possible, given the differing lower size detection limits of these instruments.

On 9/5/2000 (at the Caterpillar performance cell), no direct measure of leaky filter dilution ratio was made. Based on comparison of CPC and SMPS integrated number, the dilution ratio for this day was found to be consistent with that of 9/7/2000, so this value was used on 9/5/2000 as well.

Particle Losses

After the start of the E-43 project, a team was appointed to oversee the quality assurance aspects of the project. The QA team commenced work after completion of the Cummins on-road chase tests and the wind tunnel study. One issue addressed by the QA team was particle losses and the need to conduct *in situ* experimental loss studies. Given the complexity of the E-43 sampling program, this was seen as an enormous task both by the QA and research teams. It was agreed that loss experiments would be conducted to the extent possible with time and cost being the major constraints. Neither the QA or research teams consider the loss studies comprehensive in scope; in fact, both teams agree that further loss studies are required. However, the experiments that were conducted give an indication of the losses that should be expected in a project of this type. *Data in this report are not corrected for particle losses except in several indicated example cases, which is consistent with current literature practices.*

Bag Sampler

The bag sampler used in the MEL is shown schematically in Figure 12. Electro-pneumatically controlled valves operated from the computer console in the MEL allowed the bag to be purged, filled with filtered air, purged and filled again with sample air. It was not possible to completely purge the entire contents of the bag. Thus, "clean air bag fills" were evaluated with the SMPS to determine how successfully the bag was purged. These data are summarized in Table 6 and Figure 13. On average, between 3,000 and 4,000 particles/cm^3 remained in the bag following a clean air bag fill and the size

distributions did not show a clear trend. Remaining particles are included as part of the background correction.

Table 6. Summary statistics for clean air bag fills

Phase	Number of samples	Particles/cm^3		
		Mean	SD	SDOM
Cummins Chase	8	3190	2149	760
Cat Chase	43	3023	2068	315
Wind Tunnel	3	4042	847	489

SD = standard deviation, SDOM = standard deviation of the mean

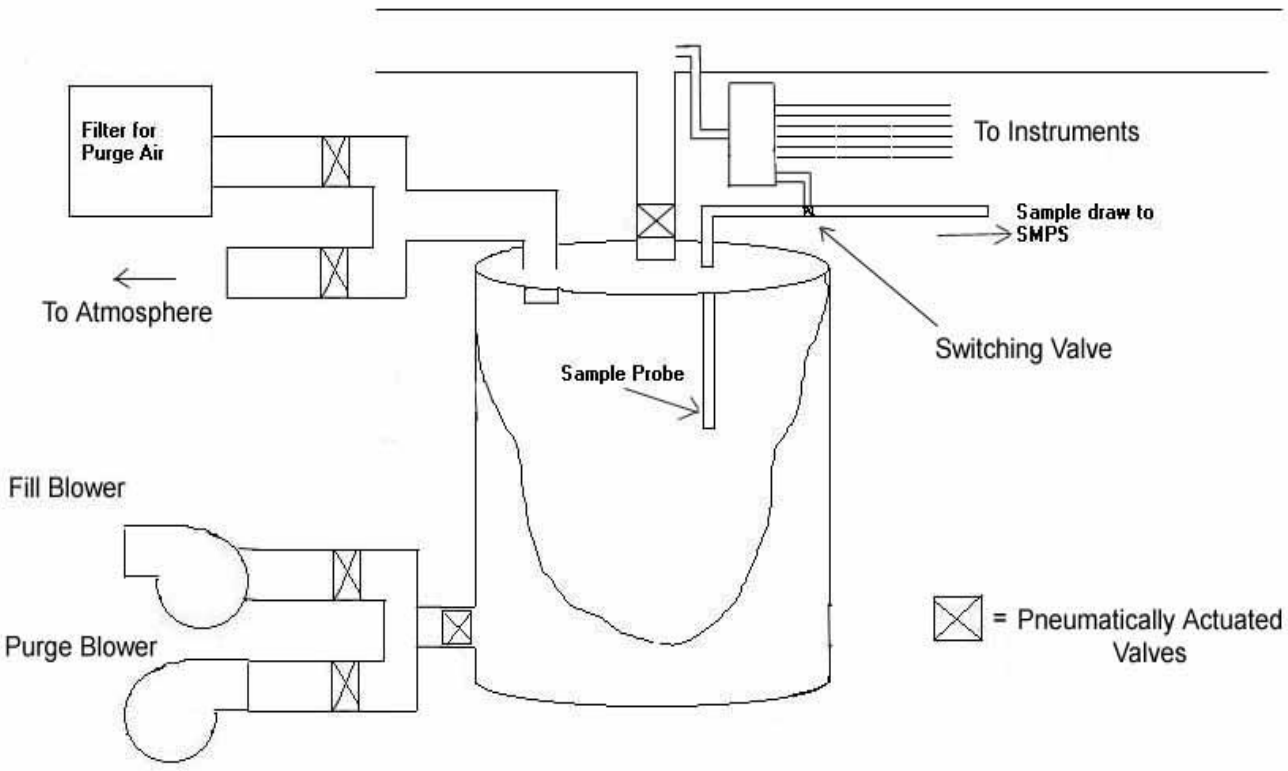

Figure 12. Schematic of the MEL bag sampler

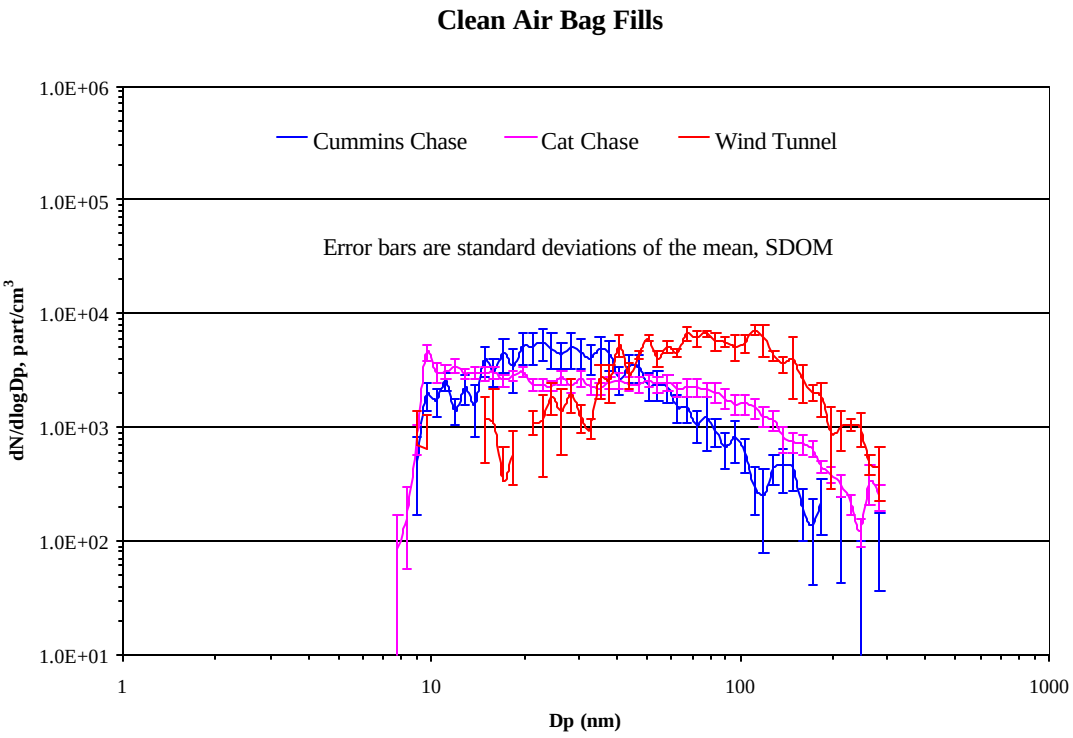

Figure 13. Clean air bag fill size distributions

To evaluate particle losses within the bag, it was necessary to have a constant aerosol source. The Langley wind tunnel, with its recirculating airflow, provided an optimal aerosol. A series of bag loss experiments was conducted during periods when the aerosol source in the tunnel was either background aerosol or ISM truck exhaust generated from operation at the 55 mph cruise condition. In these experiments, alternating SMPS samples were collected between the bag and the boom. Thus, a bag sample was collected and the size distribution was determined with the SMPS. This was followed by a continuous sample drawn directly from the boom. This series of scans was repeated for approximately one hour for each of the two conditions (background and 55 mph cruise) resulting in the average size distributions shown in Figure 14. Note how closely the shape of the wind tunnel background size distribution resembles the clean air bag fill size distribution shown in Figure 13 with a mode between 90 to 100 nm. This seems reasonable, because the clean air bag fill first purges the sample from the bag and then dilutes the remaining aerosol with filtered air.

To determine the sampling efficiency of the bag, the concentration of particles in each size channel of the SMPS is calculated. The ratio of the bag to boom concentration is plotted against particle size. The ratios are determined from nearest neighboring samples, assuming that the aerosol size distribution has not changed; a reasonable assumption given the data shown in Figure 14 that has relatively small error bands. Figures 15 and

16 show the efficiency plots for background and 55 mph cruise samples, respectively, and Tables 7 and 8 summarize the results.

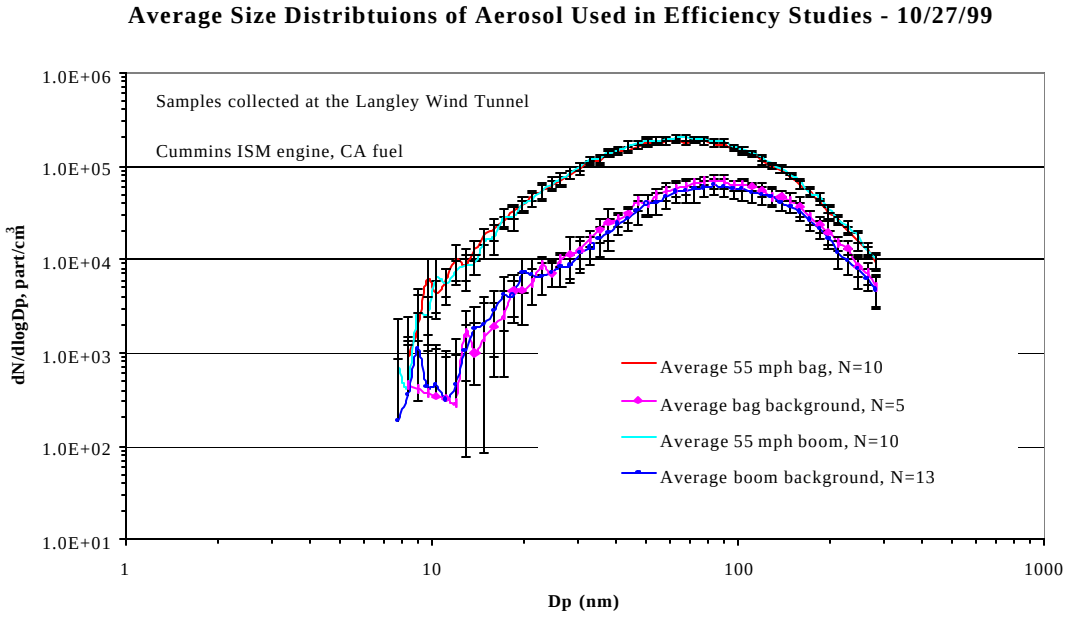

Figure 14. Average size distributions for bag sampler efficiency measurements

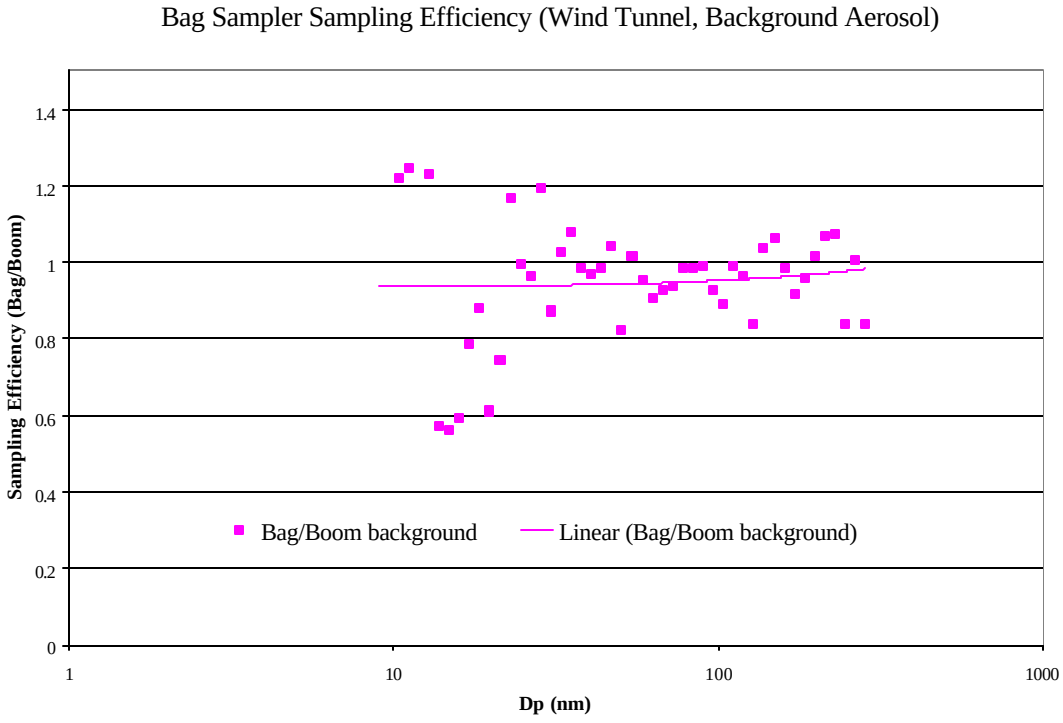

Figure 15. Bag sampler sampling efficiency, wind tunnel background aerosol

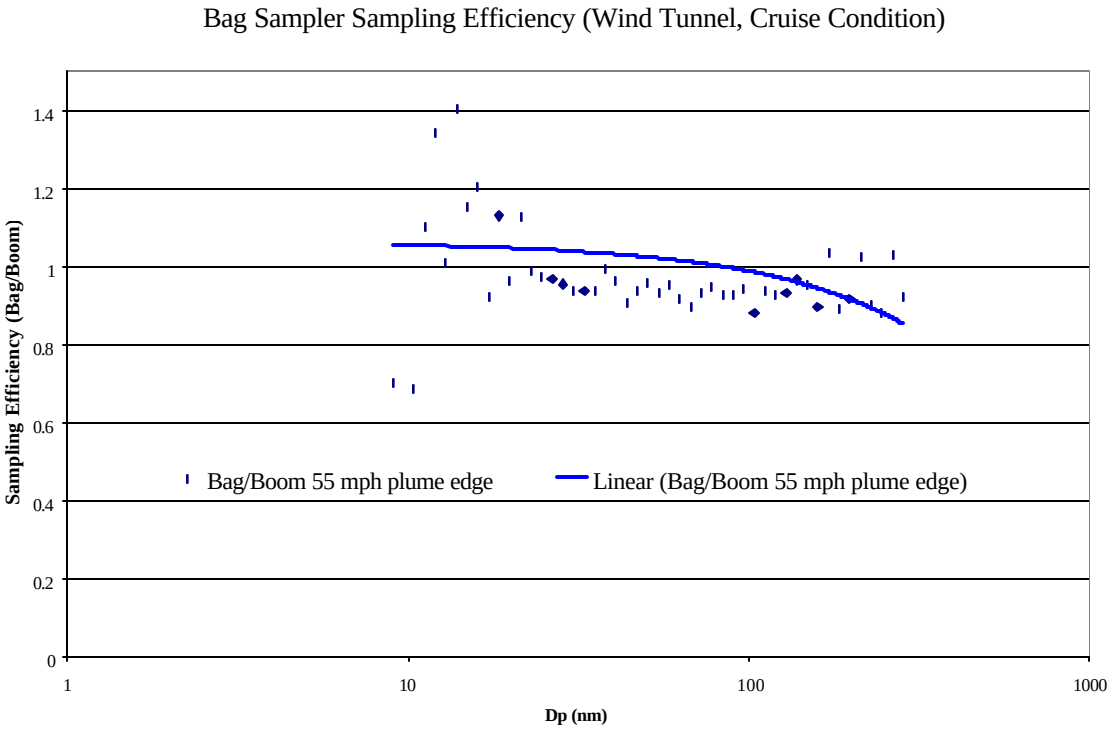

Figure 16. Bag sampler sampling efficiency, wind tunnel cruise condition aerosol

Table 7. Summary bag vs. boom sampling efficiency

Condition	Mean efficiency	SD efficiency
Cruise, > 8 nm	1.00	0.25
Cruise, > 10 nm	0.98	0.12
Background, > 10 nm	0.95	0.16

Table 8. Summary bag vs. boom DGN

	Bag DGN		Boom DGN	
Condition	mean, nm	SD, nm	mean, nm	SD, nm
55 mph, cruise	61.6	0.5	62.6	1.3
Background	80.2	0.6	79.5	1.7

The largest scatter in Figures 15 and 16 is in the range of 10 to 20 nm, with no clear trend towards the bag/boom ratio being above or below 1.0. The scatter is also observed in Figure 14, and probably is related to the relatively low concentration of particles in this size range in the wind tunnel. Table 7 shows that for the cruise condition, the bag sampler has 98 % sampling efficiency for particles > 10 nm and 95 % efficiency for

background samples. There is no statistically significant difference in the DGN measured by the SMPS samples from the bag or boom as shown in Table 8.

QA Team Particle Loss Experiments

The QA team, with assistance from the research team, conducted experiments to evaluate particle losses associated with the MEL instruments. What follows is a summary of the findings as reported in Ayala, *et al*., 2002.

Early in the study, the SMPS was evaluated for internal particle losses. Aerosol was simultaneously introduced to both the CPC and the SMPS through a Y-junction. The TSI Electrospray was used to generate a monodisperse 10 nm diameter sucrose aerosol. The atomizer was used to generate 30 nm ammonium sulfate and 50 nm PSL aerosols. The number concentration obtained from the SMPS and CPC was compared. Table 9 shows the results of these tests.

Table 9 shows particle losses of 73 % for 10 nm sucrose particles and no measurable losses for 30 and 50 nm size particles. The QA team stated that the losses at 10 nm were typical for the SMPS. Results reported by Reineking and Porstendorfer, 1986 indicate that losses at this size should be less than 48 %. Thus, since these losses are higher than expected, they should be viewed with caution. The QA team report states that the relatively long residence times associated with the laminar flow required by the SMPS, and the high diffusion losses associated with 10 nm particles contribute to the low penetration efficiency.

Table 9. SMPS loss evaluation

Comparison between SMPS Reported Total Concentation and Stand-alone CPC

Dp, nm	Material	GSD	Generation Method	CPC, #/cc	SMPS, #/cc	Penetration, %	
10	Sucrose	1.15	Electrospray	6.10E+04	1.63E+04	26.7	
30	Am. Sulfate	1.6	Atomizer	5.81E+04	6.02E+04	103.6	*
50	PSL	Bi-modal	Atomizer	2.70E+04	2.70E+04	100.0	*

*Well within 10% flow tolerance of each CPC used.

Source: QA team final report

The QA team also evaluated sampling manifold and line losses for the instrumentation in the MEL. This appears to be the most comprehensive set of loss data available for the E-43 project. The evaluation was done *in situ* and illustrates how line losses affect the measurements. It should be noted that the changes made to the MEL after this loss study was completed were minor in nature and should not affect the experimental losses to a significant extent.

Monodisperse sucrose aerosol was generated by the Electrospray and introduced into the sampling manifold. Two CPCs were used to measure the aerosol concentration. Three experiments were conducted with the CPCs located before and after the manifold, at the beginning and end of the sample line, and before the manifold and the end of the sampling line. Figure 17 illustrates the test setup used for these measurements.

Table 10 shows the bypass and instrument flows and the length of tubing used to transport the sample to the instrument and within the instrument. Losses were calculated for the manifold and for the individual lines going to the instruments and are summarized in Figure 18.

The QA team reported, "as expected, diffusion losses to the transport line wall (1 - penetration) were found to be significant for nuclei mode particles and decreased with increasing particle size." The SMPS sampling line losses were greater than those for any other instrument, because of the greater sampling line length needed to accommodate the thermal denuder and switching valves. Since the thermal denuder was not always used, these represent worst-case losses. Valves were required to switch the sample source from the bag or boom and to route the sample either through or around the TD.

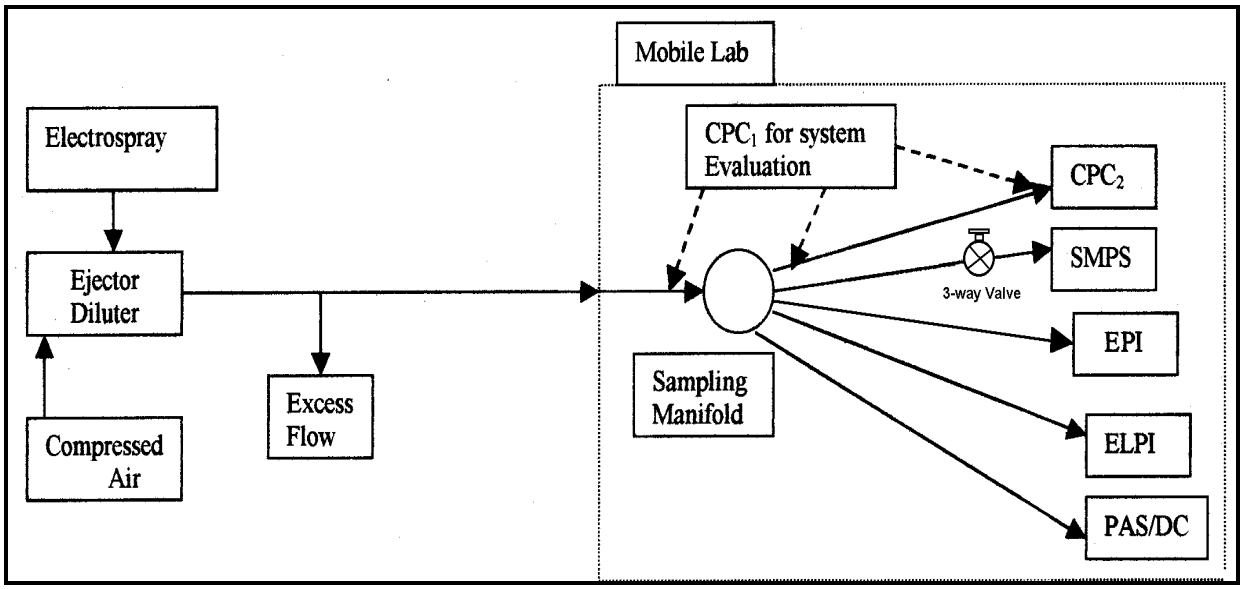

Figure 17. Schematic of MEL line loss evaluation
Source: QA team final report

Table 10. Aerosol flows and line lengths in the MEL

	Flow, L/min		Tubing length, cm	
Instrument	Bypass	Instrument	Transport	Instrument
ELPI	0.0	9.3	167.6	167.6
CPC + Diluter	8.5	1.5[a]	284.5	66[b]
PAS/DC	7.2	3.5	297	15.2
SMPS	7.7	1.5	838.2[c]	43.2
EPI	8.3	1.5	241.3	43.2

[a] The CPC also had an additional 1.0 L/min pressure balance flow
[b] The CPC had a line length of 50.8 cm and a diluter length of 15.2 cm
[c] The 838.2 cm represents the maximum tubing length as it includes the thermal denuder
Source: QA team final report

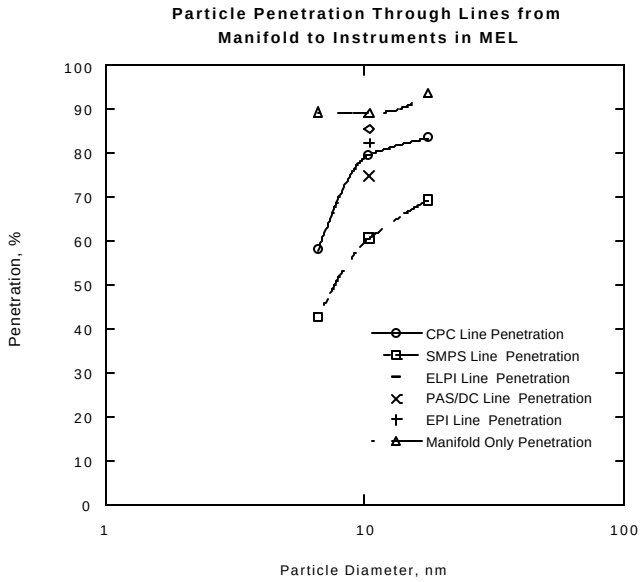

Figure 18. Particle penetration through the manifold and transport lines
Source: QA final report

The QA team compared the experimentally determined loss results to those determined by theory, based on particle deposition by diffusion for laminar and turbulent flow for each instrument in the MEL. It was expected that the experimental data would closely follow that predicted by laminar flow theory since the Reynolds number was approximately 1,350. However, the experimental results more closely resembled that predicted by turbulent flow theory, probably because turbulence was created in the transport lines by connectors or other obstacles. Other problems may be associated with

the use of the Electrospray aerosol generator. The Electrospray produces a smaller satellite peak and a primary peak (Chen, *et al*., 1995). The ratio of the primary/satellite droplet size is approximately 8; thus, the Electrospray is producing very small particles that would experience extremely high diffusion losses. On the other hand, these particles are likely to have little effect on the loss measurement because they fall below the size detection limit of the CPC. In addition, the Electrospray produces very highly charged particles. The instrument has a built in neutralizer, but if it does not work properly, particle losses will be increased. It should be noted that a very limited set of data was generated for these experiments. The results shown in Table 11 summarize the estimated penetrations for a given particle size and include the losses predicted in the MEL sampling boom.

Table 11. Total particle penetration to the MEL instruments
Source: QA team final report

Instrument	Dp, nm	Line Penetration, %	Line+Manifold Penetration, %
SMPS	6.6 *	41	35
CPC	6.6 *	58	47
SMPS	10.4	62	53
CPC	10.4	82	67
PAS/DC	10.4	75	65
EPI	10.4	82	72
ELPI	10.4	86	78
SMPS	17.2	71	66
CPC	17.2	83	77

* Estimated size

Further discussion of the impact of particle losses is found later in the report in the section titled Influence of Particle Losses on Size Distribution Measurement.

Transient Response, System Delays

To determine DRs during chase experiments, it was necessary to measure NO in the exhaust plume, the stack and the background. Because of the highly transient nature of on-road chase experiments, information on the dynamic response of the NO instruments is needed to shift these results onto a common time base. In addition, dynamic response information for all of the real time instruments is needed to make meaningful comparisons.

Dynamic response experiments were performed during the Langley wind tunnel study by switching between continuous samples taken from the wind tunnel and absolute filtered

air inside the mobile laboratory itself. This allowed the combined response characteristic of an instrument and its sampling line to be determined. A low restriction ball valve was used to switch between the sample and the zero condition. Experiments were done over roughly a 30 min period in which the system was switched between ambient samples and filtered lab samples at two-minute intervals. This switching procedure allowed a change in concentration from a relatively high ambient level to essentially zero for the particle instruments and a change between the level at the sampling point in the wind tunnel and inside the lab ambient for the gas instruments. In all cases, a distinct and sharp step in concentration was observed upon switching.

Data were modeled assuming first order instrument response plus a line lag from the sample manifold to the instrument. No consideration of laminar dispersion in the sample line was included in the model. Model parameters were obtained by minimizing the squared difference between the observed and predicted values. The resulting analysis gave a line lag and a first order time constant, τ, for each instrument. The final instrument lag time was taken as the experimentally determined line lag time plus the instrument first order half time, $t_{1/2} = -\tau*\ln(2)$. Figure 19 shows typical CPC and NO data and fitted results obtained in these transient experiments. The system was switched from the filtered MEL sample to the wind tunnel sample at 60 s and back to the filtered sample at 180s. This approach led to the following instrument lags.

Instrument	Lag time (s)
CPC	9
NO	8
CO_2	6
CO	6
DC	3

All of the instruments except the PAS fit this model rather well. In its fastest response mode, the PAS updates every 8 s with a sliding average of data collected over the previous 16 s. Consequently, second by second transient data from the PAS should not be compared with the other instruments.

Some attempts were made to correct for the first order time response characteristics of the instruments by adding a differential correction term to the data. However, since this involved differentiating rapidly changing signals, it added a great deal of noise to our results, and we felt that the use of this procedure was consequently not justified.

During chase experiments, it was necessary to synchronize stack NO measurements with plume measurements made with the MEL to determine dilution ratios. The ECOM used for stack NO measurements had a relatively long response time. To compensate for ECOM lag time, ECOM NO data were time shifted to match changes in engine speed and load recorded on the engine computer. This computer was synchronized with the computer in the MEL. We assumed that the transit time from the stack to the MEL sample manifold was 2 s. Thus, at any given time the NO value measured in the MEL corresponded to the stack NO value t lag + t transit, or 10 s earlier. NO values measured

in the 6 s window of bag sampling were averaged and used with corresponding values of stack NO to determine bag dilution ratios.

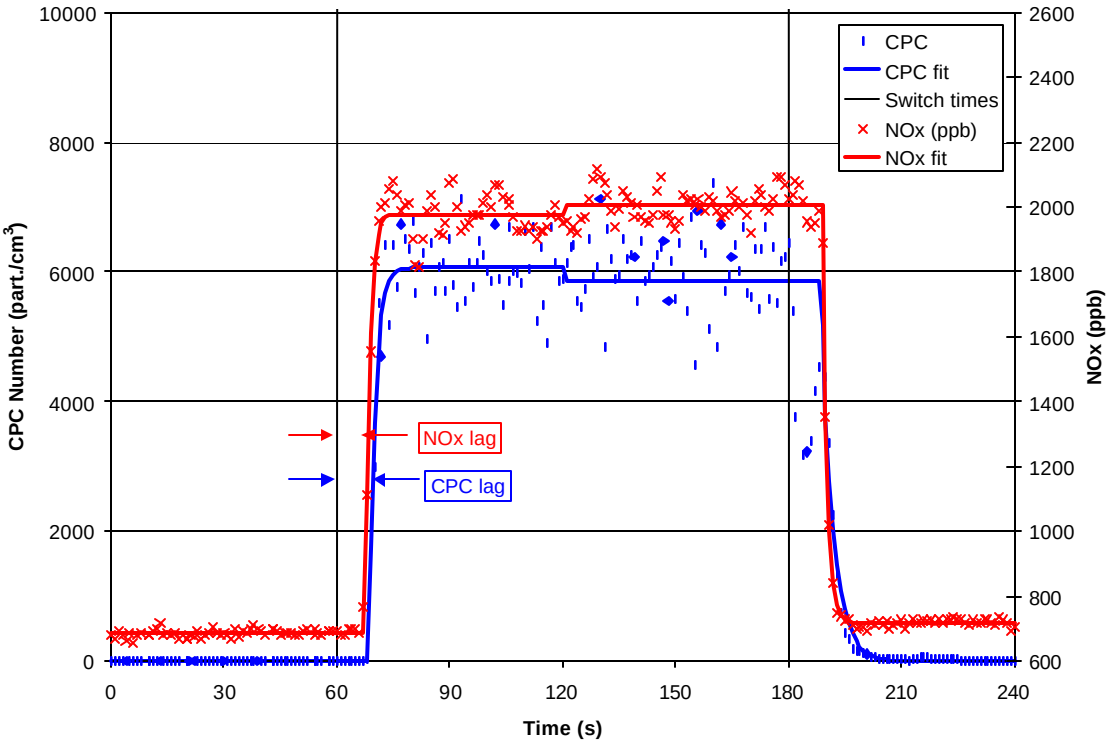

Figure 19. Typical raw and fitted results from instrument transient response tests [Data obtained on 25 October 1999 during Langley wind tunnel experiments.]

Chapter 2 Summary

The objective of this chapter was to describe the methods and materials of the E-43 project. This includes the engines, fuels and operating conditions tested, as well as the instrumentation employed and the calibration procedures used. Of particular interest was the evaluation of dilutors, particle losses, and transient response of the instrument suite.

Engines, Fuels, and Test Facilities

- On-road chase tests, chassis dynamometer tests and engine dynamometer tests were conducted as part of this research on Cummins and Caterpillar engines.
- ISM and L10 Cummins engines were tested on-road and in the laboratory. Caterpillar 3406E and 3406C engines were tested on-road and at the chassis dynamometer facility. Two additional 3406E engines were tested in the Caterpillar engine dynamometer facilities. Due to the differences between the Cummins and Caterpillar engines tested, no inter-comparisons were made.
- Tests of Cummins engines were conducted either with a loaded trailer or with no trailer. Tests of Caterpillar engines were conducted with a loaded trailer or an empty trailer. The use of an empty trailer assisted in directing the exhaust plume so that it could be more easily sampled.

- In all locations and phases of this work, an EPA certification fuel was used for testing. For tests of the ISM and 3406E engines, a market basket blend CA fuel was also used.
- In addition to E-43 work, Cummins sponsored a project to evaluate the effect of specially formulated fuel and lube oil on nanoparticle emissions.

Instrumentation

- The MEL contains a suite of instruments to measure particle number and size (CPC, SMPS, ELPI), particle surface area and surface characteristics (DC, PAS, epiphaniometer) and ambient level gas concentrations (NO, CO, CO_2). Separate data acquisition systems record MEL data and engine performance data from the test trucks. A separate portable ECOM-AC exhaust gas analyzer is used to measure raw exhaust gases from the test trucks.
- The high sensitivity CPC detects particles down to 3 nm in diameter, while the SMPS classifies particles to 7 nm; thus, the CPC is beneficial for measuring particles below the size range of the SMPS.
- The upper limit of the high sensitivity CPC is 100,000 particles/cm^3. This limit was frequently exceeded in the E-43 project so two types of passive dilution systems were used with the CPC. These systems were a parallel flow dilutor and a leaky filter dilutor. Selection of a dilutor for the CPC requires special attention be paid to minimizing particle losses, especially nanoparticle losses, and aerosol mixing.
- The ELPI was problematic throughout this work. Difficulties related to software, the corona charger, and substrate configuration were encountered. Some uncertainties regarding particle bounce and calibration have been reported by others.
- The PAS was a robust instrument that performed well throughout, but the PAS lacks specificity. Further calibration of the PAS is required to determine exactly what portion of Diesel aerosol is being measured.
- The performance of the DC was intermittent. The corona charger was prone to fouling after constant use and a leak was encountered when sampling at reduced pressures.
- Both MOUDIs were modified from their original configuration. The nano-MOUDI was the first produced, making it, essentially, a research instrument. Complete particle size calibrations were not performed for either the MOUDI or the nano-MOUDI as configured for the E-43 project.
- The Epiphaniometer worked well when used in the E-43 project, but the slow response time of the instrument makes it less useful for inherently unsteady on-road plume or transient test cell measurements.

Test Conditions and Procedures

- Successful on-road test conditions consisted of cruise, acceleration and idle.

- Engine and chassis dynamometer conditions were a blend of standard ISO test conditions and those designed to simulate on-road conditions. These conditions were largely steady-state conditions, though some transient tests were conducted.
- The effects of 2-stage ejector, CVS/ejector, and BG1/ejector dilutors on particle formation were examined. To accommodate the test facilities at Cummins and Caterpillar, the 2-stage ejector dilutor was configured with a transfer line that was too long. Loss of volatile precursor material can be a problem in a long transfer line. This can result in an underestimation of nanoparticle concentrations. The CVS/ejector dilutor was designed to simulate the dilution scheme used by MTU for their HEI study (Bagley, *et al*, 1996.) The BG1/ejector dilution system was used as an alternative to the 2-stage system.
- For all conditions, dilution ratios were calculated as the ratio of exhaust NO to dilute NO, corrected for the presence of NO in the background. The dilution ratio estimate is one of the single greatest sources of error in this study. Substantial variations in background NO contributed greatly to this error in all cases, as did the difficulty in synchronizing engine/exhaust gas data with MEL instrument data for on-road tests. This variation, while of note for laboratory testing, was substantially greater for on-road testing.
- A bag sampler was used for on-road testing to capture plume samples for analysis with SMPS. Based on tests conducted during the wind tunnel study, there were minimal losses in the bag and no significant change in the aerosol size distribution of the bag-sampled aerosol was observed.
- The QA team, assisted by the research team, conducted particle loss studies of the sampling system. Both teams feel that further study is required to better quantify particle loss estimates.

CHAPTER 3 - RESULTS AND DISCUSSION

Atmospheric Size Distributions

On-road Plume and Background Samples

During the on-road chase experiments, two types of bag samples were collected: background samples and plume samples. There was a great deal of sample-to-sample variation in plume samples so a criterion was developed to accept or reject a sample for the purpose of data analysis. Most of the variation was related to the dilution ratio, which was affected by the position of the MEL boom in the plume, the distance of the MEL from the test truck when the plume was sampled and wind conditions. Despite this, it is useful to show the dynamic range of on-road samples regardless of dilution ratio and regardless of acceptance criteria. This demonstrates the consistent shape of the size distribution regardless of the dilution ratio and shows how the nuclei mode fluctuates over two orders of magnitude while the accumulation mode remains relatively constant. Figure 20 illustrates the point. The size distributions shown are for the Caterpillar 3406E engine operated on EPA fuel at the 60 mph cruise condition. A total of 20 bag plume samples were collected on three different days. Figure 20 shows every SMPS size distribution for this condition. The spread in the accumulation mode indicates the wide range of dilution conditions.

The reason these data were chosen was because this particular condition had the most bag samples (20) collected over multiple sampling days (3). Further, the Caterpillar on-road plume data are of higher quality than the Cummins on-road plume data. The on-road Cummins data were the first data collected using the MEL and, as will be shown, had far more variability than the Caterpillar plume data. This variability is not a function of the Cummins engines, but rather a function of the research team's initial inexperience in conducting on-road chase measurements.

While there is considerable uncertainty in the Cummins results, the Caterpillar results are much more consistent and clearly show nanoparticles. Even changing the bag sample acceptance criteria to prevent biasing toward plumes with large nuclei modes did not prevent the demonstration of a significant nuclei mode in on-road plume samples.

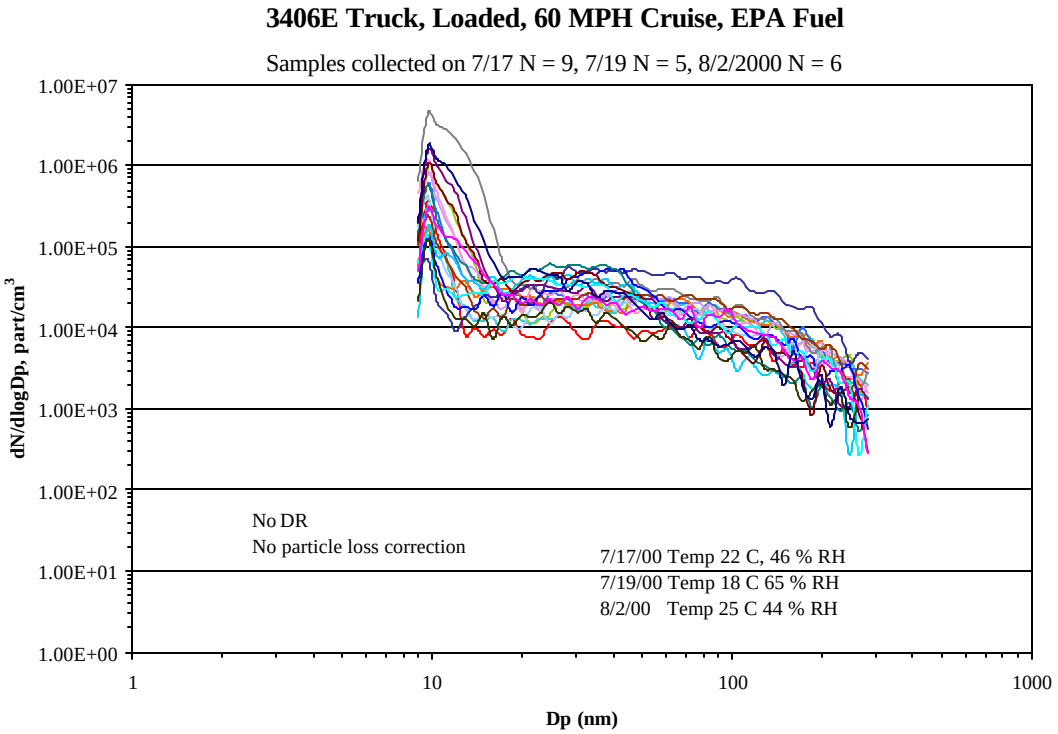

Figure 20. Dynamic range of on-road SMPS size distributions

A total of 212 background samples were collected for the on-road chase tests, 83 for Cummins engine tests and 129 for Caterpillar engine tests. All 212 samples were included in the analysis of the on-road data. The majority of the samples were bag samples, but boom samples were also collected. Most of the Cummins background samples were collected north of the Twin Cities metropolitan area from 9/99 to 11/99, while most of the Caterpillar samples were collected south of the Twin Cities from 7/00 to 8/00. Cummins background samples were collected during cooler weather with winds predominately from the north, while the Caterpillar samples were collected during warmer weather with winds from the south.

Figure 21 shows the average daily bag background samples, number of samples and average ambient temperature for days in which plume samples were collected from Cummins vehicles. The average of all background bag samples for all days is also shown.

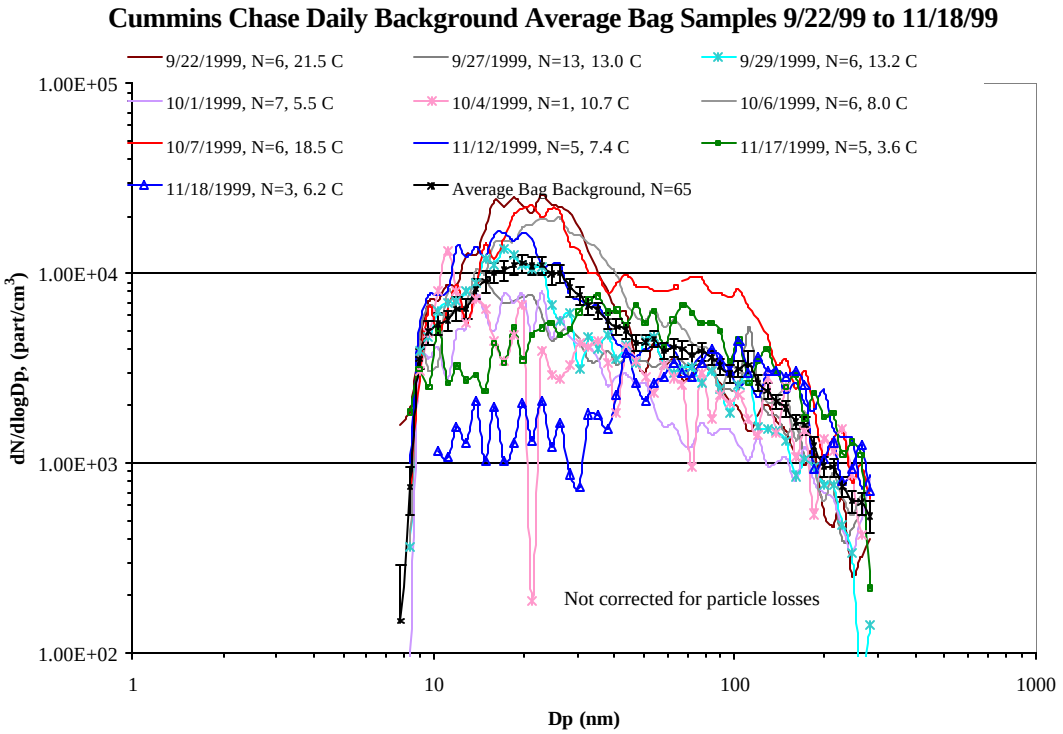

Figure 21. On-road background bag samples collected for Cummins tests

Figure 22 shows the average daily bag background samples, number of samples and average ambient temperature for days in which plume samples were collected from the Caterpillar vehicles. The average of all background bag samples for all days is also shown. The shapes of the grand average background size distributions shown in Figures 21 and 22 are different. The accumulation mode is broader with a higher concentration during the warm summer days of the Caterpillar chase tests and the nuclei mode is smaller.

The grand average SMPS integrated number concentration for all on-road Cummins background samples was lower (7,300 particles/cm^3, SDOM of 60 particles/cm^3) than measured for the Caterpillar tests (11,400 particles/cm^3, SDOM of 90 particles/cm^3). A T-test of the mean concentrations revealed that the means are significantly different. [The typical highway aerosol measured in the Twin Cities metropolitan area has a concentration of 150,000 particles/cm^3 (Kittelson, Watts, Johnson, 2001).] The Cummins on-road tests were conducted north of the Twin Cities with winds mostly from the north while the Caterpillar on-road tests were conducted south of the Twin Cities with winds mostly from the south. Differences observed in the background aerosol size distributions and concentrations are most likely related to the different locations used for the Cummins and Caterpillar on-road tests. The Cummins on-road tests were conducted north of the Twin Cities with a prevailing north or northwest wind while the Caterpillar tests were conducted south of the Twin Cities with a south or southeasterly prevailing wind.

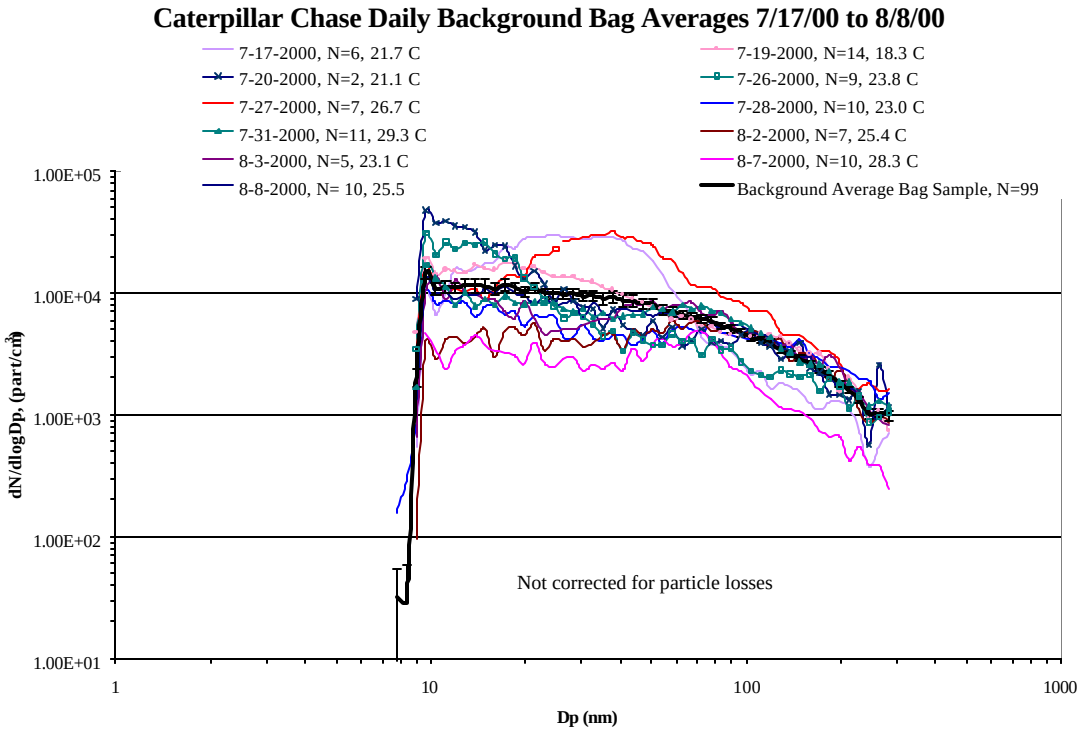

Figure 22. On-road background samples collected for Caterpillar tests

Figure 23 summarizes the grand average, E-43, background and plume samples for the entire Caterpillar and Cummins on-road data set regardless of engine, fuel, test condition or dilution ratio. Also shown is the average Minneapolis freeway size distribution determined from the MnDOT study regardless of traffic or highway speed conditions (Kittelson, Watts, Johnson, 2001). For comparison, the average wind tunnel background size distributions determined by DRI before engine startup, during engine testing and after engine shutdown at the end of the day. No acceptance or rejection criteria were applied to the E-43 distributions shown in the chart, except that the samples were considered valid on-road bag samples when all instrumentation was functioning properly. The SDOM is shown on Figure 23 for each average size distributions.

Figure 23 shows that there is a clear difference between the grand average on-road plume distribution and the grand average on-road background distribution. The sharp drop at 9 nm, for the plume distribution, suggests that there are nanoparticles below the range of the SMPS that are not being counted. The on-road background and DRI wind tunnel background distributions are also different. The DRI wind tunnel background, taken before the engine was started, shows a nuclei mode. After the engine was started the wind tunnel background accumulation mode concentration increases by a factor of 10 and the nuclei mode disappears. The wind tunnel background accumulation mode, after the engine is started, is more than a factor of three larger than the average on-road plume distribution. It is likely that the high concentration of accumulation mode particles suppressed nuclei mode particle formation, in the wind tunnel, by physical processes.

Further, note the similarity between the average Minneapolis freeway distribution and the E-43 plume distribution.

`

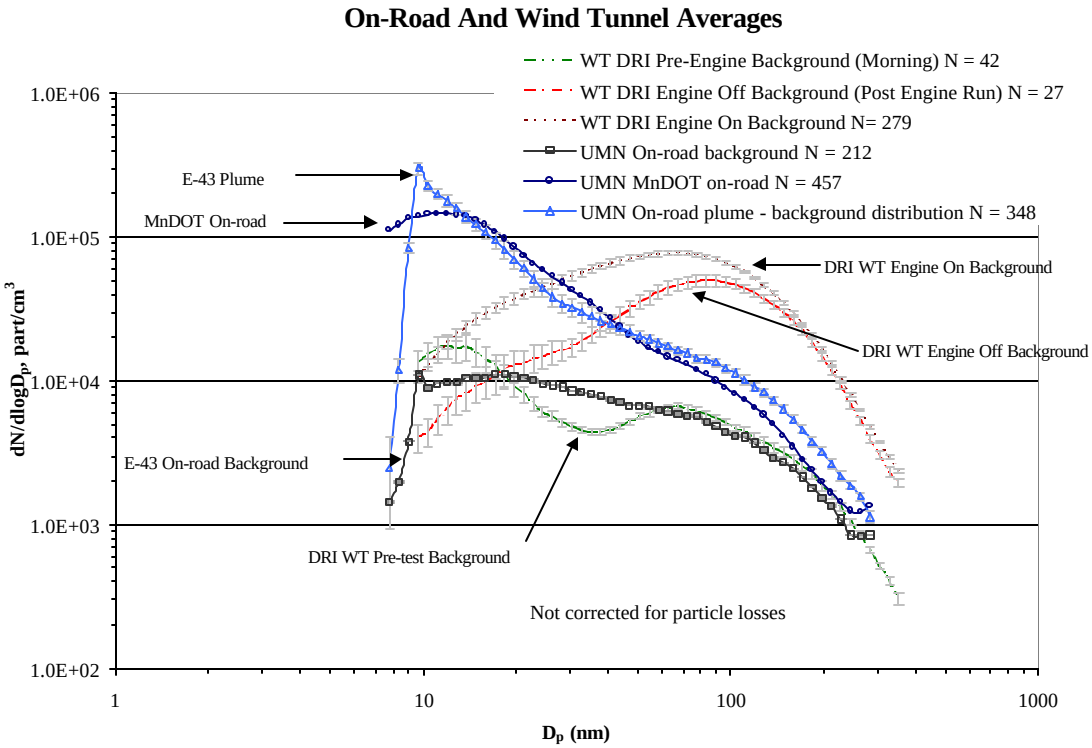

Figure 23. Mean on-road and wind tunnel background

Figure 24 compares the average background on-road size distribution to the UMN average background wind tunnel size distribution collected at the end of the day when the engine was turned off after the completion of testing. Also shown on the graph is a size distribution collected from the storage shed where the MEL is stored. The on-road background size distribution is the same as that shown in Figure 23.

The MEL storage shed distribution was collected after the E-43 data collection period was completed, but is shown because of the similarity with the wind tunnel average UMN background distribution. During the daily MEL instrument startup, scans were taken in the storage shed. Power was supplied to the MEL instruments from two Diesel generators in the MEL. Frequently, the prevailing wind direction in the morning was W NW, as it was on September 21, 2001. As a result, the background samples collected in the MEL storage shed were contaminated with Diesel aerosol from the generators. The wind blew the exhaust from outside the shed into the shed where it was contained and sampled as "background". These size distributions were useful indicators of how the SMPS was functioning, because we would expect a Diesel accumulation mode produced by the generators to center around 100 nm.

The shape of the UMN wind tunnel background and the MEL storage shed background contaminated with Diesel exhaust are remarkably similar in shape and the accumulation modes are at least a factor of 10 larger than the on-road backgrounds. The wind tunnel and MEL storage shed are aged Diesel aerosol with large accumulation modes and no nuclei mode. The large accumulation modes are associated with large surface area. We would argue that nuclei mode formation is suppressed under these conditions; precursor material is scavenged by particles in the accumulation mode before there is an opportunity to form nuclei mode particles. Further, at the wind tunnel the CA fuel was used. The CA fuel showed little tendency to form a nuclei mode in the laboratory and, although a nuclei mode was observed during on-road tests, these tests were conducted under cool climatic conditions that favor nuclei mode formation. The wind tunnel temperatures as reported in the West Virginia Wind Tunnel Report increased throughout the day and were typical of summer MN temperatures.

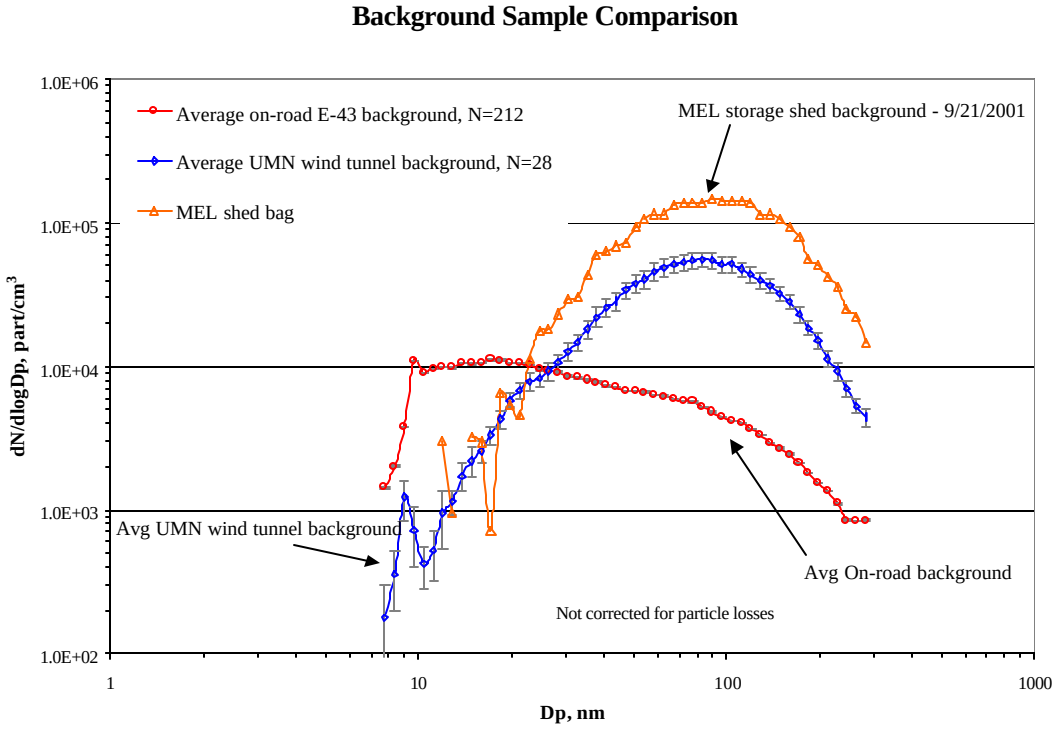

Figure 24. Background sample comparison; on-road, wind tunnel, MEL storage shed

Useful Descriptors of Particle Size Distributions

Several concentration independent descriptors are used in this report to give insights into the size and shape of atmospheric and exhaust particle size distributions. These are the particle number to volume ratio (N/V), the diameter of average volume (D_{av}), the fraction of particle number found in particles smaller than 30 nm diameter (N_{30}/N), the fraction of particle volume found in particles smaller than 30 nm (V_{30}/V), the geometric number mean diameter (DGN), and the geometric surface mean diameter (DGS). The N/V ratio

gives the number of particles formed per unit volume of emitted particulate matter (part/μm^3). Since the particle mass is proportional to particle volume, the N/V ratio gives a measure of the particles formed per unit mass emitted. For spherical particles with an effective density of 1 g/cm^3 an N/V ratio of 1 part/μm^3 corresponds to 10^{12} part/g. The N/V ratio and the diameter of average volume, D_{av} have a simple inverse relationship to one another.

$$D_{av} = \left(\frac{6}{\pi (N/V)} \right)^{1/3}$$

For spherical particle of constant density, the diameter of average volume and the diameter of average mass are the same. The N_{30}/N ratio gives an estimate of the number fraction in the nuclei mode and the V_{30}/V ratio an estimate of the volume (or mass) fraction in the nuclei mode. Both of these ratios are most accurate when the nuclei mode is much larger than the accumulation mode so that the tail of the accumulation mode smaller than 30 nm is relatively small. DGN and DGS are defined following standard aerosols practice.

$$\mathrm{Log}(DGN) = \frac{\sum \mathrm{Log}(Dp_i)\Delta N_i}{\sum \Delta N_i}$$

$$\mathrm{Log}(DGS) = \frac{\sum \mathrm{Log}(Dp_i) Dp_i^{\,2} \Delta N_i}{\sum Dp_i^{\,2} \Delta N_i}$$

Here, Dp_i is particle diameter in the i^{th} size interval and ΔN_i is its number concentration. These descriptors are instrument dependent. In this work, they will be used only with SMPS data.

Figure 25 is a scatter plot showing the usefulness of the N/V ratio plotted against D_{av}, N_{30}/N, DGN or DGS. Both plume and background samples are shown without regard to dilution ratio or acceptance criteria. Points to be made from this figure are as follows.

- N_{30}/N approaches 1.0 for large N/V ratios with nearly all of the particles in the nuclei mode. Note that N_{30}/N cannot exceed 1.0.
- D_{av} shows the expected inverse relationship with N/V with values of 86, 58, and 40 nm for N/V ratios of 3,000, 10,000 and 30,000 part/μm^3, respectively.
- Plume samples are more likely to have N/V > 10,000 while background samples nearly always have an N/V < 10,000.
- Plume samples have smaller values of DGN and DGS than background samples indicating the presence of a nuclei mode.
- Plume samples have greater variability, in part due to the variable contribution from background aerosol.
- DGS approaches DGN as particles become smaller and more monodisperse and DGS is always greater than DGN for finite (>1) σ_g.
- All diameters are limited by the lower limit of the SMPS.

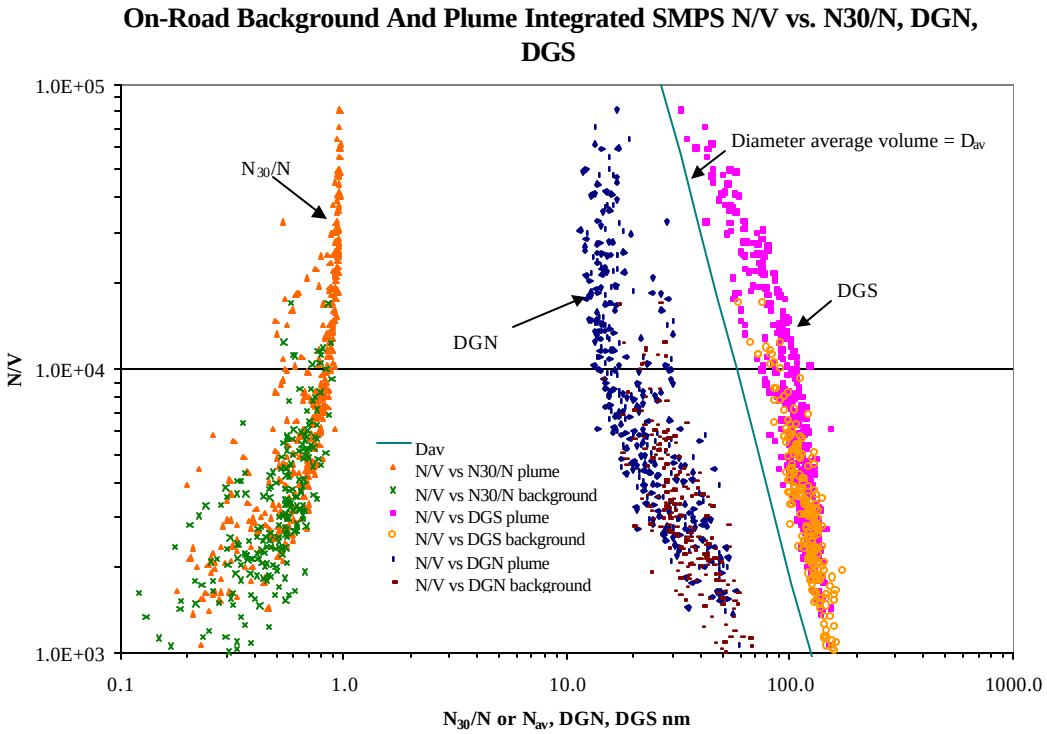

Figure 25. On-road background and plume SMPS N/V vs. N_{30}/N, D_{av}, DGN or DGS

Atmospheric Versus Laboratory Size Distributions

Caterpillar Data

One of the goals of the E-43 project was to simulate on-road size distributions in the laboratory using mini-dilution systems. Atmospheric or on-road samples present two fundamental problems. The engine condition is not steady even when cruise control is used and the dilution ratio, rate, background conditions and other parameters are uncontrolled. It is likely that the most repeatable on-road engine condition was full throttle acceleration, and this condition was reproduced in the laboratory by simulated, steady-state acceleration conditions. Figures 26 through 30 show size distributions for the Caterpillar 3406 engines collected on-road and in the laboratory. Both EPA and CA fuels were used in these tests.

Figure 26 shows the average on-road size distributions for 3406E engine accelerations using both fuels with and without the loaded trailer. There is a wide range in the average dilution ratio for the 4 lines shown in the figure (780 to 2680:1). A nuclei mode is present for both fuels with the EPA fuel giving the larger nuclei mode. The accumulation modes are similar in shape but differ in concentration mainly as a result of uncertainties in dilution ratio.

The variability in dilution ratio measurement is illustrated in Figure 23. In that figure, the average on-road size distribution, unadjusted for dilution ratio, was shown. The size distribution was based on 348 valid bag samples regardless of engine, fuel or test condition. After further examination, 244 (70 %) were included for further analysis. Samples were excluded primarily due to either computer data logger failure or the failure to be able to determine any valid dilution ratio. After application of the screening criterion, defined as the total particle number in the plume accumulation mode (defined as > 30 nm) being twice as great as the total particle number in the background accumulation mode, 178 or 51 % of the samples remained for analysis. The screening criterion essentially excluded samples with very high dilution ratios. Finally, 66 of the 178 samples were collected for Cummins on-road tests and 112 were collected for Caterpillar on-road tests. The Caterpillar on-road data set is substantially larger, which is a major reason why we have greater confidence in the Caterpillar on-road data. Unlike the Cummins data, all the Caterpillar data were collected in warm weather as shown in Table 4; thus, results obtained from EPA and CA fuel are unlikely to be influenced by ambient temperature.

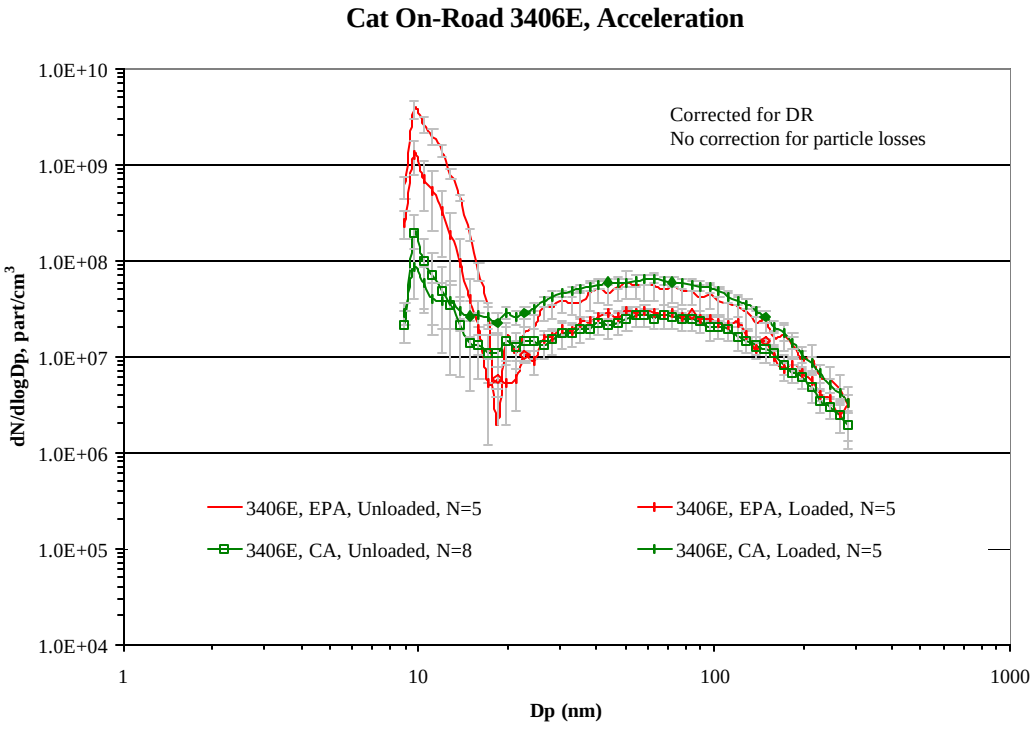

Figure 26. On-road acceleration with and without load, 3406E, EPA and CA fuel

An alternative method of analysis is available to lessen the effect of errors in the dilution ratio measurement. This method normalizes the distributions using the number distribution to total volume ratio ((1/V)dN/dlogDp) as shown in Figure 27. The SMPS size distribution is made up of 32 channels, and the number size distribution is calculated from the total particle count in each channel. If the total number of particles in each channel is then divided by the total aerosol volume determined from the size distribution,

the (1/V)dN/dlogDp distribution can be plotted. The ratio (1/V)dN/dlogDp has units of particles/μm^3 that when multiplied by 10^{12} yields number of particles/g assuming spherical particles with a density of 1.0. This is a very useful metric that relates mass emissions to the number of particles.

The normalization procedure used in Figure 27 more clearly illustrates the differences between the two fuels for the on-road chase tests. The EPA fuel produces an order of magnitude larger nuclei mode for both the loaded and unloaded test configurations while the accumulation modes are virtually identical. It is not as clear whether placing an increased load on the engine, which changes the rate of acceleration but not the load, makes a significant difference. Figure 27 also applies the best-fit lognormal distribution size distribution to the normalized size distribution. The fitting procedure is discussed in more detail in the section on the thermal denuder.

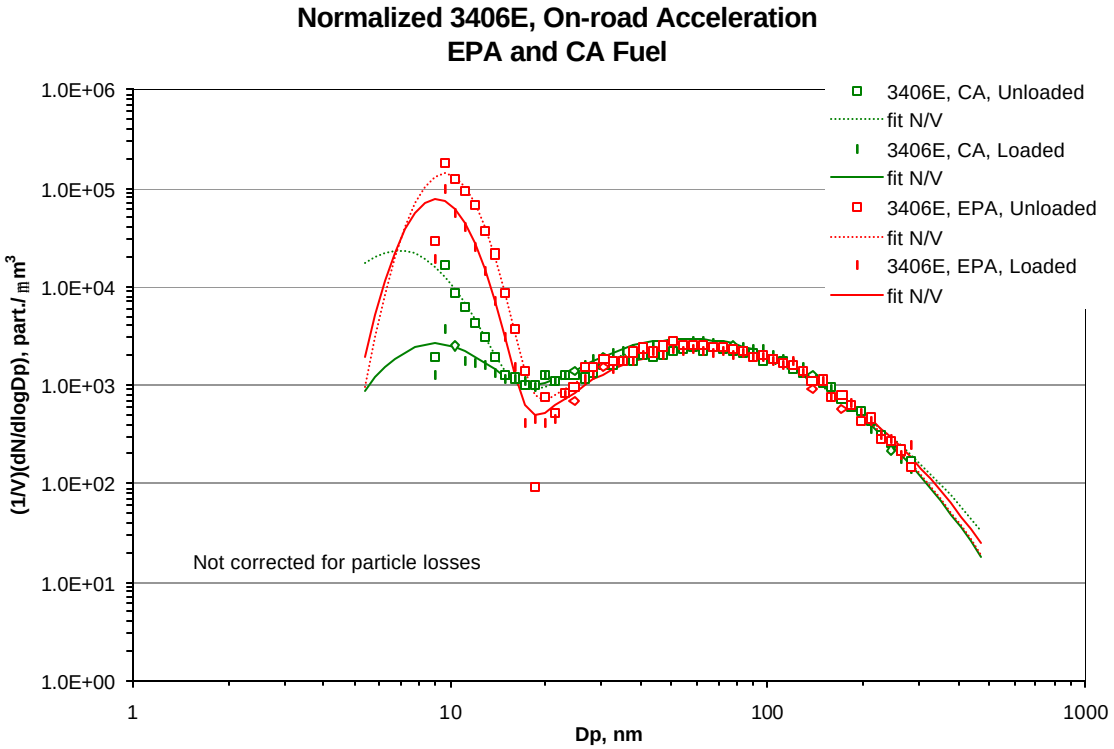

Figure 27. Normalized Cat 3406E on-road acceleration data

Figures 26 and 27 can be compared to the simulated "acceleration conditions" tried in the laboratory and illustrated in Figures 28 and 29. Laboratory dilution introduces a new set of parameters not found on-road. In the lab, the engine condition is very repeatable and the plume is contained in a dilution tunnel. The exhaust system in the laboratory may or may not resemble the exhaust system in a truck and to the extent it is different, the loss of volatile particle precursors to the walls of the exhaust system is affected. Further, losses may occur in the transfer line from the exhaust pipe to the dilution system, and dilution is achieved with filtered, temperature and humidity controlled air as opposed to on-road ambient air. The residence time and dilution rate in the dilution system are unlikely to be

well matched to the atmospheric parameters, although the goal is to simulate the atmospheric process. Laboratory testing will be far less variable than the on-road situation.

Figures 28 and 29 show the 1800-RPM, 2250 N-m and 1610-RPM 2012 N-m (EPA fuel) or 1658-RPM 2072 N-m (Ca fuel) conditions for the 3406E series of engines with EPA fuel (Figure 28) and CA fuel (Figure 29) for multiple dilution tunnel configurations. The engine used in the chase experiments and on the chassis dynamometer is denoted 3406E while the one used in the CVS facility is 3406E-1. The 1800-RPM, 2250 N-m load (ISO 1) is the rated power condition. The other condition shown for each fuel is our simulated acceleration condition based upon engine data. ISO-1 was selected for this comparison because it was a test condition that was evaluated in every phase of the Caterpillar laboratory work. Multiple 3406E engines were evaluated at this test condition as well as all of the dilution systems, although the performance cell data and engine comparison are discussed later. Further, the condition had a sizeable nuclei mode that allows a comparison between both the accumulation and nuclei modes.

The EPA fuel makes a larger nuclei mode than CA fuel, and the BG-1/ejector reproduces the nuclei mode better than the CVS/ejector dilution system or the 2-stage system used in the CVS. The accumulation modes are similar in shape but differ in concentration. In Figure 29, the BG-1/ejector again provides a better match in the nuclei mode. Also in Figure 29, the shape of the CA fuel accumulation modes are similar to those produced by the EPA fuel although the on-road unloaded and loaded conditions do not match with the EPA counterparts. This difference is likely attributable to dilution ratio estimation. The accumulation mode of the CA fuel shown in Figure 29 is larger than the accumulation mode produced by the EPA fuel even though the nuclei mode is smaller. Both Figures 28 and 29 show that the emissions from engine 3406E-1 in the CVS facility are lower than from 3406E running on the chassis dynamometer with the BG-1/ejector dilution system. This is likely to be due to engine to engine differences.

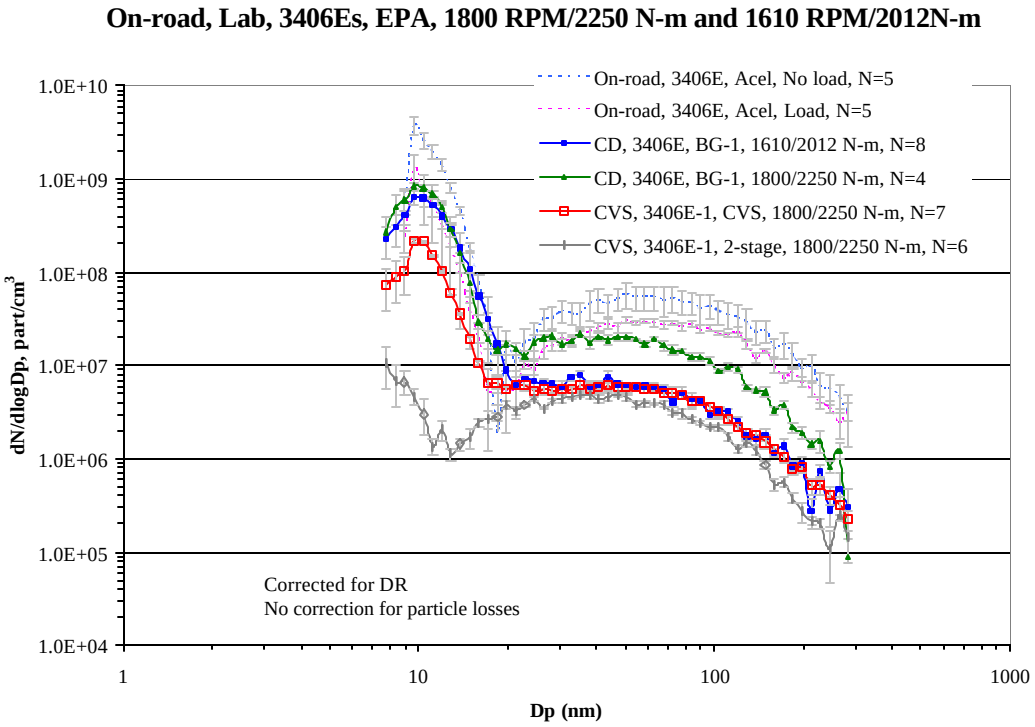

Figure 28. On-road and laboratory dilution conditions, 3406E engines, EPA fuel

Data shown in Figures 28 and 29 can be normalized to remove the differences caused by dilution ratio measurement. Figures 30 and 31 show the effect of normalization. In both cases, the on-road size distributions are included on the figures. Now the shapes of the accumulation modes are more easily seen. Note that the on-road size distributions for both fuels are narrower and show a larger accumulation mode diameter. The BG-1/ejector appears to somewhat overestimate the nuclei mode concentration while the CVS/ejector dilution systems used at the CVS nearly matches the normalized on road nuclei mode. This difference may not be significant because we are comparing two different engines. The 2-stage system underestimates the nuclei mode, as it did in Figures 28-29.

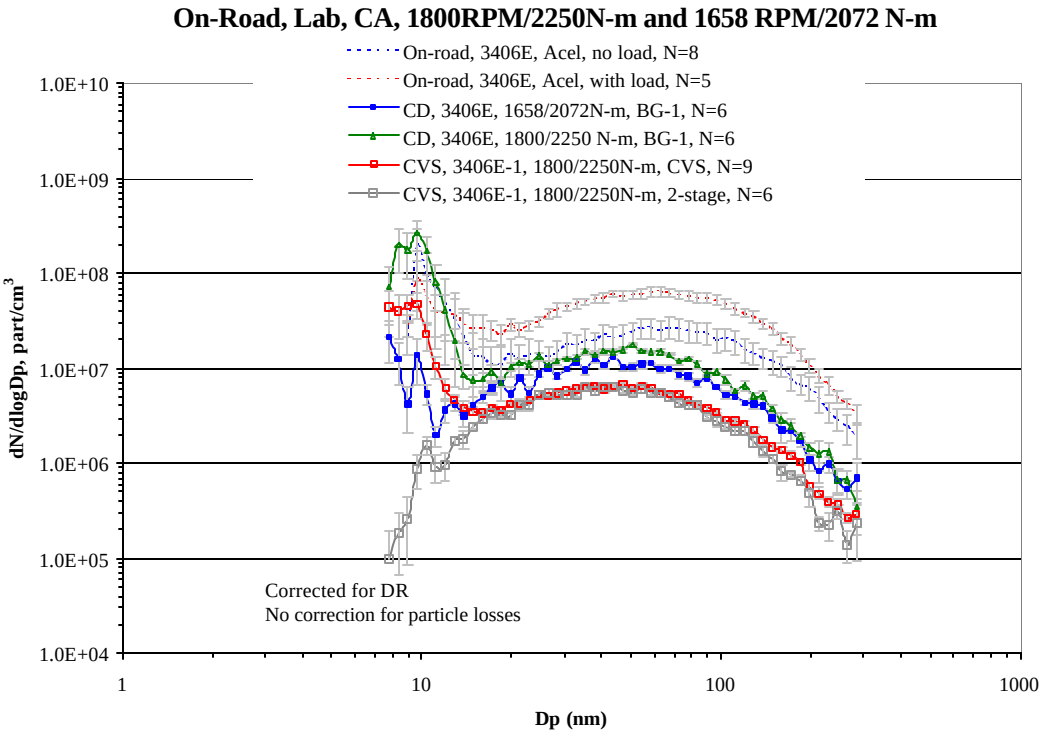

Figure 29. On-road and laboratory dilution conditions, 3406E engines CA fuel

The fitting procedure used in Figure 27 is used again in Figure 32, where the 3406E chassis dynamometer data are compared for the two fuels. Two engine conditions are shown, ISO-1 (1800 RPM, 2250 N-m) and a simulated acceleration condition that was similar to the on-road acceleration. For the EPA fuel, this condition was 1610 RPM and 2012 N-m and for the CA fuel it was 1658 RPM and 2072 N-m. The BG-1/ejector dilutor was used in the chassis dynamometer. All plots in Figure 32 show essentially identical accumulation modes, while the nuclei modes are smaller for the CA fuel.

Figure 33 repeats data from Figures 27 and 32 to show how the chassis dynamometer distributions compare to the on-road distributions, and the fitting parameters are summarized in Table 12, which compares various features of the size distributions. The first 5 columns show parameters calculated directly for the size distributions, while the remaining columns show characteristics of log-normal bimodal distributions fitted to the data. The bimodal fitting is useful because it allows features of the overlapping nuclei and accumulation modes to be quantified.

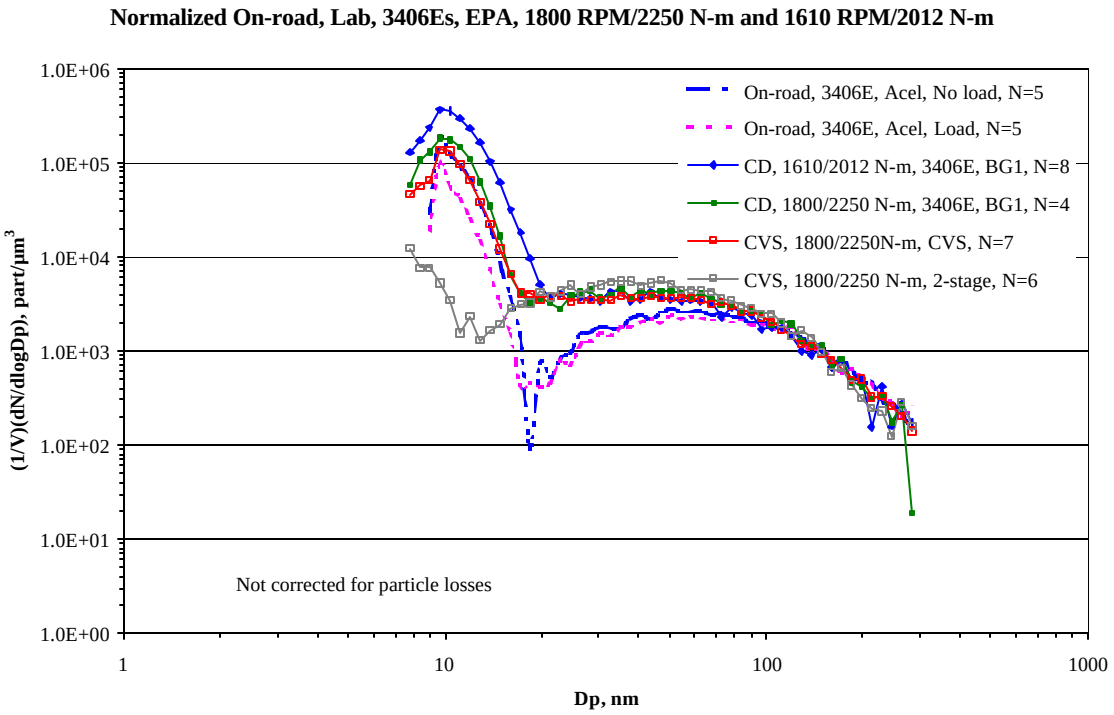

Figure 30. Normalized on-road vs. laboratory data, EPA fuel, acceleration

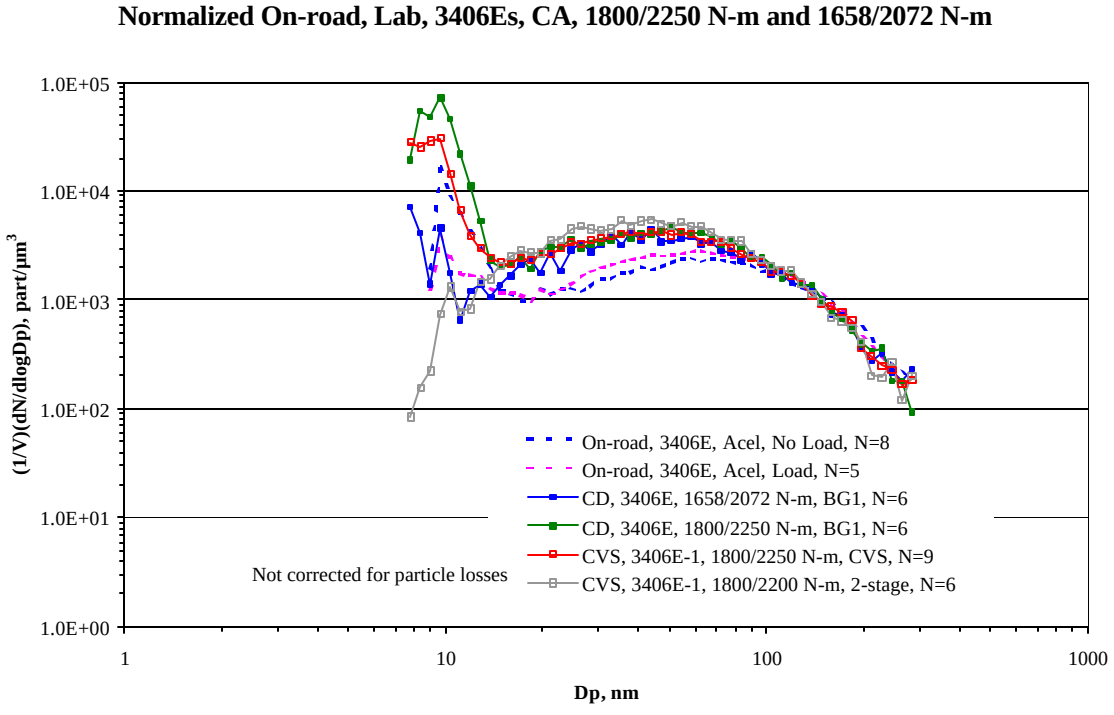

Figure 31. Normalized on-road vs. laboratory data, CA fuel, acceleration

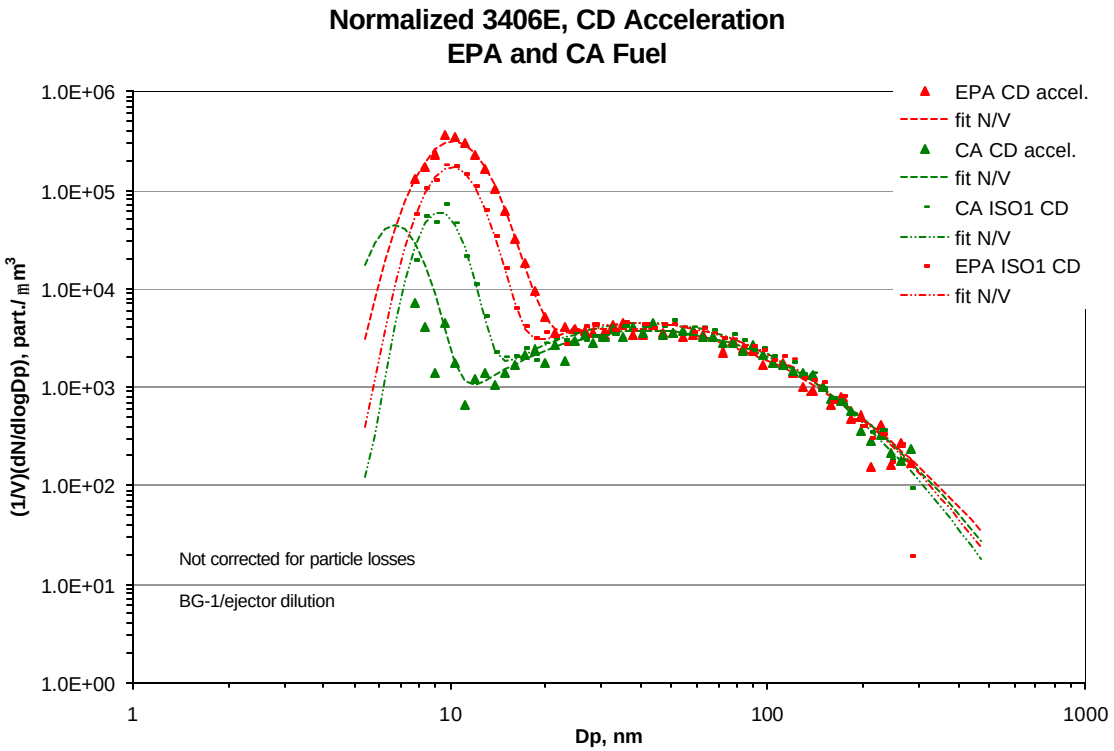

Figure 32. Normalized Cat 3406E, chassis dynamometer, simulated acceleration

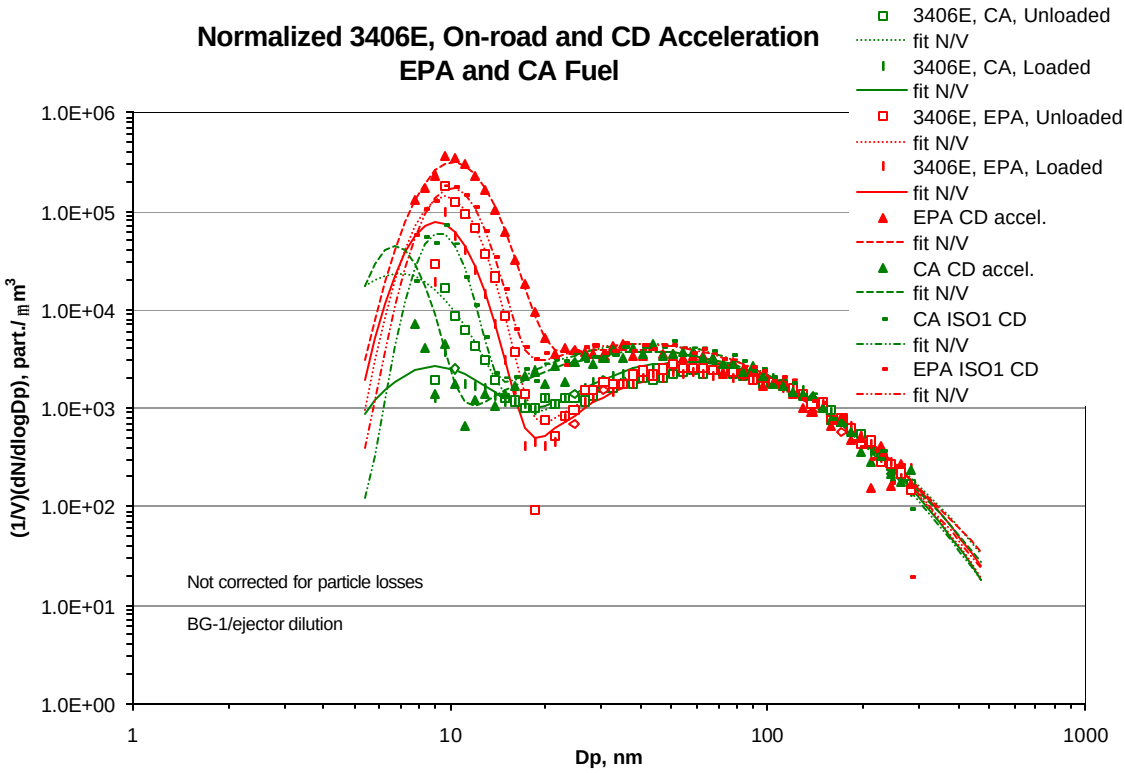

Figure 33. Normalized comparison of on-road to chassis dynamometer 3406E engine

Table 12. Fit parameters for on-road and CD BG-1/ejector distributions for Figures 27-33

Condition	N/V (part./µm^3)	N30/N	V30/V	DGN (nm)	DGV (nm)	DGN nuc (nm)	s_g nuc (nm)	DGN acc (nm)	s_g acc (nm)	N fract nuc	V fract nuc	Nfit/N
Chassis Dynamometer												
1800/100%, EPA	3.51E+04	0.933	0.0260	11.8	131	10.1	1.19	39.4	2.15	0.896	0.0121	1.03
1800/100%, CA	1.19E+04	0.803	0.0093	14.5	137	9.3	1.15	41.7	2.07	0.721	0.0029	1.06
1658/100%, CA	3.57E+03	0.402	0.0047	34.1	147	6.7	1.17	42.1	2.16	0.706	0.0008	3.00
1610/100%, EPA	7.00E+04	0.970	0.0534	11.2	131	10.2	1.23	35.3	2.32	0.951	0.0252	1.06
On-road Chase												
EPA, Unloaded	1.93E+04	0.917	0.0138	12.6	149	9.7	1.20	59.7	1.93	0.936	0.0103	1.54
EPA, Loaded	9.91E+03	0.853	0.0067	14.1	158	9.1	1.21	63.3	1.95	0.906	0.0047	1.82
CA, Loaded	2.55E+03	0.325	0.0027	42.0	149	8.9	1.40	55.8	1.95	0.305	0.0004	1.21
CA, Unloaded	3.20E+03	0.535	0.0030	27.8	156	6.9	1.35	54.9	2.08	0.799	0.0011	2.99

Raw data parameters include; N/V = total number/total volume, N_{30}/N = number of particles $\leq$ 30 nm/ total N, V_{30}/V = volume of particles $\leq$ 30 nm/ volume N, DGN = geometric number mean diameter, DGV = geometric volume mean diameter

Fitted parameters include; DGN nuc = geometric mean diameter nuclei mode, sg nuc = σ_g nuc = geometric standard deviation nuclei mode, DGN acc = geometric mean diameter accumulation mode, sg acc = σ_g acc = geometric standard deviation accumulation mode, N frac nuc = number fraction in nuclei mode, V fract nuc = volume fraction in nuclei mode, N_{fit}/N = total N fitted distribution/total N.

The N/V and V_{30}/V ratios that are calculated from the raw data give good indications of the relative number and mass of particles in the nuclei mode. These measures show some significant differences between laboratory and on-road measurements. With the EPA fuel, the on-road and laboratory measurements give N/V ratios ranging from 10,000 – 19,000 and 35,000 – 70,000 part/µm^3, for the on-road and chassis dynamometer/BG-1 measurements, respectively. Similarly, the V_{30}/V ratios range from 0.007 – 0.014 and 0.026 – 0.053 %, for the on-road and chassis dynamometer/BG-1 measurements, respectively. These differences are not readily apparent in the plots shown in Figures 30-33. All three measures clearly indicate the additional nanoparticle formation associated with the EPA fuel compared to the CA fuel. All three measures suggest that the BG-1 dilution system, as configured, may overestimate the amount of material in the nuclei mode, at least for these conditions. However, the BG-1/ejector may be appropriate for measuring nanoparticle emission characteristics similar to on-road observations.

Parameters of the bimodal lognormal fit to the size distributions are shown in the right hand side of Table 12. The bimodal fitting procedure allows separation of the accumulation mode, mainly formed in the engine, from the nuclei mode, mainly formed during dilution. The procedure allows fitting to part of a mode so that the fitted nuclei mode extends below the sizing range of the SMPS and the fitted accumulation mode extends above it. N_{fit}/N gives an estimate of the number of particles below the sizing range of the SMPS. N_{30}/N and V_{30}/V are intended as estimators of fitted values of the number and volume fractions in the nuclei mode. Differences between N_{30}/N and N fraction in nuclei mode are small and result mainly from particles below the lower limit of the SMPS and degree of overlap between the nuclei and accumulation modes. Values of V_{30}/V are typically larger than those of V fraction nuclei mode. This is mainly a result of overlap between the modes; i.e., the lower end of the accumulation mode is included in V_{30} and the upper tail of the fitted accumulation mode, which extends above the upper end of the SMPS measurements.

Particles in the nuclei mode are very small, with number mean diameters ranging from 5 to 10 nm. Their size and concentration is very dependent on dilution conditions and fuel. Accumulation mode particles, on the other hand, are expected to be less sensitive to conditions. It is somewhat surprising that the number mean diameters for the accumulation mode determined from on-highway data, 35 – 43 nm, are considerably smaller than those determined from lab data, 54 – 64 nm. Mismatch between on-highway and lab engine conditions or over correction for background in the 10-40 nm range are possible explanations for this difference.

Cummins Data

On-road, wind tunnel and CVS data can only be compared for the ISM engine using CA fuel, the only condition repeated in all three cases. As shown in Figure 34, the on-road acceleration distributions have a sizeable nuclei mode that we believe was, in part, due to the cold temperatures during test, in the 5° – 11°C range. The dilution ratio measurements on-road and at the wind tunnel were not as good as those at the Cummins CVS as illustrated by the distributions shown in Figure 34 where the CVS accumulation modes fall on top of one another. The CVS tunnel was run in two different ways for this engine condition, full flow and partial flow leading to primary dilution ratios of 5 and 8, respectively. Interestingly, the nuclei mode disappeared at the higher primary dilution ratio. Further investigation of these data has shown that the nuclei mode shown was entirely due to a very high nuclei mode in the first scan of the full flow test. It is likely that release of volatile material from the walls of the CVS tunnel at high temperature resulted in the nuclei mode.

The size distribution measured in the wind tunnel does not match with either on-road or laboratory measurements. We believe that acceleration at the wind tunnel was poorly replicated and the background aerosol concentrations were much higher than on-road, as was previously discussed. The continuous recirculation in the wind tunnel, and the lack of good background measurements, made it difficult to determine instantaneous dilution ratios. Consequently, the dilution ratio for the acceleration condition was a cumulative one based on the buildup of aerosol in the tunnel during the day.

Figure 35 shows the normalized size distributions corresponding to those shown in Figure 34. The lines drawn through the data are bimodal lognormal fits. The relatively large size of the nuclei mode measured on-road compared to laboratory and wind tunnel measurements is obvious. We believe that the formation of this mode was mainly associated with the low temperatures encountered during this phase of on-road testing.

Table 13 provides the UMN fit parameters for comparable conditions using the Cummins ISM engine and CA fuel on-road, at the wind tunnel and in the Cummins CVS laboratory using the CVS/ejector dilution system. The N/V ratios for the loaded and unloaded on road acceleration conditions are 3.3×10^4 and 5.7×10^4, respectively, and the DGN is < 20 nm in both cases, indicating the presence of a large nuclei mode. On the other hand, neither the lab nor the wind tunnel data show a large nuclei mode and all N/V values are

less than 10^4. Fitted DGNs of the nuclei mode for the on-road data are 13 and 16 nm. This is rather large for nuclei mode DGNs, for example Table 12 showed values in the 5 to 10 nm range. The relatively large size suggests that the driving force for formation and growth is strong, apparently as a result of the low temperature operation. The fitted results show DGNs for the accumulation mode ranging from 38 to 52 nm, except for the unconstrained fit of the on-road loaded acceleration. This fit gave an unreasonably high σ_g, most likely due to variability in on-road conditions and background interference. Consequently, the fit was constrained to a maximum σ_g of 2.2. Both constrained and unconstrained results are shown in the table, but the plotted results are the constrained fit. DGNs of the accumulation mode are slightly larger for the on-road test. This may be an artifact resulting from the overlapping with the very large nuclei mode or a result of the difference between simulated lab and actual on-road accelerations.

Table 13. Fit parameters for ISM engine and CA fuel for comparable on-road, wind tunnel and CVS conditions

Condition	N/V (part/mm^3)	N30/N	V30/V	DGN (nm)	DGV (nm)	DGN nuc (nm)	s_g nuc (nm)	DGN acc (nm)	s_g acc (nm)	N fract nuc	V fract nuc	Nfit/N
CVS												
1800/1552 Nm, UMN-2	4.73E+03	0.384	0.0090	37.3	133	20.0	1.40	38.4	2.07	0.079	0.0019	1.01
1800/1552 Nm, CVS-1, Full Flow, N=15	4.12E+03	0.369	0.0075	38.5	137	17.1	1.38	40.0	2.08	0.064	0.0008	1.01
1800/1552 Nm, CVS-1, Full Flow	7.83E+03	0.658	0.0107	21.8	133	9.8	1.25	37.8	2.08	0.571	0.0026	1.29
Wind Tunnel												
Wind Tunnel, Acceleration	3.97E+03	0.437	0.0053	33.4	142	11.3	1.35	47.8	1.99	0.305	0.0011	1.06
On-road Chase												
On-road, Acceleration, Unloaded	5.70E+04	0.957	0.1623	17.0	103	15.9	1.33	52.2	1.96	0.964	0.1242	1.03
On-road, Acceleration, Loaded	3.28E+04	0.946	0.0553	14.7	144	13.0	1.32	45.1	2.20	0.927	0.0272	1.06
On-road, Acceleration, Loaded (Unconstrained σ_g)	3.28E+04	0.946	0.0553	14.7	144	13.0	1.30	27.4	2.74	0.892	0.0176	1.07

Raw data parameters include; N/V = total number/total volume, N_{30}/N = number of particles $\leq$ 30 nm/ total N, V_{30}/V = volume of particles $\leq$ 30 nm/ volume N, DGN = geometric number mean diameter, DGV = geometric volume mean diameter

Fitted parameters include; DGN nuc = geometric mean diameter nuclei mode, σ_g nuc = geometric standard deviation nuclei mode, DGN acc = geometric mean diameter accumulation mode, σ_g acc = geometric standard deviation accumulation mode, N frac nuc = number fraction in nuclei mode, V fract nuc = volume fraction in nuclei mode, N_{fit}/N = total N fitted distribution/total N.

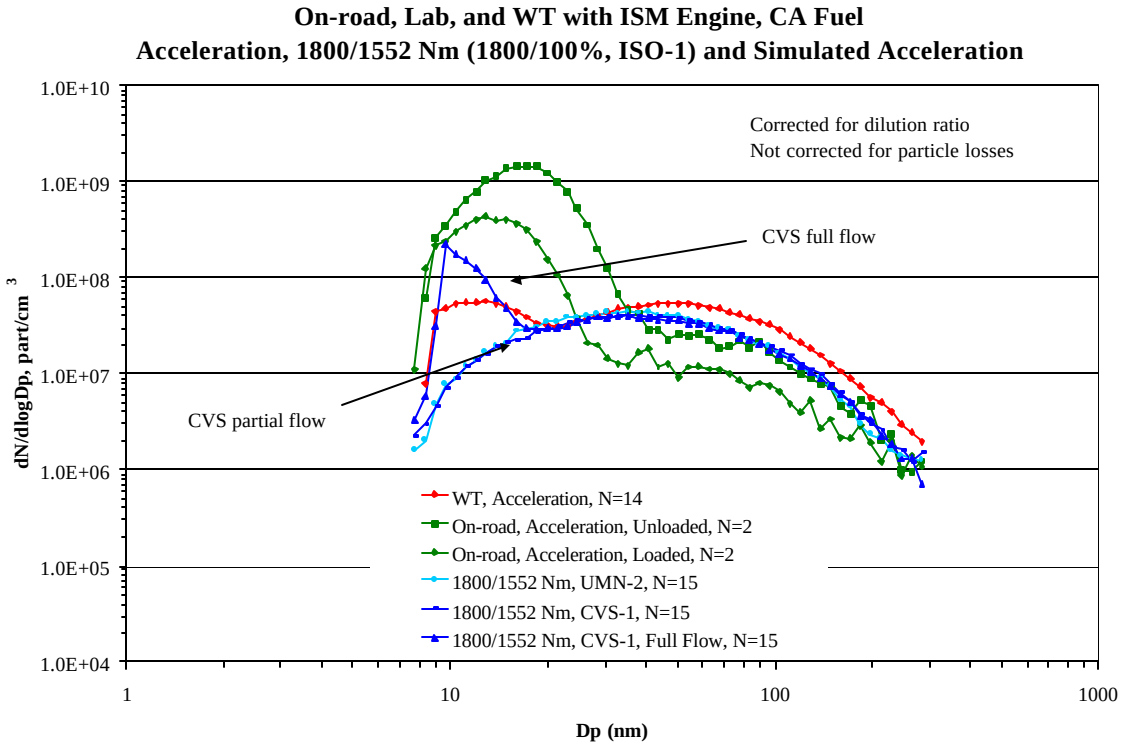

Figure 34. On-road, lab, wind tunnel, ISM, CA fuel, ISO-1 and simulated acceleration

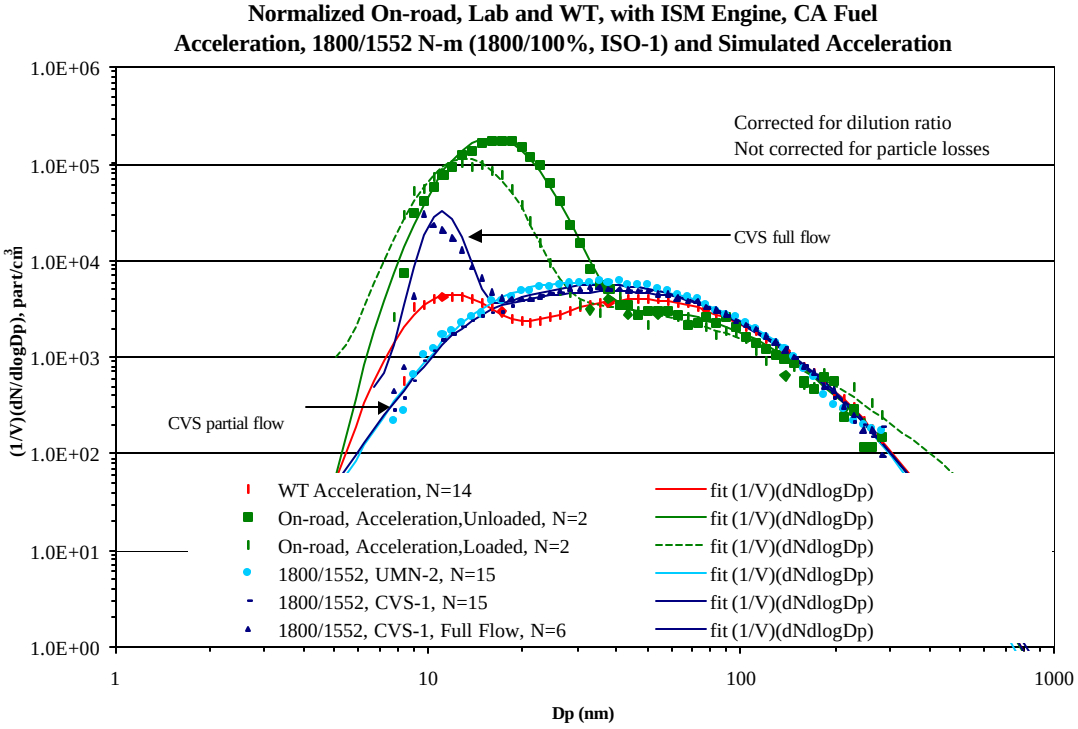

Figure 35. Normalized on-road, lab, WT, ISM, CA, ISO-1 and simulated acceleration

Sampling and Dilution System Comparison

To allow comparisons between dilution tunnels, fuels and engines, composite size distributions and statistics were compiled. These size distributions are shown in Appendix A, Figures A-1 through A-26. Thirteen composite groups were created and both non-normalized and normalized graphs are shown, for a total of 26 figures. SDOM error bars are shown for the non-normalized data. For visual clarity, SDOM error bars are not shown on the normalized figures, but they are of the same relative magnitude. Figures A-27 through A-32 are bar charts that summarize the principle features of the size distributions. Table A-1 summarizes the principle statistics of the size distributions and gives parameters of bimodal lognormal fits to the distributions. It also shows characteristics of some of the size distributions reported by Bagley *et al*., (1996). Tables A-2 and A-3 show detailed SMPS statistics and the continuous instrument data.

Table 14 shows the composite categories that were created by weighting the averaged cruise and acceleration data. Averaged data were weighted so that no single condition would disproportionately affect the results, and heavier weights were assigned to cruise conditions. Where there was only a single 55 mph cruise condition, the weighting factor was 0.6, while accelerations were assigned a weight of 0.4. Where there were multiple cruise conditions, the weighting was 0.5 for 60 mph cruise, 0.2 for 40 mph cruise and 0.3 for acceleration. Conditions such as wiggle, steady-pedal and idle were not included in the composite averages. Also shown are the composite average temperatures for the on-road tests. Average daily temperatures were averaged to give the condition average with each day's average weighted by the number of scans for that condition and that day. Composite weighting, as for the size distributions, was then done to give the temperature shown in table 14.

As mentioned before, the CA fuel was tested with the ISM engine in the Fall with temperatures around 7°C while the 3406E engine with CA fuel was tested in the Summer with temperatures around 28°C. We believe the difference in ambient temperature was a contributing factor in the differences between the observed size distribution between the CA fuel evaluated in the ISM and 3406E engines.

Table 14. Composite categories

Category	Temperature, °C
Cummins Chase ISM, CA Fuel	7.7
Cummins Chase ISM, CA Fuel (55 Cruise Only)	
Cummins Chase ISM, EPA Fuel	17.9
Cummins Chase ISM, EPA Fuel (55 Cruise Only)	
Cummins Chase L10, EPA Fuel	6.5
Cummins Chase L10, EPA Fuel (55 Cruise Only)	
Cummins Chassis Dyno 55 Cruise ISM, CA Fuel (55 Cruise Only)	
Cummins Chassis Dyno ISM, EPA Fuel (55 Cruise Only)	
Cummins Chassis Dyno L10, EPA Fuel (55 Cruise Only)	
Cummins CVS ISM, CA Fuel	
Cummins CVS ISM, EPA Fuel	
Cat Chase 3406C, EPA Fuel	24.3
Cat Chase 3406E, CA Fuel	27.9
Cat Chase 3406E, EPA Fuel	22.6
Cat Chassis Dyno 3406C, EPA Fuel	
Cat Chassis Dyno 3406E, CA Fuel	
Cat Chassis Dyno 3406E, EPA Fuel	
Cat CVS 3406E, CA Fuel	
Cat CVS 3406E, EPA Fuel	

On-road Distributions vs. Tunnel Distributions

The purpose of the laboratory dilution systems used in the E-43 project was to simulate on-road plume size distributions. Several systems were tried, including the 2-stage tunnel in several configurations, the CVS/ejector dilution system in several configurations and the BG-1/ejector. We believe that the 2-stage tunnels were configured, in most cases, with a TL that was too long, from the exhaust pipe to the tunnel. This resulted in the loss of particles and particle precursors to the walls and an underestimation of the nuclei mode. This was clearly demonstrated in the Caterpillar CVS tests where 3406E-1 was evaluated with both the CVS/ejector dilution system and the 2-stage system using EPA and CA fuel. When the engine produced a nuclei mode with the EPA fuel, the mode was not present or was substantially smaller with the 2-stage tunnel with TL. Thus, in most instances, the 2-stage tunnel provided a poor comparison due to the long TL length, except at the Cummins chassis dynamometer where the 2-stage tunnel was configured with a short TL.

Figures A-1 and A-2 show average composite data for the Cummins chase experiments in dilution corrected and normalized form. Our lab data show that the accumulation modes for the EPA and CA fuel match closely, so differences in on-road concentrations of accumulation mode particles are likely due to uncertainties in dilution ratio, background

aerosol variability and on-road operating conditions. The normalized plots bring the accumulation modes together and make the very large nuclei mode, apparently due to cold weather sampling, measured with the CA fuel, more distinct. The L10 engine emits larger accumulation mode particles and a smaller nuclei mode than the ISM engine running on the same fuel.

In Figures A-3 and A-4 (normalized), the Cummins chassis dynamometer composite L-10 distribution is shown along with the corresponding on-road size distribution for EPA fuel. The 2-stage tunnel configuration at the chassis dynamometer had the shortest transfer line possible (5 in), but it was not heated. Comparisons are shown for the 55 mph cruise conditions only because the on-road accelerations could not be simulated well on the chassis dynamometer. The on-road size distribution shows a larger nuclei mode and an accumulation mode that is broader and shifted to larger particle size. Such differences between the on-road and chassis dynamometer nuclei modes are likely to be associated with differences in dilution conditions, in particular ambient temperature. The on-road Cummins tests were conducted in cool climatic conditions. Variability in on-road engine operating conditions also affects the comparisons and may be responsible for differences in the accumulation mode that should not be influenced by dilution conditions. [Tables 3 and 4 show the ambient temperature for the on-road tests, and Table 14 shows the composite average temperatures.] The on-road data show a clearer separation of the nuclei and accumulation modes than the lab data. The same behavior was shown by Caterpillar data and is probably due to quicker quenching of nanoparticle growth under on-road conditions where dilution ratios reach several thousand in seconds. On-road stack to sample boom distances were typically 50-75 m at 55 mph giving residence times of 2-3 s to reach dilution ratios averaging 1000-2000:1.

Figures A-5 and A-6 compare on-road and chassis dynamometer data for the ISM engine running on EPA fuel. The on-road accumulation mode falls above the lab result suggesting on-road dilution ratios are erroneously high. The data show a third mode between the nuclei and accumulation modes. This may be due to non-representative operating conditions. Alternatively, it may be due to uncorrected background interference because it was impossible to make simultaneous plume and background measurements. Again, we see that the nuclei mode is underestimated by the lab dilution system. The on-road data will favor nanoparticle formation; thus, affecting the comparison to the laboratory data.

Figures A-7 and A-8 compare on-road and 2-stage tunnel size distributions for the ISM engine with CA fuel. The relative sizes of the accumulation modes suggest the on-road dilution ratio estimates are low. The on-road accumulation mode is shifted to larger particle sizes and has a longer tail. This is likely due to unsteady on-road conditions and variable background aerosol contributions. The on-road data show a very large nuclei mode that is nearly absent in our lab data. We have no plausible explanation for this large difference in the nuclei mode except that the on-road tests were conducted in cold weather in Minnesota as shown by the mean ambient temperatures recorded in Table 3 and Table 14. In laboratory studies conducted at the UMN, the impact of dilution air temperature on the formation of nanoparticles has been demonstrated and the effect

cannot be underestimated (Abdul-Khalek, *et al.*, 1999; Wei, *et al.*, 2001b, 2002). The CVS/ejector dilution system at the CVS facility also showed a poor match (Figures A-9 and A-10) to the on-road CA fuel ISM size distribution.

Figures A-9 and A-10 compare ISM engine, CA and EPA fuel composite size distributions made on-road and at the CVS using partial flow, primary dilution in the CVS tunnel and secondary dilution with the CVS/ejector system. This approach should have lower losses of particle precursors [due to lower mass transfer of material in the transfer line] compared to the two-stage system. The CVS system does a better job of matching the nuclei mode for the EPA fuel, than it does for the CA fuel, where the match is very poor. The odd third mode located between the nuclei and accumulation modes, seen in the on-road data with EPA fuel, is absent from both the chassis dynamometer data and the CVS data. This mode is an artifact of the averaging process, generated by a single atypical scan. We believe that this "mode" is associated with either an unusual engine operating condition or an inadequate correction for background aerosol. On the other hand, the normalized plot shown as Figure A-10, demonstrates that upper ends of the accumulation modes match very well. [Figures A-11 and A-12 show just the Cummins CVS ISM engine, EPA and CA fuel size distributions without the on-road distributions for easier comparison.]

The Caterpillar chase experiments were performed about nine months after the Cummins experiments. During this period, the on-road measurement protocol was improved, and modifications were made to the MEL and data acquisition software. Further, the Caterpillar measurements were made during the summer under similar ambient temperatures. The Caterpillar on-road measurements are more consistent than the Cummins measurements. Warmer ambient temperatures and improved sampling methods contributed to this consistency.

Figures A-13 and A-14 show on-road composite data for the 3406E engine running on CA and EPA fuel and the 3406C engine running on EPA fuel. The dilution (A-13) corrected and normalized (A-14) comparisons are shown. Distinct bimodal structure is apparent in all cases. The accumulation modes have very similar lognormal shapes and both engines and fuels show a nuclei mode. The CA fuel gives a much smaller nuclei mode than the EPA fuel with the 3406E engine. It should be pointed out that the CA fuel used at Caterpillar was not the same CA fuel used for the on-road tests. It came from the second batch of CA fuel shown in Table 1 and had a higher fuel sulfur content. There is little difference between the nuclei modes measured with the 3406E and 3406C engines, the mode for the 3406E is slightly higher, but the one from the 3406C is broader. This results in a larger volume fraction, V30/V, in the nuclei mode for the older engine [0.11 versus 0.009, Table A-2]. Normalized descriptors of the size distributions like V30/V are discussed in more detail below.

The BG-1/ejector dilution system used at Caterpillar in the chassis dynamometer test facility did a good job of matching the on-road 3406E size distribution for both the EPA and CA fuels, as illustrated in Figures A-15 through A-18. Figures A-15 and A-16 show good agreement between on-road and chassis dynamometer measurements for the 3406E

engine running on EPA fuel. The main difference is slightly less merging of the two modes in the on-road measurements. This is likely due to the rapid quenching of growth under on-road dilution conditions discussed above.

Figures A-17 and A-18 compare on-road and chassis dynamometer measurements for the 3406E engine running on CA fuel. The on-road data in Figure A-17 show a higher concentration in the accumulation mode suggesting an error in the dilution ratio estimates. The size and shape of the nuclei modes are similar for on-road and lab measurements.

Figures A-19 and A-20 compare on-road and chassis dynamometer size distributions for the 3406C engine running on EPA fuel. The 3406C nuclei mode is narrower with the chassis dynamometer but the height is the same after normalization. The error bars are larger for the on-road nuclei mode in Figure A-19. This may be due to variability in on-road operating conditions, and/or an error in the dilution ratio estimate. The mismatch between accumulation modes suggests that the on-road dilution ratio is too high. The normalized results show a nearly perfect match of accumulation modes.

Figures A-21 and A-22 show a comparison of composite on-road size distributions measured for the Caterpillar 3406E engine with corresponding size distributions measured in the CVS facility using the CVS/ejector dilution system for the 3406E-1 engine. Results are shown for both CA and EPA fuels. The on-road DR looks a little high, especially for CA fuel. The fact that the CVS tests were done with a different engine of the same family may account for some of the difference. The normalized plots show near perfect matching of accumulation modes. Note the distinct lognormal shape. The nuclei modes measured in the CVS facility are smaller than on-road for both of the fuels.

Figures A-23 and A-24 show the CVS results for the 3406E-1 engine with CA and EPA fuels without the corresponding on-road results. The EPA fuel produces a larger nuclei mode. Differences in the accumulation modes are likely due to dilution ratio measurements. Figures A-25 and A-26 compare chassis dynamometer tests of the 3406E with CA and EPA fuels and the 3406C with EPA fuel. The accumulation modes are very similar. The size distribution for the 3406C has a longer tail of larger particles and slightly larger nuclei mode. Normalization shows how a larger mass emitter may look relatively better because it has more volume in the accumulation mode.

Additional bar charts in Appendix A summarize some of the principal features of the sizes distributions shown in Figures A-1 to A-26. Figures A-27 and A-30 compare mean total particle number measured with the SMPS, number of particles in the accumulation mode measured with the SMPS, number of particles > 30 nm (Nacc), and the total number of particles measured with the CPC for the composite results of the Cummins chase and CVS experiments, and the Caterpillar chase, chassis dynamometer and CVS experiments, respectively. In most cases, the CPC number is higher than the SMPS number indicating particles below the range of the SMPS.

The accumulation mode number is shown in Figures A-27 and A-30 because this mode consists mainly of solid particles that should not be strongly influenced by sampling. Differences in N_{acc} between labs and on-road measurements result mainly from differences in engine operating conditions, background aerosol contributions and uncertainties in on-road dilution ratios. The Caterpillar experiments show much better agreement between on-road and laboratory measurements and even better agreement between chassis dynamometer and CVS measurements.

Figures A-28 and A-31 show corresponding mean values of V30/V, N30/N and N/V. None of these parameters are influenced by errors in dilution ratio. With the exception of the Cummins chase experiments with the ISM engine and CA fuel (cold weather), the volume fractions in the nuclei mode are 2% or less. On-road measurements give slightly higher fractions of particles in the nuclei mode than laboratory measurements, but the differences are small, especially in the case of the Caterpillar experiments.

Figures A-29 and A-32 compare composite means of measurements made with the DC and PAS, as well as active surface areas calculated from SMPS data. DC data are not available for all conditions, primarily because the DC was overloaded at higher concentrations. In most cases, where data are available, the DC active surface and the active surface calculated from SMPS data agree within 20-30 %. The photoemission activity of the particles measured by the PAS does not show a clear relationship between laboratory and chase data. This is likely to be largely due the odd transient response characteristics of the PAS. Although the sensor itself is fast and capable of response times on the order of 1 s, the commercial instrument that we used was configured to run an average over the previous 8 or 16 s. While this does not cause difficulty for steady-state laboratory measurements, it makes synchronization with the 5 s bag fill interval used in on-road sampling very difficult. The lab measurements themselves exhibit fairly consistent response with little difference between the CA and EPA fuels for the conditions tested.

Figure A-33 shows plots of the composite size distributions described above and compares them with some other recent measurements. Bimodal lognormal fits to the data are also shown. Table A-1 summarizes the principal characteristics of the size distributions and shows the parameters of bimodal lognormal size distributions fits to the data. The characteristics used to describe the distributions themselves are the number to volume ratio, N/V, the estimates of number and volume fractions in the nuclei mode, N30/N and V30/V, and the geometric number and volume mean diameters, DGN and DGV. The fitted parameters include the geometric mean diameters, DGN, and standard deviations, σ_g, of the nuclei and accumulation modes and the fractions of total number and total volume found in the nuclei mode. No fit was obtained for the chase experiments with the ISM engine because of the unusual shape of the size distribution. However, the characteristics of the original size distribution are shown. No lab data are shown for the L10 engine because we were not able to simulate on-road accelerations with the chassis dynamometer, and it was not tested on the engine dynamometer. Characteristics of the size distributions presented in the HEI report (Bagley, *et al*., 1996) are also shown. The parameters and fits were calculated from data given in the HEI

report for the "modern" 1991 engine without aftertreatment. The three engine modes that MTU tested are shown along with a composite average distribution.

Also shown in Table A-1 are the parameters of size distributions measured during on-road chase experiments in the CRC AP-2 program (Kittelson, *et al.,* 1988). These measurements are the average of chase experiments done for on-highway cruise conditions with a Cummins NTC 350 powered tractor-trailer running on road fuel with about 3,000 ppm S.

The most significant parameters of the size distributions to the E-43 program are N/V and V30/V. The N/V ratio gives the number of particles formed per unit volume of emitted particulate matter (part/μm^3). Since the particle mass is proportional to particle volume, the N/V ratio gives a measure of the particles formed per unit mass emitted. For spherical particles with an effective density of 1 g/cm^3 an N/V ratio of 1 part/μm^3 corresponds to 10^{12} part/g. Thus, if an engine emits 0.25 g/bhp-hr (grams per break horsepower-hour) particulate mass and the N/V ratio is 10,000 part/μm^3, the number emission rate would be 2.5 x 10^{15} part/bhp-hr. For an engine emitting 0.1 g/bhp-hr at the same N/V ratio, the particle emission rate would be 10^{15} part/bhp-hr.

In general, higher N/V ratios were observed in the on-road chase experiments than in the lab experiments. However, even the highest ratio observed on-road, 37,000 part/μm^3, is smaller than the 130,000 – 370,000-part/μm^3 range reported in the HEI report (Bagley, *et al*., 1996). Furthermore, the highest ratio we observed was associated with on-road operation in relatively cold weather and was not observed in any of the laboratory tests with the same engine and fuel. A more typical value for our on-road tests was 10,000 part/μm^3.

The V30/V ratio is important because it gives an estimate of the volume fraction of particles in the nuclei mode, which in turn is related to the mass fraction in the nuclei mode. We have found that the nuclei mode is comprised primarily of volatile material, unlike the accumulation mode that consists of mainly solid carbonaceous agglomerates. The V30/V ratios show a similar pattern to N/V ratios. The highest ratio we observed was 0.08 during the cold weather, on-road tests. This ratio was much lower than the ratio range (0.39 to 0.49) calculated from the HEI data (Bagley, *et al*., 1996). More typical values for our on-road tests ranged from 0.005 to 0.02. It should be noted; however, that we have observed N/V and V30/V ratios approaching levels like those observed in the HEI study (Bagley, *et al*., 1996) in some of the specially formulated fuel and lubricating oil tests described later in this report. In Figure C-1, the ISM engine was evaluated at 1200 RPM/482 N-m, standard 4000 ppm S oil, with 1 and 49 ppm S fuel. No nuclei mode was observed. For the same engine condition with specially formulated oil (385 ppm S) and 26, 49 and 325 ppm S fuel an enormous nuclei mode was observed. We believe this mode is associated with the special lube oil emitting large amounts of hydrocarbons that nucleated to form nanoparticles. This is likely to be due to a combination of inherent characteristic of the formulation and the relatively short time available to break-in recently changed lube oil.

The highest observed values for N/V and V30/V were 150,000 part/μm^3 and 0.33, respectively. These values were observed for the ISM engine running at 1200 rpm, 25 % load on 49-ppm sulfur fuel and specially formulated, reduced sulfur, lubricating oil. These values are **not** representative of normal engine operation. When the engine was tested at exactly the same operating condition with the same fuel, but with conventional lubricating oil, the values were only 3,400 part/μm^3 and 0.004 for N/V and V30/V, respectively. This shows the large influence the lubricating oil can have on nanoparticle formation and that nanoparticle formation is not simply related to fuel sulfur level.

It is apparent from figure A-33 that, in general, the observed size distributions fit bimodal log normal distributions. Nuclei mode number fractions range from 70 to 90 % when a significant nuclei mode is present. If there is not a significant nuclei mode, i.e., a number fraction in the mode less than about 30 %, the fitting procedure gives a small broad nuclei mode that is barely distinguishable from the lower end of the accumulation mode. Accumulation mode number mean diameters for the newer engines, the ISM and 3406E, range from 41 to 56 nm. For the older engines, the L10 and 3406C, the range is from 55 to 62 nm. In the cases where a significant nuclei mode is present, the volume fraction in the nuclei mode is less than V30/V. This is because the lower tail of the accumulation mode overlaps with the upper tail of the nuclei mode. Thus, the V30/V ratio gives a conservative estimate of the volume fraction in the nuclei mode.

The fit also gives parameters to estimate the number of particles, N_{fit}/N, and volume of particles, V_{fit}/V above and below the sizing range of the SMPS. In several cases, the fit suggests that a significant number of particles are below the range of the SMPS. In these cases the N_{fit}/N approaches 2. This is consistent with our observations that the total number measured with the CPC was generally larger than that measured with the SMPS.

BG-1/ejector vs. 2-stage Tunnel at the Caterpillar Performance Cell

Table 15 summarizes the calculated dilution tunnel settings for the BG-1/ejector and 2-stage tunnel used in the Caterpillar performance cell for the 3406E engine comparison. The nominal setting for the BG-1 primary dilution stage gave a dilution ratio of 7.5:1. For the 0.48 mm orifice, the orifice flow was calculated by assuming the compressible flow at the orifice. Compressed air flow for the TD 260 ejector was obtained from the manufacturer's manual. All dilution ratios were calculated for cold flow. For hot flow (first stage where the hot exhaust enters), the dilution ratios will be higher than those shown in the table.

The BG-1/ejector dilution ratio predicted from Table 15 is on the order of 1100:1, which agrees with our target dilution ratio of 1000:1. This also agrees, for the most part, with our measured data reported previously in our Caterpillar final report.

The 2-stage dilution ratios were lower than would be expected based upon the values shown in Table 15. Table 15 suggests our overall dilution ratios should be about 1600:1 but our measured mean dilution ratio range calculated from Table B-1 was 580:1. One possible explanation for this discrepancy is that the secondary ejector was subject to

downstream restriction that would lower the dilution ratio. The primary ejector vents to the atmosphere and is not subject to this problem. In any case, actual overall dilution ratios were measured regularly using NO as the tracer.

The 2-stage and the BG-1/ejector system were used together in the Caterpillar performance cell during tests of two engines, 3406E-2 and 3406E-3 running on the EPA fuel. The engines were run on the EPA fuel at idle, 1200 rpm at 260, 1280, and 2560 N-m, 1800 rpm at 1130 and 2250 N-m, 1290 rpm at 800 N-m and 1530 rpm at 860 N-m torque. The last two conditions are simulated highway cruise. The two dilution systems gave quite similar accumulation modes but the nuclei modes were consistently underestimated by the 2-stage. Measurements made with the BG-1/ejector system indicated that idle, 1200 rpm 260 and 2550 N-m and 1800 rpm, 2250 N-m produced a significant nuclei mode with N/V greater than 10^4. On the other hand, the 2-stage only showed a large nuclei mode at idle. We believe that this is due to the loss of particle precursors in the transfer line used with the 2-stage. Details of the comparison between size distributions measured with the two systems are given in the Caterpillar Data Report.

Table 15. Average dilution tunnel settings for the BG-1/ejector and 2-stage systems

Tunnel	Stage	Ejector	Orifice size, mm	Compressed air pressure, psi	Orifice flow, lpm	Compressed air flow, lpm	DR
UMN-3	Primary	TD110	0.70	20	3.11	31.6	10
UMN-3	Secondary	TD260	0.48	32	1.28	189.6	150
UMN-3	Secondary	TD260	0.48	36	1.28	200.9	160
BG-1	Secondary	TD260	0.30	50	2.30	268.9	120
BG-1	Secondary	TD260	0.30	35	1.30	198.1	150

CVS vs. 2-stage system at Caterpillar

The 3406E-1 engine size distributions were measured using both the CVS/ejector dilution system consisting of the CVS tunnel followed by a secondary ejector and the 2-stage dilution system. Both the EPA and CA fuels were evaluated. The engines were run at idle, 1200 rpm at 2560 N-m, 1800 rpm at 2250 N-m, simulated highway cruise and simulated acceleration. Measurements made with the CVS/ejector system showed that only idle, and the simulated acceleration conditions gave large nuclei modes as indicated by N/V ratio exceeding 10^4 for both fuels. The EPA fuel also showed large nuclei modes at 1200 rpm, 2560 N-m and 1800 rpm, 2250 N-m. The 2-stage dilution system, with its long transfer line, consistently underestimated the nuclei mode, and only gave N/V ratios greater than 10^4 for idle with both fuels and for simulated acceleration for EPA fuel.

Idle and other very light load conditions that have low exhaust temperatures and relatively long residence times in the exhaust system show little sensitivity to dilution conditions. Apparently gas to particle conversion of volatile particle precursors to form a nuclei mode takes place in the exhaust system before sampling and dilution.

Engine Comparison

3406E Engine comparison

Four 3406E engines, designated as 3406E, 3406E-1, 3406E-2 and 3406E-3, were tested either on-road or at Caterpillar. Engine 3406E was tested on-road and in the chassis dynamometer test facility with both EPA and CA fuel. Engine 3406E-1 was tested only in the CVS test facility with both the EPA and CA fuels, and engines 3406E-2 and 3406E-3 were tested only in the performance cell with EPA fuel. The engines were evaluated using the 2-stage dilution system and/or the BG-1/ejector dilution system. Thus, these engines were evaluated in multiple test cell configurations on different days with the purpose of demonstrating the type of variability that might be expected between engines of the same series.

Three of the engines (3406E1-3) were evaluated in the laboratory with the 2-stage dilution system. This was the largest number of different engines tested with a single dilution system, so data from these tests are used in this comparison. Additional data for the other dilution systems is available in the Caterpillar Data Report. There are five engine test conditions for this comparison idle, 1800 RPM and 2250 N-m, 1530 RPM and 857 N-m, 1287 RPM and 804 N-m, and 1200 RPM and 2555 N-m. Appendix Figures B-1 to B-15 show number, volume, and normalized number sized distributions and Table B-1 summarizes the dilution ratio statistics (average, minimum and maximum), the integrated average number of particles, the integrated average total volume of particles and the number/volume (N/V) ratio, the N_{30}/N and the V_{30}/V ratios for each of the five engine test conditions, fuels and engines. The SDOMs are also shown in the table. Figures B-1, 2, and 11 show number, volume, and normalized number for idle. All distributions show a distinct nuclei mode. Size distributions shown for the three engines running on the EPA fuel are very similar. Only 3406E-1 was run with the CA fuel and this combination gives the smallest nuclei mode. Figures B-3, 4, and 12 are the corresponding plots for the 1800 rpm, 2250 N-m condition (rated power). Here only the 3406E-1 engine with the EPA fuel shows a small nuclei mode. The accumulation mode concentration with the 3406E-2 engine is about 1/3 lower but Figure B-12 shows that the shape of the accumulation mode is very consistent. Size distributions for the two cruise conditions (1530 rpm, 857 N-m and 1287 rpm, 804 N-m) are shown in Figures B-5 to 8 and B-13 and 14. These conditions give essentially monomodal size distributions with only a hint of a nuclei mode for the 3406E-1 engine running with the EPA fuel. The 3406E-3 engine produces the highest number and volume concentrations for these conditions. Size distributions for the 1200 rpm, 2560 N-m condition (rated torque) are shown in Figures B-9, 10, and 15. For this case, the 3406E-1 shows slightly higher particle concentrations than the other two engines. It also shows a small nuclei mode when running with the EPA fuel.

Table B-1 shows engine 3406E-3 consistently had the highest overall dilution ratios, but not necessarily the highest average total number, volume or N/V ratio. The 3406E-3 engine was tested on a day when the dilution air background NOx concentration was high. This leads to considerable uncertainty in dilution ratio. Sources of such uncertainty are considered in more detail below after discussion of the size distributions. The data for

idle and the two highway cruise conditions suggest that engine 3406E-3 is the highest emitter but the trend does not appear to be statistically significant because of overlapping SDOM error bars. The normalized Figures B-11 to B-15 suggest that there is no significant difference in the accumulation mode for the engines.

There does not appear to be a remarkable trend with the CA fuel although it was only evaluated in engine 3406E-1 while in the CVS facility. Figures B-1 through B-10 show that engine 3406E-1 had nearly identical accumulation modes regardless of fuel, but differed in the nuclei mode with the CA fuel producing fewer nuclei mode particles, although the difference in some instances (Figure B-7 for example) is not great. The largest difference can be seen at idle.

With the exception of idle, none of the size distributions in Appendix B have a large nuclei mode as indicated by the N/V ratio being $>10^4$, although the tendency of the 3406E-1 engine running on EPA fuel to form a nuclei mode at the rated power and torque conditions is evident in the plots. For idle, the N/V varied from 10^4 to nearly 10^5 indicating a substantial nuclei mode. The 2-stage system tends to suppress nuclei mode formation because of the long transfer line from the exhaust to the first stage ejector dilutor. Thus, with the exception of idle, which is relatively insensitive to dilution conditions, the tendency to form a nuclei mode will be underestimated in these results. However, directional trends should be correct.

Dilution Ratio Uncertainty

The performance cell tests at Caterpillar using the 3406E engines provided an opportunity to examine uncertainties in dilution ratio caused by NOx measurement. Figure 36 shows plots of average dilution ratios and exhaust NOx values observed during the performance cell tests of engine 3406E-3. The estimated uncertainties associated with the dilution ratio are also shown. Results are shown for each of the engine conditions tested on September 7, 2000. These uncertainties are unusually high, the worst encountered in an engine test facility. The DR uncertainty shows the problem with a varying, high background concentration of NOx. However, there is no physical reason to believe that there are significant changes in DR from run to run. Furthermore, these uncertainties are for a single measurement, and in most cases, the DR is based on multiple measurements. The DR has no influence on the shape of the size distribution.

When the exhaust NOx concentration is low, the diluted NOx concentrations are only slightly higher than background leading to larger uncertainty. This is evident in Figure 36, which shows a consistent drop in uncertainty as the concentration of NOx in the exhaust and thus in the diluted exhaust increases. The characteristics of the 2-stage tunnel are such that the DR should not significantly change with changing engine conditions. Thus, the changes shown are likely due mainly to uncertainties in the background NOx. Only one high sensitivity NOx analyzer was available, so the plume and background NOx could not be measured simultaneously. While background values were measured regularly, rapid changes in background NOx are the likely cause of the apparent DR variations, rather than real changes in overall DR. The use of a single

overall DR for the two-stage system operating with fixed geometry and ejector pressures can be justified on scientific grounds and might have reduced scatter in the results.

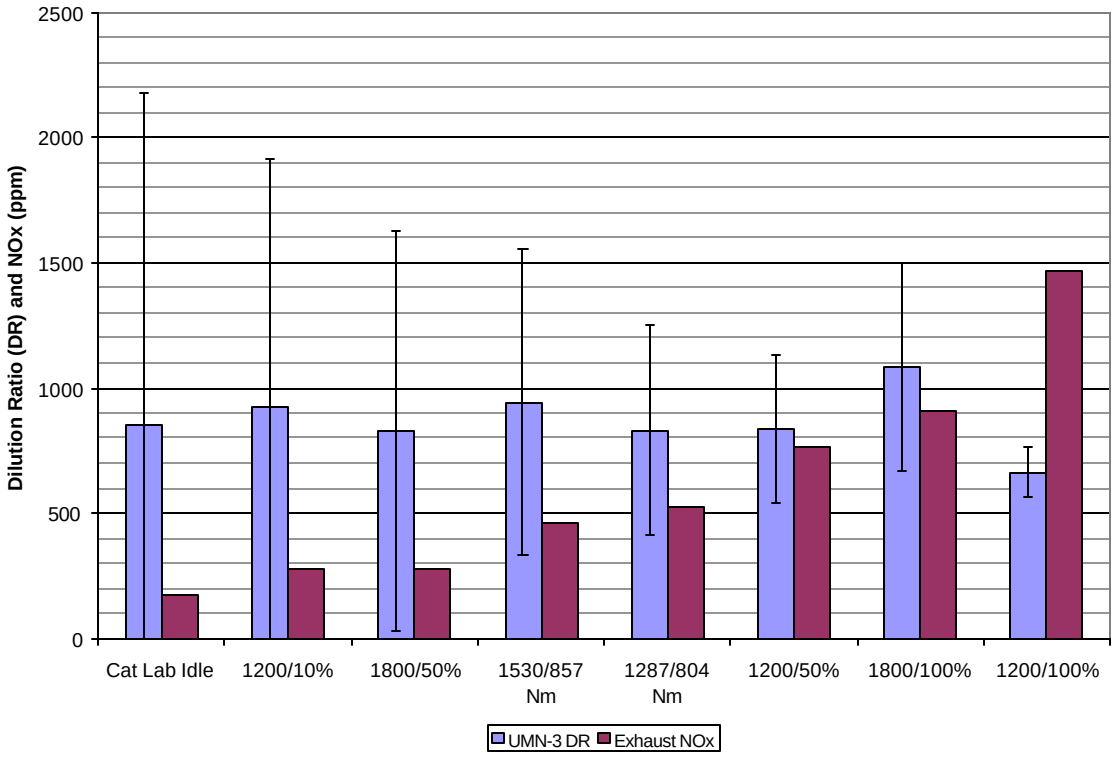

1200/100% = 1220/255 N-m. 1800/50% = 1800/1125 N-m, 1200/50% = 1200/1278 N-m, 1800/100% = 1800/2250, 1200/100% = 1220/2555 N-m

Figure 36. Dilution ratio uncertainty and NOx concentration

Specially Formulated Fuel and Lube Oil Experiments

The specially formulated fuel and lube oil experiments were conducted immediately following the completion of the Cummins portion of E-43 project and took advantage of the engine, test apparatus and aerosol instrumentation already set up in the Cummins CVS facility. The purpose of the tests was to evaluate the impact of specially formulated fuel and lube oil fuel on nanoparticle emissions. The Cummins ISM engine was used for all tests. Samples were collected from the 2-stage and CVS/ejector dilution system (CVS tunnel with an additional air ejector for secondary dilution). Cummins provided the specially formulated fuel and lube oil and the fuel and oil analyses. Break in periods for new fuels were typically about an hour at a heavy load condition selected by Cummins. The break in for the specially formulated oil was between 4-6 hrs and occurred on the night shift. A longer break in period would have been better, but the test schedule did not permit it. We will see that at lighter loads the lubricating oil has a strong influence on the nuclei mode, while at high loads the fuel becomes important.

The discussion of the specially formulated fuel and lube oil tests will focus on three operating conditions, 1200 rpm, 25 % load (482 N-m), 1800 rpm, 10 % (154 N-m), and

1800 rpm, 50 % load (776 N-m). Results from these tests are shown in appendix Figures C-1 through C-6 as size distributions, Figures C-7 through C-15 as summary bar charts, and in Tables C-1 and C-2.

Figures C-1, 2, and 3 show size distributions measured running with regular lubricating oil (4000 ppm S) with fuels of two sulfur levels, 1 and 49 ppm. The combinations of the specially formulated low fuel and normal sulfur lube oil did not create a nuclei mode at either the 1800/776 N-m or 1200/482 N-m conditions as illustrated in Figures C-1 and C-3. There is a hint of a nuclei mode at the low load condition of 1800/154 N-m shown in Figure C-2, but the error bars are large suggesting an error in one of the SMPS scans. The N/V ratios shown in Figures C-10 through C-12 and in Table C-1 rows 15-20 are all below 10^4 and the V30/V ratio less than 0.01 for all cases with the regular lube oil, except with the 1 ppm fuel at 1800 rpm, 154 N-m, the condition that showed the peculiar intermediate mode.

Figures C-4, 5, and 6 show size distributions for tests done with the specially formulated low sulfur lubricating oil (385 ppm S) for the same three engine conditions. Specially formulated fuels with four sulfur concentrations, 1, 26, 49, and 325 ppm were tested. A large nuclei mode is present for the 26, 49 and 325 ppm S fuel with 385 ppm S oil at the 1200 RPM/482 N-m and for 1, 26, 49 and 325 ppm S at 1800/154 N-m conditions (Figures C-4 and C-5). The N/V ratios are > 10^4 and V30/V ratios > 0.01. At the higher load condition of 1800/776 N-m, only the 325 ppm S fuel created a nuclei mode, and again the N/V ratio is > 10^4 and V30/V ratio greater than 0.01. Also shown on Figures C-4 through C-6 is the impact of the thermal denuder (TD) on the nuclei mode. The TD was only displayed in the charts with the condition that gave the biggest nuclei mode, 325-ppm S fuel and low S oil. When present, the nuclei mode disappeared when the TD was connected to the SMPS suggesting that the nuclei mode is composed of volatile material.

Figures C-13 through C-15 compare active surface area measurements made with the DC, with the calculated active surface from the SMPS size distributions. The photoemission characteristics of the particles measured with the PAS are also shown. A linear scale rather than logarithmic is used. In most cases, the DC and SMPS active surface areas agree to within about 25 %. The PAS response was nearly independent of fuel and lubricating oil for the 1200 rpm, 25 % load case at roughly $3x10^6$ fA. The exception was the 1-ppm S fuel, regular lube oil case which exceeded $10x10^6$ fA. As noted above, this case also showed an unusual size distribution. At 1800 rpm, 10 % load PAS levels are higher and more variable, ranging from about 10 to $23x10^6$ fA. The PAS levels at 1800 rpm, 50 % load are lower again and less variable, ranging from roughly 7 to $10x10^6$ fA. The PAS is claimed to respond to particle bound PAH, but it also responds to the PAH like character of carbonaceous agglomerates. A further complication is that liquid layers on the particle surface reduce the PAS response. Taking all the engine conditions together, it may be seen that there is a slight reduction in response with the 325-ppm sulfur fuel. This may be related to particle bound sulfuric acid.

The most surprising result of these tests is the unexpected influence of the specially formulated lubricating oil. Contrary to expectations, the specially formulated low sulfur lubricating oil led to an increase in nanoparticle formation in nearly all cases. This was particularly clear for the 1200 rpm, 25 % load case. Here, with the specially formulated low sulfur lube oil, both 26 and 49 ppm fuels gave much higher total number concentrations, N/V ratios, and V30/V ratios than the 49 ppm fuel running with regular lube oil. The same was true but to a lesser extent at 1800 rpm, 10 % load. The fuel sulfur also influenced nanoparticle formation. The 1800-rpm, 10 % load case showed a consistent increase in the size of the nuclei mode as the fuel sulfur content was increased. The effect was strongest at 1800 rpm, 50 % load where there was essentially no nuclei mode for 1, 26, and 49 ppm S fuel and a large one for the 325-ppm sulfur fuel. Thus, the lube oil composition had the strongest influence on nanoparticle formation at light load conditions while fuel sulfur played a greater role at higher speed and load.

At this point, it is only possible to speculate on why the specially formulated low sulfur oil led to increased nanoparticle formation. The proprietary chemical formulation of the oil may be different to compensate for the removal of sulfur containing additives. In addition, the test with the specially formulated low sulfur oil began after only an overnight break in of the oil. Consequently, the oil could have still been releasing volatile components that led to nanoparticle formation. In any case, whether the increased nanoparticle formation resulted from the lack of adequate break in time, the oil formulation, or some combination of the two, these tests clearly show the important role the lube oil can play in nanoparticle formation. They are consistent with the observations made by others (Sakurai, *et al.*, 2001, Ziemann, *et al*., 2002) that suggest that the heavy ends of lube oil are a major component of the nanoparticles formed by a Diesel engine.

Effect of Catalyzed Diesel Particulate Filter

A catalyzed Diesel particulate filter (CDPF) was evaluated during the fuel sulfur experiments. Only specially formulated low S oil and specially formulated 1 and 26 ppm S fuel were used with the CDPF tests. Figures C-16 to C-19 show SMPS size distributions without the trap and with the trap in place with and without the TD. The filter reduces the concentrations of particles (mainly solid) in the accumulation mode by two orders of magnitude or more. However, at high load conditions (1800 rpm, 1552 N-m (rated power) and 1200 rpm and 1927 N-m (rated torque)) a nuclei mode is apparent after the CDPF when the TD is not being used. The nuclei mode disappears when the aerosol passes through the TD at 300°C prior to entering the SMPS demonstrating that the particles are volatile. For the 1200 rpm, 1927 N-m condition, particle concentrations in the nuclei mode region are more than ten times higher with the filter than without. This is especially true with the higher sulfur (26 ppm) fuel. Exhaust temperature was > 400°C for these engine conditions, making it likely that sulfur is oxidized from SO_2 to SO_3 by the catalyzed filter. The SO_3 forms sulfuric acid that nucleates during the cooling and dilution.

CPC data shown in Figure C-20 also show the influence of engine operating conditions on the formation of volatile particles downstream of the CDPF. At about 16:00, the

engine is operating at its rated power condition with the thermal denuder, operating at 300°C, placed ahead of the CPC. The CPC concentration is < 10^4 particles/cm^3. At about 16:05, the TD is removed and the CPC concentration increases to >10^8 particles/cm^3 indicating the particles emitted from the CDPF were volatile. At 16:12 the engine is set to a light load condition and the CPC count falls dramatically. Apparently, the low exhaust temperature associated with the light load condition prevents the penetration through (or formation of) the particle precursors that lead to nanoparticles forming downstream of the CDPF. At this condition, volatile particles are still being formed but their concentration is much lower. Adding the TD at 16:23 only drops the total number by about a factor of 10. The TD is then removed and the engine is set to its rated torque condition at 16:31. This engine condition saturates the CPC and causes the DC signal to increase sharply and then decay. Apparently, switching from the light load to the heavy load condition caused the creation of significant particle surface area as well as number downstream and the CDPF. The DC signal drops back down into the noise level of the instrument within about 5 minutes. This peak is probably due to high temperature causing the release of stored materials from the CDPF. When the TD is added upstream of the CPC the number concentration again drops and continues to decay. Since the CPC/TD combination should mostly detect solid particles, this decay suggests a transient release of solid particles although the concentrations are low. When the TD is removed at 16:47, the CPC saturates again indicating that very large number of tiny particles continues to be released. This high number count is consistent with the large nuclei mode shown in Figure C-17 for the same engine and fuel combination. The last engine mode at 17:06 is an intermediate load and speed. At this condition, number emissions are low and the response to the TD suggests that they are mainly solid because the drop is not far from the TD losses for very small particles.

TD Effects, Transient Tests and MOUDI Samples

Effect of Thermal Denuder in Laboratory Transient Tests

The influence of the TD has been investigated in many different ways during the E-43 program. In addition to the steady-state tests described above, it was used during transient testing for the Cummins fuel and lube oil sulfur studies. The TD was connected at times to the SMPS, the CPC, or the surface area instruments (PAS and DC) and operated at 300°C. At this temperature, highly volatile organic carbon and sulfuric acid (30° – 125°C), ammonium sulfate and bisulfate (125°-175°C) and low volatile organic carbon (175°-300°C) will be volatilized (Burtscher, *et al*., 2001). Aerosol was directed either through the TD to the instruments or around the TD to the instruments. The sample line length was approximately the same in both cases. Penetration of 20 nm particles through the TD at an operating temperature of 300°C, at a flow rate of 0.3 l/min, was determined experimentally to be about 63 %. Burtscher, *et al*., 2001, report details on the TD, including information on particle losses.

Figure 37 illustrates the responses of the CPC and surface area instruments during the FTP transient cycles that were run during the Cummins specially formulated fuel and lube oil tests in the Cummins CVS laboratory. In this case, the ISM engine was fueled

with Diesel fuel containing 1 ppm S and the engine was using oil with 300 ppm S. The TD reduces the CPC particle number concentration (shown in blue) much more than the surface area concentration. There is nearly an order of magnitude reduction in the CPC concentration. This is because in a typical Diesel aerosol size distribution, often more than 90 % of the particles are in the nuclei mode, but less than 20 % of the surface area is in this mode. We believe, based on our data and the data collected for the TDPBMS portion of the project, that most of the particles in the nuclei mode are composed of volatile material. Thus, the TD has a greater impact on reducing the CPC number concentration than it does on reducing the surface area concentration.

Figure 38 illustrates the consistency of the FTP cycle. To prepare this chart, multiple FTP cycles were overlaid on each other and an adjustment was made in the time base. During this period the SMPS was operated in the single channel mode. In this mode, the SMPS acted as a classifier for the CPC so particle counts were measured for an individual channel. Three particle sizes were obtained by adjusting the SMPS voltage, 10 nm, 34 nm and 100 nm, and the calculated size distribution is shown in Figure 40 and discussed below. During these cycles, the TD was switched from the SMPS in the 10 nm single size mode, to the stand alone CPC, to the DC/PAS, which have a common sample inlet.

The impact of the TD on the 10 nm size particles is shown in Figure 39. Again, it is clear that the particles are composed mainly of volatile material, as there is typically a 1 to 2 order of magnitude reduction in the concentration of 10 nm particles when the TD is on. Also note that the three particle sizes shown in Figure 39 do not track with each other, as the size distribution is changing throughout the cycle. Of the three sizes, the 10 nm particles show the most variation.

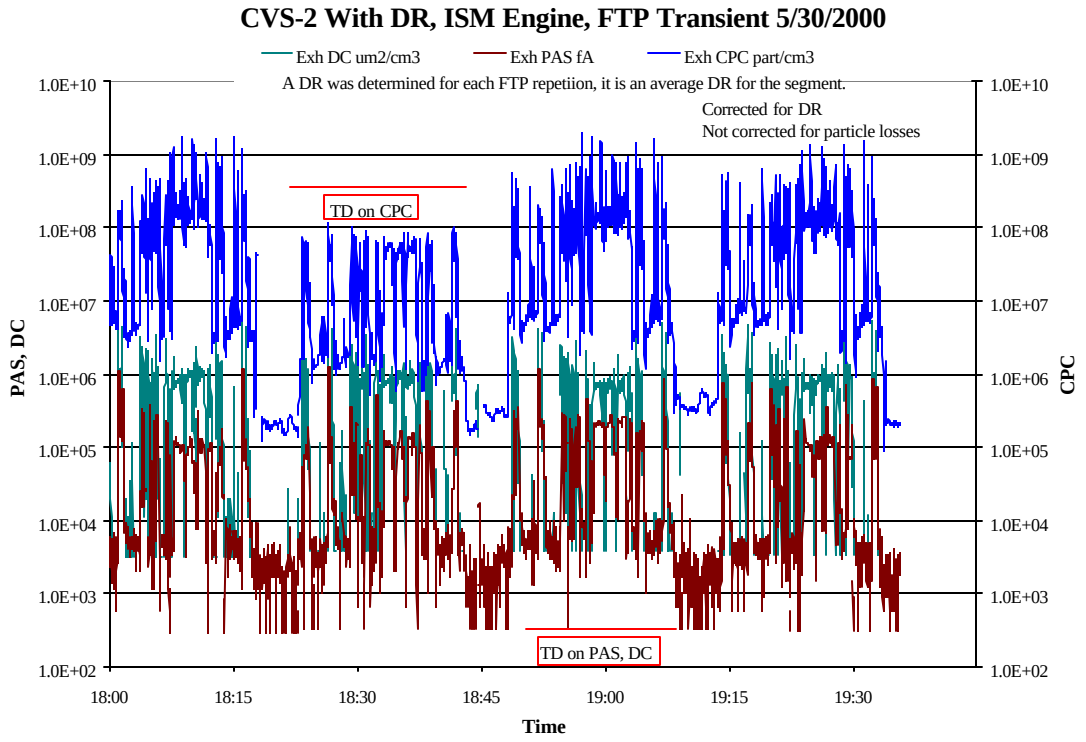

Figure 37. Impact of TD on CPC, PAS and DC during multiple FTP transient cycles

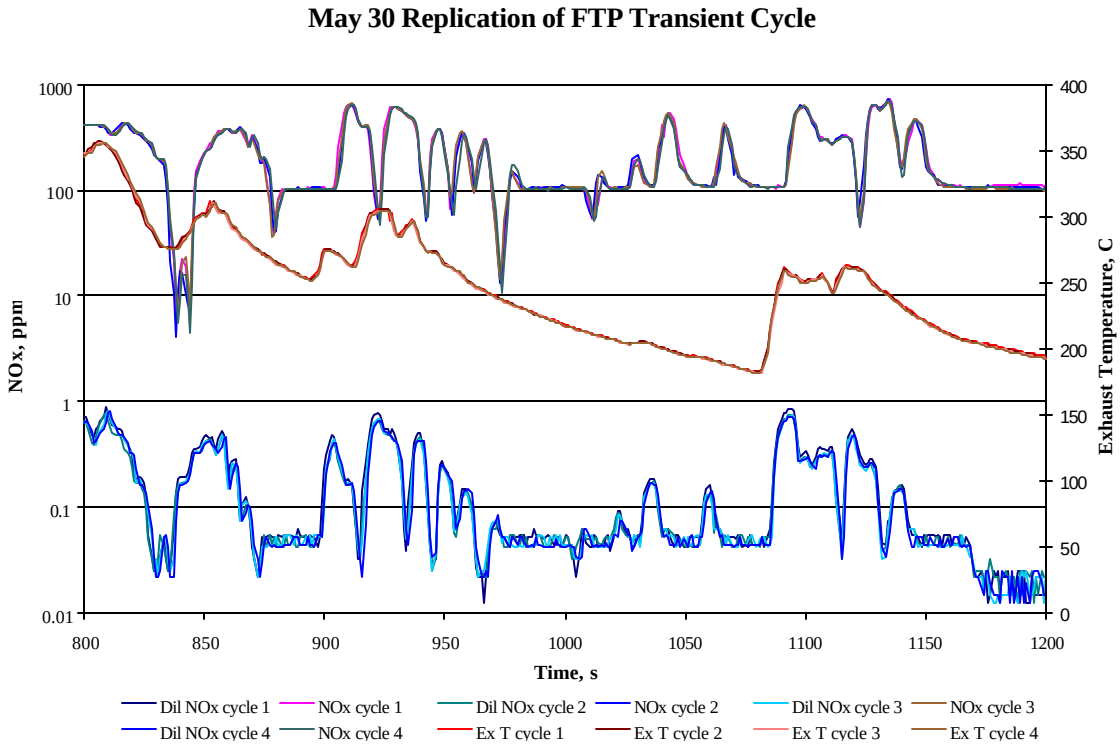

Figure 38. Replication of the FTP transient cycle in the Cummins CVS laboratory

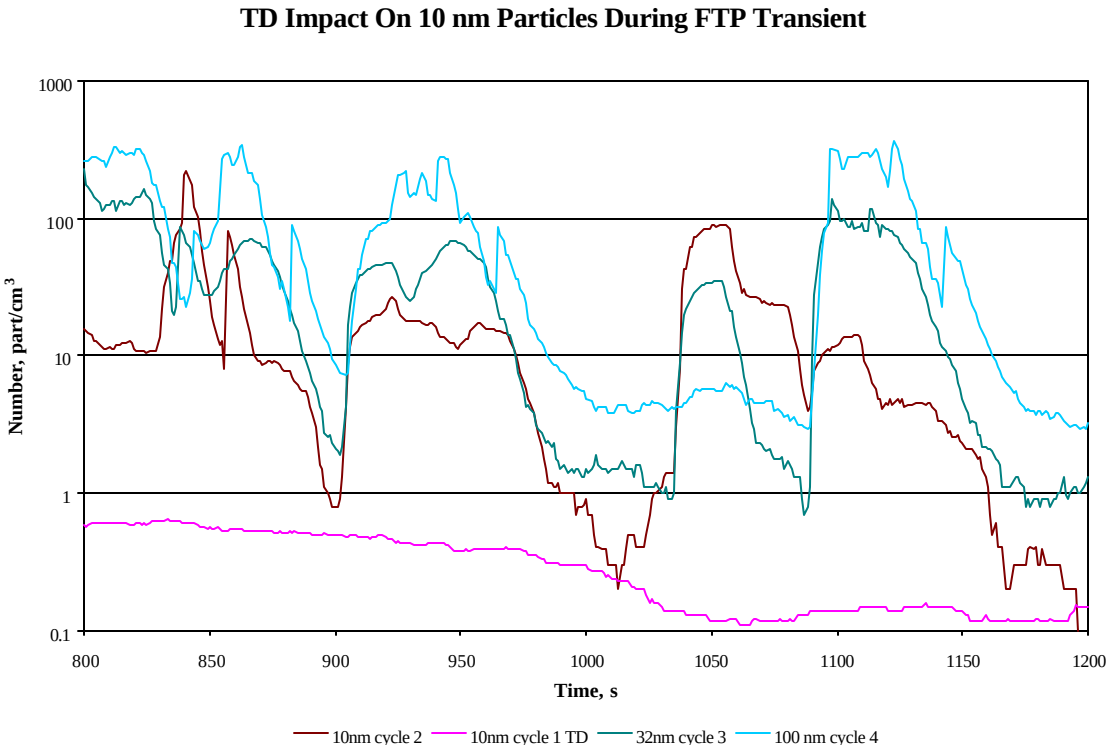

Figure 39. Impact of TD on 10 nm size particles during FTP transient cycle

Table 16 summarizes the transient cycle thermal denuder data shown in Figure 37. For these calculations, the dilution ratio, which constantly changes over the FTP cycle was not used. Note the repeatability of the CPC from cycle to cycle. The trend of decreasing CPC count from test to test might reflect the storage and release phenomenon that we have observed. At 10 nm nearly all the material (ratio of TD/no TD = 0.018) is volatile by number count. On the other hand, by DC surface area that fraction is 0.81. This is consistent with particle surface area dominated by solid particles. It is interesting to note that the PAS value increases slightly when the TD was placed on the inlet to the DC and PAS. It has been reported by PSI that the PAS response increases in the absence of volatile material.

Table 16. Transient cycle summary with the TD in various positions

Cycle	TD position	CPC part/cm^3	DC um^2/cm^3	PAS fA	10 nm part/cm^3	32 nm part/cm^3	100 nm part/cm^3
1	10 nm	6690	377	65	0.27		
2	CPC	1020	310	47	15		
3	DC/PAS	5550	254	73		37	
4		5340	307	70			100
Mean no TD		5860	313	64			
SD no TD		730	61	12			
Ratio TD/no TD		0.17	0.81	1.14	0.018		

Finally, the transient FTP data were converted to an equivalent size distribution and shown in Figure 40 without consideration to the dilution ratio. The four transient cycles were aligned in time using exhaust temperature and NOx data as references of cyclic events. Then the average concentration in each size channel (10, 32, and 100 nm) was

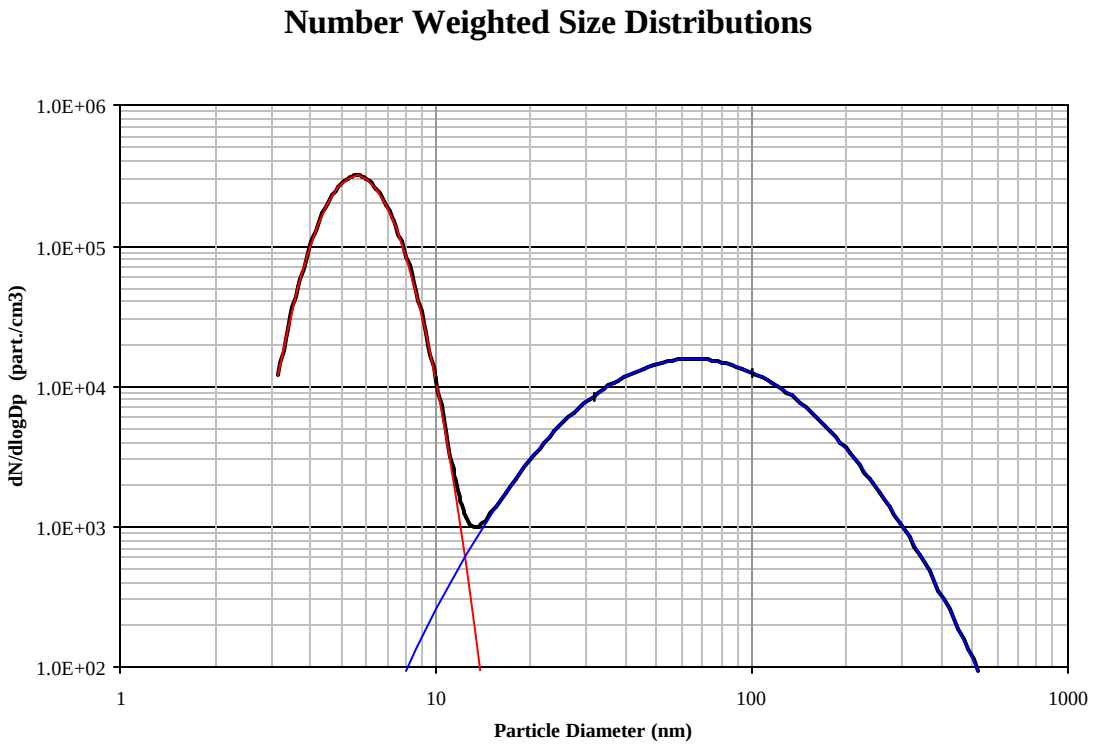

Figure 40. Calculated number weighted size distribution for FTP transient cycle

calculated for each of the cycles. The 10 nm channel with the thermal denuder did not enter into these calculations. The particle number concentrations in each channel were converted into dN/dlogDp using the following relationship:

$$dN/d\log Dp = dN/(\log Dp_{upper} - \log Dp_{lower})/f_{(charged\ x\ Tr)}$$

Here, dN is the CPC concentration in a particular channel, Dp_{upper} and Dp_{lower}, are the upper and lower diameter limits of a given size channel and $f_{charged}$ is the fraction of particles charged at that particle size (Wiedensohler, 1988) and Tr is the transfer function assumed to be the ideal value of ½(Knutson, 1975). The upper and lower diameter limits are a function of the instrument resolution. For our experiments, the resolution (res) given by the ratio of sample flow to sheath airflow, was 0.15. The resolution determines the upper and lower electrical mobility bounds of a particular channel and these mobility bounds in turn determine the diameter bounds. The governing relationships are:

$$Z(Dp_{upper}) = Z(Dp_{center})*(1 + res)$$

and

$Z(Dp_{lower}) = Z(Dp_{center})*(1 - res)$

The values of dN/dlogDp at the three sizes were converted to a bimodal log normal distribution. This distribution requires 6 parameters for its specification, the concentration, geometric mean diameter, and geometric standard deviation for each mode. Thus, we have three equations and six unknowns and the system is under-specified. However, we also have the average total number concentration from the CPC, which gives us another equation. Finally, we have observed that although the size and concentration of the particles in the various modes can vary, the standard deviations are usually in a fairly limited range. We used typical values observed on the steady-state tests for these parameters. The values assumed are geometric standard deviations of 1.25 and 1.92 for the nuclei and accumulation modes, respectively. The number fraction in the nuclei mode and the geometric mean diameters of the nuclei and accumulation modes are the remaining unknowns. Solution of the system of equations with these assumptions leads to a number fraction in the nuclei mode of 0.87 and mean diameters of 5.6 and 65 nm for the nuclei and accumulation modes, respectively. The combined use of the CPC and SMPS allows the number of particles below the sizing range of the SMPS to be estimated. Examination of Figure 40 reveals that for this low sulfur fuel, most of the nuclei mode is below 10 nm and below the sizing range of the conventional, long column SMPS.

Figure 41 shows another instance in which the TD was alternately connected and not connected to the CPC. In this case, the Cummins ISM engine was operated at 1800 rpm, 50% load with 325 ppm S fuel and 385 ppm S oil. The reduction in the CPC concentration with the TD is even more drastic in this case than the preceding situation where the ISM was operated with 1 ppm S fuel and 385 ppm S oil. The role of volatile sulfur compounds is apparent. The average CPC count without the TD was 6.63×10^8. When the TD was placed in line before the CPC the average dropped by more than 90 % to 4.36×10^7. Additional TD data were also given in the description of the fuel and oil sulfur tests.

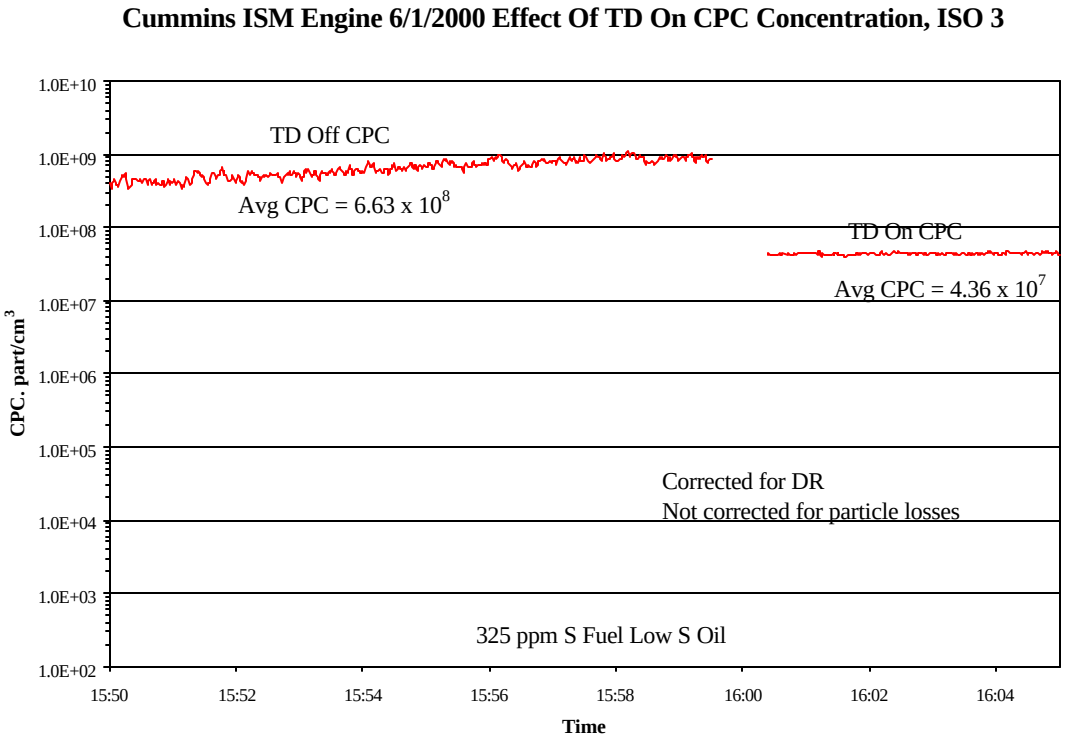

Figure 41. Impact of thermal denuder on CPC concentrations, ISM engine, ISO mode 3 (1800 rpm, 50% load)

Effect of TD in On-road Tests

During the Caterpillar chase experiments, the TD was used in conjunction with bag-sampled aerosol and the SMPS. Data were obtained for the 3406E engine with loaded trailer and EPA fuel at 40 cruise, 60 cruise, and acceleration conditions. Data were also acquired for the 3406C engine (with EPA fuel) for the 60 cruise condition, in both loaded and unloaded trailer configurations.

In the following charts (Figures 42 - 46), the average SMPS distributions for each of these conditions was plotted with the average SMPS distributions for the same condition, but with the aerosol passed through the TD at a temperature of 300°C. In addition, the pre-loss non-volatile fraction (prior to any TD or sampling system loss corrections) is also plotted. The volatile fraction can be computed from these data by subtracting the non-volatile fraction from 1.0.

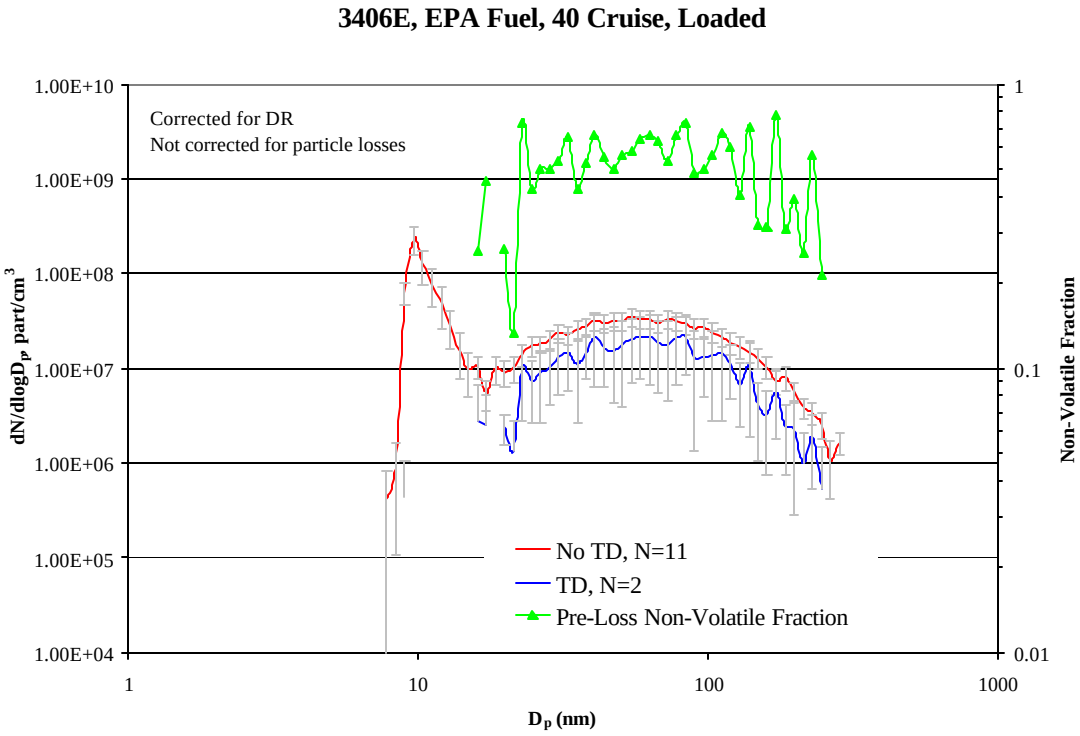

Figure 42. 3406E engine, EPA fuel, 40 cruise, loaded, with and without TD

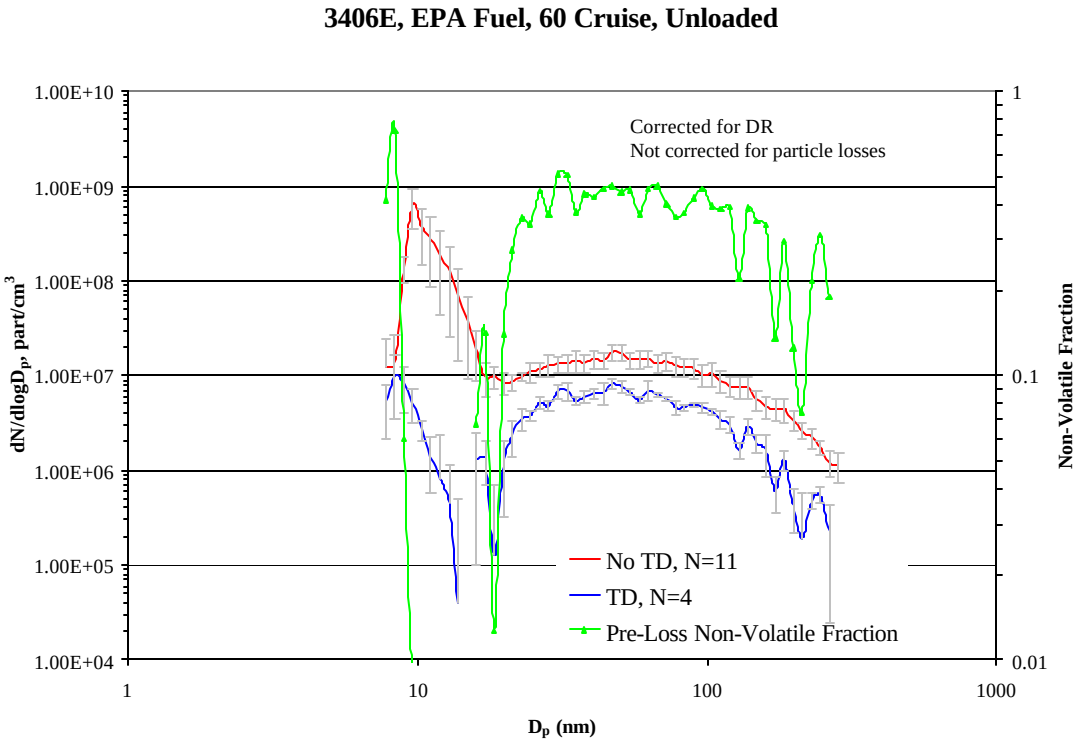

Figure 43. 3406E, EPA fuel, 60 cruise, no load, with and without TD

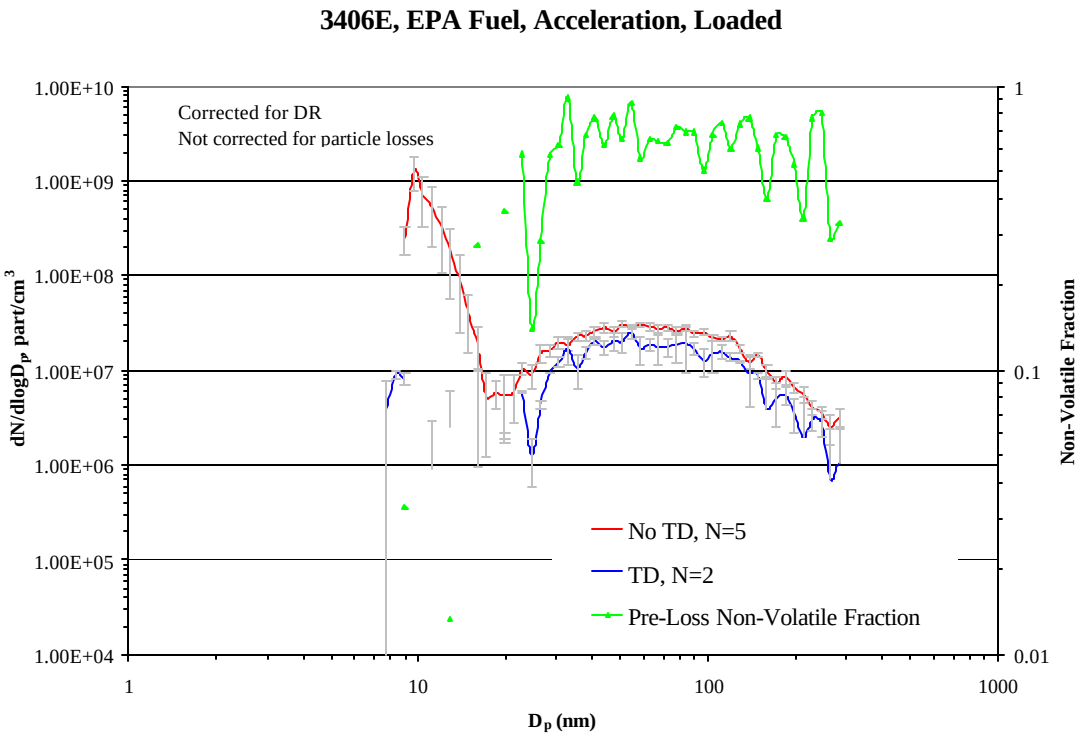

Figure 44. 3406E engine, EPA fuel, acceleration, loaded, with and without TD

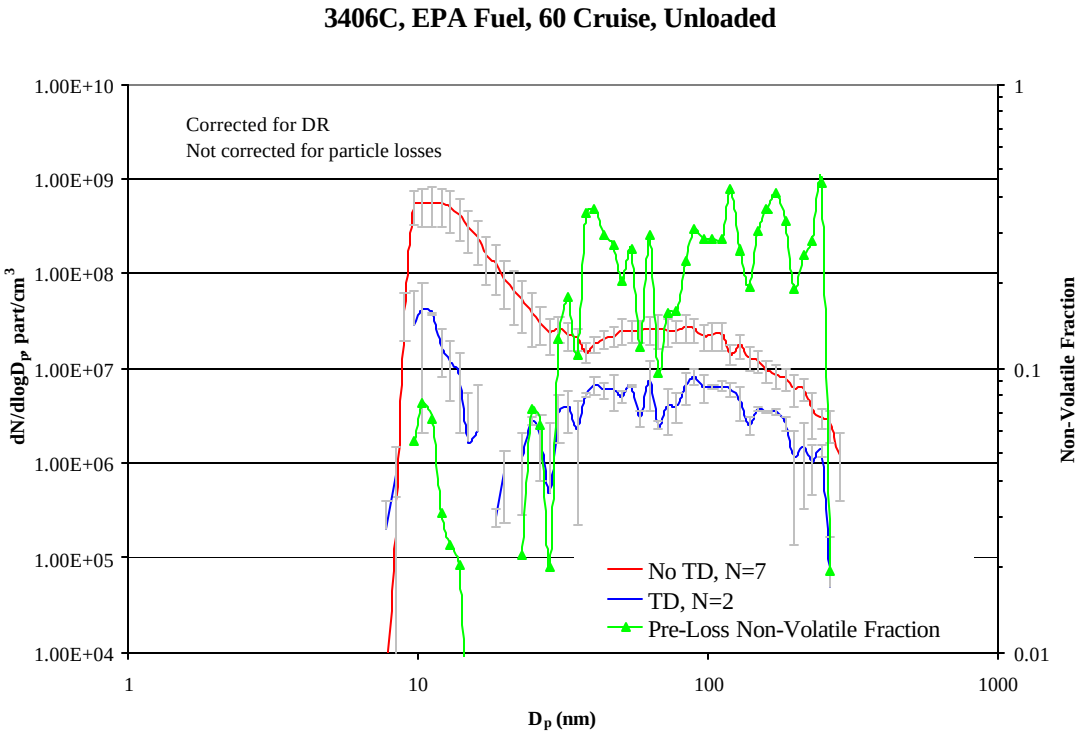

Figure 45. 3406C engine, EPA fuel, 60 cruise, no load, with and without TD

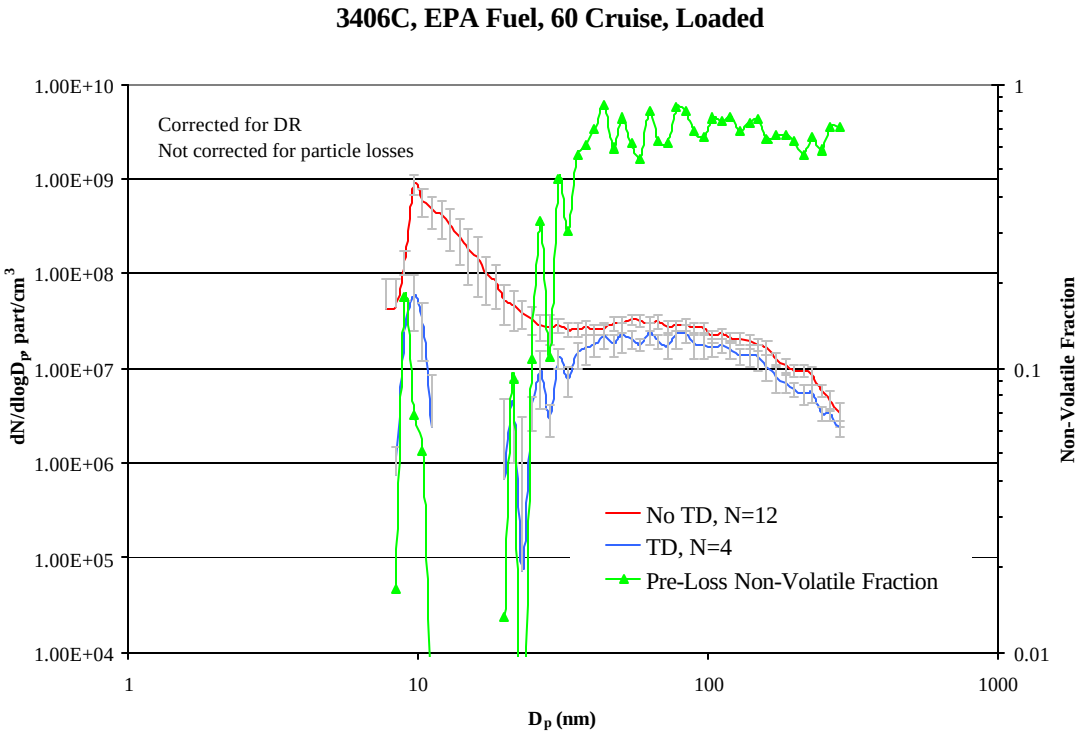

Figure 46. 3406C engine, EPA fuel, 60 cruise, loaded, with and without TD

The error estimates for volatile and non-volatile fraction for on-road work are substantial and further research is necessary to adequately characterize the statistical significance of these results. However, these data do suggest a few findings of interest.

As suggested elsewhere, it appears that the on-road nuclei mode is largely volatile in nature. For all cases, the non-volatile fraction for particles less than 20 nm in diameter is less than 0.1. Even more interesting for all cases, except the 40 cruise, loaded trailer case for the 3406E engine, is the appearance of a small mode at 7-10 nm when the aerosol is passed through the thermodenuder (see Figured D-2 through D-5). This finding suggests that the nuclei mode is composed largely of volatile particles, but the smallest particles may be as much as 10 % or more non-volatile, possibly metal compounds from lube oil ash or the like. Abdul-Khalek, *et al*., (1998a) used a catalytic stripper, a device similar to the TD, and reported a non-volatile residue after heating Diesel aerosol. However, he reported a lower fraction, ~1 %. On the other hand, there is little evidence of a solid residue except the usual lower end of the accumulation mode in the Cummins fuel and oil sulfur tests. Again, further study is required to answer these questions.

MOUDI Samples

During the course of the E-43 project, MOUDI and nano-MOUDI samples were collected. These samples were primarily intended for chemical analysis, but additional experiments were conducted to determine particle bounce and to compare the MOUDI and SMPS size distributions. The MOUDI is an inertial impactor that classifies aerosols

using the particle aerodynamic diameter while the SMPS classifies aerosols using the electrical mobility of the particle. The volume distribution calculated by the SMPS is often compared to the mass distribution determined from the MOUDI because a volume of 1 $\mu m^3/cm^3$ corresponds to a mass of 1 $\mu g/m^3$ for particles with a density of 1 g/cm^3. However, this comparison is only valid when the density of the particle is approximately 1 g/cm^3. Park, *et al*., (2001) have shown that the actual effective density of Diesel exhaust particles decreases as size increases from about 1 g/cm^3 at 50 nm to 0.3 g/cm^3 at 300 nm SMPS mobility diameter. The effect of this variable density is illustrated in the section below on the MOUDI data obtained with the C-12 caterpillar engine.

A variety of 37 mm substrates were evaluated during the E-43 project. These include the following: greased and ungreased substrates made of Al, Teflon, and Mylar. Either 37 or 47 mm Teflon or quartz filters were used on the last stage. The grease used to coat the substrates was Apiezon L grease dissolved in HPLC grade toluene.

Wind Tunnel

The UMN collected nano-MOUDI samples at the Langley wind tunnel in Langley, VA. The nano-MOUDI was on a scaffold that was situated directly behind the test truck and dynamometer. The scaffolding was positioned so that the nano-MOUDI was sampling just below the plume centerline. Five nano-MOUDI samples were collected with an average sampling time of 4 hr 31 min. No plume dilution ratio measurements are available for this location, but WVU estimated a 75:1 dilution ratio in the plume centerline 200 in behind the exhaust stack. This estimate of dilution ratio was used in Figures 47 and 48 for the nano-MOUDI. The individual size distributions are shown in Figure 47 and the average size distribution compared to the SMPS volume size distributions are shown in Figure 48. The samples were sent to DRI for chemical analysis.

Figure 48 shows the comparison of the average SMPS volume size distribution compared to the nano-MOUDI average mass distribution. A total of 79 scans were grouped and averaged to determine the three SMPS distributions shown in Figure 48. These scans were collected while the nano-MOUDI was operating. Two periods of cruise condition with the wind speed at either 25 or 55 mph, and one period of background sampling are shown for the SMPS distributions. The shape of the volume and mass size distributions obtained from the SMPS and nano-MOUDI respectively are very similar with the difference coming in the absolute concentration in each size range. The nano-MOUDI dilution ratio was estimated from the WVU CO_2 data (DR of 75:1 at 5 m from stack) while the SMPS dilution ratio was based upon measurements in the MEL (79, 37, 68:1). It is highly likely that errors in the DR ratio measurement are responsible for much of the discrepancy observed in these data. These results have not been corrected for particle density and differences between aerodynamic and electrical mobility diameter. This correction has been done for data from a Caterpillar engine shown in Figure 62. Transforming an SMPS volume size distribution based on mobility or Stokes diameter to a mass size distribution based on aerodynamic diameter shifts it down and to the right as shown in Figure 62. Such a transformation would bring the SMPS data and MOUDI data

in Figure 48 into much closer agreement. This density correction has only been applied to Figure 62 as an example, because the density distribution used was not for the engine tested. It is likely that the form of the transformation will be the same, but it is not appropriate to apply this correction to all of our data without density information specific to the conditions in question.

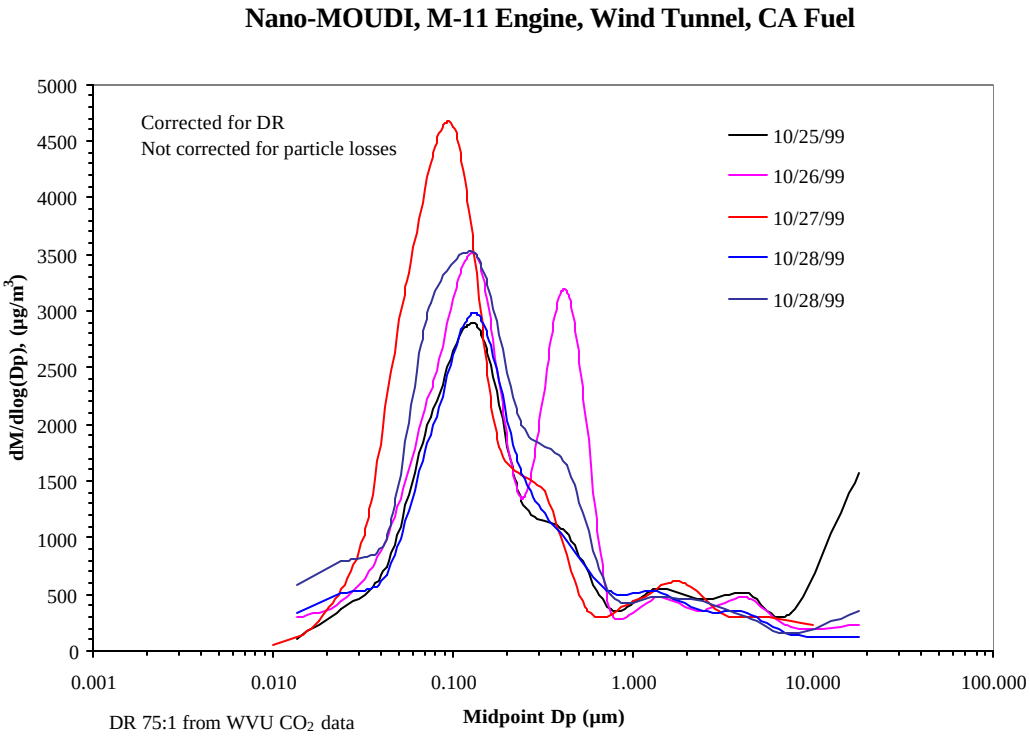

Figure 47. Nano-MOUDI size distributions from the Langley wind tunnel

The two bottom stages of the nano-MOUDI, with mean diameters of 13 and 24 nm, show much higher concentrations than the SMPS. Differences are much too large to be explained by density effects and are likely to be an impactor artifact. The nano-MOUDI was located on scaffolding at the wind tunnel, and was subject to a lot of vibration. It is possible that excess vibration adversely affected the performance of the nano-MOUDI. However, a similar artifact was found in the particle bounce experiments suggesting particle bounce or other artifacts play a role.

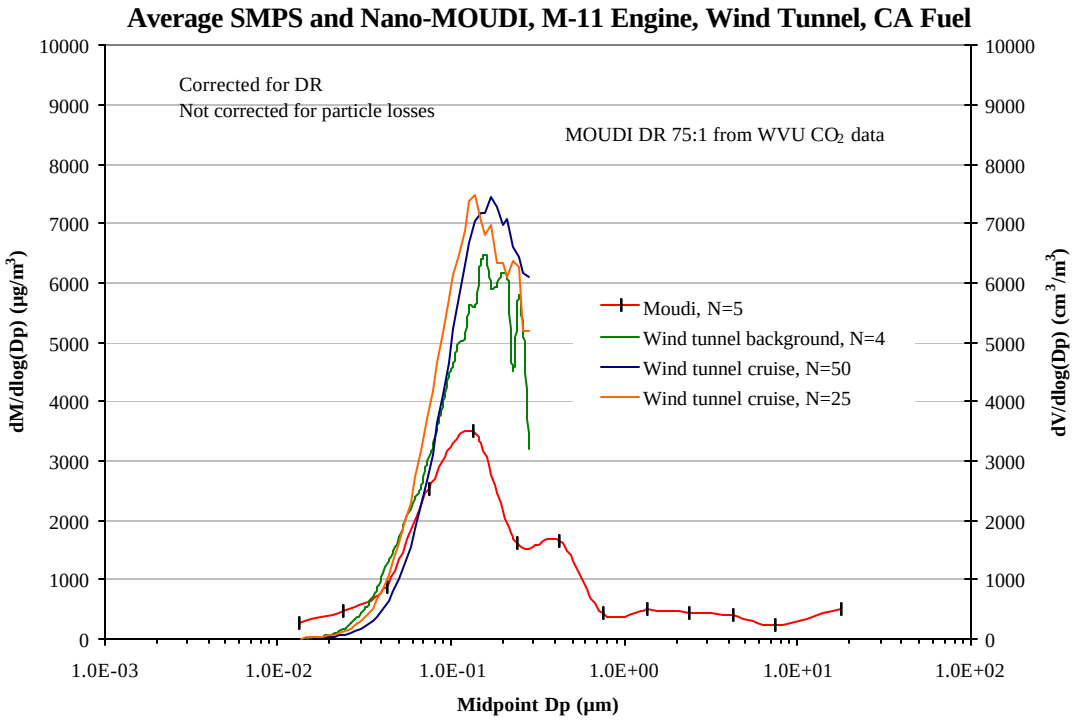

Figure 48. Average SMPS and nano-MOUDI distributions from the wind tunnel

Bounce Experiments

The objectives of the bounce tests were to determine the extent of particle bounce within the nano-MOUDI and to recommend a scheme for greasing substrates that would minimize bounce while at the same time allow for chemical analysis of some substrates. Particle bounce occurs when large particles are not retained on the proper stage of the impactor but instead pass on to lower stages where incorrect classification occurs, thus distorting the resulting size distribution. Normally, inertial classifiers like the MOUDI are operated with substrates that are coated with oil, grease or other substances that tend to hold particles on the surface of the substrate, thus minimizing bounce. However, these coatings are generally incompatible with chemical analysis.

The aerosol instrumentation used for these tests included the nano-MOUDI, MOUDI, and UMN built SMPS. The MOUDIs, provided by NIOSH, were not a "matched" set. One MOUDI was altered to accommodate the nano-stack loaned to UMN by the EPA. The other MOUDI was modified to accept a 0.056 µm stage prior to the after filter and was further modified for use with a MOUDI turner that rotated the stages to create uniform deposition on the substrates. The SMPS was used to monitor the exhaust aerosol to evaluate day-to-day exhaust aerosol consistency. The SMPS was also used to measure size distributions downstream of the 56-nm stage of the nano-MOUDI to estimate particle bounce and inter-stage losses.

Sample streams for the MOUDI and nano-MOUDI were obtained using a 2-stage dilution system similar to the ones used during the Cummins and Caterpillar experiments. The MOUDI sample was obtained after primary dilution (DR 13:1) and the SMPS sample was obtained after secondary dilution (DR 300:1). Figure 49 shows the test setup.

EPA certification fuel was used for all tests, and a Deere 4045 engine, operated at 1,000 RPM and 200 Nm (66 % load), was used as the test engine. The coatings used on the MOUDIs are shown in table 17. This relatively heavy load condition is expected to produce a relatively dry aerosol that would be likely to bounce.

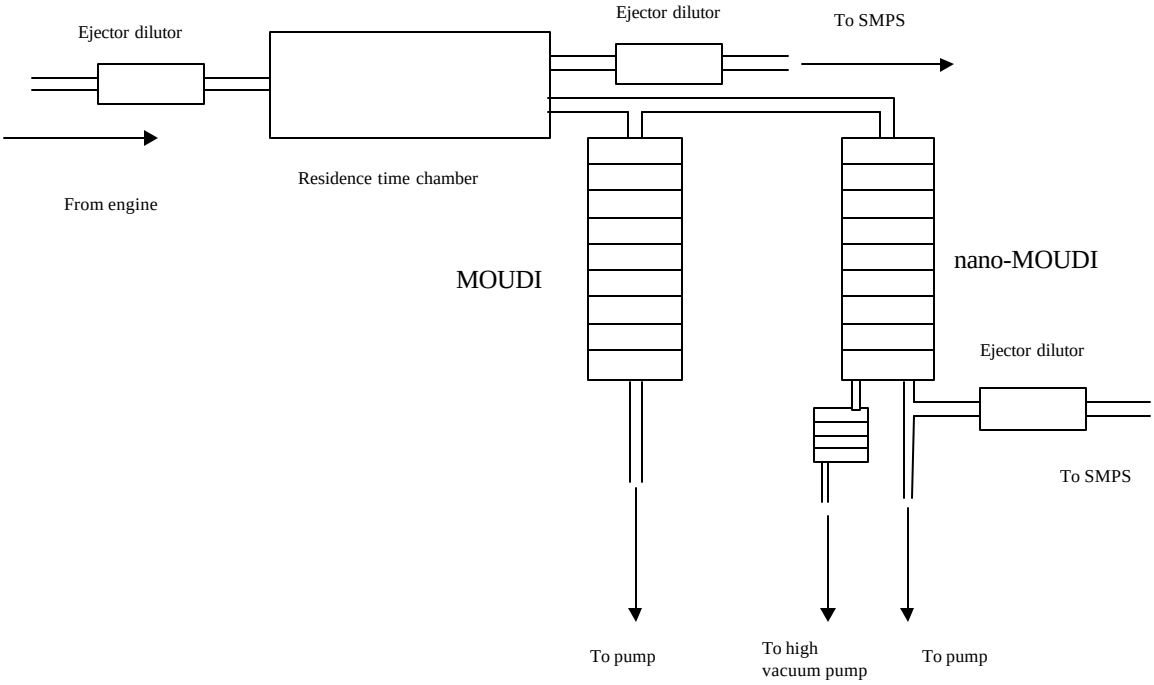

Figure 49. MOUDI particle bounce setup

Table 17. Substrate coatings used for the bounce tests

Sampler	Configuration	Number of tests
nano-MOUDI	All stages ungreased	1
nano-MOUDI	All stages greased	1
nano-MOUDI	Stages > 1000 nm greased	1
nano-MOUDI	Stages > 320 nm greased	1
nano-MOUDI	Stages > 56 nm greased	1
MOUDI	All stages greased	4
	Total number of tests	9

Tables 18 and 19 show the mass collected on each of the 9 samples. MOUDI sample number 2 was eliminated from the analysis because the substrate on stage five popped allowing unimpeded flow to pass through the stage. It is not clear why the MOUDI after filters show such great differences in mass from run to run. All MOUDI after filters showed a distinctive light brown color. Further, filter deposition, as determined by color

pattern, was uneven. The total mass collected on the greased MOUDI Al foil substrates above the after filter was 0.542 mg, 0.522 mg, and 0.463 mg, for the three samples, respectively. This is reasonable agreement between three sample runs of approximately 30 min each in duration.

Nano-MOUDI data are similar in that there is quite a variation in after filter mass; however, the filters were white in color. The total amount collected in the nano-stack (stages 0.032 µm to 0.010 µm), excluding the after filter, is shown below in table 20 as is the total amount collected on stages 10 µm through 0.056 µm. Grease appears to reduce the amount of mass collected by the nano-MOUDI stack. Thus, bounce appears to be a problem, at least for this engine and operating condition.

Table 18. MOUDI mass, all stages greased

Stage	Cut size, um	MOUDI mass by sample, mg			
		Sample 1	Sample 2	Sample 3	Sample 4
1	10.000	0.013	0.019	0.013	0.012
2	5.623	0.013	0.008	0.017	0.007
3	3.162	0.013	0.011	0.012	0.021
4	1.778	0.028	0.018	0.017	0.019
5	1.000	0.026	0.402	0.029	0.025
6	0.562	0.017	0.022	0.031	0.027
7	0.316	0.036	0.050	0.066	0.055
8	0.178	0.197	0.138	0.184	0.151
9	0.100	0.134	0.135	0.094	0.089
10	0.056	0.065	0.058	0.059	0.057
Subtotal		0.542	0.861	0.522	0.463
Filter		0.653	0.018	0.074	0.250
Control			0	0.002	-0.001

Note: Sample 2 substrate on stage 5 popped

The weighing accuracy of the Cahn 31 microbalance is $\pm$ 3 µg.

Table 19. Nano-MOUDI mass data

Stage	Cut size, um	Nano-MOUDI mass by sample, mg				
		All greased	None greased	> 1000 nm greased	> 320 nan greased	> 56 nm greased
1	10.000	0.012	0.001	0.018	0.014	0.010
2	5.623	0.016	0.007	0.014	0.010	0.015
3	3.162	0.014	0.019	0.017	0.015	0.015
4	1.778	0.018	0.020	0.027	0.021	0.021
5	1.000	0.032	0.011	0.024	0.047	-0.053
6	0.562	0.020	0.015	0.011	0.026	0.034
7	0.316	0.027	0.036	0.039	0.037	0.037
8	0.178	0.056	0.069	0.092	0.071	0.046
9	0.100	0.221	0.248	0.169	0.217	0.266
10	0.056	0.144	0.110	0.111	0.170	0.253
11	0.032	0.001	0.028	0.008	0.01	0.009
12	0.018	-0.055	0.009	0.004	0.001	0.000
13	0.010	0.008	0.004	0.006	0.005	0.002
Subtotal		0.514	0.577	0.540	0.644	0.655
Filter		0.738	0.116	0.093	0.045	0.022
Control			0.001	-0.004	-0.005	-0.002

It appears from Figure 50 that the two MOUDIs do not have the same stage cutpoints from 0.056 to 10 µm. The nano-MOUDI indicates smaller particles and a higher concentration in the size range of overlap. These MOUDIs were modified to accommodate the test matrix and the modifications were made in the MOUDI stack. Both MOUDIs are among the first MOUDIs made by MSP and the nano stack was the first made by MSP for EPA. A complete particle size calibration in the current instrument configurations has not been done, but should be done in the future in to fully interpret data collected during the E-43 project. Other tests comparing the nano-MOUDI and SMPS suggest that the nano-MOUDI is overestimating particle size in the accumulation mode region.

Table 20. Total mass collection for various nano-MOUDI stages

Grease	Stages 0.010 – 0.032 µm	Stages 0.056 – 10 µm
All greased	-0.046 mg**	0.560 mg
No grease	0.041	0.536
> 1000 nm greased	0.018	0.522
> 320 nm greased	0.016	0.628
> 56 nm greased	0.011	0.644

**One stage had a significant weight loss probably due to mishandling of the substrate.

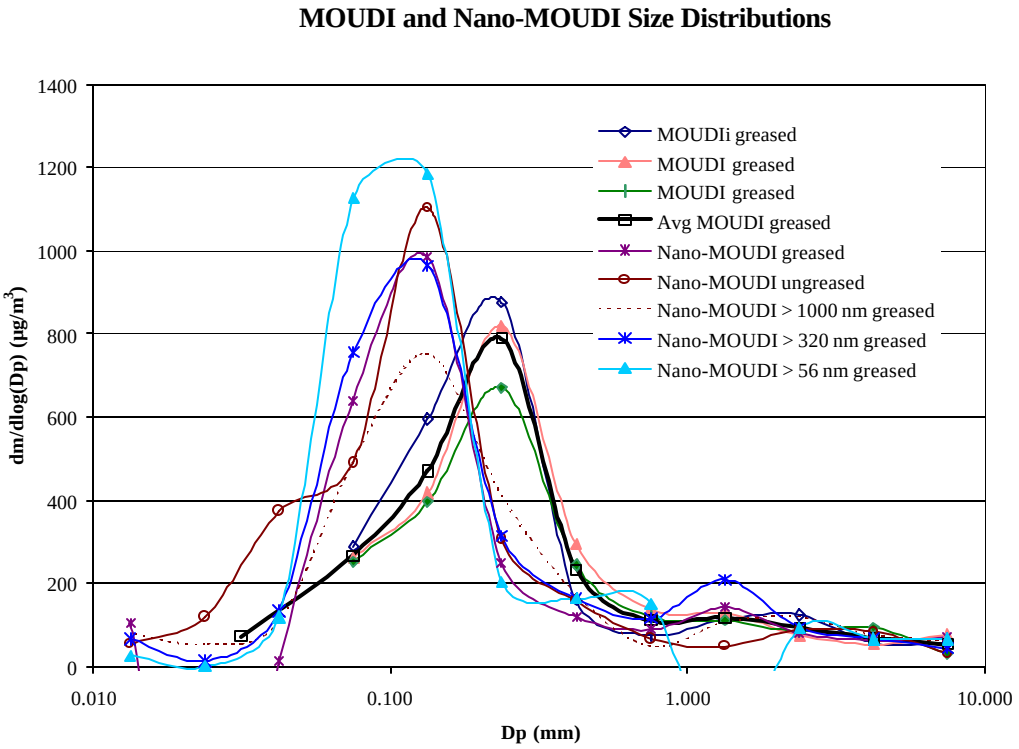

Figure 50. MOUDI and nano-MOUDI mass size distributions

A second experiment was conducted to evaluate particle bounce in the nano-MOUDI. In this experiment, the effectiveness of greased substrates for reducing particle bounce was evaluated using the SMPS. SMPS data were collected upstream and downstream of the nano-MOUDI. This approach also allowed an estimate of particle losses for particles < 56 nm in the MOUDI stages above 56 nm. The sample aerosol produced by the Deere engine is quite steady, as illustrated by Figures 51 and 53, where the dN/dlogDp peak centers around 90 to 100 nm in both cases. The penetration through the upper stages of the MOUDI is determined by taking the ratio of the downstream to upstream concentration. Figures 52 and 54 are based on figures 51 and 53 and show quantitatively the cumulative penetration through the nano-MOUDI stages above 56 nm. It is possible that, as particles collect on the greased or ungreased substrates, the efficiency of collection improves. The peak penetration efficiency occurs for 20 to 30 nm particles and ranges from about 55 to 65 %. This suggests significant losses of small particles in the upper stages.

On the other hand, it is surprising that there is a significant percentage of 100 nm particles passing though the lower stage of the MOUDI stack (56 nm). This is likely due to a combination of particle bounce and the difference between aerodynamic diameter, by which the MOUDI sizes, and Stokes diameter, by which the SMPS sizes. As an example, for spherical particles, an aerodynamic diameter of 56 nm corresponds to Stokes diameters of 99 and 165 nm for densities of 0.5 and 0.25 g/cm^3, respectively. The problem is further complicated when one considers the irregular shapes of Diesel agglomerates. Whatever the reasons, these experiments suggest that a significant fraction

of relatively large particles reach the lower stages of the nano-MOUDI. This will lead to overestimates of the mass of particles in this size range.

We did not perform a comprehensive set of experiments, but these limited data suggest that greased substrates collect more particles; thus, minimizing the deposition of larger particles on the nano-MOUDI stages (< 0.056 μm).

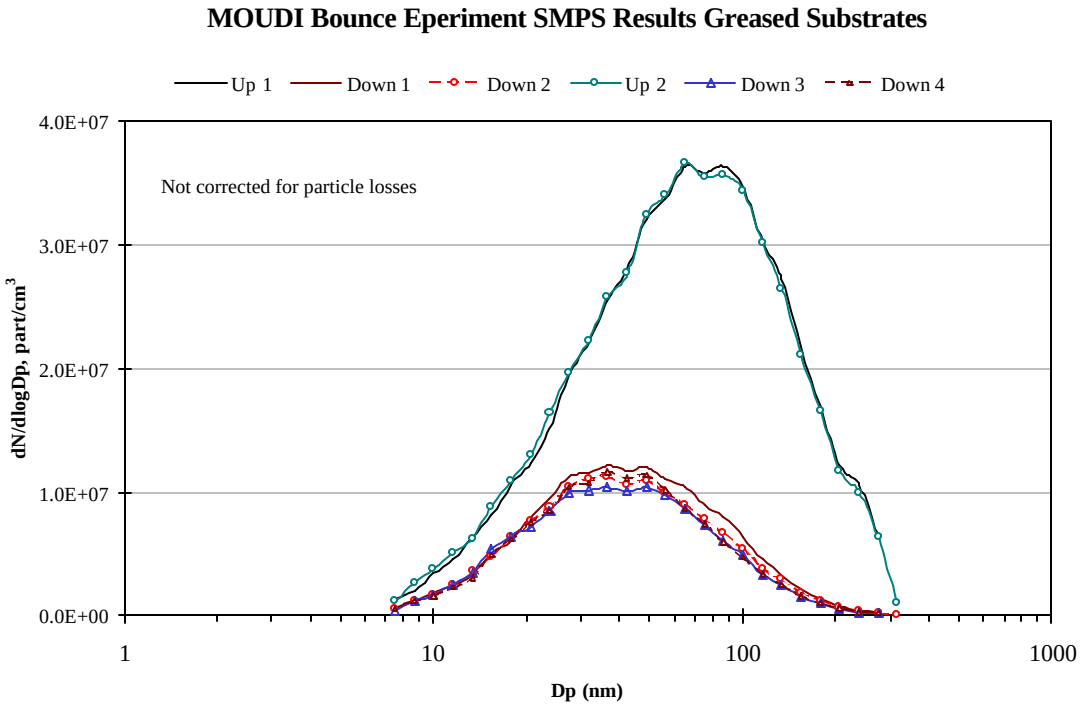

Figure 51. Nano-MOUDI up and downstream SMPS size distributions for ≥56 nm stages, all stages greased

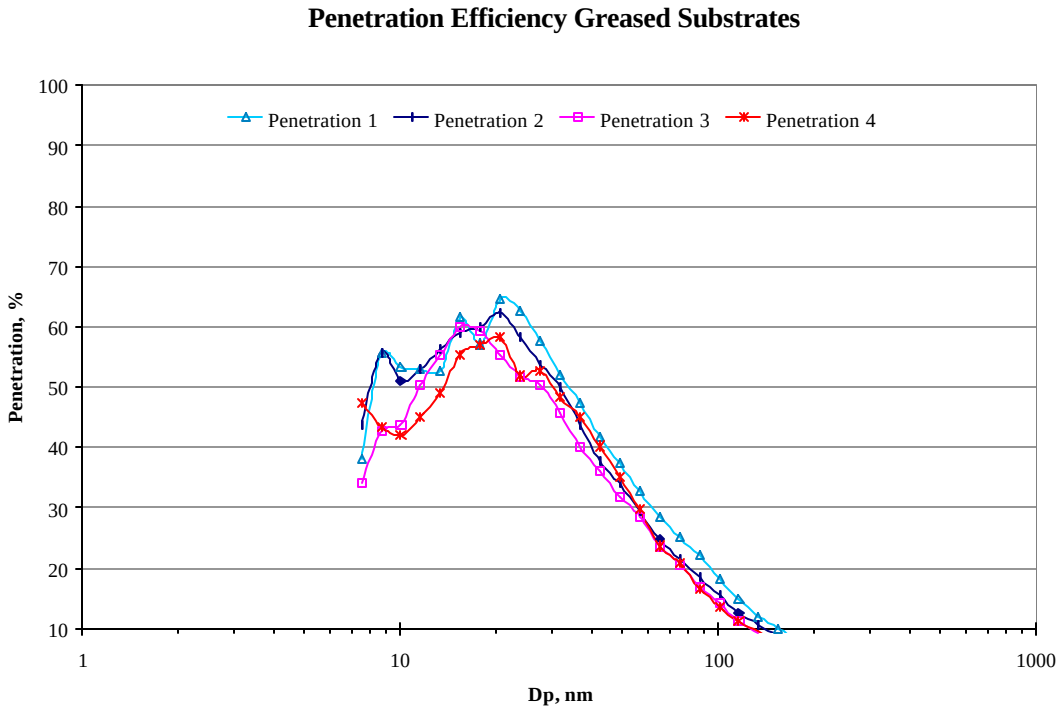

Figure 52. Change in penetration efficiency of a 30 min, greased, nano-MOUDI test

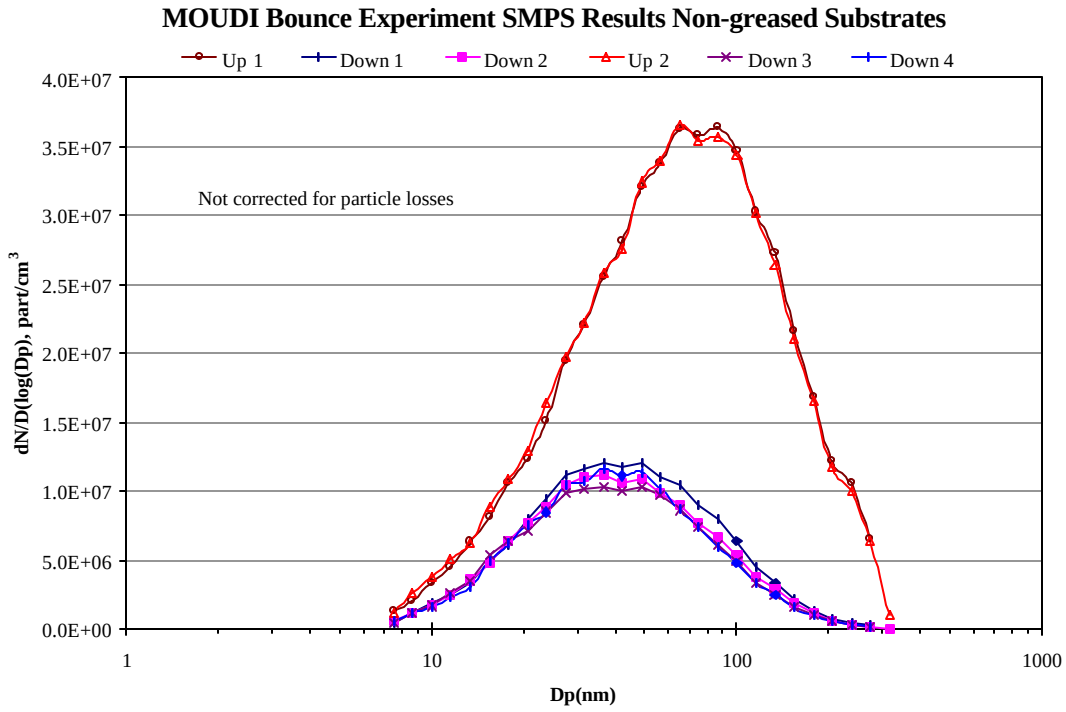

Figure 53. Nano-MOUDI up and downstream SMPS size distributions for ≥56 nm stages, all stages ungreased

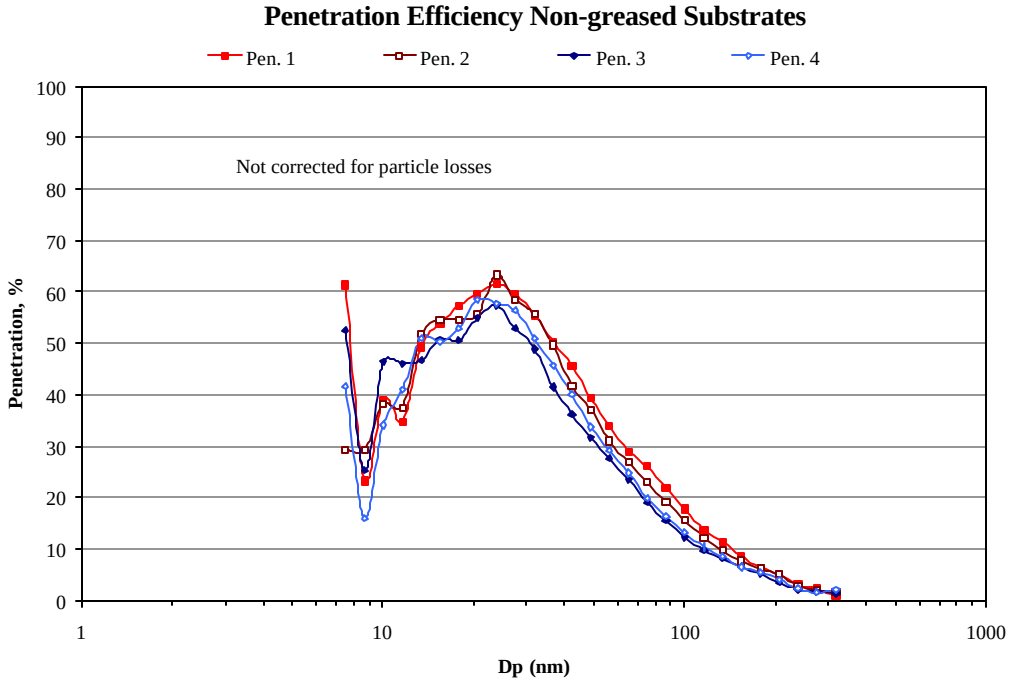

Figure 54. Change in penetration efficiency for a 30 min, non-greased, nano-MOUDI

Cummins MOUDI Samples

MOUDI and nano-MOUDI samples were collected from the Cummins CVS tunnel for chemical analysis. The ISM engine fueled with CA or EPA certification fuel generated the samples. A list of these samples is shown in Table 21. The DR in the CVS tunnel varied from 7-15:1. The MOUDI samples were taken following secondary dilution from a dilutor designed for filter sampling. For the E-43 experiments, the secondary dilution ratio was about 2:1. It was varied to control sample temperature and to maintain as high a concentration as possible for more accurate weighing of the substrates. The best estimates of the total dilution ratio for the MOUDI samples are 15:1 for the 1400 rpm, 366 N-m case and 20:1 for the 1800 rpm, 777 N-m and 1800 rpm, 1553 N-m cases.

Figures 55-58 show the size distributions. Results from four other nano-MOUDI samples were collected but are not shown because of problems in handling the substrates that preclude the results from being analyzed properly. California fuel samples are shown in green with larger symbols, and the nano-MOUDI samples are shown with dashed lines and no symbols. Corresponding SMPS data are also shown as open symbols with colors matched to MOUDI and nano-MOUDI runs. The MOUDI and nano-MOUDI are presented with no dilution ratio correction, but the SMPS data are dilution ratio corrected. The scales for the SMPS data have been adjusted to reflect the approximate dilution ratios for the MOUDI and nano-MOUDI runs. Thus, the SMPS full scale in Figure 55 is 20,000 $\mu m^3/cm^3$, which for unit density spheres corresponds to 20,000 $\mu g/m^3$, 20 times

(since the estimated dilution ratio for this run is 20) the MOUDI and nano-MOUDI scale of 1000 $\mu g/m^3$.

Table 21. MOUDI sample matrix, Cummins CVS

Date	Sample	Substrate coating	Fuel	RPM	Load, N-m	Quality	Condition
5/19/2000	M-4	B	EPA	1400	366	Good	light cruise condition
5/19/2000	NM-4	B	EPA	1400	366	Good	light cruise condition
5/22/2000	M-2	C	EPA	1800	1553	OK	ISO 1
5/22/2000	M-3	C	EPA	1800	777	OK	ISO 3
5/22/2000	M-8	B	EPA	1400	366	Good	light cruise condition
5/22/2000	NM-2	A	EPA	1800	1553	Fair	ISO 1
5/22/2000	NM-8	B	EPA	1400	366	Good	light cruise condition
5/24/2000	M-10	B	CA	1400	366	Good	light cruise condition
5/24/2000	M-5	C	CA	1800	1553	OK	ISO 1
5/24/2000	M-6	C	CA	1800	777	OK	ISO 3
5/24/2000	NM-10	B	CA	1400	366	Good	light cruise condition
5/24/2000	NM-6	A	CA	1800	777	Good	ISO 3
5/31/2000	M-7	C	NA	NA	NA	OK	Background
6/1/2000	M-11	D	NA	NA	NA	OK	Dynamic Blank - Abs Filter

A = greased to 0.056, no grease below; B = no grease; C = alternating grease
D = 10, 3.2, 0.56 stages only greased

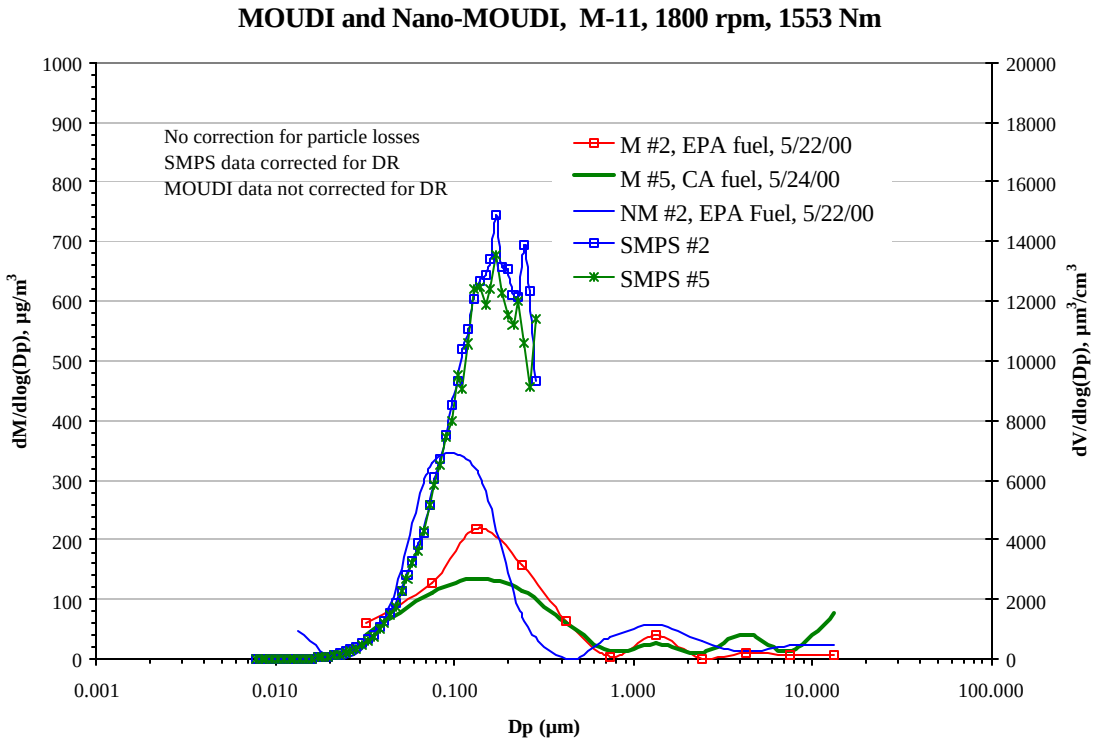

Figure 55. Cummins ISM MOUDI samples 1800 RPM, 1553 Nm

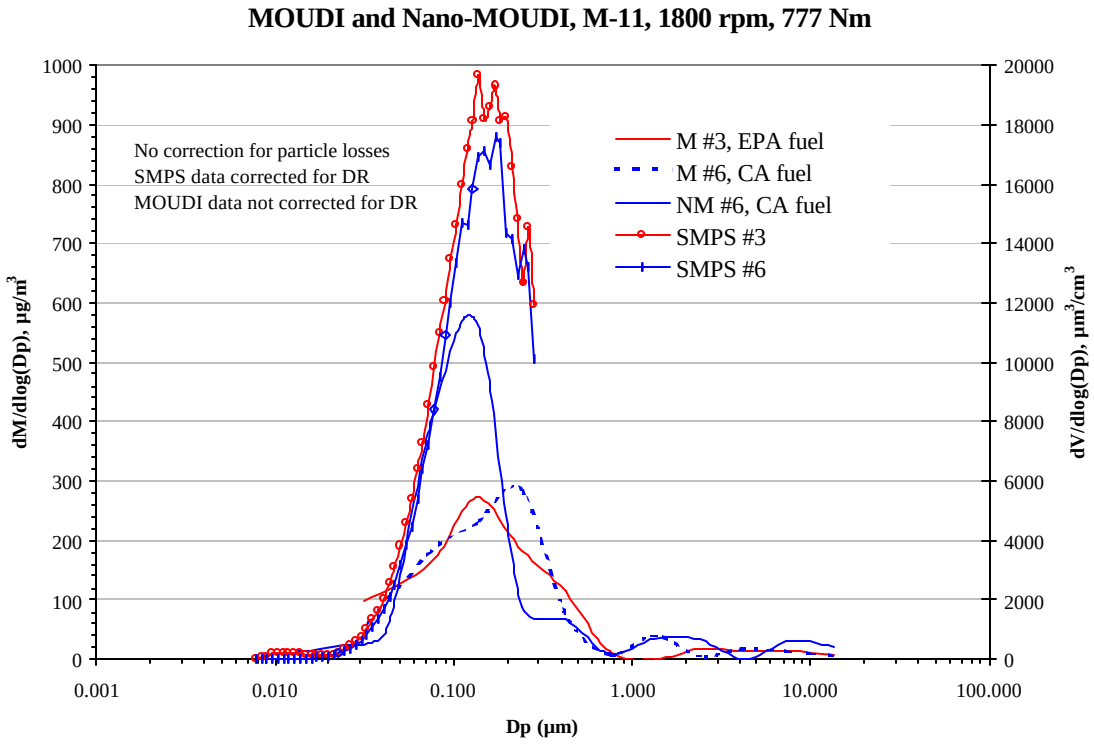

Figure 56. Cummins ISM MOUDI samples 1800 RPM, 777 Nm

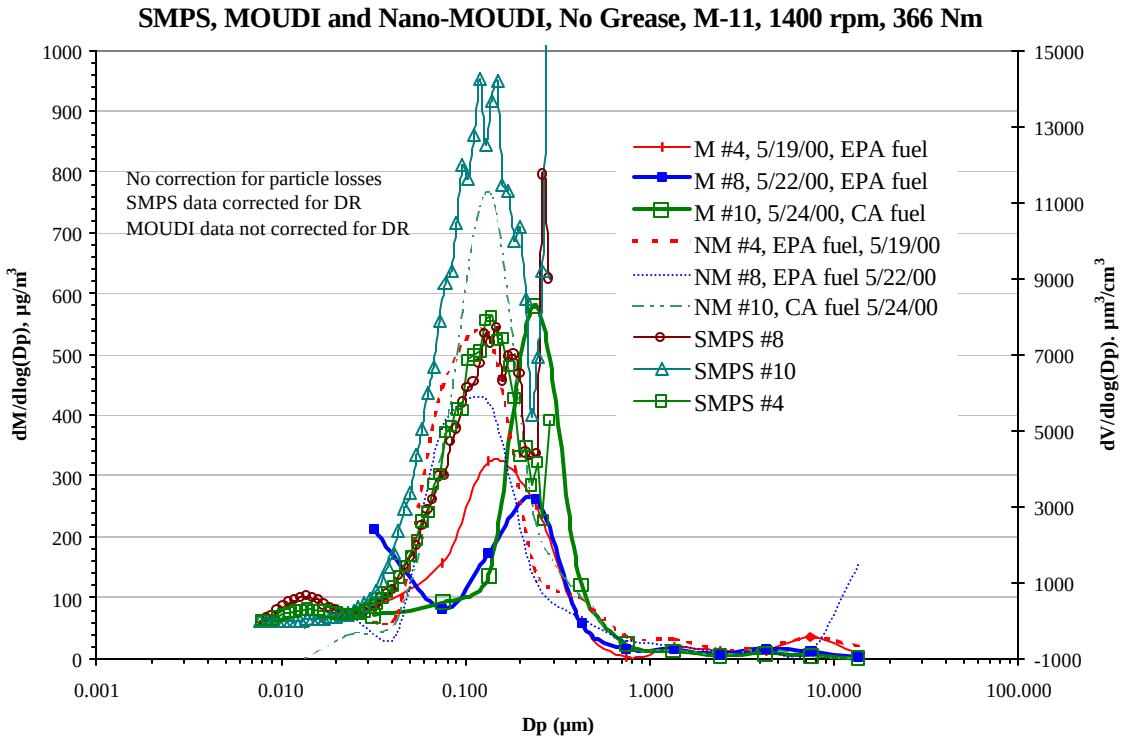

Figure 57. Cummins ISM MOUDI samples 1400 RPM, 366 Nm

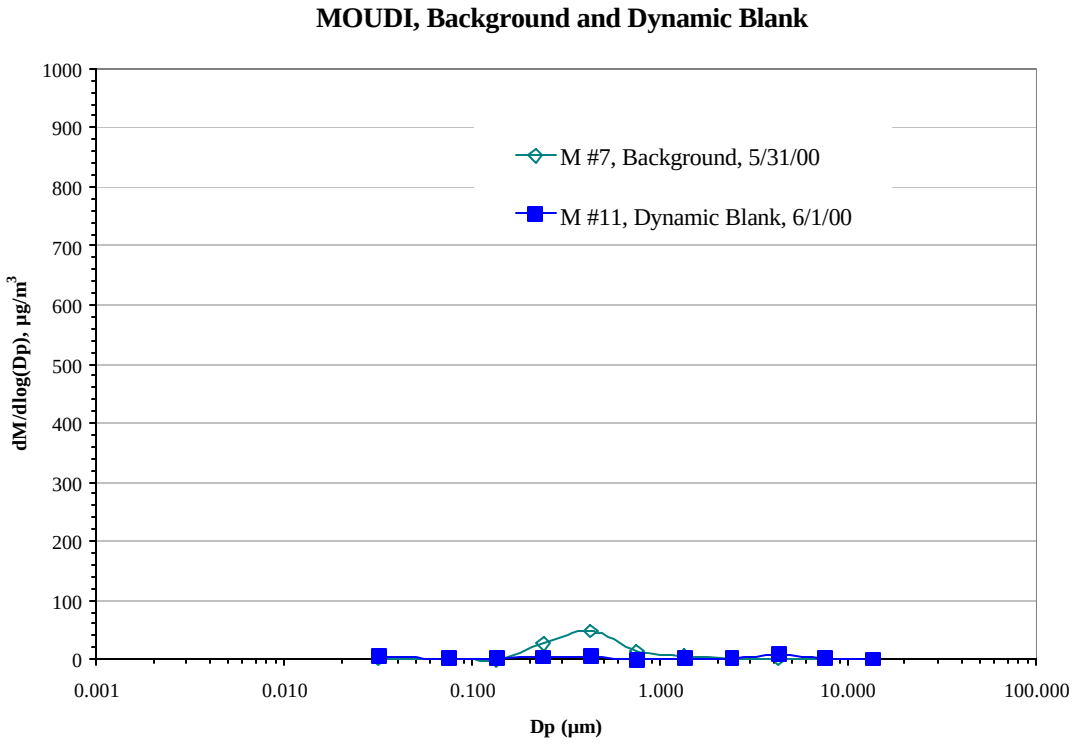

Figure 58. MOUDI background and dynamic blank samples

Based on data shown in Figures 55 through 57, it appears that the nano-MOUDI tends to measure a smaller size distribution than the MOUDI and it collects more mass. This is consistent with the observations we made in the UMN engine lab in the experiments examining the influence of greased substrates on particle bounce. The MOUDIs were not a matched set, but were modified for this project. These MOUDIs were among the first manufactured by MSP, and some of the parts were used a great deal in underground mine studies. It is quite possible that the modifications and prolonged use have adversely affected their performance. It is also likely that the flows through the two MOUDIs were not the same. For the five cases in which the two MOUDIs were successfully operated simultaneously, the mass collected by the MOUDI (through 56 nm stage) was 35 % less than the mass collected through the nano-MOUDI. It is unlikely that flow alone is responsible for the observed differences.

The SMPS volume distributions generally track with the nano-MOUDI distributions but exhibit larger size. However, these SMPS distributions are volume, not mass distributions. We will see below that when density effects are taken into account, mass size distributions calculated from SMPS data match nano-MOUDI quite well. This suggests that the sizing inconsistencies reported above are due to the MOUDI rather than the nano-MOUDI.

Caterpillar C-12 MOUDI Samples

Eleven nano-MOUDI samples were collected using the Caterpillar C-12 engine operated at the simulated highway cruise condition of 1530 rpm and 704 N-m fueled. The C12 was fueled with California Diesel fuel. It is a 435 hp, 6-cylinder, 1998 post-consent decree status engine. That is very similar to the 3406-E engines evaluated at Caterpillar. It has the same combustion and fueling system, but the cylinder displacement is 80 % of the 3406E size. Emissions are expected to be very similar to the model year 2000 3406-E engine. Samples were sent to DRI for chemical analysis.

The coatings and substrates for each sample are discussed below and the size distributions are shown in Figure 59. Figure 60 shows the tunnel blank size distributions. At the same time, 47 mm filter samples were collected using a BG-1 dilution system. The estimated dilution ratio is between 12 and 20:1. The first 8 runs were conducted in random order followed by the 2 tunnel blank runs. Run 7 was repeated because of difficulties encountered during the first run. UC Davis provided the Mylar substrates and the Al substrates were baked at DRI prior to use.

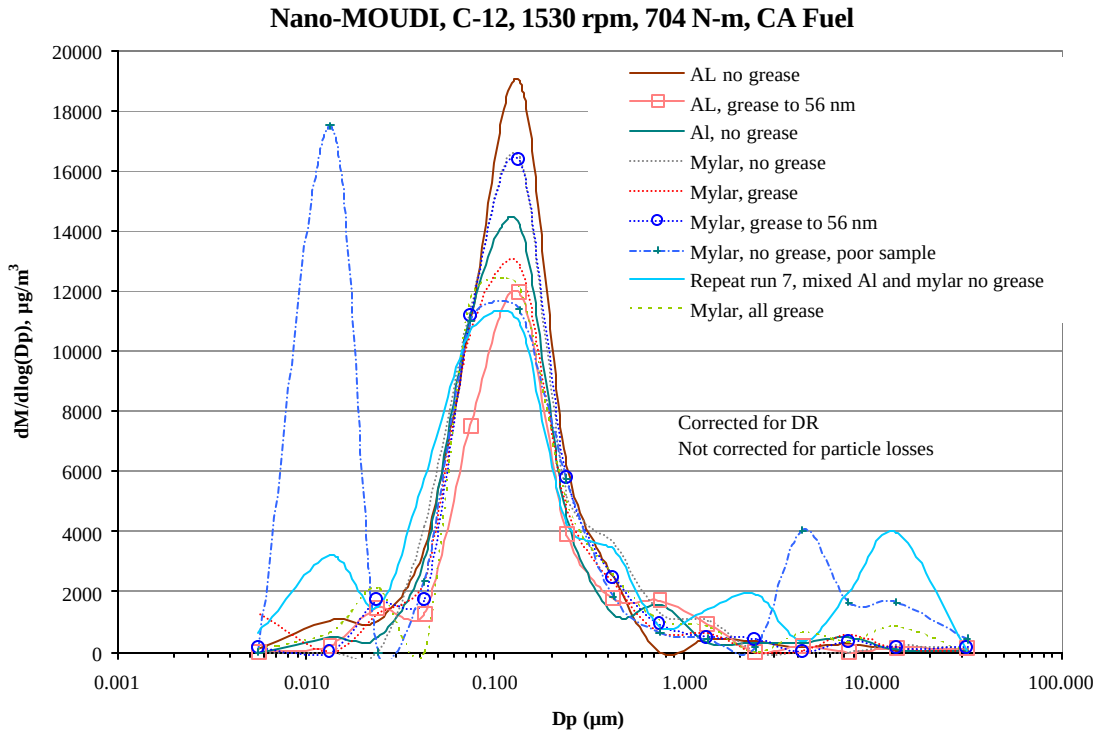

Figure 59. CAT C12 nano-MOUDI size distributions

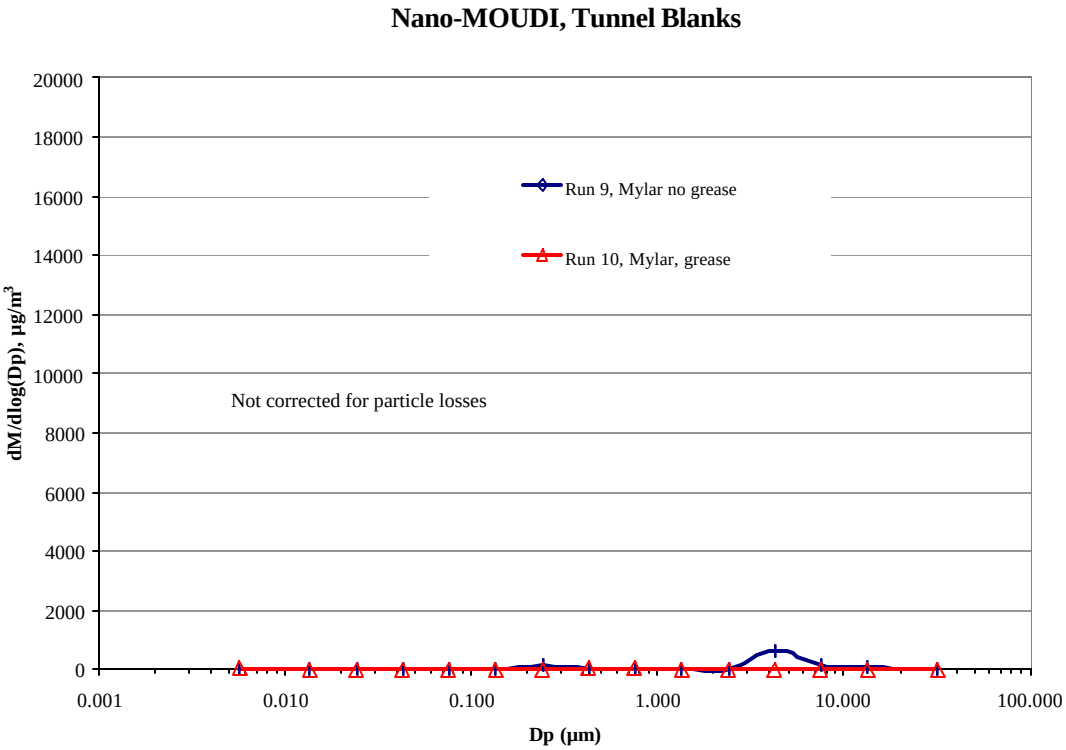

Figure 60. Nano-MOUDI tunnel blanks

Prior to the collection of these samples, 4 preliminary samples were collected from the Caterpillar C-12 operated at rated torque speed and 10 % load and CA fuel. The purpose of these samples was to evaluate Mylar as a substrate material. Figure 61 compares the average of these 4 samples to the average of the samples shown in Figure 59, excluding run 7, which was abnormal.

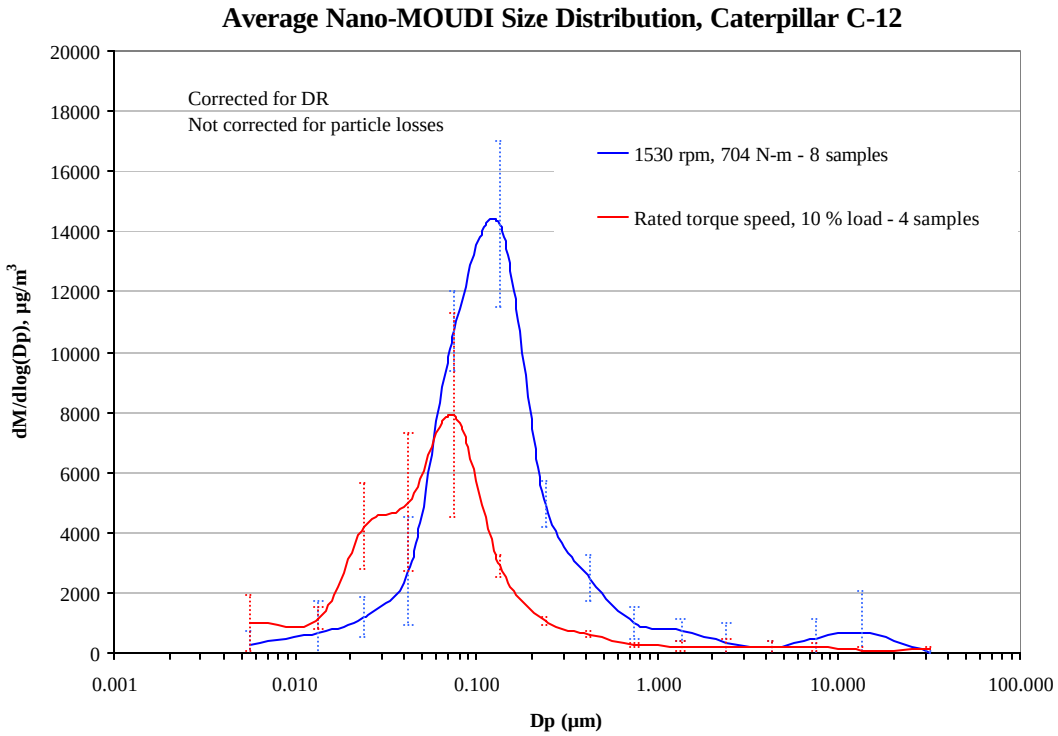

Figure 61. Caterpillar C-12 average size distributions at two engine conditions

Figure 62 shows a comparison between the average nano-MOUDI size distribution measured for the C12 engine under the highway cruise condition (1530 rpm, 704 N-m) and SMPS measurements made during the nano-MOUDI sampling period. All concentrations are those measured in the first stage of dilution with the BG-1 dilutor.

The SMPS data are shown in Figure 62 plotted in three ways. The first plot is a traditional volume distribution calculated from the number distribution assuming spherical particles. It is plotted on the same scale as the mass distributions because a volume of 1 $\mu m^3/cm^3$ corresponds to a mass of 1 $\mu g/m^3$ for particles with a density of 1 g/cm^3. The other two SMPS plots correspond to the mass distribution calculated from the SMPS volume and the size dependent effective particle density recently measured by Park, *et al.*, (2001) using either the Stokes or aerodynamic diameters.

Park's density measurements were made with a different Diesel engine (Deere 4045), but are the best estimates currently available. Park found that the density decreased from 1 to 0.3 g/cm^3 as particle size increased from 40 to 300 nm. The variation of particle mass with SMPS diameter gave a fractal dimension of 2.38. This density function makes the

SMPS mass distribution agree much better with the MOUDI results, although the SMPS distribution is lower and shifted to the right, toward larger particle size. However, it is not strictly correct to compare the mass distribution calculated from SMPS data with impactor data because an impactor sizes by aerodynamic diameter and an SMPS by Stokes diameter. For densities less than one, the Stokes diameter is larger than the aerodynamic diameter.

To perform a more rigorous comparison between the two instruments, the SMPS data have been recalculated based on aerodynamic diameter. This transformation shifts the SMPS results to the left and upward. The later shift is due to a decrease in the dlogDp intervals associated with the transformation. When the SMPS data are transformed in this manner, the agreement with the MOUDI data is much better, especially in the 50 to 150 nm range, where most of the mass resides. Note that the nano-MOUDI shows more mass in the nanoparticle range than the SMPS. This difference is outside the error bounds of the SMPS data. We believe that the nano-MOUDI overestimates mass in this range due to bounce and other artifacts associated with impactors.

The transformation of the SMPS data to aerodynamic diameter is interesting because it allows comparison between SMPS and MOUDI data. However, the use of aerodynamic diameter instead of mobility (or Stokes) diameter may not be appropriate in many cases. Often size distributions are used to estimate biological effects like lung deposition. In the ultrafine and nanoparticle range, this deposition is dominated by diffusion (Lippmann, 2001), which depends on the Stokes diameter, not the aerodynamic diameter.

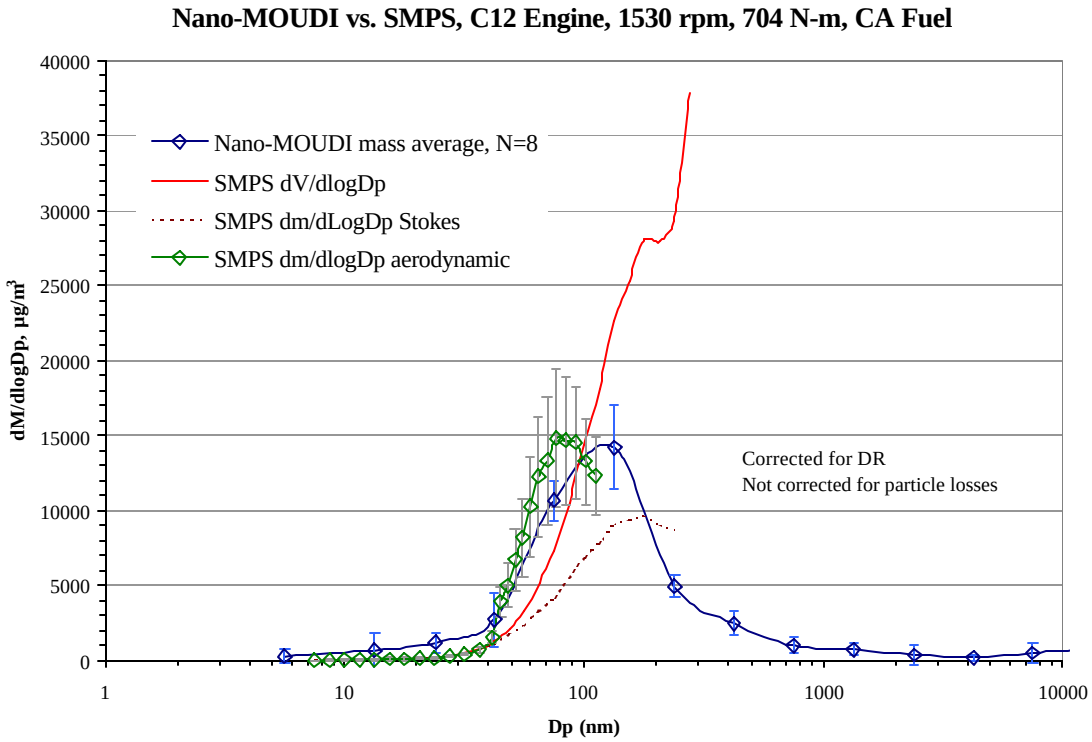

Figure 62. Comparison of the average nano-MOUDI size distribution to the SMPS

Other Results

Thermal Desorption Particle Beam Mass Spectrometer (TDPBMS)

The CRC E-43-4 project, titled "Chemical Analysis of Diesel Nanoparticles Using a Nano-DMA/Thermal Desorption Particle Beam Mass Spectrometer," was collaboration between the research groups of Professor Paul Ziemann at the University of California, Riverside (UCR) and Profs. Peter McMurry and David Kittelson at UMN (Ziemann, *et al*., 2002). The primary objective of this project was to use the Nano-DMA/TDPBMS to obtain information on the chemical composition of Diesel nanoparticles formed in a laboratory environment under various engine-operating conditions. The focus was on the chemistry of nucleation-mode particles, but for comparison larger particles were also analyzed. The goal was to combine the composition data with the measurements of physical properties (e.g., size, concentration, etc.) collected during the CRC E-43 project to develop an understanding of the chemical mechanisms of nanoparticle formation in Diesel exhaust. Engines evaluated in the project included the Cummins ISM engine used in the E-43 project, a Caterpillar C-12 and a Deere engine. Measurements were performed over a range of engine loads and the test fuels included CA fuel supplied by the E-43 project, Fischer-Tropsch, EPA certification and EPA pump fuel. This project did not fall under the review of the E-43 QA team.

Findings from this research project support our hypothesis of nanoparticle formation (Ziemann, *et al*., 2002). The main conclusions are listed below:

- The organic component of total Diesel particles and nuclei mode particles appears to be comprised predominantly of unburned lubricating oil, whereas the fuel contribution to the total organic component appears to be relatively small, no more than 20 % and probably much less.

- Low volatility oxidation products (e.g., organic acids) and PAHs, which are compounds of interest and are known to be present (from previous GC-MS analyses), do not appear to be a major portion of the organic mass.

- The major organic compound classes (alkanes, cycloalkanes, and aromatics) appear to be distributed fairly uniformly across the volatility spectrum.

- Sulfuric acid containing nanoparticles were formed using EPA pump fuel, which contains 410 ppm S. Fuel sulfur enhances nucleation. No sulfuric acid was detected in nanoparticles formed using CA (96 ppm S) or Fischer-Tropsch, (< 1 ppm S) fuel.

- Nuclei-mode particles and accumulation-mode particles are externally mixed across a wide size range, with the chemical components being distributed between two particle types: (a) "less volatile" particles, probably comprised of an elemental carbon core with a small organic component; and (b) "more volatile" particles, containing predominantly organics, sometimes small amounts of sulfuric acid, and possibly, a non-volatile core (elemental carbon or metal oxide) < 4 nm in diameter.

- The volatility of nanoparticle components exhibits no dependence on fuel or engine load.

The general model of nanoparticle formation that emerges from these results is that particles form by nucleation of low volatility organics or, when present in sufficient quantities, sulfuric acid and water. It is possible that non-volatile particles of either elemental carbon or a metal oxide may also serve as nuclei for nanoparticle formation, but this is still an open question. Once nucleation occurs, growth appears to involve condensation of organic compounds from unburned lubricating oil. The resulting particles are an external mixture; some are completely volatile, whereas others contain a significant non-volatile core. The resulting nuclei-mode particles are predominantly the "more volatile" particles whereas the accumulation mode is predominantly "less volatile" particles.

Particle Density Measurements

Park, *et al.*, (2001) obtained the density estimates used to convert the Caterpillar C-12 engine SMPS volume distribution to a mass distribution. This research was supported by

EPA and will be fully reported in Park's Ph.D. dissertation. These density estimates are important in understanding the E-43 MOUDI data.

Density experiments were done in the UMN engine lab with a Deere 4045 and VW TDI engines, and Figure 63 shows the experimental setup.

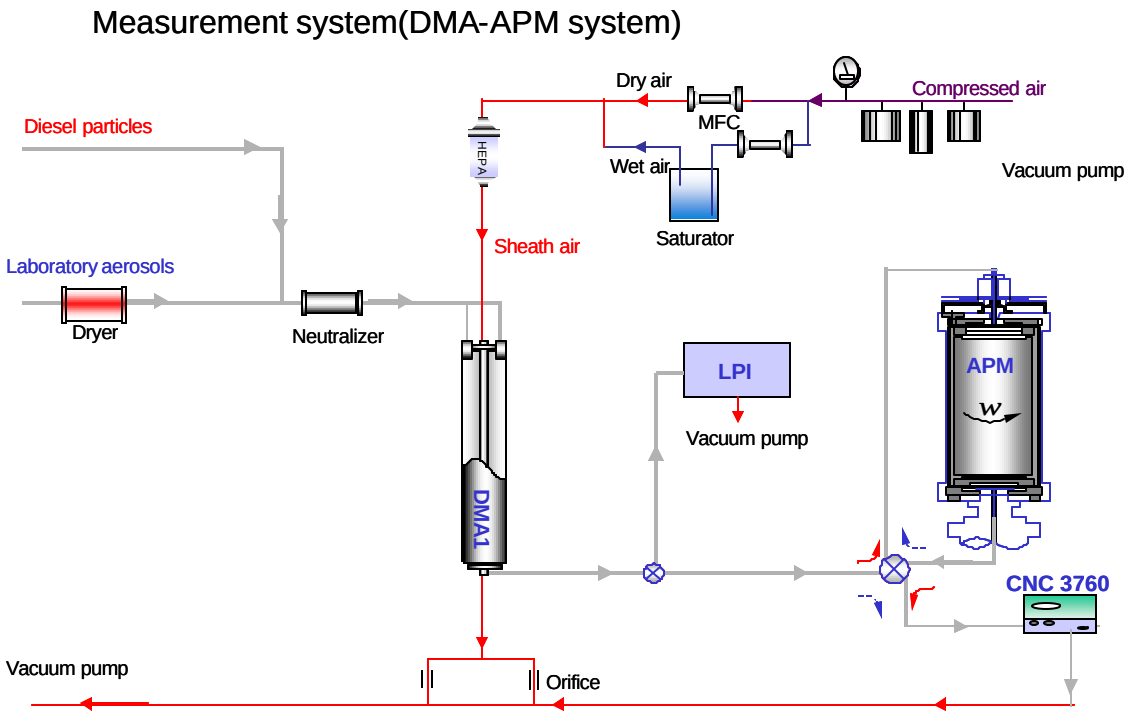

Figure 63. System for measuring Diesel particle density (Park, *et al*., 2001)

The key component in the system is the Aerosol Particle Mass Analyzer (APM) (Ehara, *et al*., 1996) that classifies aerosol particles according to mass-to-charge ratio. The APM measures a fundamental aerosol property, mass, in-situ. In this case, the APM is combined with the sizing column from an SMPS, a differential mobility analyzer (DMA), to measure the aerosol mass size distribution. A CPC is connected in parallel with the APM so both mass and number distributions are obtained simultaneously. DMA volume distributions are calculated from the number distribution. Comparison of particle volume and mass yields effective particle density. Figures 64 and 65 show typical density data obtained for the Deere engine and VW TDI engines. These figures show the influence of engine load and fuel type on particle density.

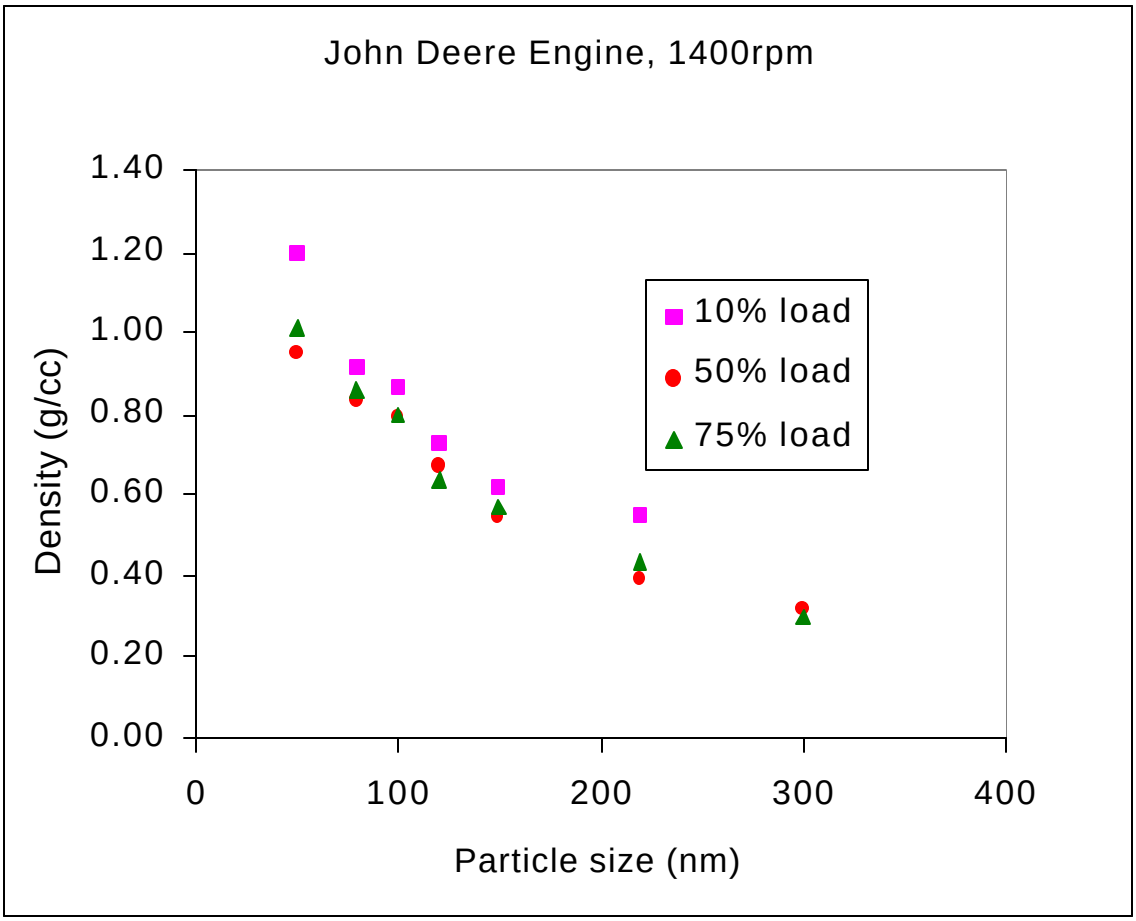

Figure 64. Influence of particle size and engine load on particle density
(Source: Park, *et al*., 2001)

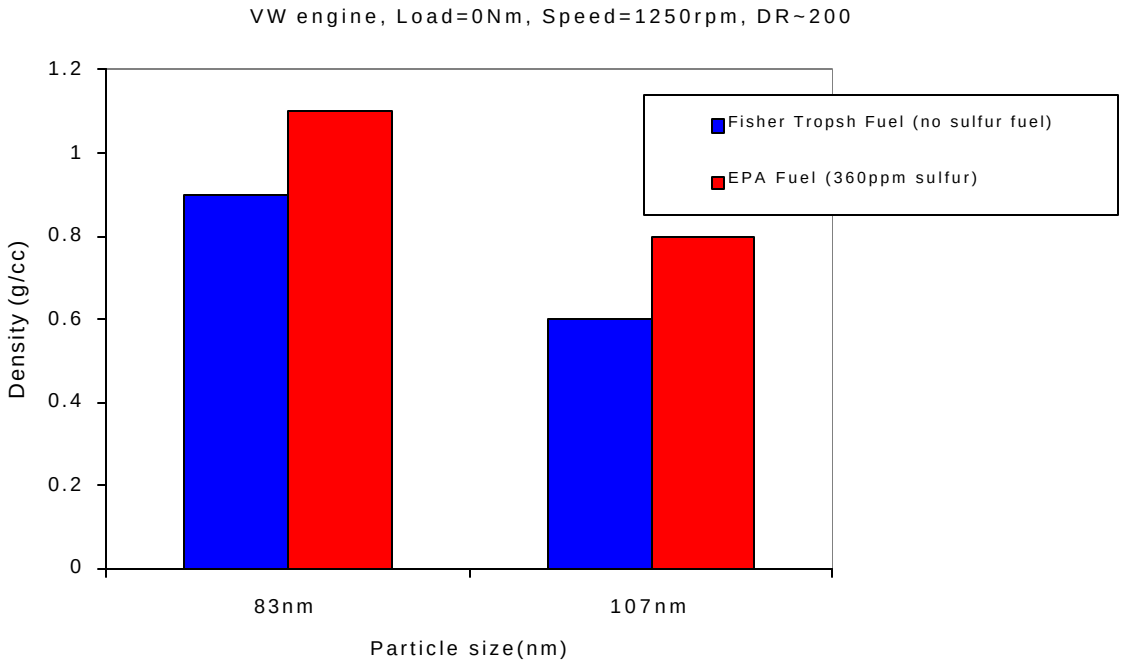

Figure 65. Variation of effective particle density with size and fuel composition (Source: Park, *et al*., 2001)

Park's data show that effective particle density depends upon a number of factors including particle size, engine operating conditions and fuel properties. However, it appears that the most important parameter influencing Diesel particle density is particle size. Simultaneous measurements of DMA- APM and MOUDI mass size distributions for several engines and operating conditions are planned in the future.

Park's effective density data for the Deere engine operating at 50 % load on EPA fuel were used to convert SMPS data to mass data for the C-12 engine reported above in the Caterpillar C-12 MOUDI section. This is a representative operating condition and fuel.

Size Distribution Measurements at the UMN Lab with Caterpillar C-12 Engine

We have continued to develop and improve sampling and dilution practices in the UMN laboratory in a program mainly supported by Caterpillar, but partially supported by the E-43 program, but not covered by the E-43 QA program. A single stage dilution tunnel designed to simulate the atmospheric dilution process was designed, built and evaluated (Wei, *et al.*, 2001a, 2001b and Wei, 2002). An early version of this dilution system was tried during chassis dynamometer tests at Cummins, but technical difficulties prevented its use. Since then, the system has been improved and used with the C-12 engine to make a variety of measurements, including comparisons with other dilution systems.

As a result of the single stage tunnel evaluation, the impact of exhaust transfer line losses and dilution air temperature on nanoparticle formation was documented (Wei, *et al.*, 2001b and Wei, 2002). These tests help explain why the two-stage tunnel with a transfer

line that was too long formed much lower concentrations of nanoparticles than either the CVS partial flow tunnel/ejector combination or the BG-1/ejector combination. These tests also demonstrate the impact that dilution air temperature has on nanoparticle formation. Lower dilution air temperatures favor increased nanoparticle formation. This observation is consistent with what was observed in the E-43 project with the ISM engine running on CA fuel.

As part of this program, the performance of the two-stage dilution system, a BG-2 with a secondary ejector dilutor and the single stage dilution system were compared. The BG-2 is an upgraded version of the BG-1. The goal of the comparison was to determine how close each of these dilution systems could come to matching the on-road size distributions obtained under the E-43 project for the Caterpillar 3406E engine operated on EPA fuel. The C-12 engine is very similar to the 3406E engine. The C-12 has the same high-pressure electronic fuel injection system and the same combustion chamber design, but only 80 % of the displacement of the 3406E. To compensate for this difference the C-12 was operated at the same engine speed and brake mean effective pressure as the 3406E. Using this approach, the C-12 operating condition that corresponded to on-road cruise with the 3406E was 1530 rpm, and 704 N-m torque.

Figure 66 compares the size distributions measured with the three different dilution systems to the 3406E on-road 60 mph loaded cruise condition. The three dilution systems were operated at different conditions of dilution air temperature (Dair), DR, primary residence time (PRT), primary dilution temperature (PDT) and flow (coaxial and counter).

The single-stage dilution system was operated with a 1 s residence and mixing time, 16°C dilution air, and two sample introduction schemes, coaxial flow leading to a DR of 203 at the sampling point and counter flow, leading to a dilution ratio of 154 at the sampling point.

The BG-2 dilution system was modified to include an aging chamber after primary dilution that was maintained at 35°C. The chamber had a 1 s residence time and was followed by a secondary ejector. The BG-2 system was operated at two different primary DRs, 9.2 and 12.3, and a fixed secondary DR of 43.

The two-stage ejector system was the same one used at the Cummins CVS facility and the Caterpillar performance cell. The principle difference was that it was used with a very short transfer line from the tailpipe to the dilution system, about 20 cm. This system was run with a primary DR of 11.1, a secondary DR of 20, a residence time of 0.8 s and an aging primary dilution temperature of 44°C.

The plots in Figure 66 show that the two single-stage operating conditions underestimate the on-road nuclei mode. The two BG-2 dilution conditions bracket the on-road nuclei mode, and the two-stage system conditions come very close to matching the mode. The full range of dilution conditions that these systems can achieve was not explored, but it

appears that with suitable adjustment, any of them could closely match the on-road condition.

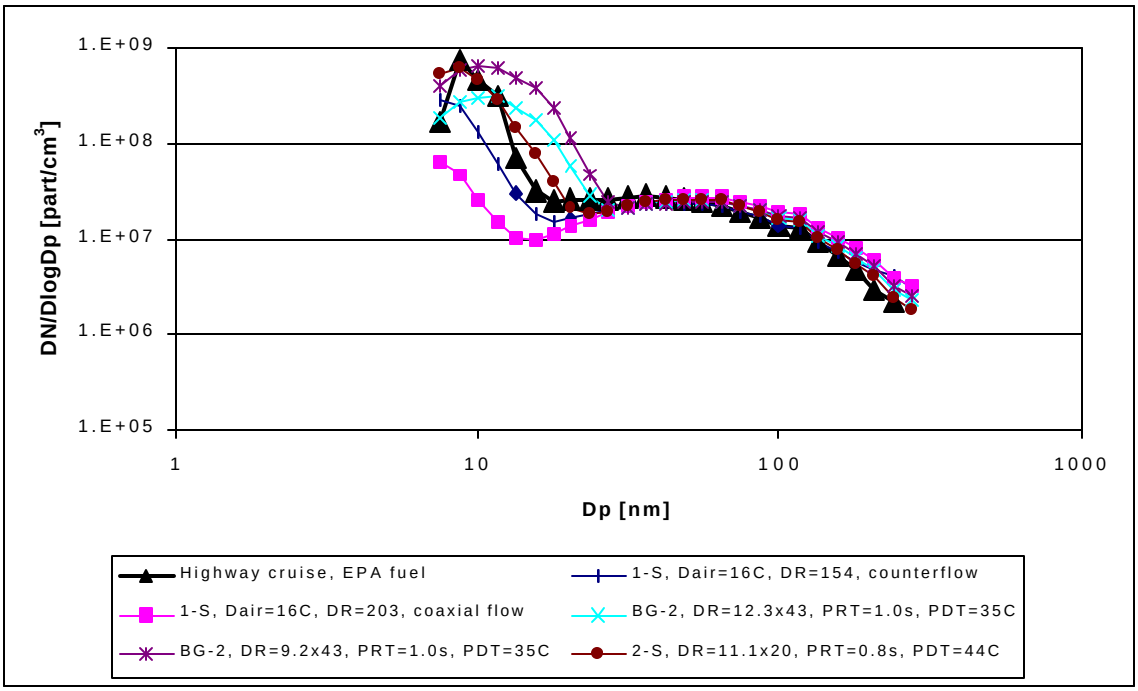

Figure 66. Comparison of laboratory and on-road size distribution measurements using three different dilution systems

Each of the three systems has advantages. The single stage system produces a nuclei mode that is quite monodisperse, much like the on-road mode. The two-stage ejector system is inexpensive and robust, and the BG-1/BG2 system is a commercial system that also works well for filter sampling. More details of this work are available in Wei, 2002.

Nano-SMPS Measurements with the C-12 Engine

In many cases, both on-road and in the laboratory, we have found that the CPC number count is higher than that of the SMPS. We have always had some reservations about making this case too strongly because of uncertainties in the performance of the leaky filter dilutor that was used in the E-43 program for most CPC measurements. However, recent work in our laboratory confirms that under some engine and sampling conditions large numbers of particles below the sizing range of the conventional SMPS are formed. Two types of evidence support this hypothesis: comparison of CPC and SMPS number measurements and nano-SMPS measurements. The CPC and SMPS comparison is similar to what was reported in the E-43 program with one major difference, the CPC used a well-characterized ejector dilutor rather than a leaky filter dilutor.

Figure 67 shows the comparison of the CPC with ejector dilutor to the SMPS for total number concentration with the single stage dilution system for the cruise condition 1530 rpm and 704 N-m. The SMPS with a lower limit of about 7 nm underestimates the total

number of nanoparticles. The cycling of the CPC number concentration is due to small variations in the mixing rate and dilution ratio in the single-stage dilution tunnel caused by air compressor reservoir pressure fluctuations. These changes illustrate the sensitivity of nucleation to very small changes in dilution conditions. Note that CPC concentrations are 3 to 10 higher than SMPS concentrations for these conditions. Side by side calibration of the same SMPS and CPC with larger particles reveal that the two instruments agree within 20%. Thus, Figure 67 is a clear indication of the formation of very small particles below the sizing range of the conventional SMPS.
Measurements with a nano-SMPS provide further evidence of the formation of very small particles. The nano-SMPS extends the range of the SMPS downward to 3 - 4 nm. Details of this instrument are described elsewhere (Chen, *et al*., 1996, 1998). It should be noted that the nano-SMPS measurements were not subject to the E-43 QA program and that the instrument was designed to minimize particle losses.

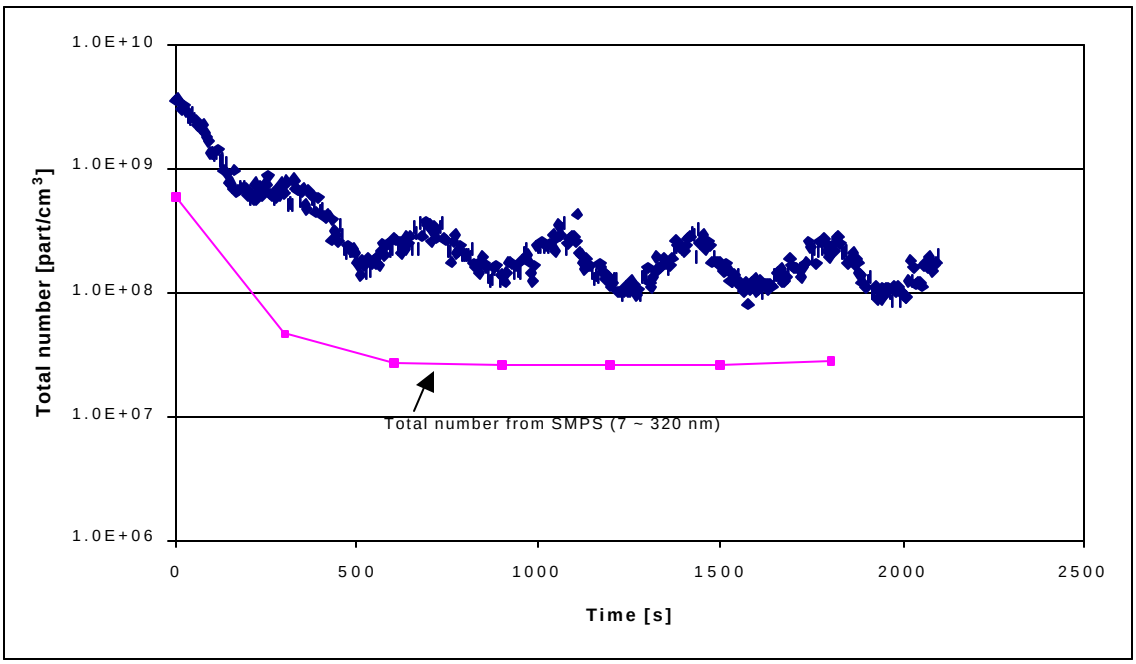

Figure 67. CPC and SMPS number concentration measurements made on C-12 engine during transition from idle to cruise condition (1530 rpm. 704 N-m)
Single-stage dilution tunnel, counter flow, DR = 325, RT = 1.0s, Tair = 21°C.

Figure 68 shows the comparison of the nano-SMPS with the SMPS using the BG-2 dilutor. Again the SMPS underestimates the number of nuclei mode particles. These measurements were made with the CA fuel that only showed a hint of a nuclei mode with the standard SMPS, but a large nuclei mode with the nano-SMPS. This is consistent with the ideas presented in Appendix D, suggesting that the size of the particles in the nuclei mode is related to the concentration of volatile particle precursors, such as sulfuric acid. Apparently, the concentrations of these precursors are lower with the CA fuel. Nucleation still occurs, but there is less growth, so the particles are smaller with the dilution conditions illustrated here.

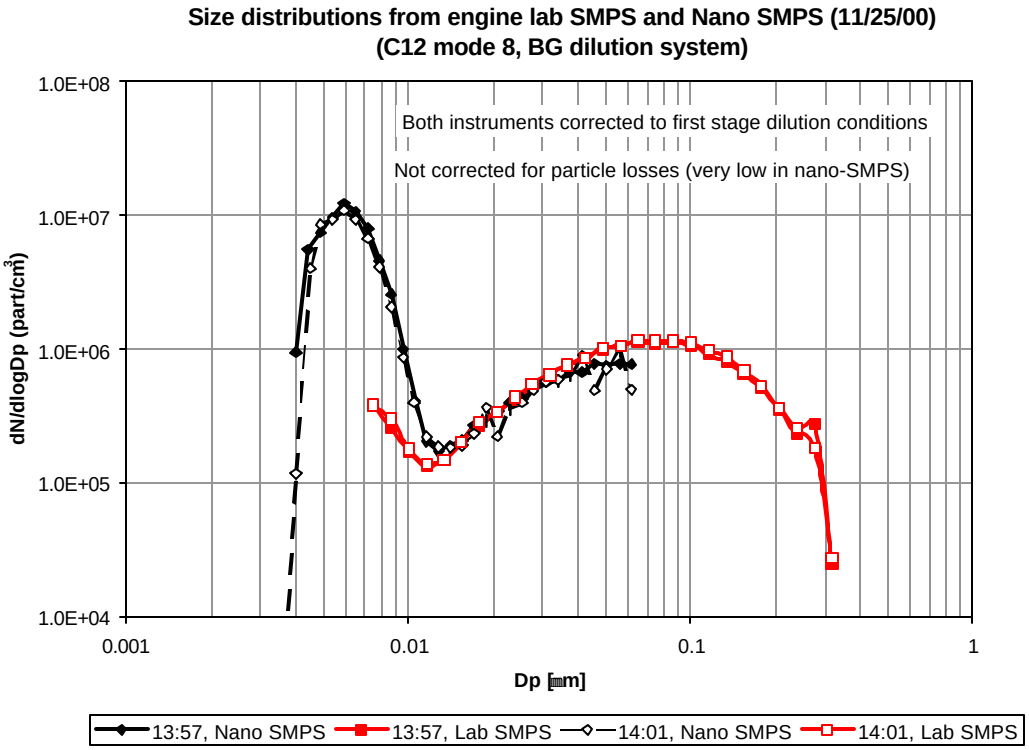

Figure 68. Comparison of nano-SMPS and conventional SMPS measurements made on C-12 engine
1200 rpm, 50 % load, BG-2 dilution system, primary DR = 15, concentration corrected to primary tunnel concentration.

Particle Volatility Measurements Made on ISM Engine

Volatility and hygroscopicity measurements were made at the same time as the Cummins TDPBMS measurements were made. TDPBMS experiments showed that Diesel nanoparticles consist mainly of alkanes with a small fraction of sulfuric acid. The objectives of the particle volatility measurements were to determine the volatility and hygroscopicity of Diesel nanoparticles to draw inferences about the particle composition. While these measurements give useful insights about the composition of volatile and/or hygroscopic nuclei mode particles, they reveal little about the composition of material adsorbed on solid accumulation mode particles. The mobility size of solid accumulation mode particles is unlikely to be influenced by adsorption/desorption processes.

Volatility

Figure E-1 shows the test setup used in these experiments. The same Cummins ISM engine used in the E-43 program was used for these tests. The key instrument for measuring particle volatility was the nano-tandem differential mobility analyzer (nano TDMA). This instrument consists of two differential mobility analyzers (DMAs) with a heating or humidification section between the two DMAs. It allows a single particle size to be selected with the first DMA. This particle size was then treated by heating or humidification, and the resulting size change determined with the second DMA.

The expected outcome from these experiments was the demonstration that solid particles consisting primarily of carbon and semi-volatile or volatile particles consisting primarily of hydrocarbons would be differentiated. Volatile particles shrink and eventually disappear upon heating, while solid particles shrink far less as any volatile materials on the surface are removed. It was expected that on the larger end of the size scale we would find accumulation mode particles that are mainly composed of carbonaceous soot or solids. Little shrinkage of these particles was expected. In the size range where there is overlap between the nuclei mode and accumulation mode, we expected to find two kinds of particles. Solid particles representing the lower size end of the accumulation mode, and volatile particles in the upper size range of the nuclei mode. For the smallest particles in the range of a few nanometers, we expected to find mainly a volatile material.

Figure E-2 shows results of experiments in which 30 nm particles were heated after exiting the first DMA. The 30 nm particles exhibited the behavior of particles near the boundary between the nuclei and accumulation mode. As a result of heating, the particle size distribution split into two modes: a solid fraction, that had very little shrinkage, which was associated with the tail of the accumulation mode, and a volatile fraction that shrunk progressively as the heating process continued.

Figure E-3 is an example of what happens to 7 nm diameter particles as they are heated. These particles shrink progressively towards the lower limit of detection of the nano TDMA. Another way of looking at this effect is to plot the diameter change as a function of temperature, starting with different initial size particles. This is shown in Figure E-4. Here, initial sizes of 50, 30, 12 and 7 nm are shown. The 50 nm particles split clearly into a mainly solid mode that shrinks down to a diameter of 43 nm, and a volatile mode that rapidly shrinks between 100-150 to 15 nm. The 30 nm particles show a similar splitting, as do the 12 nm particles. However, the 7 nm particles simply shrink as they are heated, and don't show evidence of consisting of two different types of material.

Figure E-5 shows the volume fraction remaining in the particles after heating. It shows that the non-volatile residue remaining after heating particles initially in the 12-30 nm range is as little as 2-3 %. The decrease in particle volume as a function of temperature may be related to its vapor pressure. Evaporation rates were calculated for particles consisting of normal alkanes in the C20-C36 range. These rates were used to determine the amount of shrinkage expected in the volatility experiments.

In Figure E-6, the predicted diameter decrease as a function of temperature for various normal alkanes is compared with the observed diameter decrease for particles of various initial sizes. It shows that the shrinkage of particles from Diesel engines observed is in the same range as expected for C28-C36 normal alkanes. Also shown on the plot, is the experimentally shrinkage of a C32 alkane that was generated in the laboratory and subjected to the same heating experiment. The behavior is quite similar to the disappearance of the 30 nm Diesel nanoparticles.

The evaporation calculations were done for the residence time (about 0.26 s) in the heater that is used between the DMA columns in the volatility experiments. It is noteworthy that they indicate, for example, that a C20 normal alkane nanoparticle will shrink in diameter by about 10 nm at 30°C and 30 nm at 40°C. Thus, fuel related hydrocarbons, mainly lighter than C20, would be expected to evaporate from nuclei mode particles very quickly under normal ambient conditions.

In all of the heating experiments, the particles seemed to shrink down to a diameter near the lower limit of detection of the nano TDMA. It is not clear whether this indicates a real solid residue from these particles or an instrument artifact. Note that even the pure C32 normal alkane did not totally disappear.

Hygroscopicity

The hygroscopicity experiments were performed by selecting a given size range, setting the humidity in the DMA and dilution air to a very low value (approximately 6 %) and then adding humidity in the second DMA of the nano-TDMA to raise the humidity to approximately 85 %. Size distributions with and without this addition of humidity are shown in Figure E-7. For an initial diameter of 6.5 nm, particles grow by about 5 %. Larger particles, 12 and 30 nm particles grow by about 2 %. These experiments were performed with a standard EPA on highway fuel with about 350-ppm sulfur. When these experiments were performed with the 96-ppm S CA fuel used in the Caterpillar experiments, no significant uptake was observed for any of these particle sizes. These growth factors were used to estimate the mass fraction of sulfuric acid present in the particles. These mass fractions increased with decreasing particle size, ranging from 5 percent at 30 nm, to 19 percent at 6.5 nm. This suggests that, at least for higher sulfur fuels, binary nucleation and sulfuric and water provide sites for heterogeneous nucleation and/or absorption of the heavy hydrocarbons that comprise most of the material in the nuclei mode particles. Tandem DMA characterizations of nanoparticles formed downstream of catalyzed aftertreatment systems would be a useful follow-on to this work.

Summary

The volatility experiments indicated that, except for the smallest particles, heating could differentiate between volatile and solid particles. The fraction of solid particles decreased as particle size decreased, and only a volatile mode was detectable for the

smallest particles tested (7 nm). It was found that more than 97 % of the volume of the volatile constituents of 12 and 30 nm particles disappeared on heating to 400°C. The volatility of the Diesel nanoparticles was found to resemble that of C24-C32 normal alkanes, which implies a significant contribution of lubricating oil to these particles.

The hygroscopicity experiments suggest the presence of sulfuric acid in Diesel nanoparticles when the engine was run with a normal 350-ppm sulfur fuel. The hygroscopicity experiments could not detect sulfuric acid in particles produced by the engine when running on the 96-ppm sulfur CA fuel. When hygroscopic particles could be detected, it was found that the smallest particles were the most hygroscopic, suggesting that the smallest particles were relatively enriched with sulfuric acid.

Carnegie Mellon Report

CMU prepared a subcontract report, entitled "Lifetimes of Ultrafine Diesel Aerosol," for UMN as part of the E-43 program (Capaldo and Pandis, 2001). A computer model was used to determine the lifetime and evolution of particle size distributions measured during on-road testing by UMN. Their report addressed the following three questions:

1. What is the lifetime of particles emitted from on-road Diesels under typical conditions?
2. How far are these particles going to be transported, and what is the range of influence of these mobile sources?
3. Which are the most important factors influencing the lifetime of the ultrafine aerosols?

A one-dimensional Lagrangian trajectory model was used to simulate the evolution of the plume size distribution. This model simulated the dispersion, mixing with ambient particles, coagulation and dry removal of the emitted particles. The effects of meteorology, topography, ambient aerosol and model assumptions were examined. Baseline calculations were done assuming the roadway plume mixed with an urban influenced continental background aerosol, with a concentration of 6500 part/cm^3, mainly in an accumulation mode centered at 100 nm.

Particle lifetimes, τ_{90} and τ_{99}, were defined as the times necessary for the reduction of the *total number (nearly all in the ultrafine range) concentrations* from their initial plume values by 90 % and 99 %, respectively. Similarly, particle transport distances, s_{90} and s_{99}, were defined as the distance of transport of the emitted particles, measured along the prevailing wind direction, necessary to reduce the initial plume number concentrations by 90 % and 99 %, respectively. The τ_{90} and τ_{99} times reflect number concentration reductions by dilution, coagulation, and deposition and for most cases simple dilution is the dominant factor. An additional characteristic time, t_{50}, was defined to describe actual removal of nanoparticles from the atmospheric boundary layer by coagulation and deposition.

Major conclusions of the report are:

- For typical urban conditions, τ_{90} is on the order of a few minutes and τ_{99} is on the order of 20-30 min.
- s_{90} can vary from 100-1000 m, and s_{99} from 0.5-10 km. Typical values for these transport distances are 300 m for 90 % reduction and 2 km for 99 % reduction. These results indicate that Diesel trucks and other mobile ultrafine particle sources will have an effect on the aerosol particle number concentrations in a wide area around roadways.
- t_{50} is on the order of 20 minutes and relatively independent of mixing conditions. This indicates that coagulation plays a relatively minor role for the base case background aerosol.
- The degree of atmospheric mixing (dilution) is the most important variable affecting characteristic times (τ_{90} and τ_{99}.) As wind speed increases from 1 to 10 m/s, τ_{90} and τ_{99} decrease by an order of magnitude.
- Characteristic transport distances (s_{90} and s_{99}.) are rather insensitive to wind speed.
- For a given wind speed, ultrafine particles are expected to survive and travel a factor of ten greater distances in a rural flat area as compared to an urban downtown location. This is because of faster coagulation due to higher background particle concentrations and faster mixing and deposition due to rougher terrain in urban areas.
- For the same meteorological conditions and topography, τ_{90}, τ_{99}, and t_{50} are expected to be about a factor of two, ten, and ten less, respectively, in a polluted urban area, with a background particle number concentration three times higher than baseline, than in a rural area. The dramatic decrease in τ_{99} and t_{50} result from increased scavenging of nuclei mode particles by coagulation with polluted urban background particles.
- On-road concentrations, emissions rates, and initial particle size have a minor influence on the τ_{90} and τ_{99} lifetimes.

PSI Reports

The Paul Scherrer Institute (PSI) submitted a report (Bukowiecki, *et al.,* 2001) detailing the use and performance of the surface area measurement instruments used in the E-43 program. The DC and epiphaniometer, along with the PAS, were provided for this research as part of the PSI subcontract. These instruments were included to examine their utility for characterizing the surface properties of Diesel aerosols. PSI, in collaboration with the UMN, also published a paper titled "Real-time Nanoparticle Information Obtained with a Diffusion Charger, a Photoelectric Aerosol Sensor and a Condensation Particle Counter" (Bukowiecki, *et al.,* 2002). This paper is based upon data collected in the E-43 project.

In the project report submitted by PSI, the performance of the epiphaniometer and its correlation with the DC were examined. The instrument handling and data analysis methods for the epiphaniometer were also discussed. This discussion included the epiphaniometer operating principles, the inversion method for epiphaniometer data,

considerations for long-term usage and calibration of the epiphaniometer, and the presence of saturation effects.

Major conclusions of this report are:

- The epiphaniometer is not a rapid response instrument. The instrument has a recommended time resolution of 15 min for measuring particle surface area.
- When compared to 15 min averages of DC measured surface area, the epiphaniometer/DC ratio determined by regression analysis is 0.933 with an R^2 value of 0.852 for on-road testing. The epiphaniometer-DC correlation is surprisingly good, especially for on-road experiments.
- The epiphaniometer is ideal for measuring accumulated surface area concentrations, as may be required for inhalation and/or exposure studies.
- Signal saturation [related to the mathematical processing of data at high concentrations] is a problem with the epiphaniometer that will have to be addressed in future investigations.
- The DC, used as an important plume indicator, had multiple breakdowns and hence, a repair and subsequent re-calibration. These problems were mainly due to overloading the corona with high aerosol concentrations.
- The long-term stability of the DC was checked with the epiphaniometer. Only a minor shift in the relationship between the DC and the epiphaniometer occurred after the aforementioned repair/re-calibration, indicating the DC calibration did not significantly change during the time period analyzed for this report (autumn 1999 to spring 2000).

The findings of this report suggest that the epiphaniometer is not an appropriate instrument to collect real-time data during chase experiments. However, the rapid response time of the DC made it a useful instrument in the chase tests. The epiphaniometer may be useful in steady-state engine testing, but it is clearly most useful as an ambient-level monitor of long-term particle surface area concentration.

Bukowiecki, *et al.*, (2002) concluded that based upon comparison to the epiphaniometer, the DC provided a reasonable measure of surface area, although more study of its usefulness is required. Neither the DC, which required repair due to excess aerosol deposits on the corona, nor the epiphaniometer, which suffered from signal saturation effects, were particularly well suited for the measurement of high concentrations of Diesel aerosol for long periods of time. On the other hand, the very high sensitivity of the epiphaniometer might make it appropriate for making measurements of the very low concentrations of particles from future engines meeting 2007 and later emission standards. The slow time response might not be a factor in determining the average concentration during a transient cycle.

The diameter of average surface calculated with DC and CPC data ($D_{Ave,S(A)}$) provided useful information on the relative concentration of nuclei mode particles throughout an experiment, assuming a fairly constant size and concentration of the Diesel accumulation mode particles (Bukowiecki, *et al.*, 2002). Since the physical principles to determine the DC active surface and the CPC particle number concentration are basically independent

of each other, $D_{Ave,S(A)}$ can be considered as a reliable relative parameter. It was also shown that the relationship between $D_{Ave,S(A)}$ and $D_{Ave,S(SMPS)}$ was in good agreement with the Fuchs theory.

Chassis dynamometer experiments, as well as the ambient monitoring during the Cummins phase of E-43, confirmed that the response of the PAS is strongly influenced by volatile or semi-volatile species, which partially condense on the accumulation mode particles and are responsible for the formation of nuclei mode particles. In PAS/DC plots there are two branches with hardly any data points between the two branches, which often are found in plots from urban ambient aerosol measurements (Bukowiecki, *et al.*, 2002). The low PAS response branch is associated with conditions leading to a large nuclei mode, while the high response branch is associated with conditions leading to mainly accumulation mode particles.

For a series of measurements, a triangle-like arrangement of the data was obtained in PAS/DC vs. $D_{Ave,S(A)}$ plots (Bukowiecki, *et al.*, 2002). The corner regions of these plots can be assigned to three different situations regarding the composition of the sampled aerosol in the particle size range D < 200 nm. The plot helps to distinguish between the presence/absence of nuclei mode particles and the presence/absence of an adsorbed layer on accumulation mode particles. The high time resolution of the involved instruments allows for stand-alone and real-time monitoring of exhaust particles and enables qualitative, but reliable statements about the quality of the measured air, which can give valuable input to the ongoing discussion about the influence of particle surface and number concentrations on health and environment. These statements can be obtained without simultaneous SMPS measurements. Quantitative statements are not possible since no simple physical or chemical parameters can be assigned to the PAS measurements according to current knowledge. Further limitations are the relatively large signal variability and a certain threshold aerosol concentration (higher than approx. 1000 particles per cm^3) that is needed for a reasonable interpretation of the results. However, for most urban or motor traffic measurements concentrations are sufficiently high (Bukowiecki, *et al.*, 2002).

Wind Tunnel Report

In conjunction with the UMN, WVU researchers (Clark, *et al.*, 2001) conducted exhaust dilution experiments at the Langley wind tunnel from October 22nd through 28th, 1999. WVU sub-contracted with the Desert Research Institute for monitoring tunnel background aerosol concentrations.

The objective of the WVU Langley wind tunnel experiment was to examine the nature of plume dilution and to gather PM size and concentration information from the plume and far field while the truck was operated in the wind tunnel. Truck 61 with the Cummins ISM test engine was used for the wind tunnel experiments and cruise, acceleration and idle conditions were simulated. Because of weight restrictions in the wind tunnel, only unloaded conditions could be simulated, as flywheel weights could not be lifted onto the

wind tunnel platform and be added to the WVU portable dynamometer. Only CA fuel was used in these experiments, due to time and other constraints.

Gas and particle instruments were mounted in a roving gantry that could sample at various points within the diluted exhaust plume. Background particulate was measured with an SMPS set up near the truck's front wheel. During simulated accelerations, the gantry SMPS was operated in single-channel mode at up to five different sizes (12, 25, 65, 100, and 300 nm).

Major conclusions from the WVU report are:

- The plume was mapped and dilution ratios were determined. At steady-state conditions, dilution ratios of 75 and 125 were measured at distances of 200 and 337 inches along the plume centerline.
- PM size distributions were predominantly unimodal throughout the plume and showed GMD values of 54-58 nm with peak concentrations in the range of 10^6-10^7 particles/cm^3.
- Increased PM production was evident during simulated accelerations. Near the stack, exhaust stack particle concentrations at 65 nm dominated those of the 25, 100, and 300 nm sizes. This was also true on the plume edge and along the plume centerline (at 200 and 337 inches).
- Along the plume centerline, the concentration of 65 nm particles was one to two orders of magnitude greater than the concentration of 12 nm particles.
- Background PM in the wind tunnel was dominated by accumulation particles, though the transient appearance of nuclei mode particles was observed early in the test day (prior to starting the engine).
- A nuclei mode was observed under idle operation with a GMD of from 14 to 24 nm. It is likely that these particles were formed at the lower idle exhaust temperatures within the exhaust stack itself. These particles persisted and were detected in the background.
- No appreciable count of nuclei mode particles was detected during cruise (steady-state) or transient operation. A nuclei mode was detected during idle operation.
- Ambient sampling of PM mass during the study showed a rise in PM levels in the tunnel over the day, although they were not higher than those found in some major metropolitan areas.
- WVU researchers believe that nuclei mode particles detected during laboratory studies are strongly dependent on dilution conditions, including the type of dilution system employed.
- The WVU researchers recommend further research "to determine the effect of background on plume PM size and that these results are used in conjunction with known urban PM levels."

As shown earlier in this report, the wind tunnel background particle size distributions were characteristic of size distributions measured when running a Diesel engine in a confined space. Further, the range of dilution ratios achieved in the wind tunnel was not consistent with those achieved on the roadway. Based on the WVU discussion and the UMN results presented in this report, it is clear that the wind tunnel tests did not

adequately simulate on road dilution conditions as experienced in the E-43 project or the conditions experienced on Minnesota roadways in the Twin Cities area as reported by Kittelson, *et al.,* (2001).

Recent work done in a road tunnel in Austria (Sturm, *et al*., 2002) has shown that while a significant nuclei mode is present near the tunnel inlet where aerosol concentrations are lower, it disappears further into the tunnel were a very high background concentration has built up. The aerosol size distribution observed under these conditions is quite similar to that observed in the wind tunnel. This provides further evidence that nuclei mode formation may be suppressed by high background aerosol concentrations.

Comparison of E-43 Results with Earlier AP-2 Results, and Results of HEI Study

One finding from the HEI sponsored Diesel research program conducted at MTU (Bagley, *et al.,* 1996) was that new technology engines produced higher number emissions even though mass emissions were reduced. This finding was regarded as preliminary by both HEI and MTU. The E-43 program used an MTU-like dilution system (CVS/ejector) throughout the project in an effort to duplicate the MTU test methods. In this section, particle size distributions measured in the HEI program are compared with measurements made in the E-43 program and measurements made 20 years ago in the CRC AP2 program (Kittelson, D. B., *et al.,* 1988).

Figures 69 – 71 compare particle emissions from the Cummins 1991 LTA10-310 engine evaluated in the HEI program, the Cummins 1999 ISM engine, the Caterpillar model year 2000 3406E engines tested in the E-43 program, and a 1979 NTC 350 engine tested in the CRC AP2 program (Kittelson, *et al.,* 1988). Size distribution measurements were made with electrical aerosol analyzers in the HEI and AP2 programs and with an SMPS for the E-43 program. The size distributions shown are:

- HEI (Bagley, *et al.,* 1996) - an average of the three modes tested, 1900 rpm, 25, 50, and 75 % load. Sampling was done from a partial flow tunnel with a secondary ejector dilutor. Results are shown for a low sulfur (~100 ppm S) fuel.
- E-43 – composite averages corresponding to on-highway cruise and acceleration conditions. Sampling for ISM engine was done on-road and in a partial flow CVS system with secondary dilution. Sampling for 3406E engine was done on-road and on a chassis dynamometer using BG-1 primary and ejector secondary dilution. Results are shown for the EPA certification fuels (326 - 406 ppm S).
- AP2 (Kittelson, D. B., *et al.,* 1988) – average size distribution for on-highway cruise condition. Sampling was done on-road, with standard 1979 on highway fuel (~3000 ppm S).

Figures 69 and 70 show number weighted size distributions on log and linear scales, respectively[1]. The newer engines were tested with a higher sulfur fuel than the 1991

[1] The linear-log size distribution used in Figure 70 allows a better visual comparison of data from different studies. The log-log plot in figure 69 is the normal way of displaying size distributions because more detail of the ordinate value is shown along the whole abscissa range.

engine tested in the HEI program. Despite this, the new engines produce much smaller nuclei modes than the engine tested in the HEI program. This is especially clear in Figure 70 where the number scale is linear. The NTC 350 engine tested in the AP2 program produced the largest nuclei mode (Kittelson, *et al.*, 1988). This illustrates that the presence of a nuclei mode is not a new finding. Previous research, conducted nearly 30 years ago, documented very high on-road number concentrations of nuclei mode size particles (Whitby, 1975, Whitby and Cantrell, 1975, Wilson, *et al.*, 1977).

Figure 71 shows volume weighted size distributions. The difference in the size of the nuclei mode between the HEI engine and the engines tested in the E-43 program is striking. The newer engines show very little volume (and consequently mass) in the nuclei mode or nanoparticle range, while the HEI engine shows that nearly half its total aerosol volume is in the nuclei mode. The engine tested in the AP2 program shows the largest nuclei mode volume, but it is a smaller fraction of the total volume emitted than for the HEI engine.

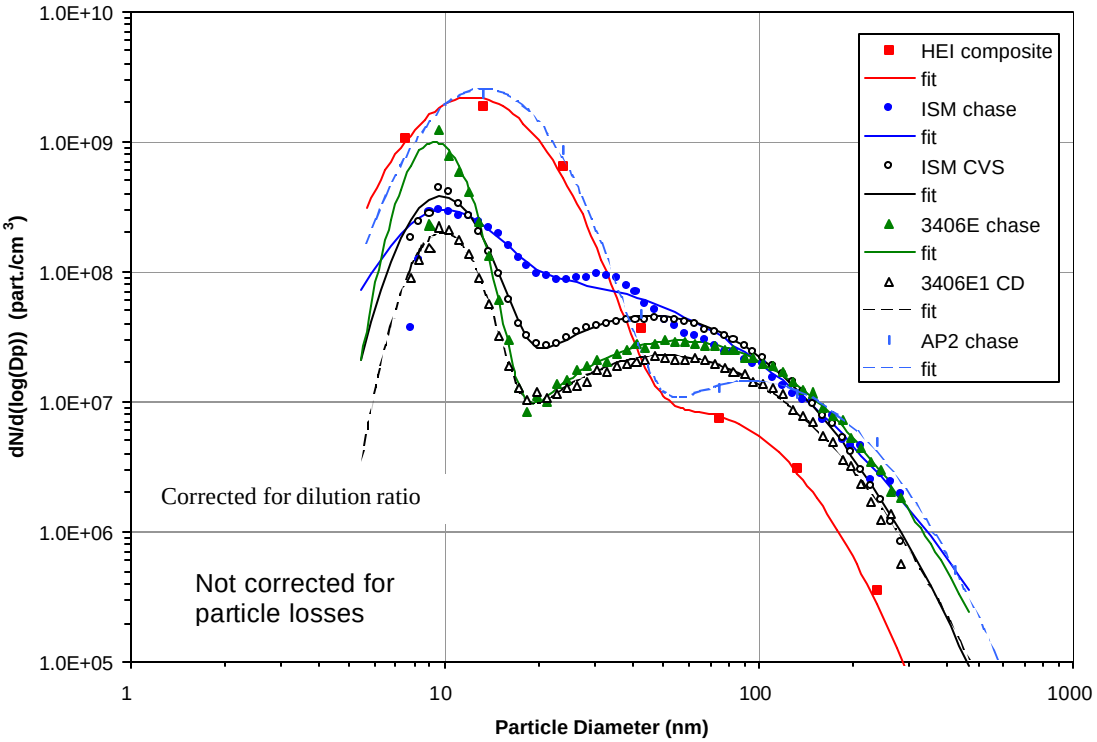

Figure 69. Number weighted size distributions measured during HEI, E-43, and AP2 research programs

Logarithmic number scale - Sources: (Bagley, *et al.*, 1996, Kittelson, *et al.*, 1988)

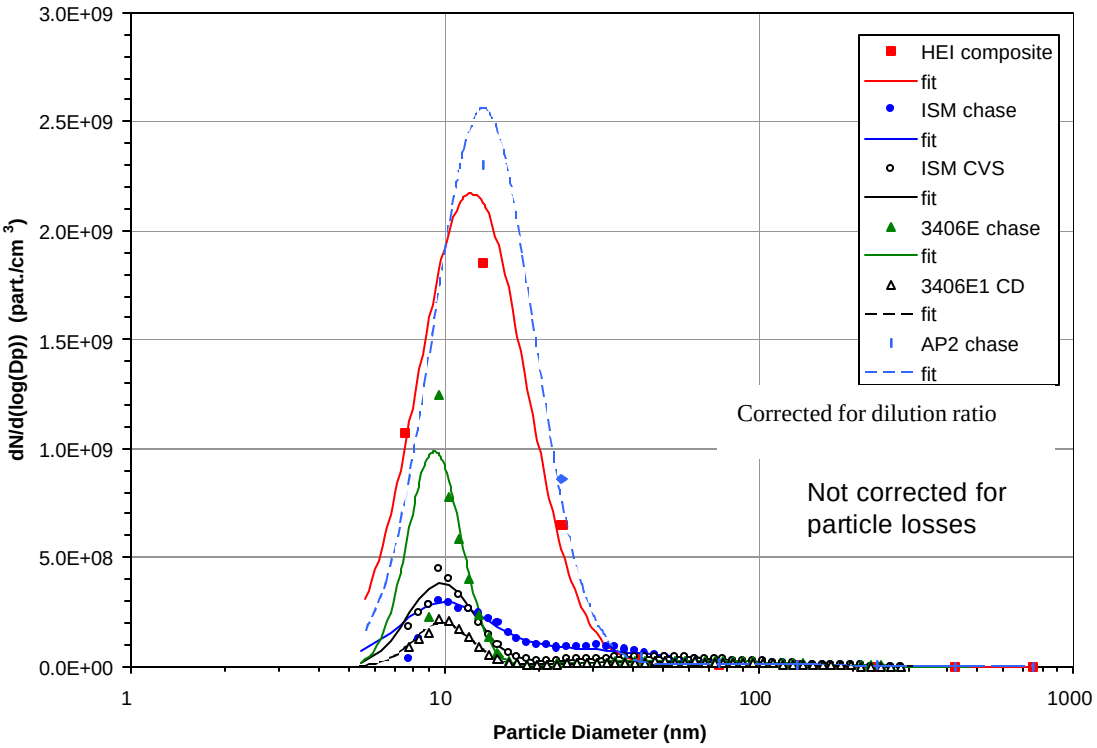

Figure 70. Number weighted size distributions measured during the HEI, E-43, and AP2 research programs

Linear number axis - Sources: (Bagley, *et al*., 1996, Kittelson, *et al*., 1988).

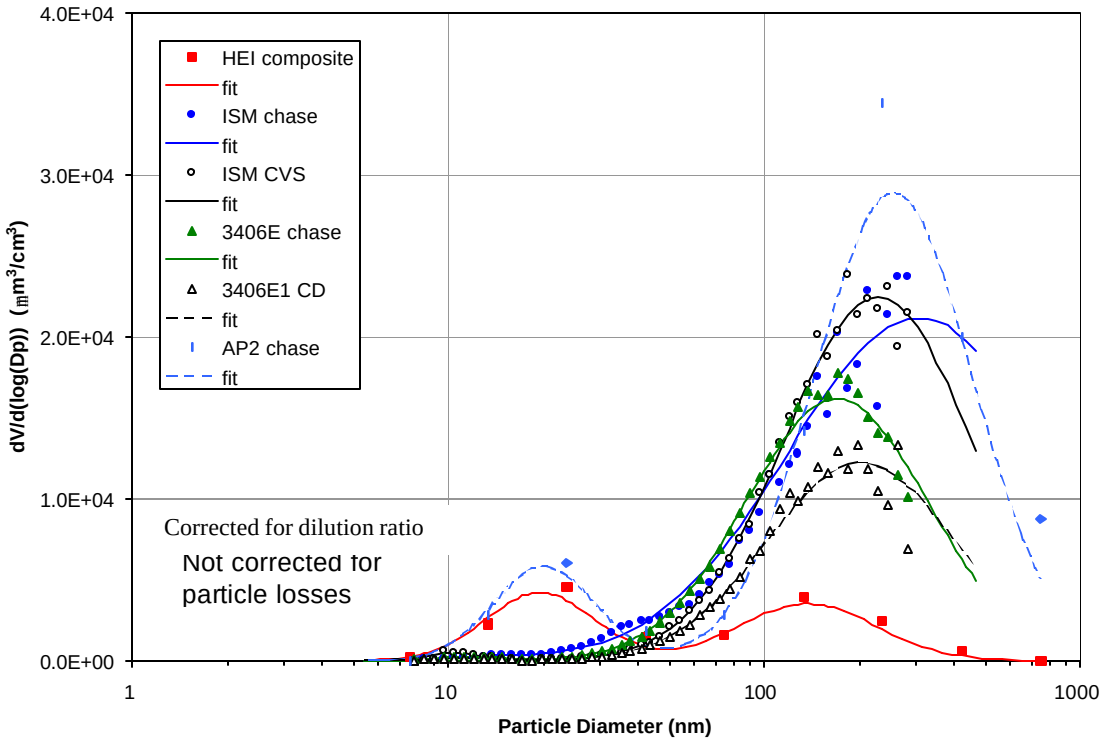

Figure 71. Volume weighted size distributions measured during the HEI, E-43, and AP2 research programs

Linear volume axis - Sources: (Bagley, *et al*., 1996, Kittelson, *et al*., 1988)

The on-road size distributions measured in the AP2 program gave larger nuclei modes than measured on-road with new technology engines in the E-43 program. As newer technology engines make up a larger part of the fleet, a decrease in number concentrations emitted over roadways can be expected.

Summary parameters for the size distributions are shown in Table A-1. The relative size of the nuclei mode of the new technology engines has been reduced compared to the engines tested 20 years ago. Since these results are plotted in terms of the normalized N/V ratio, the absolute number emissions will be proportional to the mass emissions of a given engine type. The number of particles produced per unit volume is lower, and since the mass emissions have been reduced by roughly a factor of 10, this would suggest that the number emissions have been reduced by at least this much.

The HEI results, suggesting rather low number emissions for older technology engines, and very high number emissions for new technology engines, stand in stark contrast to the E-43 results. We believe that this is a result of an unusual set of circumstances. The HEI measurements were done in a two-stage partial flow dilution system, with about a 1 second residence time in the first stage, and a dilution ratio of 15:1. These conditions, as discussed in Appendix D, allow time for nanoparticle nucleation and growth, and time for carbonaceous soot present in the exhaust to suppress nanoparticle formation. The old technology engine had a rather low SOF content, about 30 %, whereas the new

technology engine had a very high SOF content, about 75 %. As discussed in Appendix D, the formation of nanoparticles is directly related to the amount of growth precursors; thus, the high SOF fraction engine provided a high concentration of growth precursors, leading to a high concentration of nanoparticles. The difference between the old and new technology engine was magnified, because under the dilution conditions of the HEI study, the carbonaceous soot content of the exhaust played a significant role in suppressing nucleation and growth in the older engine resulting in lower nanoparticle concentrations for that engine.

For on-road conditions, the formation of nanoparticles is driven largely by the concentration of growth precursors, but is not strongly influenced by the carbonaceous soot content in the exhaust, which has inadequate time to act in suppressing the nucleation growth of nanoparticles. On the other hand, laboratory dilution conditions with relatively long residence times at fairly low dilution ratios allow suppression of particle growth with high carbonaceous soot emitting engines. Thus, under typical laboratory conditions, not only does the concentration of the growth species play a role in the growth of nanoparticles, but the concentration of carbon also plays an important role. Additionally, longer residence times available for growth in laboratory dilution systems may lead to over estimating nanoparticle formation with low carbon emitting engines.

In summary, on-road measurements have shown that nuclei modes were formed in the past and continue to be formed by modern engines. Laboratory dilution conditions may magnify the difference between nuclei mode formation tendencies of old and new technology engines and must be interpreted with care. The engines tested in the E-43 program produce smaller nuclei modes, both on-road and in the laboratory, than reported in the past in the HEI and AP-2 studies. Thus, engine improvements that have reduced mass emissions have reduced number emissions as well. This reduction is likely to be the result of reductions of volatile particle precursors, like sulfuric acid and heavy hydrocarbons.

Influence of Particle Losses on Size Distribution Measurement

Most of the results shown in this report are without a correction for particle losses in the sampling lines and in the instruments. However, our work with the QA team revealed significant losses in the sample lines and in the SMPS itself. The reason for not showing corrected results is that most of the other data found in the literature has been presented in that manner. Nevertheless, it is essential that the influence of these losses be understood. In this section three representative size distributions, with typical, smaller, and negligible nuclei modes are shown with and without the loss correction found by the QA team. We believe that the sampling line losses determined by the QA team may be erroneously high because they are so much larger than predicted by well developed theory. Despite this, we have used these loss estimates for the corrections shown below. We feel that this will show the upper extreme of the effect of losses in our laboratory setup.

Figure 72 shows composite size distributions measured for the 3406E engine running with EPA and CA fuels on the chassis dynamometer and for the ISM engine running on

CA fuel in the CVS facility. Results are show with and without loss corrections. The BG-1 / ejector dilution system was used for the chassis dynamometer tests, the CVS / ejector system for the CVS tests. The uncorrected data are also presented in Appendix A. Error bars are not shown in Figure 72 for readability, but are shown in the original plots in Appendix A.

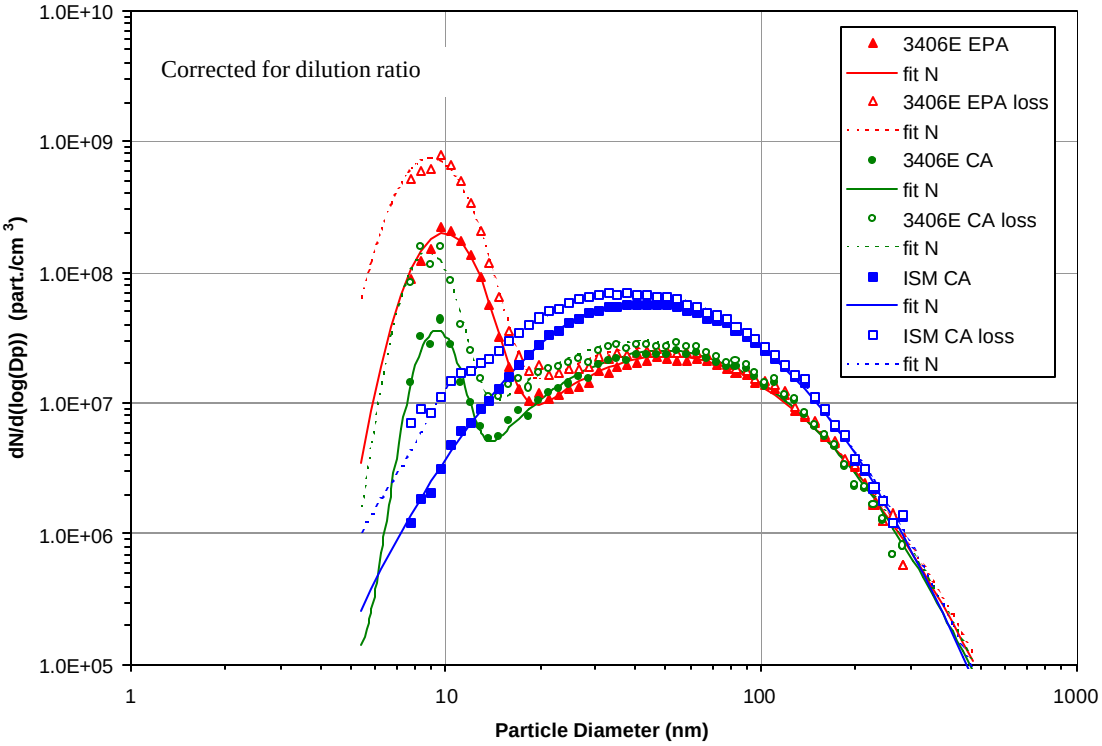

Figure 72. Typical number weighted size distributions, with and without loss corrections

Loss estimates are based on sampling line and SMPS losses reported by the QA team.

Figure 72 shows both measured data and bimodal lognormal fits to the data. It is clear that the losses cause the nuclei mode to be significantly underestimated but do not change the basic structure of the size distribution. The basic parameters of the corrected and uncorrected size distributions, as well as the parameters of the fitted results, are shown in Table 22. The loss correction has the expected effects on the parameters, increasing the number and volume fractions in the nuclei mode and decreasing mean diameters. It has a surprisingly modest influence on some of the fitted parameters. The geometric mean diameters of the nuclei and accumulation modes both decreased by about 10%. The geometric standard deviations of the nuclei modes hardly change while the accumulation modes become slightly broader. Applying the loss correction to the ISM CA size distribution that has no nuclei mode does not create one. In fact, the fitting procedure finds a larger fraction in the nuclei mode for the case without losses. This is an artifact associated with trying to fit a nuclei mode that isn't there.

The loss correction has the strongest influence on N/V ratios and volume fractions in the nuclei mode. For example, for the 3406E running on EPA fuel, the loss corrections increase the N/V ratio and the volume fraction in the nuclei mode from 8,800 to 23,000 part/μm^3 and 0.003 to 0.009, respectively. Even with loss corrections, these are far lower than the N/V ratio of 210,000 part/μm^3 and volume fraction in the nuclei mode of 0.49 calculated from a composite of the size distributions reported by Bagley, *et al*., 1996 and shown in Table A-1.

Even given the worst case losses presented here, as stated elsewhere, any loss correction does not change the conclusions of this report. Loss corrections would have minimal effect on the qualitative and quantitative outcomes of this study.

Table 22. Characteristics of typical size distributions with and without loss correction

Condition	N/V (part./μm^3)	N30/N	V30/V	DGN (nm)	DGV (nm)	DGN nuc (nm)	s_g nuc (nm)	DGN acc (nm)	s_g acc (nm)	N fract nuc	V fract nuc	Nfit/N
Original Data												
3406E EPA	8.81E+03	0.771	0.0073	16.4	142	9.9	1.23	50.4	1.98	0.730	0.0031	1.40
3406E CA	3.68E+03	0.392	0.0039	34.3	138	9.4	1.15	48.6	1.97	0.218	0.0003	1.37
ISM CA	3.85E+03	0.265	0.0060	44.6	130	25.3	1.23	45.1	1.90	0.023	0.0008	1.18
Original Data Corrected for Worst Case Losses												
3406E EPA	2.31E+04	0.907	0.0159	12.0	137	9.0	1.25	45.2	2.04	0.898	0.0087	1.46
3406E CA	6.42E+03	0.625	0.0063	21.0	135	8.8	1.17	42.9	2.04	0.509	0.0010	1.43
ISM CA	4.69E+03	0.348	0.0083	38.9	127	10.7	1.13	39.3	1.98	0.011	0.0000	1.20

Chapter 3 Summary

This summary section does not include summaries from the subsections included in "Other Results" as these sections are themselves summaries.

Atmospheric Size Distributions

- There is a large sample-to-sample variation in atmospheric exhaust plume size distributions. There is a modest level of difficulty in differentiating background and plume when sampling particle size distributions, but it was possible and the rate of success rate for capturing a plume sample increased over time.
- Background SMPS number concentrations for on-road testing were 7300 +/- 100 particles/cm^3 for Cummins and 11,400+/-100 particles/cm^3 for Caterpillar. This compares to 150,000 particles/cm^3 measured on Twin Cities Metro Area highways (Kittelson, Watts, Johnson, 2001.) The average plume concentration for chase experiments (engine contribution plus background) was approximately 86,000 particles/cm^3.
- Plume samples were corrected for background and an average difference distribution was calculated for each on-road condition.
- Background size distributions for wind tunnel tests were substantially larger in size and greater in concentration than on-road backgrounds. On average, wind

tunnel background was even greater than average on-road diluted plume aerosol for particles sized >40 nm. Wind tunnel background concentrations were high because air was recirculated within the wind tunnel. This resulted in the buildup of truck emissions over time and caused the background concentration to increase steadily throughout the test period.

Atmosphere Lab Comparison

Caterpillar Data

- In on-road tests for the 3406E with EPA fuel, summary data from Table 12 show N/V ratios ranged from 10-20,000 part/μm^3, V_{30}/V ranged from 0.7-1.4%, N_{30}/N ranged from 0.85-0.92, DGN of the nuclei mode was typically at 9 nm and DGN of the accumulation mode ranged from 60-63 nm.
- In on-road tests for the 3406E with CA fuel, summary data from Table 12 show N/V ratios ranged from 2500-3200 part/μm^3, V_{30}/V ranged from 0.27-0.3%, N_{30}/N ranged from 0.33-0.54, DGN of the nuclei mode was typically from 5-8 nm and DGN of the accumulation mode ranged from 54-58 nm.
- The comparison of on-road and laboratory conditions was complicated by the uncertainty in on-road dilution ratios. The comparison of N/V size distributions made for a more robust comparison. The comparison of size distribution based on N/V_{total} (actually $(dN/dlogD_p)/V_{total}$), as opposed to on a $dN/dlogD_p$ basis, yields a dilution ratio independent way of comparing distributions. This approach gives a normalized size distribution that gives number at a given size per unit total volume, and by extension, as a function of total mass of particulate.
- The results of the Caterpillar analysis focus on accelerations because this condition was found to be the most repeatable with the least uncertainty for both on-road and laboratory conditions.
- For 3406E engine under acceleration condition, nuclei mode present for both fuels and loads with the EPA fuel yielding a larger nuclei mode. On a normalized, N/V basis, the EPA fuel produces an order of magnitude larger nuclei mode than does CA fuel.
- The 2-stage dilution tunnel poorly reproduces the on-road size distribution in the nuclei mode range, but matches on-road size distributions fairly well in the accumulation mode range. Constraints on access necessitated the use of an excessively long transfer line from the exhaust to the first stage of dilution. This transfer line was the probable cause of the tunnel's poor performance.
- For laboratory tests involving 3406E engines, the EPA fuel makes a larger nuclei mode than does the CA fuel. On a dilution ratio corrected basis, the BG-1 reproduces the EPA fuel on-road nuclei mode better than the CVS/ejector dilution system or the 2-stage. This is also true for CA fuel.
- On a normalized basis (for 3406E engine, both fuels, and the acceleration conditions), the BG-1 somewhat overestimates the nuclei mode concentration while the CVS/ejector dilution systems at the CVS nearly match the normalized on-road nuclei mode. This difference may not be significant because different

test engines were used on-road and in the laboratories. Again, the 2-stage underestimates nuclei mode formation.

- The number mean diameters of the accumulation mode determined from lab data (35-43 nm) are less than those determined from on-road data (54-64 nm.) This may be due to mismatch in engine conditions or to condensation onto accumulation mode particles during dilution.

Cummins Data

- For the Cummins phase of the work, on-road, wind tunnel and CVS data were compared for the ISM engine and CA fuel only (EPA fuel and the L10 engine were not used at the wind tunnel).
- For the ISM engine and CA fuel, the on-road distributions show a nuclei mode, while the laboratory distributions do not generally show a nuclei mode. We believe that this was due to cold temperatures (5 – 11 °C) during on-road testing of the CA fuel.
- Again, for the ISM engine and CA fuel, the CVS tunnel was run at two different primary dilution ratios (5 and 8). A nuclei mode formed at the lower dilution ratio, but it was still much smaller than for on-road conditions where one size distribution had a large influence on the average.
- The wind tunnel size distribution, especially in the nuclei mode range, is a poor match for on-road and laboratory conditions. This is likely due to high background particle concentrations, and possibly due to the relatively low tendency for the ISM engine running on the CA fuel used in these tests to produce a nuclei mode except at very light loads or with cool dilution air.

Sampling and Dilution System Comparison

- Composite size distributions were compiled to allow overall comparisons between dilution tunnels, fuels, and engines. These composites are described in the text and are weighted composites of cruise and acceleration conditions, with cruises weighted most heavily.
- In general, the observed size distributions fit a bimodal log normal distribution. Nuclei mode number fractions range from 70-90 % when a significant nuclei mode is present.
- Data from Table A-1 show that the accumulation mode number mean diameters for the newer engines (the ISM and 3406E) range from 41 to 56 nm and for the older engines (the L10 and 3406C) range from 55 to 62 nm.
- N/V and V_{30}/V are useful parameters of the size distributions for the E-43 program. The N/V ratio gives the number of particles formed per unit volume of emitted particle matter. Since the particle mass is proportional to particle volume, the N/V ratio gives a measure of the particles formed per unit mass emitted. The ratio of V_{30}/V gives an estimate of the volume fraction of particles in the nuclei mode, which in turn is related to the mass fraction in the nuclei mode.
- The highest on-road value of N/V observed was 37,000 part/μm^3. This is smaller than the 130,000 to 370,000 part/μm^3 range reported in the HEI report. The on-

road maximum value for E-43 was observed during cold weather operation and this value was not reproduced for a similar laboratory condition.

- Data from table A-1 show the highest on-road observed value of V_{30}/V was 0.08, which is substantially lower than the 0.39-0.49 calculated from the HEI data.
- The highest values of N/V (1.52×10^5) and V_{30}/V (0.329) were measured in the laboratory for the ISM engine at 1200 rpm, 482 N-m for 49-ppm sulfur fuel and specially formulated lube oil (values from row 13 of table C-1). These values are not representative of normal operation. For a similar condition with conventional lube oil, N/V and V_{30}/V were 3,400 part/μm^3 and 0.004, respectively. This shows the large influence that lube oil can have on nanoparticle formation.
- With the exception of the Cummins ISM experiments with CA fuel, on-road measurements gave similar fractions of particles in the nuclei mode, to CVS and BG-1 dilution conditions.
- During Cummins testing, the CVS (CVS/ejector) system does a better job of matching the on-road nuclei mode for EPA fuel than for CA fuel, where the match is very poor. This may have be due to the low ambient temperatures encountered when testing the CA fuel on-road.
- In general, the BG-1 system (in the configuration used) tended to slightly overestimate the nuclei mode formation and the CVS system tended to underestimate nuclei mode formation.
- The 2-stage tunnel was configured with too long a transfer line. This may have led to the loss of particle precursors in the transfer line and suppression of nuclei mode formation. The 2-stage tunnel underestimated on-road size distributions in the nuclei mode range.
- During Caterpillar testing, there was little difference between the nuclei modes measured with the 3406E and 3406C engines. The 3406E nuclei mode is slightly larger, but the 3406C nuclei mode is broader. This results in a larger volume fraction, V_{30}/V, in the nuclei mode for the older engine.
- In most cases at both Caterpillar and Cummins, for all engines, fuels, and conditions, the CPC number is higher than the SMPS number concentration, indicating particles below the range of the SMPS.

Engine Comparison

- Four 3406E engines were tested either on-road or in the Caterpillar laboratory dynamometer facilities.
- There is no significant variation amongst the members of the 3406E engine family that were tested in the Caterpillar CVS and performance cell facilities.

Specially Formulated Fuel and Lube Oil Experiments

- The effect of different combinations of specially formulated fuel and lube oil on the formation of nanoparticles was examined. The major difference between the fuels was sulfur content and the lube oil was specially formulated to have a low sulfur concentration.

- For conventional lube oil and both 1 ppm and 49-ppm sulfur fuel, there is no significant formation of a nuclei mode. N/V ratios are all $<10^4$ and V_{30}/V is less than 0.01 for most cases.
- For low sulfur lube oil, a large nuclei mode was formed for all fuels at 1800 rpm/154 N-m and for all fuels but the 1-ppm fuel for the 1200-rpm, 482 N-m condition. At the high load condition, 1800/776 N-m, only the 325-ppm sulfur fuel created a substantial nuclei mode.
- When present, most of the nuclei mode was removed when the TD was connected to the SMPS, suggesting that the nuclei mode is composed of volatile particles.
- DC and SMPS active surface area measurements agreed within 25 %.
- The most surprising result was the large influence of specially formulated lube oil. Contrary to expectations, low sulfur oil led to an increase in nanoparticle formation in nearly all cases. It is possible that the increase in nanoparticle formation by low sulfur oil was related to the formulation of the oil necessary to compensate for the removal of sulfur. It could also be due, in part, to the release of volatile components from the oil, related to the lack of oil break-in.
- Increasing fuel sulfur also increased nanoparticle emissions, especially at high load.
- The observations of the importance of lube oil in nanoparticle formation are consistent with those made by others (Sakurai, *et al.*, 2001)

Aerosol Composition, Transient Tests, and MOUDI Samples

- It is believed, based on TDPBMS experiments and various experiments with the thermal denuder, that most nuclei mode particles are composed of volatile material.
- There appear to be substantial numbers of particles below the size range of the SMPS that are within the size range of measurement of the CPC. Based on TD experiments with these aerosols, it appears that these particles are substantially volatile.
- FTP transient cycles were conducted at the Cummins CVS facility with the SMPS acting as a size classifier. Nearly all of the 10 nm particles were found to be volatile.
- A transient equivalent size distribution was calculated for the FTP cycle. This size distribution can be found in the text. This size distribution reveals that most of the nuclei mode is less than 10 nm and is below the sizing range of the SMPS used. This is consistent with the CPC measurements, as compared to SMPS size distribution number concentration measurements.
- Thermal denuder measurements for on-road tests also showed that on-road nuclei modes are largely volatile, but may posses as much as 10 % non-volatile material by number. This is greater than, but consistent with, the results obtained by Abdul-Khalek, *et al.*, (1998a) using a catalytic stripper where about 1 % of the material was composed of a non-volatile residue. Given large uncertainties in on-road data, further study of this finding is required.
- MOUDI and nano-MOUDI samples were collected primarily for chemical analysis.

- At the wind tunnel, MOUDI and nano-MOUDI size distribution shapes are similar to those measured by the SMPS, especially when particle density effects are considered.
- Experiments were conducted to determine the extent of particle bounce within the nano-MOUDI and to recommend a scheme for greasing substrates to minimize bounce and maximize the opportunity for chemical analysis.
- Greasing appears to reduce the amount of mass collected by the nano-MOUDI stack and bounce appears to be a problem. The data suggest that greased substrates collect more particles, minimizing the deposition of larger particles on the nano-MOUDI stages (<0.056 µm).
- An SMPS was used to measure particle concentrations upstream and downstream of the MOUDI stages (all stages $\geq$ 56 nm). Downstream measurements showed significant penetration of particles larger than 56 nm mobility diameter, but showed peak penetrations of only about 70 %. This finding suggests that there were significant interstage losses of small particles in the upper stages. The penetration efficiency in the nano-MOUDI decreased during a 30-min sample run. It is possible that as particles collect on greased or ungreased substrates, the efficiency of collection increases.
- When measuring the same aerosol, the nano-MOUDI produced size distribution with a smaller particle size than the MOUDI. However, modifications were made to both the nano-MOUDI and MOUDI for this study and particle size cutpoints for the individual stages were not checked using standard calibration aerosols. It is likely that differences in calibration would account for these differences.
- The SMPS volume distributions for tests at Cummins generally track with the nano-MOUDI distributions but exhibit larger size. When density effects are considered, SMPS data matches nano-MOUDI data quite well.
- SMPS and nano-MOUDI measurements were made on the Caterpillar C-12 engine in the UMN laboratory. When the SMPS volume size distribution was converted to a mass distribution using density data from Park, *et al*., (2001), good agreement between the nano-MOUDI in the accumulation mode range was obtained, but the nano-MOUDI overestimated the size of the nuclei mode.

Other Results

- Comparisons of CPC and nano-SMPS with conventional SMPS measurements made on the C-12 engine reveal that significant numbers of particles may be found below the lower sizing limit of an conventional SMPS. This is consistent with CPC and SMPS measurements made during the main on-road and laboratory tests in the E-43 program.
- Comparisons of E-43 on-road and laboratory size distributions with earlier results from the HEI report (Bagley, *et al*, 1996) and the CRC AP-2 study shows similar bimodal structure but much smaller number and volume fractions in the nuclei mode for the E-43 data.
- The influence of particle losses in sampling lines and in the SMPS on typical size distributions was examined. Correcting for losses decreased DGNs by about 10 %. N/V ratios and the volume fractions in the nuclei mode increased by

factors of 2 to 3 when a significant nuclei mode was present but did not cause one to appear when one was not observed in uncorrected data.

CHAPTER 4 – TECHNICAL SUMMARY AND CONCLUSIONS

Introduction

Diesel engines are used extensively in transportation. In the U.S., Diesel engines are most commonly used in the over-the-road trucking industry due to their power, durability and efficiency. However, like other sources of combustion pollution, Diesels emit exhaust gases and particulates that are subject to regulation by State and Federal authorities. To meet these regulations, engine manufacturers have significantly lowered exhaust emissions, primarily by improving engine design and efficiency. Emission control technology and improved fuel and lube oil formulations have also led to a reduction in emissions. However, recent research suggests that there are still concerns related to health effects from exposure to fine particulate matter (< 2.5 micrometers in diameter, $PM_{2.5}$) in the atmosphere (Health Effects Institute 2001, 2002a). These concerns apply to Diesel exhaust and are discussed in depth elsewhere (Health Effects Institute 1995, 2002b).

Particulate emissions from internal combustion engines have traditionally been regulated solely on the basis of total particulate mass emissions; no reference is made either to the size or the number concentration of the emitted particles. Modern engines emit much lower particle mass concentrations than older engines. Another Health Effects Institute funded study reported, that for Diesel engines, the reduction in particle mass was accompanied by an increase in the number of nanoparticles < 50 nanometers (nm) in diameter (Bagley, *et al*., 1996 and Johnson and Baumgard, 1996). The low emission engine used in this study was a prototype engine with unusual emission characteristics characterized by a disproportionately high soluble organic fraction associated with the particulate matter. It is likely that excess volatile material in the exhaust contributed to the formation of the large number of nanoparticles. The Health Effects Institute and the investigators were careful to note that their results were preliminary and subject to confirmation by other investigations.

The University of Minnesota and partners under contract to the Coordinating Research Council undertook the study titled "Diesel Aerosol Sampling Methodology" to sample, characterize, and quantify nanoparticles in Diesel exhaust. The goal of CRC E-43 was to develop Diesel aerosol sampling methods for the laboratory that would produce results similar to those obtained under real-world roadway conditions. To accomplish this goal, a fundamental investigation was required to understand the physical processes that affect aerosol formation, transformation, measurement, and the resulting aerosol size distribution. These processes include dilution, nucleation, condensation, adsorption and coagulation. In addition to the physical processes, the nature of the particulate matter emitted in exhaust is affected by the engine condition, fuel, lube oil, exhaust system, sampling system, and other factors. The influence of these parameters on particulate matter emissions must be understood before real-world, on-road combustion aerosols can be duplicated in the laboratory. Results of this research have identified key parameters

that must be controlled so that on-road Diesel aerosol size characteristics can be reproduced in the laboratory.

Diesel Aerosol

Diesel and other aerosols are often characterized by measuring particle diameters of the individual particles making up the aerosol. The aerodynamic diameter, defined as the diameter of a unit density (1 g/cm^3) spherical particle that has the same settling velocity as the measured particle, is frequently used to classify particles for determining their mass size distribution by gravimetric measurement. Typically, the electrical mobility diameter is used to classify aerosols for determining their number size distribution. The electrical mobility diameter is a close approximation of the Stokes diameter, which is defined as the diameter of a spherical particle having the same density and settling velocity as the measured particle. The Stokes diameter determines the particle diffusion coefficient and its diffusional deposition characteristics. The densities of Diesel particles are typically less than 1 g/cm^3 so that aerodynamic diameters are less than Stokes diameters. Other parameters, such as surface area and volume, are also useful in characterizing aerosols. In the E-43 project, multiple measures were used to characterize Diesel aerosols including particle number, volume, surface area and mass.

Figure 73 shows a typical Diesel particle size distribution weighted by number, surface area, and mass. Diesel particle size distributions typically fit a lognormal, trimodal form like those shown in Figure 73, with the concentration in any size range being proportional to the area under the corresponding curve in that range. The nuclei, accumulation, and coarse modes make up the trimodal size distribution. Nuclei mode particles range in diameter from ~ 0.003 to 0.03 micrometers (μm) or ~ 3 to 30 nm. In the past, the nuclei mode was defined as particles between 5 and 50 nm. However, in light of the E-43 investigations, it is appropriate to redefine the nuclei mode to encompass the range between 3 and 30 nm. These particles consist mainly of volatile organic and sulfur compounds in varying proportions as well a small amount of solid material likely to consist of carbon and metallic compounds. Most of the volatile particles form during exhaust dilution and cooling. The nuclei mode typically contains 0.1-10 % of the particle mass and up to 90 % or more of the particle number. The accumulation mode ranges in size from roughly 0.03 to 0.5 μm (30-500 nm). Most of the mass, composed primarily of carbonaceous agglomerates and adsorbed materials, is found in the accumulation mode. The coarse mode consists of particles larger than 1 μm (> 1,000 nm) and contains 5-20 % of the Diesel aerosol mass. These relatively large particles are formed by reentrainment of particulate matter, which was deposited on cylinder and exhaust system surfaces (Kittelson, 1998).

Figure 73 also shows some size definitions, notably, ultrafine and nanoparticles that have diameters less than 100 and 50 nm, respectively. There is some disagreement about the most appropriate boundary for the nanoparticle range, but 50 nm is widely used. Note that the nuclei mode falls nearly entirely within the nanoparticle range while the accumulation mode straddles the fine, ultrafine and nanoparticle ranges. The nuclei and accumulation modes of Diesel engine exhaust are formed at different times and have

different compositions. It is more convenient and meaningful to describe Diesel exhaust size distributions in terms of the characteristics and sizes of the nuclei and accumulation modes rather than focusing on ultrafine and nanoparticle fractions; however, if there is a significant nuclei mode, nearly all of the nanoparticles are found in this mode and the terms are nearly synonymous.

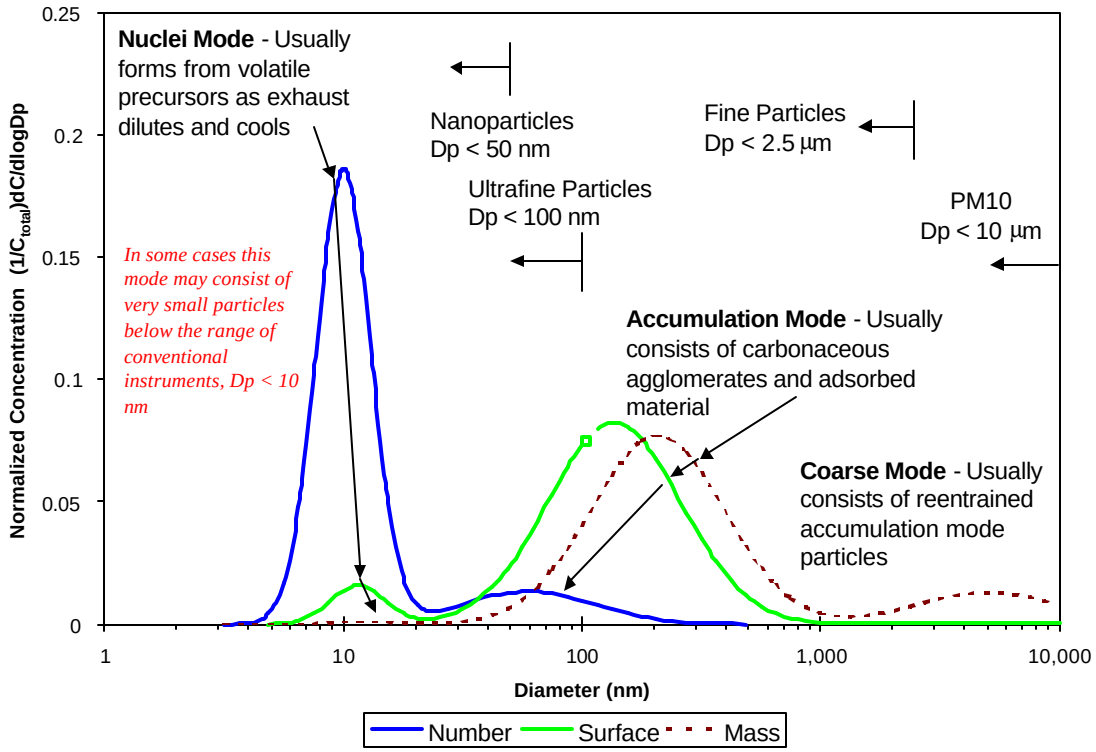

Figure 73. Diesel aerosol size distribution
D_p = particle diameter, C_{total} = total concentration

Approach

Field studies were carried out using four test trucks powered by Caterpillar and Cummins engines. Environmental Protection Agency certification (EPA fuel) and market basket blends of California fuels (CA fuel) were used for all tests. On-road, chase studies were carried out in Minnesota and a wind tunnel study was carried out at the Langley wind tunnel in Langley, Virginia. Both Caterpillar and Cummins engines were tested on-road, but only one Cummins engine was tested at the Langley wind tunnel. Engine and chassis dynamometer laboratory studies were carried out at Caterpillar and Cummins in Peoria, Illinois and Columbus, Indiana, respectively. Engine dynamometer studies were also done at the University of Minnesota.

Several mini-dilution systems were evaluated during the laboratory portions of the project. A 2-stage ejector system was used in multiple configurations throughout the project (Abdul-Khalek, *et al*., 1998a, 1998b and 1999). Another system was used at Caterpillar and Cummins laboratories to simulate the dilution system used in the Health

Effects Institute studies conducted by Michigan Technological University (Bagley, *et al*., 1996 and Johnson and Baumgard, 1996). It consisted of a constant volume sampler (CVS) dilution tunnel and a secondary air ejector dilutor (CVS/ejector). Finally, a Sierra Instruments BG-1 dilution system followed by an ejector dilutor (BG-1/ejector) was used at Caterpillar.

Quality Assurance

To ensure quality processes and products for the E-43 project, CRC appointed a separate quality assurance (QA) team. The primary goal of the QA team was to provide independent opinions and guidance for the research team in the development of QA protocols for the research and final evaluation of project data. The QA team patterned their activities according to the QA requirements and guidance recommend by the U.S. Environmental Protection Agency (Environmental Protection Agency, 1998). The QA team prepared a detailed final report describing their activities and findings (Ayala, *et al*., 2002). What follows is a brief summary of the findings from this report.

QA team activities were initiated after the start of the E-43 project; thus, all aspects of the project were not subjected to the same level of QA. Specifically, the Cummins on-road chase tests and the Langley wind tunnel tests were completed before implementation of the QA plan. Due to the late introduction of the QA team's plan, it became a working document rather than a planning document. Normally, a QA plan is in place before the beginning of the project to ensure the highest quality possible, but in this case changes or updates were made to the plan as new material became available.

The quality assurance level (level 3) attained for E-43 was consistent with "projects producing results used to evaluate and select basic options, or to perform feasibility studies or preliminary assessments of unexplored areas which might lead to further work" (Environmental Protection Agency, 1991). Level 3 is consistent with a research project investigating new methods for characterization and measurement of nanoparticles. Standard procedures were not, and are still not, available for many of the measurements made during the project.

It must be pointed out that there are no calibration standards for particle number or surface area. It is impossible to obtain the equivalent of a calibration grade span gas for such measurements. Instrument to instrument consistency checks were done as part of the E-43 program but these were relative rather than absolute checks. If any measure of particle concentration other than mass is to be used as a standard, reference calibration systems need to be developed.

QA team audits of project records indicate that data generated during the project are generally valid. QA team performance audits of the aerosol instruments revealed that the equipment was capable of generating consistent and valid measurements. The instruments were used in a manner consistent with standard operating and research procedures throughout the project. Surveillance visits by the QA team to the test sites documented that field activities were conducted in accordance with the agreed-upon

protocol. Audits of the record archive revealed that the information collected by the research team was in conformance with the QA plan. The QA team concluded that the UMN research team demonstrated conformance with the QA plan for most of the experimental tasks. The QA team also noted non-conformances and recommended corrective actions to the project investigators (Ayala, *et al*., 2002).

QA Report Recommendations

QA recommendations for project planning and execution were made in the QA final report (Ayala, *et al*., 2002) based on the E-43 project. These recommendations are summarized below. It should be emphasized that the points discussed below are meant to optimize the effectiveness and efficiency of a QA plan, and that not all of these points were integrated into the E-43 project.

- It is essential to determine QA goals and develop a QA plan before project activities are initiated.
- QA responsibility should be clearly assigned and the QA team should be involved in project planning.
- Quality control measures and procedures should be jointly developed and approved by the research team, the QA team and the sponsor.
- The QA plan should become an integral part of the execution plan.
- To ensure QA for field experiments, procedures should be developed and followed rigorously by project staff.
- Random audits of sampling systems and instruments should be conducted as frequently as required to meet QA goals.
- Instrument audits should be exhaustive and prescribed during project planning so as to establish the accuracy (precision and bias) of the sampling instruments.
- When attempting to measure the number and size of ultrafine emissions, transport losses by diffusion or other potentially relevant mechanisms such as turbulent deposition and thermophoresis should be quantified and reported. Losses may be considered a system bias or "persistent distortion of the measurement process" (Environmental Protection Agency, 1998). Thus, if instrument and sampling system precision and biases are established, the accuracy of the measurements may also be determined. [Particles smaller than about 15 nm have high diffusion coefficients and are subject to large losses in sampling and dilution systems and in instruments. Although particle losses in the sampling systems used in this program were determined as part of the QA effort, the loss studies were not comprehensive in scope, and the QA and research teams agree further work in this area is required. However, representative measurements with and without loss corrections are shown in the final report, but most data in the final report are uncorrected for particle losses. Particle losses of more than 50 % are not uncommon and are often not reported in the literature. By not correcting for particle losses, E-43 data can be compared to other published data.]
- The quantification of losses is likely to require additional experimentation due to the limitations of theoretical predictions. Therefore, if the performance of the sampling methods is ensured, including particle losses, and dilution conditions are

known precisely, an accurate ultrafine particle number emission rate can be estimated.
- A record of all field activities should be submitted for custody, and a chain of custody mechanism should be implemented.
- Data post-processing procedures and software development should be decided upon during project planning and approved by the project staff, QA personnel, and the sponsor; and the final data format, data reduction, acceptance criteria, handling, and retrieval procedures should be delineated before activities are initiated.

When these measures are considered, it is feasible to design a quality integrated work plan for non-routine academic research that meets stringent quality assurance requirements.

Specific Objectives And Findings

The objectives of the E-43 project are listed below. Underneath each objective is a list of the pertinent findings relevant to that objective. Further details of the E-43 project are found in Cummins and Caterpillar data volumes and associated reports (Kittelson, *et al*., 2000, 2002a,b,c). Details on the wind tunnel study are available in two reports (Kittelson, *et al.*, 2002d and Clark, *et al.*, 2001). Detailed information on the findings from the surface area instruments used in the E-43 project is available in reports prepared by the Paul Scherrer Institute (Bukowiecki, N., *et al*., 2001 and 2002).

Objective 1. Conduct on-road chase and wind tunnel experiments to determine the actual particle size distribution and particle number concentration in the exhaust plume from heavy-duty Diesel vehicles operated on the road or in the wind tunnel.

The Diesel aerosol exhaust size distribution is influenced by many factors. These include engine condition, fuel and lube oil composition, exhaust system configuration, sampling system and sampling conditions. Engine and sampling system stabilization and previous engine operating history play important roles in determining the size distribution. Furthermore, ambient weather conditions, such as temperature, wind speed and direction also affect the on-road size distribution and the ability to capture a plume sample. These factors made the on-road sampling conditions less repeatable than what is normally encountered in an engine test laboratory. However, a consistent pattern of nuclei mode formation emerged supporting earlier roadside and on-road observations of nuclei mode particles (see for example Whitby *et al*., 1975, Kittelson, *et al.*, 1988). The findings below are based on on-road composite size distributions.

On-Road Findings:

- All of the test vehicles were found to have bimodal distributions under cruise and acceleration test conditions with both EPA and CA fuels.
- Nuclei mode geometric mean number diameter (DGN) ranged from 6-11 nm.
- Accumulation mode DGN ranged from 52-62 nm.

- The nuclei mode was highly variable. This variability was partly real and depended upon engine, fuel and environmental conditions, but it was also partly a function of the difficulty in capturing a plume, distinguishing the plume from background and measuring the dilution ratio.
- Cold temperatures (5 to 11 ^{o}C) favored nuclei mode formation.
- California fuel produced fewer nanoparticles under most conditions, but the accumulation modes produced by EPA and CA fuels were similar.
- Both old and new technology engines produced nuclei modes of similar magnitude, but the newer technology engines produced smaller accumulation modes. This finding is consistent with new engine technology that has reduced mass emissions.
- When a thermal denuder was used to heat the sample to 300°C prior to passage to the instruments, the nuclei mode was found to shrink in size. This finding implies that the aerosol consisted largely of volatile compounds.
- On-road dilution is rapid, typically on the order of 1,000:1 in 2 s.
- On-road studies require fast response instruments with wide dynamic ranges.

Several ratios were used to describe the size of the nuclei mode relative to the accumulation mode to determine the relative contribution of nanoparticles. These ratios are the number fraction in the nuclei mode, the volume fraction in the nuclei mode, and the ratio of total particle number to total particle volume as determined by the Scanning Mobility Particle Sizer. We observed the following based on these ratios:

- The number fraction in the nuclei mode ranged from 37 to 87 %.
- The volume fraction in the nuclei mode ranged from 0.3 to 2.1 %.
- The number to volume ratio ranged from 2500 to 37000 particles/μm^3. Number to volume ratios greater than about 10^4 part/μm^3 generally indicated the presence of a distinct nuclei mode.

West Virginia University Wind Tunnel Findings:

- The plume was mapped and dilution ratios were determined. At steady-state conditions, dilution ratios of 75 and 125 were measured at distances of 5 and 8.5 m along the plume centerline. This range of dilution ratios was substantially lower than the typical on-road dilution ratio (1,000:1).
- In contrast to the on-road size distributions, the wind tunnel size distributions were predominantly unimodal throughout the plume and showed DGN values between 54 and 58 nm.
- Increased particulate matter production was evident during simulated accelerations. Near the stack, particle concentrations of 65 nm particles were dominant. This was also true on the plume edge and along the plume centerline, at 200 and 337 inches.
- Along the plume centerline, the concentration of 65 nm particles was one to two orders of magnitude greater than the concentration of 12 nm particles.
- Background particulate matter in the wind tunnel was dominated by accumulation mode particles that gradually increased in concentration throughout the day. This

is consistent with recirculation of Diesel exhaust. A nuclei mode was observed early in the test day (prior to starting the engine), but disappeared shortly after engine testing began.

- o A nuclei mode was observed under idle operation with a DGN ranging from 14 to 24 nm. It is likely that these particles were formed at the lower idle exhaust temperatures within the exhaust stack itself. These particles persisted and were detected in the background.
- o No appreciable count of nuclei mode particles was detected during cruise (steady-state) or transient operation.
- o Ambient sampling of particulate matter mass during the study showed a rise in particulate matter levels in the tunnel throughout the day. This was consistent with recirculation of Diesel exhaust.

The wind tunnel sampling conditions were quite different from those encountered on-road. On the highway, the closest point of plume capture was about 30 m under extremely turbulent mixing conditions. In the wind tunnel, samples were collected 2 to 10 m behind the vehicle stack under far less turbulent conditions. Wind tunnel background particle size distributions were characteristic of size distributions measured when running a Diesel engine in a confined space. Further, the range of dilution ratios achieved in the wind tunnel was not consistent with those achieved on the roadway; thus, the difference observed between the on-road and wind tunnel size distributions was a reasonable finding.

Objective 2. Conduct laboratory tests to compare on-road aerosol data with data generated in emissions test facilities to determine if current emission test facility sampling and analysis methods are adequate for characterizing particle size observed on the road.

Since transient engine dynamometer testing was not part of the E-43 program and only limited transient tests were performed, our results and recommendations are most appropriate for steady-state testing.

Duplication of on-road size distributions in the laboratory is made difficult because of unsteady conditions encountered during normal truck operation. Thus, those who attempt duplication of exhaust particle size distribution results need to be aware that current and past engine operating conditions, fuel, lubricating oil, dilution ratio, dilution rate, environmental conditions (temperature, humidity, background air quality), sampling system design features and other parameters are important influences on the size distribution. Tight control of these parameters is not possible during on-road chase tests, but can be achieved in the laboratory. Most nanoparticles are found in the nuclei mode. The nuclei mode is the most difficult part of the size distribution to reproduce because it consists mainly of volatile particles that are usually formed during dilution. The accumulation mode, which consists primarily of solid carbonaceous agglomerates, is much easier to reproduce.

While it was difficult to match on-road size distributions for individual test conditions with laboratory size distributions, much better agreement between on-road and laboratory was achieved for composites of several test conditions. On-road measurements consistently showed the presence of a nuclei mode. Laboratory measurements also showed the presence of a nuclei mode under some conditions. The agreement between on-road and laboratory measurements improved as more experience was gained with sampling protocols. Consequently, more consistent results were obtained during the second year of the program (Caterpillar engines). Laboratory size distributions obtained using either the CVS/ejector or Sierra BG-1/ejector dilution systems were similar. It was found that any dilution system with a transfer line between the engine and the first stage of dilution that allowed significant heat and mass transfer underestimated the nuclei mode.

Figures 74 and 75 show comparisons between composite size distributions measured on-road and in the laboratory using the Sierra BG-1/ejector dilution system for the Caterpillar 3406E engine running on EPA and CA fuels, respectively. In both plots, the shapes of the accumulation modes on-road and in the laboratory are very similar. The differences in concentration between on-road and lab conditions are primarily due to difficulties in determining on-road dilution ratios. The size of the nuclei mode relative to the accumulation mode is not influenced by uncertainties in the dilution ratios. Comparisons of lab and on-road dilution shows, for EPA fuel, that the lab underestimates the relative size of the nuclei, N/V = 8800 vs. 12,600 part/μm^3. On the other hand, for the CA fuel, the lab slightly overestimates the small nuclei mode with N/V = 3700 vs. 2600 part/μm^3.

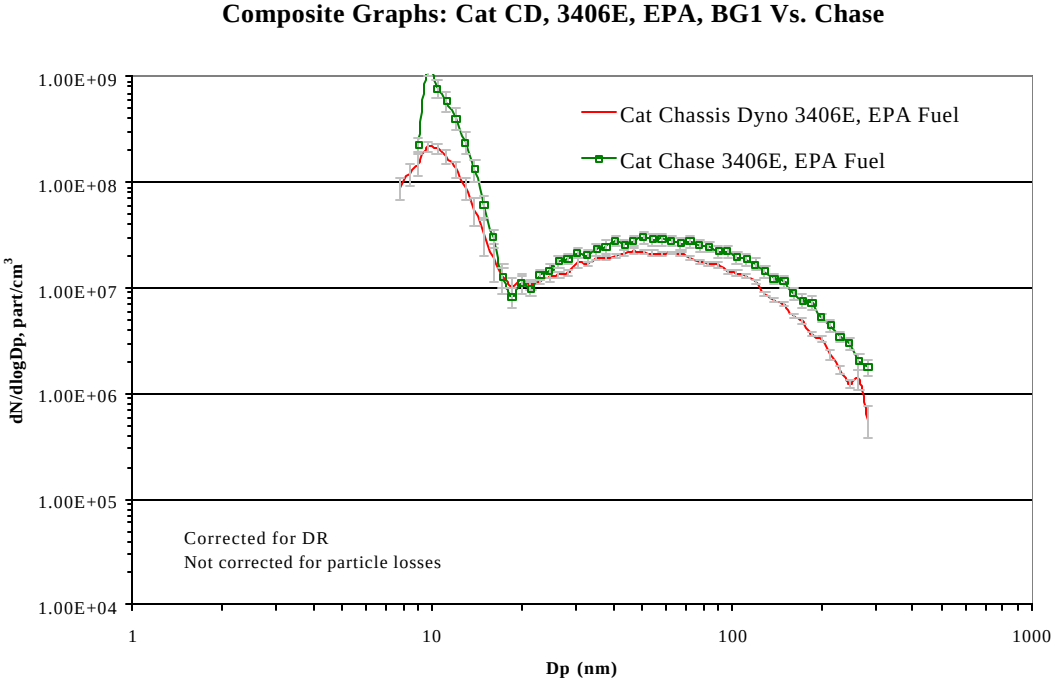

Figure 74. Composite particle number size distribution Caterpillar 3406E engines, EPA fuel, chassis dynamometer vs. on-road chase, BG-1/ejector dilution system

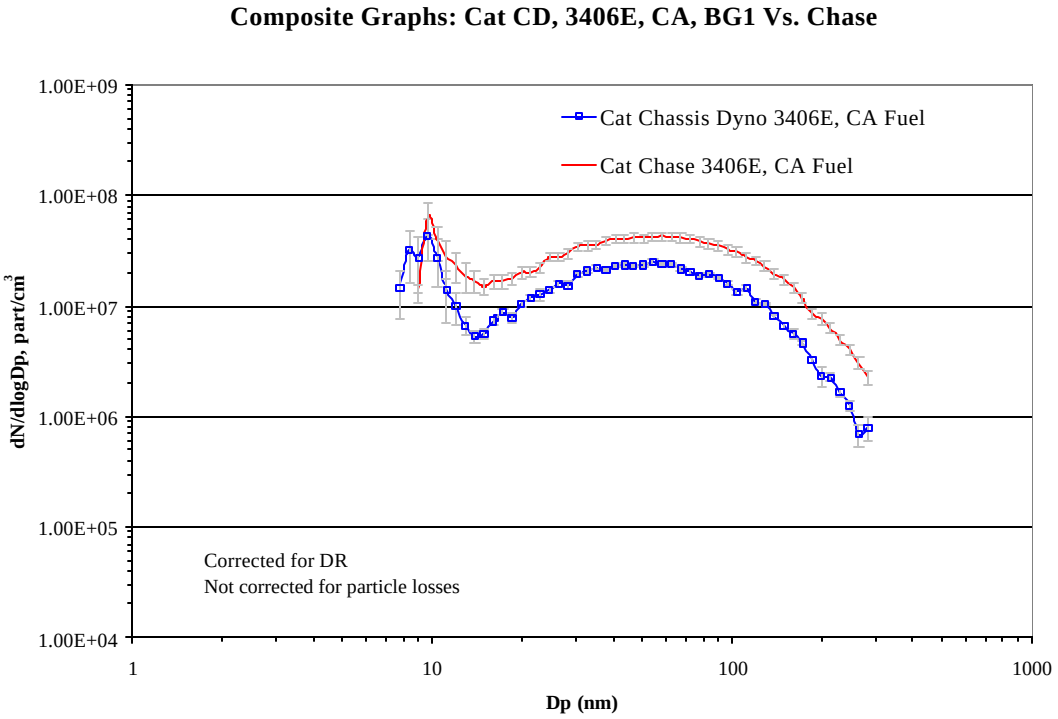

Figure 75. Composite particle number size distribution Caterpillar 3406E engines, CA fuel, chassis dynamometer vs. on-road chase, BG-1/ejector dilution system

Findings:

- Storage and release of semi-volatile material and particle precursors in the exhaust system play an important role in the formation of nanoparticles. Thus, the prior engine operating history is important when determining whether nanoparticles will be formed.
- Some engine conditions, such as idle, produce size distributions that are not appreciably influenced by the sampling conditions, while nuclei mode formation at other engine operating conditions is very sensitive to changing dilution conditions.
- It is difficult to simulate highway test conditions in the laboratory, because on-road conditions are not steady or repeatable. The on-road conditions never allow the engine to reach an equilibrium condition. In the laboratory, running at a single engine load and speed for a prolonged period can stabilize an engine. On-road conditions favor nuclei mode formation through constantly changing exhaust temperatures, traffic slow-downs that favor storage of material in the exhaust system, and release of this material at high load or under hard acceleration.
- The formation of nanoparticles from particle precursors is influenced by the residence time in the dilution tunnel or exhaust system. Short residence time in the exhaust and sampling system prior to dilution favor nanoparticle formation, while short residence time in the dilution system suppresses nanoparticle growth.
- The transfer line from the exhaust pipe to the dilution system is critical. Shorter heated lines minimize residence time, heat and mass transfer and loss of particle

precursors, while long transfer lines remove volatile material necessary for particle nucleation and growth.

- Nanoparticles are more easily formed when fuels with high sulfur content are used, but under some engine conditions, such as light load, nuclei mode formation is independent of fuel sulfur content and heavy hydrocarbons like those in lubricating oil play a major role.
- Catalyzed ceramic filters effectively remove accumulation mode (solid) particles from the exhaust, but can emit volatile precursors that lead to nanoparticle formation and a large nuclei mode under high load conditions.
- Engines of the same series tested with multiple dilution systems and in multiple locations showed engine-to-engine variability in absolute concentrations but the shapes of the size distributions were similar.
- Evaluation of nanoparticles, especially under transient conditions, requires multiple gaseous and particle instruments with synchronized data collection capabilities.

The CRC E-43 program included examination of particle size signatures from several dilution systems, including full flow tunnels and a variety of mini-dilution systems. The sampling and dilution system used in the E-43 that most closely met the goals of the program was the Sierra BG-1 / ejector combination. However, other systems that minimize transfer line losses and maintain constant dilution ratio, dilution air temperature and residence time might be appropriate.

Most full flow dilution systems run rather low primary dilution ratios under high speed and load conditions and high primary dilution ratios under low speed and load conditions. This will cause the laboratory sampling and dilution system to produce particle size distributions for different engine conditions that may be unlike those produced on-road. For example, in a full flow tunnel the exhaust plume dilutes more quickly at low engine speeds and loads than at high speeds and loads, while the opposite is likely to occur under atmospheric dilution conditions. Consequently, we recommend that with full flow dilution systems the dilution ratio be adjusted with engine condition to maintain a roughly constant dilution ratio. This would give a better simulation of what occurs in the atmosphere. However, this raises practical difficulties when doing transient cycles, and it may be difficult to measure size distributions during a transient cycle in a meaningful way using a full flow system for primary dilution. More intense study is needed in this area.

Particle losses in the instruments and sample lines were found to be significant and must be considered in the design of any laboratory dilution and sampling system. Losses in the instruments and sampling systems used in the E-43 program were significant. Correcting for losses decreased DGNs by about 10 % and increased N/V ratios and volume fractions in the nuclei mode by factors of 2 to 3, when a significant nuclei mode was present. However, correction for particle losses would not change any of the conclusions of the E-43 study.

Objective 3. Examine particle transformations as the plume disperses downwind of the roadway in a typical urban situation.

Findings:

Carnegie Mellon University (CMU) prepared a subcontract report titled "Lifetimes of Ultrafine Diesel Aerosol" as part of the E-43 program (Capaldo and Pandis, 2001). A computer model was used to determine the lifetime of ultrafine particles and evolution of particle size distributions measured during on-road testing. Their report addressed the following questions:

- What is the lifetime of particles emitted from on-road Diesels under typical conditions?
- How far are these particles going to be transported, and what is the range of influence of these mobile sources?
- Which are the most important factors influencing the lifetime of the ultrafine aerosols?

A one-dimensional Lagrangian trajectory model was used to simulate the evolution of the plume size distribution. This model simulated the dispersion, mixing with ambient particles, coagulation, and dry removal of the emitted particles. The effects of meteorology, topography, ambient aerosol and model assumptions were examined.

Particle lifetimes, τ_{90} and τ_{99}, were defined as the times necessary for the reduction of the *total number(nearly all in the ultrafine range) concentrations* from their initial plume values by 90 % and 99 %, respectively. Similarly, particle transport distances, s_{90} and s_{99}, were defined as the distance of transport of the emitted particles, measured along the prevailing wind direction, necessary to reduce the initial plume number concentrations by 90 % and 99 %, respectively.

Findings from the report are:

- For typical urban conditions, τ_{90} is on the order of a few minutes and τ_{99} is on the order of 20-30 min.
- s_{90} can vary from 100-1000 m, and s_{99} from 0.5-10 km. Typical values for these transport distances are 300 m for 90 % reduction and 2 km for 99 % reduction. These estimates indicate that Diesel trucks and other mobile ultrafine particle sources will have an effect on the aerosol particle number concentrations in areas near roadways.
- The degree of atmospheric mixing is the most important variable affecting characteristic times (τ_{90} and τ_{99}.) As wind speed increases from 1 to 10 m/s, τ_{90} and τ_{99} decrease by an order of magnitude.
- Characteristic transport distances (s_{90} and s_{99}) are rather insensitive to wind speed.
- For a given wind speed, ultrafine particles are expected to survive and travel a factor of ten greater distances in a rural flat area as compared to an urban downtown location. This is because of faster coagulation due to higher

background particle concentrations and faster mixing and deposition due to rougher terrain in urban areas.

- For the same meteorological conditions and topography, τ_{90} and τ_{99} are expected to be a factor of two and ten less, respectively, in a polluted area as compared to a rural area.
- Driving conditions have a minor effect on the τ_{90} and τ_{99} lifetimes.

Objective 4. Characterize the bulk Diesel particulate matter chemical composition and to determine surface properties and composition.

Findings:

Based upon the work done by Ziemann, Sakurai and McMurry (2002) in a project conducted simultaneously with the E-43 project, the following conclusions are made. These conclusions are based on tests done on a Deere 4045, a Caterpillar C12, and the same Cummins ISM engine used in the E-43 programs. The engines were tested at intermediate speed with light and medium loads.

- The organic component of total Diesel particles and nuclei mode particles appears to be comprised predominantly of unburned lubricating oil, whereas the fuel contribution to the total organic component appears to be relatively small, no more than 20 % and probably much less.
- Low volatility oxidation products (e.g., organic acids) and polycyclic aromatic hydrocarbons, which are compounds of interest and are known to be present (from previous analyses), do not appear to be a major portion of the organic mass.
- The major organic compound classes (alkanes, cycloalkanes, and aromatics) appear to be distributed fairly uniformly across the volatility spectrum.
- Sulfuric acid containing nanoparticles were formed using EPA pump fuel, which contains 410 ppm S. Fuel sulfur enhances nucleation. No sulfuric acid was detected in nanoparticles formed using CA (96 ppm S) or Fischer-Tropsch, (< 1 ppm S) fuel.
- Nuclei-mode particles and accumulation-mode particles are externally mixed across a wide size range, with the chemical components being distributed between two particle types: (a) “less volatile” particles, probably comprised of an elemental carbon core with a small organic component; and (b) “more volatile” particles.
- The volatility experiments showed that, except for the smallest particles, heating could differentiate volatile and solid particles. The fraction of solid particles decreased as particle size decreased, and only a volatile mode was detectable for the smallest particles tested (7 nm). It was found that more than 97% of the volume of the volatile constituents of 12 and 30 nm particles disappeared on heating to 400°C. The volatility of the Diesel nanoparticles was found to resemble that of C24-C32 normal alkanes, which implies a significant contribution of lubricating oil to these particles.
- Hygroscopicity experiments suggest the presence of sulfuric acid in Diesel nanoparticles when the engine was run with a normal 350-ppm sulfur fuel. The

hygroscopicity experiments could not detect sulfuric acid in particles produced by the engine when running on the 96-ppm sulfur CA fuel. When hygroscopic particles could be detected, it was found that the smallest particles were the most hygroscopic, suggesting that the smallest particles were relatively enriched with sulfuric acid.

Recommendations for Laboratory Dilution

The E-43 program has shown that highway dilution conditions lead to the formation of nanoparticles for both old and new technology engines. Dilution is very rapid, freezing the aerosol size distribution, and changing the time scale for further physical changes. The time scale is on the order of minutes, as described by Capaldo and Pandis, 2001, and results in nanoparticles being present near highways, with concentrations dropping over time and distance from the roadway. Nanoparticles are formed very quickly and then decay over a matter of minutes.

Supporting laboratory work and theory have shown that most nuclei mode formation and growth occurs in the low dilution ratio range between about 5 and 50:1. In this range, gas to particle conversion of volatile particle precursors, like heavy hydrocarbons and sulfuric acid, leads to simultaneous nucleation and growth of the nuclei mode and adsorption onto existing particles in the accumulation mode. Residence time and dilution air temperature are critical in this regime. In our tests, typical atmospheric dilution ratios and residence times ranged from 500 to 5000:1 and 1 to 3 s, respectively. Consequently, nuclei mode formation processes were essentially complete and on-road measurements did not significantly depend on these parameters. On the other hand, most laboratory dilution systems, at least in the first stage of dilution, operate in the critical dilution ratio regime where most nucleation and growth occur. The selection of suitable laboratory dilution ratio, temperature, and residence time will allow nucleation and growth to be varied over a wide range. Current laboratory dilution systems have a distribution of residence times at fairly low dilution ratios, but no consistent control of parameters influencing nuclei mode formation.

To best simulate atmospheric dilution processes, a dilution system must simulate the nucleation and growth conditions found in the atmosphere including the range of ambient temperatures and humidity that influence the formation and growth of the nanoparticle mode. On-road E-43 measurements showed the sensitivity of nanoparticle formation to ambient conditions and the variability of these measurements with engine and fuel combinations. The following three points should be made from the E-43 results:

- The Cummins ISM engine running on the CA fuel in cold climatic (5 to 11 ^{o}C) conditions produced a large nuclei mode that was not observed during the laboratory tests of the same engine with warm dilution air.
- On-road nanoparticle formation from Caterpillar engines did not appear to be influenced by temperature and humidity, but these tests were conducted with ambient temperatures ranging from 20°C to 30°C.

- Laboratory tests done at the University of Minnesota with Perkins and Caterpillar engines (Abdul-Khalek, *et al.*, 1998a, 1999 and 2000, Wei 2001a,b and 2002 thesis) show a nuclei mode formation increasing strongly with decreasing dilution air temperature but little or no dependence on humidity. Studies in Europe (Shi and Harrison, 2000 and Ristimaki, 2001) show similar temperature dependence, but a marked increase in nuclei mode formation at higher humidity. Further work on temperature and humidity effects is needed.

Other than ambient conditions, the main parameters influencing nanoparticle growth in the atmosphere are the composition of the growth species and the dilution rate. Evidence from E-43 and related projects suggest that these growth species are predominantly volatile or semi volatile materials such as heavy hydrocarbons (C24 and greater) and sulfuric acid. A dilution system should be designed that closely matches the concentration and time profile for these growth precursors. Wei (Wei, *et al.*, 2001a,b and 2002) built and tested a single stage dilution system that approximates the concentration time profile observed in the atmosphere, but the system is complex and needs refinement. At present, the only relatively easy method to approximate atmospheric dilution utilizes a two-stage dilution process. Two stage systems consist of an exhaust system, an exhaust transfer line that transfers exhaust from the exhaust system to the primary stage of dilution, a primary dilutor, an aerosol-aging chamber and a secondary dilutor. Design issues for these systems are described immediately below and numerical recommendations are made in the paragraphs that follow.

- Exhaust system design - Aging, storage and release processes take place in the exhaust system. It should be matched to that used in actual vehicles as closely as possible.
- Transfer line design - Samples must be taken in such a way that the growth precursors are not lost in sample lines from the tailpipe to the dilution system. The sample line should be designed for low heat and mass transfer rates. A combination of short residence times in the transfer line, achieved by high flow rates, and relatively small values of the ratio of the surface area to flow rate will allow this to be accomplished.
- First stage dilution system - The first stage dilutor should be designed to dilute quickly, with low particle losses. This is accomplished in a Sierra BG type dilutor through the use of porous walls that introduce dilution air. In a two-stage ejector dilutor, the dilution occurs very quickly in an ejector pump. Full and partial flow dilution tunnels used by industry for certification type testing combine aging and primary dilution in one stage.
- First stage residence chamber - An aging chamber is required after primary dilution in a 2-stage tunnel. Dilution and aging are combined in the full or partial flow systems. Whichever type of aging system is used, the combination of primary dilution ratio temperature and residence time must be sufficient to allow particles to grow into the size range encountered in the atmosphere.
- Conditions in primary dilution stage - The number and size of nanoparticles formed, are strongly dependent on the conditions in the first stage of dilution. Low temperatures, low dilution ratios, high humidity and long residence times

favor nanoparticle formation and growth. The BG1 system used in the Caterpillar experiments had a primary dilution ratio of 7.5 and diluted with dry, filtered air at 25° - 30°C. This system worked well under most test conditions.

- Second stage dilution - The secondary dilution system must quench further nanoparticle formation and changes caused by the physical processes of coagulation, nucleation and growth so that a stable aerosol is conveyed to the instruments. Dilution to an overall ratio of 200:1 or more is recommended, although lower ratios may be suitable for future low emission engines.

Even if all of these design factors are carefully considered, it may not be possible to exactly duplicate on-road size distributions due to the high variability of plumes, engine conditions, fuels, environmental conditions and other parameters. Based upon our experience, we believe that the best sampling strategy for measuring engine exhaust aerosol size distributions is to use representative and repeatable laboratory methods that incorporate accepted particle technology principles, rather than attempting to simulate the formation of these particles under ambient conditions that are highly variable. For a partial-flow dilution system, like the BG-1/2 or the 2-stage system, we recommend the following:

- Sampling should take place at the end of a realistic vehicle exhaust system,
- The exhaust transfer line should be designed for low heat and mass transfer,
- The primary dilution ratio should be 5-10:1,
- The residence time in the primary dilution system should be 1-2 s,
- Secondary dilution should be used to raise the overall dilution ratio to >200 to freeze coagulation and growth,
- The dilution air temperature should be 25°-30°C,
- Dilution air should be absolute filtered and charcoal scrubbed and
- Dilution air should be dry or precisely humidity controlled.

For a full flow tunnel, like those used in industry, sampling is more difficult, because it is more difficult to control the parameters that influence nanoparticle formation and growth. However, the goal should again be to measure an engine's nanoparticle emission characteristics. Thus, to the extent possible, the system should be designed to obtain the same dilution conditions recommended for the two-stage, partial flow systems.

Most full flow dilution systems run rather low primary dilution ratios under high load conditions and high primary dilution ratios under low load conditions. This will cause the growth rate of nanometer size particles to be different for different engine conditions, and the weighting of the formation of these particles will be different in a transient test cycle from what it is in the atmosphere. Consequently, we recommend that, with full flow dilution systems, the dilution ratio be adjusted with engine condition to maintain a roughly constant dilution ratio. This would likely give a better simulation of what occurs in the atmosphere. However, this raises practical difficulties when doing transient cycles, and it may be difficult to measure the nanoparticle emission characteristics in a transient cycle in a meaningful way. Recently Khalek, *et al* (2002) described possible scenarios for transient sampling, and although difficult, it may be possible to do this type of

sampling in the future. While it would be difficult to achieve a constant dilution ratio, stepping the total CVS flow in proportion to engine size would allow, at minimum, the average dilution ratio to be maintained constant for different size engines. Alternatively, average sampling zone temperature could be maintained constant. The new 2007 EPA Heavy-Duty test procedures specify an average filter face temperature of 47° ± 5°C. Following this protocol and sampling from the same zone might be an appropriate way of using a CVS system for nanoparticle measurement, but additional study and validation would be required.

Most constant dilution ratio partial flow sampling systems are not designed for proportional sampling and are not appropriate for traditional certification testing. However, meaningful transient tests may still be performed using fast response instruments like the CPC, SMPS in single channel mode, the diffusion charger, and the ELPI. New fast response SMPS-like instruments from Cambustion and TSI are expected to become commercially available in 2002.

Recommendations for Future Work

- **Calibration** - At present there are no convenient calibration standards for number concentration and surface area. A program should be established to evaluate the different types of standard particle generators available along with calibration systems based on primary measurements with the aim of developing a calibration system that could be used on routine basis in a manner analogous to span gases.

- **Chase experiments with low (mass) emission vehicles** - There are still important questions that can be resolved by doing chase experiments. Two additional types of vehicles should be characterized in chase experiments, natural gas powered trucks or buses and trucks or buses equipped with particle traps. Lubricating oil is a major contributor to nanoparticle emissions. Natural gas conversions of Diesel engines often consume as much or more oil as conventional Diesel engines. Lube oil that escapes the combustion system could be a significant source of nanoparticles. Similar arguments apply to Diesel engines equipped with particle traps. These traps are very efficient at removing solid particles but their effectiveness at removing volatile particle precursors has not been fully established.

- **On-road ambient monitoring** - When the mobile emissions laboratory is used to measure on-road aerosols in mixed traffic, the problems associated with trying to characterize a plume from a single source are eliminated. We have already demonstrated that it is possible to measure on-road mixed fleet fuel specific emission factors (Kittelson, *et al*, 2001). However, our study was only a pilot study, and a follow on study should include a variety of on-road locations and ambient conditions. Such sampling will identify areas with high concentrations of nanoparticles, $PM_{2.5}$, or gaseous pollutants, and could lead to recommendations for reducing these concentrations through traffic management. Additional sampling should also include the collection of size-fractionated samples for chemical analysis.

- **Mobile emission laboratory plume sampling** - The mobile emission laboratory is a convenient source of exhaust emissions that could be used as the platform for experiments. For instance, background measurements could be made continuously with additional instruments in the lab and stack emissions could be monitored simultaneously with onboard instruments. This would eliminate problems encountered during the E-43 program trying to capture a plume and differentiate the plume from the background. Tests could be run with different fuels, aftertreatment systems and operating conditions.

- **Single vehicle onboard plume sampling** – In our engine lab we have shown that sampling with a short heated transfer line using a two-stage dilution tunnel can simulate size distributions produced by roadway dilution conditions. This dilution system could be used in conjunction with a set of portable instruments to sample continuously from the exhaust of an individual vehicle, even a passenger car. Instruments like the condensation particle counter, photoelectric aerosol detector, and diffusion charger are available as portable units. All of these instruments could be carried onboard for real world characterization of size distributions

- **Validation of the E-43 recommended laboratory sampling methods** - One of the major limitations of the E-43 study was the difficultly in adapting our dilution and sampling procedures for use in laboratories not dedicated to research. Much of the time was spent moving and setting up equipment from one lab to another and learning about the special situations and limitations in each location. Consequently, there was insufficient time to systematically vary dilution and sampling conditions as we have done in the past in our lab. Our recommended test procedures for evaluating an engine's nanoparticle emission characteristics should be subjected to a series of validation experiments to confirm our recommendations.

- **Further research on the chemistry of nanoparticles** - It is necessary to develop a sampling system capable of generating size-fractionated samples that provides samples of sufficient mass for chemical speciation. This system should also allow for simultaneous physical aerosol characterization.

- **Fast response instruments for transient tests** - There is a need for relatively low cost instruments for near real time measurements in the nanoparticle range. Such instruments would allow size information to be obtained during transient cycles. The combination of the diffusion charger and condensation particle counter has shown promise during the E-43 program. Cambustion Ltd. has recently introduced a fast response, differential mobility particle sizer that yields SMPS like size distributions with 200 ms time response. Further testing is required to evaluate the effectiveness of these instruments, and other instruments that have recently become available, during transient engine tests conducted in the laboratory. If these instruments perform well, then they can be included in a suite of instruments used for on-board, real world, on-road tests.

Summary

The Diesel aerosol exhaust size distribution is influenced by many factors. These include engine condition, fuel and lube oil composition, exhaust system configuration, sampling system and sampling conditions. Engine and sampling system stabilization and previous engine operating history play important roles in determining the size distribution. Furthermore, ambient weather conditions, such as temperature, also affect on-road size distributions. All of these factors make precise definition and simulation of the on-road operating and dilution conditions very difficult. Measurement of the nanoparticle size range is the most difficult because it is dominated by nuclei mode particles, most of which are formed by nucleation of volatile precursors as the exhaust dilutes and cools. Nucleation is extremely dependent upon dilution conditions and these nuclei and their precursors may be strongly influenced by losses and sampling artifacts. While it was difficult to match on-road size distributions for individual test conditions, much better agreement between on-road and laboratory was achieved for composites of several test conditions. Size distributions generated in the laboratory under optimal engine, sampling, and dilution conditions can reproduce on-road size distributions. Based upon our experience, we believe that the best sampling strategy for measuring engine exhaust size distributions is to apply good particle technology principles in the laboratory using a standard set of sampling and dilution conditions that are reproducible, are sensitive to sampling the broad range of particle sizes known to exist in engine exhaust aerosols and minimize sampling artifacts. However, it is unlikely that dilution systems and methods currently used in the Diesel engine industry will be able to consistently reproduce on-road size distributions without substantial modification and strict adherence to test procedures and protocols.

REFERENCES

Abdul-Khalek, I. S. and D. B. Kittelson. 1995. Real Time Measurement of Volatile and Solid Exhaust Particles Using a Catalytic Stripper. SAE Tech. Pap. Ser. No. 950236.

Abdul-Khalek, I. S., *et al*. 1998a. Diesel Exhaust Particle Size: Measurement Issues and Trends. SAE Tech. Pap. Ser. No. 980525, 13 pp.

Abdul-Khalek, I., D. Kittelson and F. Brear. 1998b. Diesel Trap Performance: Particle Size Measurements and Trends. SAE Tech. Pap. Ser. No. 982599, 14 pp.

Abdul-Khalek, I. S., D. B. Kittelson and F. Brear. 1999. The Influence of Dilution Conditions on Diesel Exhaust Particle Size Distribution Measurements. SAE Technical Paper Series. 1999-01-1142.

Abdul-Khalek, I. S., D. B. Kittelson and F. Brear. 2000. Nanoparticle Growth During Dilution and Cooling of Diesel Exhaust: Experimental Investigation and Theoretical Assessment. SAE Tech. Pap. No. 2000-01-0515.

Adachi, M., Y. Kousaka and K. Okuyama. 1985. Unipolar and Bipolar Diffusion Charging of Ultrafine Aerosol Particles. J. Aerosol Sci. v. 16, pp 109-123.

Agarwal, J. K. and G. J. Sem. 1980. Continuous Flow, Single-Particle-Counting Condensation Nucleus Counter. J. Aerosol Sci. 11: 343-357.

Ayala , A., B. Olson, and B. Cantrell. 2002. Working Quality Assurance Project Plan for Diesel Aerosol Sampling Methodology (CRC Project E-43), 93 pp. Available from the Coordinating Research Council, Alpharetta, GA.

Bagley, S. T., *et al*. 1996. Characterization of Fuel and Aftertreatment Device Effects on Diesel Emissions. Health Effects Institute (HEI), Research Report No. 76.

Baltensperger, U., E. Weingartner, H. Burtscher, and J. Keskinen. (2001) Dynamic mass and surface area measurements. In Aerosol Measurement (Edited by Baron, P.A. and Willeke, K.), pp. 387-418. John Wiley and Sons, New York.

Baumgard, K. J. and D. B. Kittelson. 1985. The Influence of a Ceramic Particle Trap on the Size Distribution of Diesel Particles. SAE Tech. Pap. Ser. No. 850009, SAE Transactions, 95:56-69.

Booker, D. R. 1997. Urban Pollution Monitoring: Oxford City Centre, Research Report, AEA Technology, Aerosol Science Centre, Oxfordshire, UK.

Bukowiecki, N., *et al*. 2001. Subcontract Final Report CRC E-43: Surface Area Instruments Epiphaniometer. 20 pp.

Bukowiecki, N., *et al*. 2002. Real-time Characterization of Ultra Fine and Accumulation Mode Particles in Ambient Combustion Aerosols. J. Aerosol Sci. (In press).

Burtscher, H. (1992) Measurement and Characteristics of Combustion Aerosols With Special Consideration of Photoelectric Charging and Charging By Flame Ions. J. Aerosol Sci. 23:549-595.

Burtscher, H., *et al*. 2001. Separation of Volatile and Non-Volatile Aerosol Fractions By Thermodesorption: Instrumental Development and Applications. J. Aerosol Sci. (32): 427-442.

Cadle, S. H., *et al*. 1998. Measurement of Exhaust Particulate Matter Emissions from In-Use Light-Duty Motor Vehicles in the Denver, Colorado Area, 142 pp. Available at http://charon.cira.colostate.edu

Capaldo, K. and S. Pandis. 2001. Lifetimes of Ultrafine Diesel Aerosol. CRC E-43 Subcontract Final Report. Coordinating Research Council, Alpharetta, GA.

Chen, D., D. Y. H. Pui and S. L. Kaufmann. 1995. Electrospraying of Conducting Liquids for Monodisperse Aerosol Generation in the 4 nm to 1.8 μm Diameter Range. J. Aerosol Sci. 26(6):963-977.

Chen, D. R., *et al*. 1996. Nanometer Differential Mobility Analyzer (Nano-DMA): Design and Numerical Modeling. J. Aerosol Sci. 27(1): S137-S138.

Chen, D. R., *et al*. 1998. Design and Evaluation of a Nanometer Aerosol Differential Mobility Analyzer (Nano-DMA). J. Aerosol Sci. 29(5/6): 497-509.

Clark, N., *et al*. 2001. Subcontract Final Report CRC E-43 Langley Wind Tunnel Research. Coordinating Research Council, Alpharetta, GA.

Code of Federal Regulations. 2001. 40 CFR Part 86 Subpart N. 2001. Emission Regulations For New Auto Cycle And Diesel Heavy Duty Engines; Gaseous And Particulate Exhaust Test Procedures.

Dickens, C. J., *et al*. 1997. Evaluation of Instruments for Vehicle Emission Particle Sizing. AEA Technology Report: AEAT-1180, 69 pp. (restricted distribution).

Ehara, K., C. Hagwood, C. and K. Coakley. 1996. Novel Method to Classify Aerosol Particles According to Their Mass-to-Charge Ratio-Aerosol Particle Mass Analyzer. Bulletin of NRML 45, pp. 265-282.

Environmental Protection Agency. 1991. Preparation Aids for the Development of Category III Quality Assurance Project Plans, EPA/600/8-91/005, February 1991.

Environmental Protection Agency, QA/G-5. 1998. Guidance on Quality Assurance Project Plans, EPA/600/R-98/018, February 1998.

Friedlander S. K. 2000. Smoke Dust and Haze 2nd edition, Wiley and Sons. John Wiley and Sons, New York.

Gäggeler, H. W., *et al*. 1989. The Epiphaniometer, A New Device for Continuous Aerosol Monitoring. J. Aerosol Sci. 20(5): 557-564.

Gäggeler, H. W., *et al*. 1989b. Applications of the Epiphaniometer to Environmental Aerosol Studies. J. Aerosol Sci. 20(8): 1225-1228.

Graskow, B., *et al.* 1998. Characterization of Exhaust Particulate Emissions from a Spark Ignition Engine. SAE Tech. Pap. Ser. No. 980528, 10 pp.

Greenwood, S., *et al.* 1996. An Investigation to Determine the Exhaust Particulate Size Distributions for Diesel, Petrol, and Compressed Natural Gas Fuelled Vehicles. SAE Tech. Pap. Ser., No. 961085.

Harrison, R.M. 1996. Airborne Particulate Matter in the United Kingdom. Third Report of the Quality of Urban Air Review Group, R.M. Harrison, chair, The University of Birmingham, Edgbaston, England.

Health Effects Institute. 1995. Diesel Exhaust: A Critical Analysis of Emissions, Exposure, and Health Effects. HEI Special Report. Health Effects Institute, Cambridge, MA.

Health Effects Institute. 2001. Airborne Particles and Health: HEI Epidemiologic Evidence, HEI Perspectives, Health Effects Institute, Cambridge, MA.

Health Effects Institute. 2002a. Understanding the Health Effects of Components of the Particulate Matter Mix: Progress and Next Steps, HEI Perspectives, Health Effects Institute, Cambridge, MA.

Health Effects Institute. 2002b. Research Directions to Improve Estimates of Human Exposure and Risk from Diesel Exhaust. HEI Special Report. Health Effects Institute, Cambridge, MA.

Higgins, K., *et al*. 2001. Size-Selected Nanoparticle Chemistry: Kinetics of Soot Oxidation, Abstract and Presentation, AAAR Annual Conference, 2001.

Hinds, C.W. 1982. Aerosol Technology, Properties, Behavior, and Measurement of Airborne Particles, J. Wiley and Sons, Inc, 133 pp..

Hiromu, S., *et a*l. 2001. Hygroscopicity and Volatility of Diesel Nanoparticles Studied by Nano TDMA, Abstract and Presentation, AAAR Annual Conference, 2001.

Jing, L., *et al*. 1996. Einfluss des Einspritzdruckes auf die Partikelemission des DI-Dieselfahrzeuges, Zeitschrift fur das Messwesen, Volume 3, pp 7-10, (in German).

Johnson, J. H. and K. H. Baumgard. 1996. The Effect of Fuel and Engine Design on Diesel Exhaust Particle Size Distributions, SAE Tech. Pap. Ser. No. 960131.

Jones, T. J. and D. B. Kittelson. 2002. Experiments Performed on the Caterpillar C12 Test Stand: January 1st through May 1st 2002, report submitted to Caterpillar Inc., June 2002.

Jung, H., D. B. Kittelson and M. R. Zachariah. 2001. Characterization of Aerosol Surface Instruments (PAS and DC) with Soot Agglomerates, Abstract and Presentation, AAAR Annual Conference, 2001.

Khalek, I., T. Ullman, and S. Shimpi., *et al*. 2002. Performance of Partial Flow Sampling Systems Relative to Full Flow CVS on Particulate Emissions for Steady-State and Transient Engine Operation. Presented at Spring Fuels & Lubricants Meeting & Exhibition, May 2002, Reno, NV, USA, Session: Diesel Emissions (Part C). SAE Tech. Paper Ser. 2002-01-1718 and SP-175.

Kittelson, D. B., *et al*. 1988. Characterization of Diesel Particles in the Atmosphere. AP-2 Project Group Final Report, Coordinating Research Council.

Kittelson, D. B. and J. H. Johnson. 1991. Variability in Particle Emission Measurements in the Heavy Duty Transient Test. SAE Tech. Pap. Ser. No. 910738, Published in Diesel Particulate Emissions: Measurement Techniques, Fuel Effects and Control Technology SAE Pt-42, pp. 137-162, Edited by J. H. Johnson, *et al.* SAE, Warrendale, PA.

Kittelson, D. B. 1998. Engines and Nanoparticles: A Review. J. Aerosol Sci. 29(5/6):575-588.

Kittelson, D. B., J. Johnson, W. Watts, Q. Wei. M. Drayton, D. Paulsen and N. Bukowiecki. 2000. Diesel Aerosol Sampling in the Atmosphere. SAE Tech. Paper Ser. 2000-01-2212, 8 pp.

Kittelson, D. B., W. F. Watts and J. P. Johnson. 2001. Fine Particle (Nanoparticle) Emissions On Minnesota Highways. Mn/DOT Report No. 2001-12, 87 pp. Available at http://www.dot.state.mn.us/research/reports_online.html

Kittelson, D. B., W. F. Watts, G. Ramachandran, D. Paulsen and C. Kreager 2002. Exposures to Diesel Exhaust Aerosol. In Health Effects Institute Report Research Directions to Improve Estimates of Human Exposure and Risk from Diesel Exhaust. A Special Report of the Institute's Diesel Epidemiology Working Group, April 2002, 233 pp., Health Effects Institute, Boston, MA. (Available at www.healtheffects.org)

Kittelson, D. B., W. F. Watts and J. P. Johnson. 2002a. Diesel Aerosol Sampling Methodology - CRC E-43 Final Report. Coordinating Research Council, Alpharetta, GA.

Kittelson, D. B., W. F. Watts and J. P. Johnson. 2002b. Diesel Aerosol Sampling Methodology - CRC E-43 Cummins Data Volume. Coordinating Research Council, Alpharetta, GA.

Kittelson, D. B., W. F. Watts and J. P. Johnson. 2002c. Diesel Aerosol Sampling Methodology - CRC E-43 Caterpillar Data Volume. Coordinating Research Council, Alpharetta, GA.

Kittelson, D. B., W. F. Watts and J. P. Johnson. 2002d. Diesel Aerosol Sampling Methodology - CRC E-43 Wind Tunnel Report. Coordinating Research Council, Alpharetta, GA.

Keskinen, J., *et al*. 1992. Electrical Low Pressure Impactor. J. Aerosol Sci. 23(4): 353-360.

Kesten, J., A. Reineking and J. Porstendoerfer. 1991. Calibration of a TSI model 3025 ultrafine condensation particle counter. Aerosol Sci. Technol. 15: 107-111.

Knutson, E. 1975. Extended Electric Mobility Method for Measuring Aerosol Particle Size and Concentration. In Fine Particles Aerosol Generating, Measurement, Sampling, and Analysis, B. Y. H. Liu editor, Academic Press, Inc., NY, NY.

Kruger, M., *et al*. 1997. Influence of Exhaust Gas Aftertreatment on Particulate Characteristics of Vehicle Diesel Engines, Motortechnische Zeitschrift, Vol. 58.

Lippmann, M. 2001. Chapter 5 Size-Selective Health Hazard Sampling. In Air Sampling Insturments for Evaluation of Atmospheric Contaminants. 9th Edition, B. S. Cohen and C. S. McCammon, Jr., Editors, ACGIH, Cincinnati, OH. p. 93-134.

Maricq, M. 1998. Vehicle Particulate Emissions: A Comparison of ELPI, SMPS and Mass Measurement. International Seminar on Particle Size Distribution Measurement From Combustion Engines, Espoo, Finland.

Maricq, M., *et al*. 1999a. Gasoline Vehicle Particle Size Distributions: Comparison of Steady-state, FTP, and USO6 Measurements. Env. Sci. Technol. 33:2007-2015.

Maricq, M. M., *et al*. 1999b. Examination of the Size-Resolved and Transient nature of Motor Vehicle Particle Emissions. Env. Sci. Technol. 33(10): 1618-1626.

Maricq, M., D. H. Podsiadlik, and R. E. Chase. 2000. Size Distributions of Motor Vehicle Exhaust PM: A Comparison between ELPI and SMPS Measurements. Aerosol Sci. and Technol. 33(3):239-260.

Marple, V. A., K. L. Rubow and S. M. Behm. 1991. A Microorifice Uniform Deposit Impactor (MOUDI): Description, Calibration, and Use. Aerosol Sci. Technol. 14: 434-446.

Marple, V. A., K. L. Rubow and B. A. Olson. 1994. Low Pressure Stages for the Micro-orifice Uniform Deposit Impactor (MOUDI). Fourth International Aerosol Conference Abstracts.

Matter, U., Siegmann, H.C., and Burtscher, H. (1999) Dynamic field measurements of submicron particles from Diesel engines. Environ. Sci. Technol. 33:1946-1952.

Mayer, A., *et al*. 1995. Particle Size Distribution Downstream Traps of Different Design, SAE Tech. Pap. Ser. No. 950373.

Mayer, A., *et al*. 1998. Vert: Diesel Nano-Particulate Emissions: Properties and Reduction Strategies. SAE Tech. Pap. Ser. No. 980539, 12 pp.

Mayer, A., *et al*. 1999. Particulate traps for retro-fitting construction site engines VERT: final measurements and implementation. SAE Tech. Pap. Ser. No. 1999-01-0116, 15 pp.

McAughey, J. J., *et al*. 1996. Exhaust Particulate Size Distribution: Vehicle and Fuel Influences in Light Duty Vehicles, SAE Tech. Pap. Ser. No. 961980.

McAughey, J. J., *et al*. 1997. Regional Lung Deposition and Dose of Ambient Particulate in Humans by Particle Mass and Number. AEA Technology, Aerosol Science Center.

Pandis, S. N., *et al*. 1991. Inversion of Aerosol Data from the Epiphaniometer. J. Aerosol Sci. 22: 417-428.

Pandis, S. N. and K. Capaldo. 2001. Lifetimes of Ultrafine Diesel Aerosol. Final Report Prepared for the University of Minnesota and the Coordinating Research Council under the E-43 Project Diesel Particulate Sampling Methodology, 24 pp.

Park, K. D. B. Kittelson and P. McMurry. 2001. Measurements of the Effective Density of Diesel Particles Using the DMA-APM Technique. Presentation at AAAR Annual Meeting, 2001.

Paulsen, D. A. 2001. Real-time Assessment of Combustion Aerosols within a Parking Facility. Masters Thesis, University of Minnesota, 153 pp.

Ping, J. I., *et al*. 2000. Characterization of Particles from a Current Technology Heavy-Duty Engine. Env. Sci. Technol. 34(5):748-755.

Pui, D. Y. H. and D. Chen. 2001. Chapter 15. Direct-Reading Instruments for Analyzing Airborne Particles. In Air Sampling Instruments. ACGIH, Cincinnati, OH., p 377-414.

Ristimaki, J. 2001. Nanoparticle Formation During Diesel Exhaust Dilution. Master's Thesis, Department of Electrical Engineering. Tampere, Finland, Tampere University of Technology. 62 pp.

Reineking, A. and J. Porstendorfer. 1986. Measurements of Particle Loss Functions in a Differential Mobility Analyzer (TSI, Model 3071) for Different Flow Rates. Aerosol Sci. Technol. 5:483-486.

Rogak, S. N., *et al*. 1991. Measurement of Mass Transfer to Agglomerate Aerosols. Aerosol Sci. Technol. 14: 447-458.

Sakurai, H., *et al.* 2001. Hygroscopicity and Volatility of Diesel Nanoparticles Studied by Nano TDMA, Abstract and Presentation, AAAR Annual Conference.

Shi, J. P. and R. M. Harrison. 2000. Characterization of Particles from a Current Technology Heavy-Duty Diesel Engine. Env. Sci. Tech. 34: 748-755.

Siegmann, K., L. Scherrer and H.C. Siegmann. 1999. Physical and Chemical Properties of Airborne Nanoscale Particles and how to Measure the Impact on Human Health. J. Molecular Structure, 458 (1-2 Special Issue SI):191-201.

Siegmann, K. and Siegmann, H.C. 2000. Fast and Reliable "in situ" Evaluation of particles and their surfaces with special reference to Diesel exhaust. SAE Technical Paper Ser. No 2000-01-1995.

Sierra Instruments. 1998. BG-1 ™ Micro-Dilution Test Stand Instruction Manual. Part Number IM-BG-1 03.98 Revision B, 82 pp.

Sturm, P. J., *et al.* 2002. Measurement of Particulate Matter Size Distribution in a Road Tunnel. Presentation at 12th CRC On-Road Vehicle Emissions Workshop.

Suresh, A., *et al.* 2001. A Study of the Effect of a Catalyzed Diesel Particulate Filter on the Emissions from a Heavy Duty Diesel Engine with EGR. SAE Technical Paper Ser. 2001-01-0910.

Watson, J. G. *et al*. 1998. Northern Front Range Air Quality Study, final report, prepared for Colorado State University.

Wei, Q., D. B. Kittelson and W. F. Watts. 2001a. Single-Stage Dilution Tunnel Design. SAE Tech. Pap. Ser. 2001-01-0207, 14 pp. In In-Cylinder Diesel Particulate and NOx Control 2001, SAE SP-1592, p 119-131.

Wei, Q., D. B. Kittelson and W. F. Watts. 2001b. Single-Stage Dilution Tunnel Performance. SAE Tech. Pap. Ser. 2001-01-0201, 12 pp. In In-Cylinder Diesel Particulate and NOx Control 2001, SAE SP-1592, p 75-86.

Wei, Q. 2002. Systems to Simulate Engine Exhaust Dilution in the Atmosphere, Ph.D. Thesis, University of Minnesota, 2002.

Wiedensohler, A.1988. An Approximation of the Bipolar Charge Distribution for Particles in the Submicron Size Range. J. Aerosol Sci. 19(3):387-389.

Wiedensohler, A., *et al*. 1990. Experimental Verification of the Particle Detection Efficiency of TSI 3025 UCPC. J. Aerosol Sci. 21: 617-620.

Whitby, K. T., *et al*. 1975. Characterization of California Aerosols - 1. Size Distributions of Freeway Aerosol. Atmosph. Environ. 9:463-482.

Whitby, K. T. and B. K. Cantrell. 1975. Atmospheric Aerosols - Characteristics and Measurement. Proceedings. ICESA Conference.

Wilson, W. E., *et al*. 1977. General Motors Sulfate Dispersion Experiment: Summary of EPA Measurements. JAPCA 27(1):46-51.

Ziemann, P. J., H. Sakurai and P. H. McMurry. 2002. Chemical Analysis Of Diesel Nanoparticles Using A Nano-DMA/Thermal Desorption Particle Beam Mass Spectrometer. Final Report CRC Project No. E-43-4, 92 pp.

Zhu, Y., et al. 2002a. Concentration and Size Distributions of Ultrafine Particles Near a Major Highway. Accepted for publication in J. Air Waste Management Assoc.

Zhu, Y., et al. 2002b. Study of Ultrafine Particles and Other Vehicular Pollutants Near a Highway With Heavy Duty Diesel Traffic. Submitted to Atmosph. Environ.

APPENDIX A - COMPOSITE SIZE DISTRIBUTIONS AND TABLES

APPENDIX B – 3406E ENGINE COMPARISON

APPENDIX C – CUMMINS FUEL/OIL SULFUR RESULTS

APPENDIX D – FACTORS INFLUENCING FORMATION AND GROWTH OF NANOPARTICLES

APPENDIX E – VOLATILITY AND HYGROSCOPICITY